University of Szeged

Faculty of Pharmacy

Department of Pharmacodynamics

and Biopharmacy

Kaohsiung Medical University

College of Pharmacy

Graduate Institute of Natural

Products

Ph.D. Thesis

Antiproliferative and antimetastatic properties of modified estradiol analogs against gynecological cancer cell lines

Izabella Sinka Pharm.D.

Supervisors:

István Zupkó D.Sc.

Prof. Hui-Chun Wang Ph.D.

2020

Table of contents

Scientific publications related to the subject of the thesis

I. Sinka, I; Kiss, A; Mernyák, E; Wölfling, J; Schneider, G; Ocsovszki, I; Kuo, C-Y; Wang, H-C; Zupkó, I:

Antiproliferative and antimetastatic properties of 3-benzyloxy-16-hydroxymethylene-estradiol analogs against breast cancer cell lines

EUROPEAN JOURNAL OF PHARMACEUTICAL SCIENCES 123 pp. 362-370. 9 p. (2018)

IF: 3.532

II. Kiss, A; Mernyák, E; Wölfling, J; Sinka, I; Zupkó, I; Schneider, Gy:

Stereoselective synthesis of the four 16-hydroxymethyl-3-methoxy- and 16-hydroxymethyl-3-benzyloxy-13α-estra-1,3,5 (10)-trien-17-ol isomers and their antiproliferative activities

STEROIDS 134 pp. 67-77., 11 p. (2018)

IF: 2.136

III. Mernyák, E; Kovács, I; Minorics, R; Sere, P; Czégány, D; Sinka, I; Wölfling, J; Schneider, Gy; Újfaludi, Zs; Boros, I; Ocsovszki, I; Varga, M; Zupkó, I:

Synthesis of trans-16-triazolyl-13α-methyl-17-estradiol diastereomers and the effects of structural modifications on their in vitro antiproliferative activities

JOURNAL OF STEROID BIOCHEMISTRY AND MOLECULAR BIOLOGY 150: pp. 123-134. (2015)

IF: 3.985

Scientific publications not related to the subject of the thesis

I. Tastan, P; Hajdú, Zs; Kúsz, N; Zupkó, I; Sinka, I; Kivcak, B; Hohmann, J:

Sesquiterpene Lactones and Flavonoids from Psephellus pyrrhoblepharus with Antiproliferative Activity on Human Gynecological Cancer Cell Lines

MOLECULES 24: 17 Paper: 3165, 9 p. (2019)

IF: 3.060

II. Mótyán, G; Mérai, L; Kiss, M; Schelz, Zs; Sinka, I; Zupkó, I; Frank, É:

Microwave-assisted synthesis of biologically relevant steroidal 17- exo -pyrazol-5'-ones from a norpregnene precursor by a side-chain elongation/heterocyclization sequence

BEILSTEIN JOURNAL OF ORGANIC CHEMISTRY 14 pp. 2589-2596., 8 p. (2018)

IF: 2.595

III. Vlaisavljević, S; Šibul, F; Sinka, I; Zupko, I; Ocsovszki, I; Jovanović-Šanta, S:

Chemical composition, antioxidant and anticancer activity of licorice from Fruska Gora locality

INDUSTRIAL CROPS AND PRODUCTS 112 pp. 217-224., 8 p. (2018)

IF: 4.191

IV. Baji, Á; Kovács, F; Mótyán, G; Schneider, G; Wölfling, J; Sinka, I; Zupkó, I; Ocsovszki, I; Frank, É:

Investigation of pH and substituent effects on the distribution ratio of novel steroidal ring D- and A-fused arylpyrazole regioisomers and evaluation of their cell-growth inhibitory effects in vitro

STEROIDS 126 pp. 35-49., 15 p. (2017)

IF: 2.253

V. Kovács, B; Béni, Z; Dékány, M; Orbán-Gyapai, O; Sinka, I; Zupkó, I; Hohmann, J; Ványolós, A:

Chemical Analysis of the Edible Mushroom Tricholoma populinum: Steroids and Sulfinyladenosine Compounds

NATURAL PRODUCT COMMUNICATIONS 12: 10 pp. 1583-1584., 2 p. (2017)

IF: 0.809

VI. Bodnár, B; Mernyák, E; Wölfling, J; Schneider, Gy; Herman, B; Szécsi, M; Sinka, I; Zupkó, I; Kupihár, Z; Kovács, L:

Synthesis and biological evaluation of triazolyl 13α-estrone–nucleoside bioconjugates

MOLECULES 21: 9 Paper: 1212, 16 p. (2016)

IF: 2.861

VII. Csábi, J; Martins, A; Sinka, I; Csorba, A; Molnár, J; Zupkó, I; Tóth, G; Tillekeratne, LMV; Hunyadi, A:

Synthesis and in vitro evaluation of the antitumor potential and chemo-sensitizing activity of fluorinated ecdysteroid derivatives

MEDCHEMCOMM 7: pp. 2282-2289., 8 p. (2016)

IF: 2.608

Abbrevations

°C	Celsius
Ac-DEVD-pNA	Acetyl-Asp-Glu-Val-Asp *p*-nitroanilide
Ac-IETD-pNA	Acetyl-Ile-Glu-Thr-Asp-*p*-nitroanilide
APAF1	Adapter protein apoptotic protease activating factor 1
AR	Androgen receptor
ATP	Adenosine triphosphate
BL1	Basal-like 1
BL2	Basal-like 2
BLBC	Basal-like breast cancer
CA	California
CARD	Caspase recruitment domain
CYP	Cytochromes P450
dATP	Deoxyadenosine triphosphate
DED	Death-effector domain
DISC	Death-inducing signaling complex
DNA	Deoxyribonucleic acid
DR	Death receptor
ECM	Extracellular matrix
ER	Estrogen receptor
ERE	Estrogen response element
FADD	FAS-associated death domain
FAK	Focal adhesion kinase
FISH	Fluorescence in situ hybridization
h	Hour
HER2	Human epidermal growth factor receptor 2
HO	Hoechst 33258
HPV	Human papillomavirus
IAP	Inhibitors of apoptosis protein
LAR	Luminal androgen receptor
LEHD-pNA	Leu-Glu-His-Asp- p-nitroanilide
IHC	Immunohistochemistry
ME	Maine
MEK	Mitogen-activated protein kinase kinase
MMP	Matrix metalloproteinase
MPT	Mitochondrial permeability transition
MTT	3-(4,5-dimethylthiazol-2-yl)-2,5-diphenyltetrazolium bromide
PARP	Poly ADP-ribose polymerase
PBS	Phosphate-buffered saline
pFAK	Phosphorylated focal adhesion kinase
PI	Propidium iodide
PI3K	Phosphoinositide 3-kinase
PR	Progesteron receptor
RBA	Relative binding affinities
RIPK1	Receptor-interacting serine/threonine-protein kinase 1
RNAse A	Ribonuclease
Rpm	Revolutions per minute
SDS-PAGE	Sodium dodecyl sulfate–polyacrylamide gel electrophoresis
TNBC	Triple-negative breast cancer
TNFR	Tumor necrosis factor receptor
TRADD	TNF receptor-associated death domain
USA	United States
WCE	Whole-cell extraction

1. Introduction

1.1 Epidemiology and overview of breast and cervical tumors

In spite of the continuously developed new therapeutical opportunities, cancer is still an unsolved health problem and a leading cause of death globally. Based on the database of Globocan 2018, 18.1 million new cases and 9.6 million tumor-related deaths were estimated worldwide in 2018.[1] In 2012, the approximated new case and cancer death numbers were 14.1 and 8.2 millions.[2] Comparing these data to the assessment of 2018 shows the huge necessity for more efficient treatments. Among women, breast malignancy was the most frequently diagnosed and correlating to this fact, it is the leading cause of cancer death in 103 countries. Another significant gynecological tumor is cervical cancer, since it takes the fourth position in incidence and mortality.[1]

The presence of secondary tumors can be connected with approximately 90% of cancer-related deaths.[3] Steeg *et al.* have evaluated the reports of US National Cancer Institute Surveillance, Epidemiology and End Results (SEER) registries, including data between 1995–2000 and 2004–2010 that were reported in 2005 and 2015, It was found that patients with a diagnosis of metastasis had decreased overall 5-year survival rates compared to the patients with localised or regional disease. In addition, fewer than 20% of the patients with metastatic disease survived 5 years later regarding half of the examined cancer sites. The 5-year survival rate is reduced in several cancer types with distant metastases between the two reporting periods, such as breast and cervical tumors.[4] The assessment of results of randomized clinical trials covering a 30-year period could not show sustained evidence of survival improvement among women with metastatic breast cancer.[5]

The heterogeneous clinical and molecular appearance of breast cancer is expansively established; several subtypes were determined on the basis of their expressed receptors. There are various available methods to identify receptor expression. Estrogen receptor (ER) and progesterone receptor (PR) assessment can be carried out by the means of immunohistochemistry (IHC), while for determination of human epidermal growth factor receptor 2 (HER2) expression, IHC or fluorescence in situ hybridization (FISH) are utilized.[6] Breast cancer subtypes were further identified based on gene expression profiling using cDNA microarrays.[7,8] Numerous genes were found to be highly expressed in estrogen receptor (ER) positive tumors which are also expressed by the luminal cells of breast tissue.[7] We can identitify luminal A and luminal B types between hormone-positive cancers, considering that Luminal A was featured by higher expression of ER-related genes, and the

less expression of proliferative genes compared to Luminal B tumors.[8] Another clinically significant class is determined by the expression of HER2.[9]

The triple-negative subtype (TNBC) is distinguished by the lack of ER, PR and HER2 amplification.[9] Within this characteristic, heterogeneous molecular feature was described. The basal-like breast cancer (BLBC) carries the same receptor characteristic, but in addition, it is featured by a strong gene expression pattern, such as cytokeratin 5,6,17 and EGFR.[10,11] The "basal-like" term was derived from the fact, that the genes mentioned above are featuring normal basal and myoepithelial cells. TNBC subtype encompasses approximately 90% of BLBCs.[11]

Approximately 15-20% of the total diagnosed breast tumors are triple-negative. However, the fact that 25% of the total breast cancer mortality can be connected with the subtype shows its serious burden.[9] The size of the tumor is typically larger, the chance of recurrence is higher, and metastatic spread appears in a significantly shorter period from the initial diagnosis than other breast cancer subtypes.[12] Moreover, the secondary tumor of TNBC frequently occurs in the brain and viscera, which carries a poor prognosis. On the other hand, the non-TNBC metastatic evaluation mostly affects bones. Correspondingly, TNBC is featured by shorter median time to death (4.2 vs. 6 years) and worse overall survival.[9,13] Another disadvantageous fact, that TNBC patients are 5-10 years younger compared to other breast tumor subtypes at the time of diagnosis.[14]

Although extensive mutational and clonal diversity was described in connection with the progression of primary TNBC, the clinical treatment still considers TNBC as a single disease entity. Standard chemotherapeutical treatment is utilized for all stages of TNBC.[11,15–17] The reassessment of the molecular classification of TNBC by the means of gene expression profiling (previously six subgroups were described by Lehmann et al. in 2011[15]) resulted in differing basal-like 1 (BL1), basal-like 2 (BL2), luminal androgen receptor (LAR) and mesenchymal intrinsic subtypes. The previously described immunomodulatory (IM) and mesenchymal stem-like (MSL) subtypes were demonstrated to be composed of tumors with low cellularity.[16] Variable clinical courses of TNBC were observed which could be the result of its heterogenic molecular feature. Following the sensitivity examination of the subgroups towards chemotherapy, a parallel was drawn between the subtypes and TNBC cell lines with comparable gene expression. MDA-MB-231, a commonly studied triple-negative cell line was classified into the MSL subtype.[15] Another two classification of TNBC based on gene expression profiling was described with both overlaps and differences compared to the work of Lehmann et al.[18,19] It was reported that the response to neoadjuvant chemotherapy

comprising anthracycline and taxane of TNBC patients significantly varied based on their molecular subtype that was classified by utilizing the classification of Lehmann et al.[20] The differing responses to neoadjuvant chemotherapy of the subtypes were additionally confirmed by the combined analysis of over 300 TNBC patients.[16]

Several drug candidates with different mechanism of action have been examined in clinical trials against TNBC, such as poly ADP-ribose polymerase (PARP) inhibitors, phosphoinositide 3-kinase (PI3K) inhibitors, mitogen-activated protein kinase kinase (MEK) inhibitors, anti-androgen therapies, heat shockprotein 90 inhibitors, histone deacetylase inhibitors, immune-checkpoint inhibitors and their combinations. Despite the promising results of PARP inhibitors and immune-checkpoint inhibitors, the specific treatment of TNBC remains an urgent unmet medical need.[9,11]

Cervical tumor development is featured by different factors, including the most significant human papillomavirus (HPV) infection and the required genetic and epigenetic alterations for the process.[21] The main role of the persistent high-risk HPV type infection is well-established both epidemiologically and biologically; the presence of HPV was demonstrated in 99.7% of cervical cancers. The involvement of genetic and epigenetic alterations evolves the immortalization and transformation of the epithelial cells of the host.[22] "High-risk" HPV subtypes, such as 16, 18, 31, 33 and 45 have been shown carcinogenic potential in the initiation and promotion of intraepithelial and invasive cervical tumors.[23,24] HPV 16 and 18 are definied as the most dominant considering that 70-80% of all cervical cancers are affected.[25,26] The prognostic significance of HPV-DNA prevalence and viral load regarding preinvazive cervical tumors was observed in several studies.[23,24] HeLa cell line was derived from cervical cancer and has become the first cultured and most widely utilized human cell line.[27] The presence of HPV 18 DNA in HeLa cells is well-established.[28] Although the numerous available therapeutical opportunities, the outcome of the disease has not developed significantly in the last 20 years. Additionally, the appearance of relapses (10-60%) is within the first 2-3 years after finishing the treatment period.[24]

1.2 Overview of the main processes of programmed cell death

Apoptosis or programmed cell death is characterized by specific energy-dependent biochemical and genetic pathways; moreover, a distinct morphological characteristic. It is considered critical in maintaining the balance between cell survival and cell death via initiating the elimination of unnecessary and damaged cells as a homeostatic mechanism. Apoptotic signals play an essential role in several processes, including embryonic

development, physiological cell turnover, development and normal functioning of the immune system, hormone-dependent atrophy, and chemical-induced cell death. The contribution of accelerated cell death has been demonstrated in immunodeficiency, acute and chronic degenerative diseases, and infertility. On the other hand, insufficient apoptosis can lead to cancer or autoimmune diseases. Programmed cell death normally has a defender function regarding genomic integrity, while inappropriate apoptosis can result in not only carcinogenesis, but evolving resistance of tumor cells to treatment.[29,30]

Among the huge number of gene products that were identified as a participant in the cell cycle and cell death processes, definite regulatory proteins, enzymes, and receptors were connected with key regulation segments. The remarkable significance of these regulators was determined through the direct effect of their abnormal expression or mutation on cell cycle.[31] Apoptosis is determined as highly conserved since there is no alteration in the execution of the mechanism despite the different initiating stimuli.[29,32] The initiation and execution of programmed cell death depend on the activation of a family of cysteine proteases, caspases. Considering their role in the apoptotic mechanism, initiator and effector caspases can be distinguished. Following the detection of cell damage signal, effector caspases (caspases-3, -6 and -7) are activated by initiator caspases (caspases-8 and -9). This activation leads to a cascade of molecular events, such as DNA fragmentation, degradation of cytoskeletal and nuclear proteins, crosslinking of proteins, creation of apoptotic bodies, the expression of ligands for phagocytic cell receptors and finally the uptake by phagocytic cells.[29,31]

Two main apoptotic mechanisms are distinguished, the intrinsic or mitochondrial pathway, and the extrinsic or death receptor pathway. The main linkage between the execution of mitochondrial and death receptor-mediated processes is the identical terminal pathway mediated by caspase-3.[29] The intrinsic pathway is determined by various impulses which influence multiple intracellular objectives in response to different stress conditions. Negative and positive signals can either initiate this form of apoptosis. Insufficient suppression of cell death process can be caused by negative signals, including the absence of defined growth factors, cytokines and hormones. The absence of these prosurvival factors afterward leads to the initiation of the apoptotic program. On the other hand, positive signals, such as hypoxia, toxins, hyperthermia, viral infections, radiation, irreversible genetic damage and free radicals can activate the intrinsic pathway as well.[29,31]

The mechanism is initiated by caspase-9 that binds to adapter protein apoptotic protease activating factor 1 (APAF1) through its caspase recruitment domain (CARD). Basically the CARD domain is blocked and pro-caspase-9 is unable to bind it, however,

stimulation by positive or negative signals leads to the alteration of the mitochondrial membrane that results in the opening of the mitochondrial permeability transition (MPT) pore. Subsequently the mitochondria release pro-apoptotic proteins, such as cytochrome-c, Smac/Diablo and HTrA2/Omi into the cytoplasm. Cytochrome-c binds to the WD domain of APAF1 monomers and causes certain conformational changes creating the ability to bind deoxy ATP (dATP). Following an additional conformational change in APAF1 induced by binding to dATP, its CARD and oligomerization domains are exposed leading to the formation of a complex of APAF1s called „apoptosome". The exposed CARD domains of the apoptosome activate pro-caspase-9, then caspase-9 activates the executioner pro-caspase-3 to caspase-3 that induces the full process of the apoptotic mechanism. Smac/Diablo and HTrA2/Omi support the apoptotic process by suppressing the inhibitors of apoptosis proteins (IAPs).[29,31]

The extrinsic or death receptor pathway of apoptosis is initiated by transmembrane receptor-mediated interactions. Death receptors belong to the tumor necrosis factor receptor (TNFR) superfamily. The structure of TNFRs mostly can be described as transmembrane proteins containing 2–4 similar cysteine-rich domains in the extracellular fraction. The presence of a ~70 amino acid "death domain" in the cytoplasmic fraction is another factor regarding the separation of death receptors. Six death receptors have been established as the direct or indirect regulators of the process of programmed cell death: DR3 (TNFRSF25), DR4 (TNFRSF10A), DR5 (TNFRSF10B), DR6 (TNFRSF21), TNFR1 (TNFRSF1A), and Fas/Apo1/CD95 (TNFRSF6). The possible ligands of the TNFR superfamily are mostly homotrimeric transmembrane proteins and they can play a role as soluble proteins in the extracellular space, or as plasma membrane-anchored ligands at the surface of cells or secreted exosomes.[33]

The first step of the extrinsic apoptotic process is the binding of death ligands produced by patrolling macrophages and natural killers to death receptors in the target cell membrane, which results in the activation of pro-caspase 8 to caspase 8. Binding of the death-effector domain (DED) of pro-caspase 8 to a death-inducing signal complex (DISC) located on the cytoplasmic domain of the ligand-bound death receptor leads to the recruitment of monomeric pro-caspase 8. The adaptor protein FADD and TNF receptor-associated death domain (TRADD) contained in DISC additionally promote the interaction between pro-caspase 8 and DISC, which catalyze the dimerization of pro-caspase-8 monomers. Two sub-pathways were distinguished based on the classification of the apoptotic cells into type I or II.[31,34] Type I cells are characterized by the fact, that caspase-8 initiates apoptosis via cleaving

the executioner caspases directly. When IAPs inhibit the direct activation of executioner caspases by caspase 8, unless IAPs are suppressed by proteins released from the mitochondria, cells are classified into type II.[31,35]

1.3 Matrix metalloproteases and the focal adhesion kinase in cancer

Tumor cell invasion into tissue is a crucial early step in the metastasis comprising basement membrane breach and following migration through the stroma. The occurrence of further steps of the process, such as intravasation of cancer cells into the vasculature, and extravasation of cells present in circulation into the surrounding tissue leads to the spread of malignant cells via the circulatory and lymphatic system, then subsequent development of secondary tumors. Cell migration through the extracellular matrix (ECM) is a major factor for a successful invasion. In most cases, epithelial cells go through the epithelial–mesenchymal transition process that results in reaching mesenchymal state and adoption of migratory phenotype. Tumor cells are capable of navigating around other cells and via the confines of EMC with pore ranges between 0.1 μm to 30 μm during the invasion. In order to move in the matrix, cells additionally able to secrete matrix metalloproteases (MMPs).[36]

Matrix metalloproteases are calcium-dependent endopeptidases reaching their catalytic action through zinc ion coordination by means of three amino acids. All of them are synthesized in an inactive proenzyme form that is characterized by an interaction between a zinc-containing catalytic domain and a cysteine residue. The disruption of this interaction leads to partial activation of the MMP, which enhances the autocatalysis of the propeptide region resulting in the fully active enzyme. Numerous MMPs have been identified in humans; each recognizes and cleaves specific peptide sequences. The function of MMPs is complex considering that they are involved in both normal and pathological processes, such as embryogenesis, wound healing, inflammation, arthritis and cancer.[37]

It was reported that the expression of MMPs is elevated in most of the human malignancies in comparison with normal tissue.[38] The involvement of MMPs in all stages of metastasis development was observed.[39] The presence or increased expression of MMPs, such as MMP-1, -2, -3, -7, -9, -13, -14 in primary tumors and/or metastases were associated with tumor progression based on the retrospective analysis of MMP expression in cancer patients.[40] Due to the degradation of surrounding ECM components by MMPs, a migratory pathway is created that facilitates the local invasion of cancer cells. The cleavage of fibrous ECM proteins leads to the exposure of normally hidden sites and epitopes that can redound growth. Elevated MMP activity also promotes cytokine and growth factor expression subserving

angiogenesis, tumor growth, and metastasis. MMPs are potentially involved in localisation of metastases considering that they play a role in capillary wall adhesion following circulatory transport. They affect the formation of secondary tumors via enhancing the proteolysis of ECM that facilitates cancer cell motility and settling into new tissue.[39] After learning from failed clinical trials with MMP-inhibitors, such as batimastat and marimastat, the development of anticancer agents targeting MMPs is currently ongoing.[41–43]

Focal adhesion kinase (FAK) is a cytoplasmic tyrosine kinase with multiple functions regarding cell signaling within the tumor microenvironment. It is involved in signaling pathways that facilitate cancer growth and metastasis, such as kinase-dependent control of cell motility, invasion, survival, and promotion of epithelial-mesenchymal transition by transcriptional events. Cell survival or breast tumor stem cell proliferation can be affected additionally by the kinase-independent scaffolding activity of FAK.[44] Its ability to promote cell migration is based on bridging signals between integrin and growth-factor receptors.[45] The activation of FAK involves integrin receptor clustering initiated by cell binding to ECM proteins that may result in FAK dimerization. The following steps are auto-phosphorylation at Y397, binding of SRC-family kinases to the phosphorylated site, SRC-mediated phosphorylation of the FAK kinase domain activation loop (Y576 and Y577), and activated FAK-SRC complex formation.[44] FAK kinase activity is also involved in tumor angiogenesis and vascular permeability.[46] Besides its classic role in integrin and growth factor receptor signaling as a cytoplasmic kinase, FAK was demonstrated to be present in the nucleus. Nuclear FAK can facilitate p53 degradation via ubiquitination, which results in tumor cell growth and proliferation. FAK can be involved in the regulation of GATA4 and IL-33 expression leading to reduced inflammatory responses and immune escape.[47]

The gene encoding FAK is located at human chromosome 8q24, which was found to be amplificated and often associated with increased FAK expression in human tumor cells and in tumors *in vivo*.[48] Increased FAK mRNA levels were shown in invasive breast tumor and ovarian cancer in correlation with poor patient survival by large databases. Elevated Fak mRNA levels were reported regarding several other tumor types as well.[44] FAK overexpression or overphosphorylation was described to be responsible for cell migration, survival, proliferation, and adhesion in various cancer cells.[48] The elevated expression of FAK was associated with the invasive and metastatic potential of several human cancers, including breast tumors.[49,50] It was found that the activation of FAK elevates with tumor progression based on the assessment by phosphospecific antibody recognition of the Y397 auto-

phosphorylation site.[51] FAK inhibitors have been under investigation recently in several early phase clinical trials.[52–56]

1.4 Modified estrogen derivatives in anticancer research

The substantial impact of estrogens has been shown in the development of reproductive processes; moreover, they influence the progression of hormone-dependent cancers, such as, uterine, endometrial, breast and prostate malignancies.[57–60] Despite that 17β-estradiol promotes cell proliferation, the anticancer property of structurally modified estrogen derivatives was determined in several studies.[61–71] The absence of estrogenic activity is an essential demand during the development of estrane-based antitumor drug candidates. The lack of hormonal properties can be reached via the definite alteration of the estrane skeleton, including the substitution at C-2 or C-3. [61,72,73] Another option is the modification of ring D that leads to hormonally non-active D-homo and D-seco derivatives.[74,75] Members of D-ring modified compounds were demonstrated to inhibit the enzyme aromatase CYP1A19, which causes reduced estrogen production. This mechanism of action enhances their potential beneficial effect against estrogen-dependent breast tumors.[76]

In vitro and *in vivo* experiments demonstrated, that the inversion of configuration at C-13 of estradiol leads to a low binding ability to the ER and no uterotropic action in mice.[73] The reason of the insignificant affinity for ERs is probably the conformational alteration resulting from the *cis* junction of rings C and D.[77,78] The potential increase of the antiproliferative action of 3-benzyl ether moiety on the estrane core was demonstrated in previous studies.[66,79] Triazole ring was selected based on its enhancing property regarding the solubility, bioavailability, and diversity of the structure. Considering the low affinity for ER of 13α-derivatives and the antiproliferative characteristic of previously studied triazols,[80–84] 13α-estradiol series was synthesized with the incorporation of triazole ring at C-16 and benzyloxy function at C-3 to assess their anticancer activity.

To prove the loss of hormonal activity, binding qualities of possible isomers of 16-hydroxymethyl-3,17-estradiol to ER were examined using receptor protein prepared from rabbit uteri for radioligand-binding assay. Each estradiol-based compound was displayed relative binding affinities (RBA) lower than 2.0% compared to estradiol, which indicates the annulling impact of 16-hydroxymethyl group on affinity to ER, regardless its configuration.[85] Therefore, the presence of a hydroxymethylene group at C-16 notably reduces the emergence of estrogenic properties. These preliminary results, together with the findings mentioned above regarding substitution at C-3 of the estrange core, represents the applicability of 16-

hydroxymethylene-3,17-estradiol skeleton for designing biologically active estradiol derivatives with the loss of hormonal feature. In order to integrate the structural modifications responsible for an increase in the antiproliferative and a decrease in the hormonal characteristic, 3-benzyl ethers bearing electronically different substituent at the 4'-position and containing hydroxymethyl function at C-16 were synthesized.

Besides these molecules, the synthesis of the four possible isomers of 16-hydroxymethyl-3-methoxy- and 16-hydroxymethyl-3-benzyloxy-13α-estradiol derivatives was performed based on the previous experience regarding substituting C-3, attaching a hydroxymethyl group at C-16; moreover, the inversion of configuration at C-13 of the estrane skeleton. These alterations also serve the necessity for the lack of estrogenic activity and enhancement of the potential anticancer feature of the molecules.

2. Specific Aims

The current study aimed to determine the anticancer properties of newly synthesized 16-hydroxymethyl-3-methoxy- and 16-hydroxymethyl-3-benzyloxy-13α-estradiol derivatives, 16-triazolyl-13α-estradiol and their precursor molecules, furthermore 3-benzyloxy-16-hydroxymethyl-estradiol analogs on a panel of gynecological cancer cell lines *in vitro*:

- Antiproliferative screening and the assessment of cancer-selectivity of the examined compounds by means of MTT assay. Comparing the activity of the most potent analogs on different gynecological tumor cell lines and/or against breast cancer cell lines with different receptor status.
- Investigating the antiproliferative activity of selected compounds by performing cell cycle analysis, morphological examination of the cells with Hoechst 33258 (HO) and propidium iodide (PI) staining, and determining the activity of key caspases.
- Examination of the antimetastatic ability of selected agents through their activities on cell migration and invasion. Performing gelatin zymography and Western Blot analysis to further assess the antimetastatic property of the agents. Considering the previous results of the compounds and the unmet medical need of TNBC, MDA-MB-231 TNBC cell line was chosen for the antimetastatic experiments.

3. Materials and methods

3.1 Chemicals

Novel 16-triazoles and their precursors in the 13α-estradiol series, the four possible stereoisomers of 3-benzyloxy-16-hydroxymethylene-estra-1,3,5(10)-trien-17-ol and three further analogs with a substituted benzyl function at C-3; moreover, the four possible isomers of 16- hydroxymethyl-3-methoxy- and 16-hydroxymethyl-3-benzyloxy-13α-estra-1,3,5(10)-trien-17-ols were designed and synthesized by the Department of Organic Chemistry, University of Szeged, Hungary. The structures of the examined molecules are summarized in **Figure 1-3**.

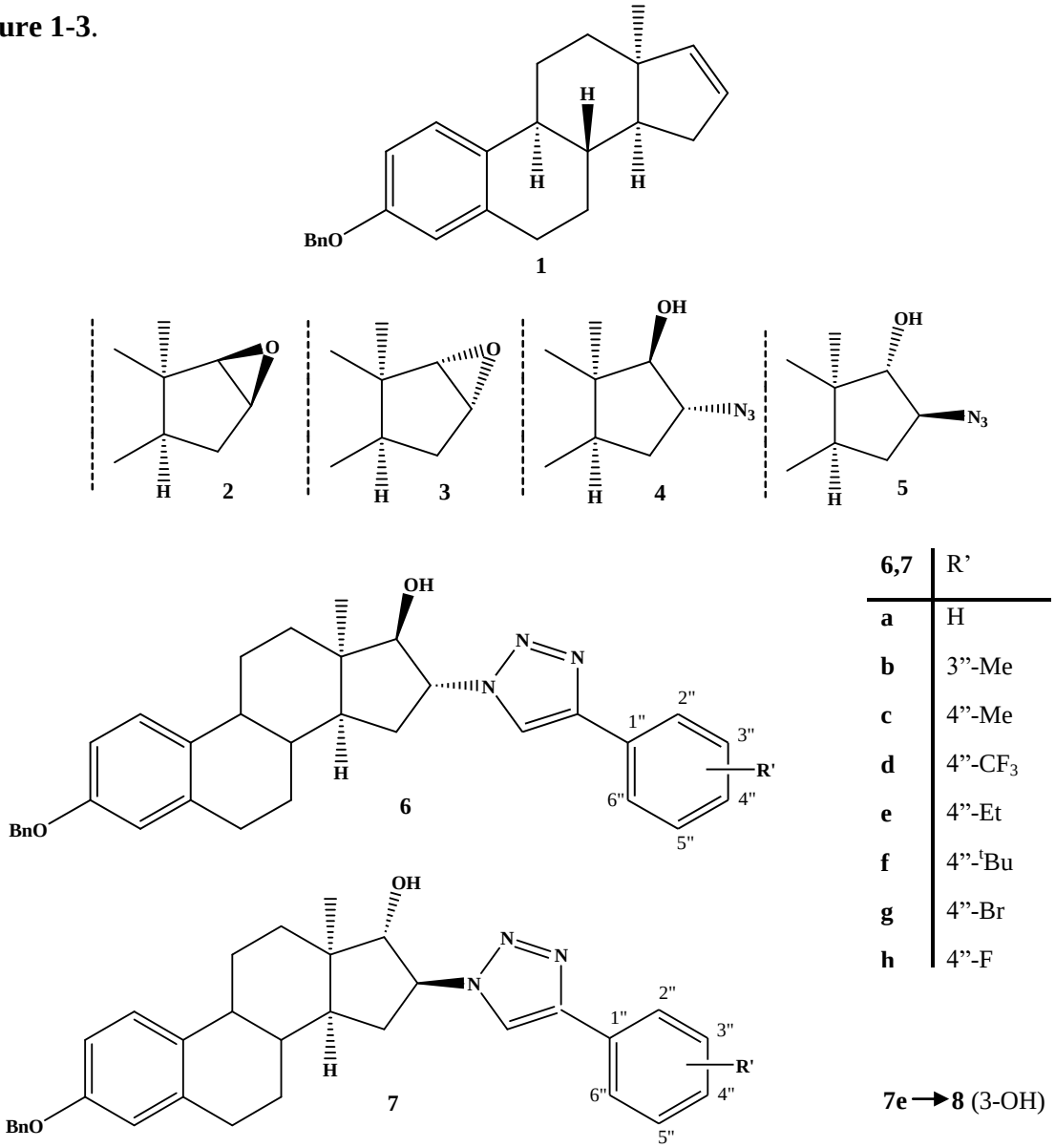

6,7	R’
a	H
b	3”-Me
c	4”-Me
d	4”-CF_3
e	4”-Et
f	4”-^{t}Bu
g	4”-Br
h	4”-F

7e → **8** (3-OH)

Figure 1. *Chemical structures of the tested compounds of the 16-triazolyl-13α-estradiol series.*

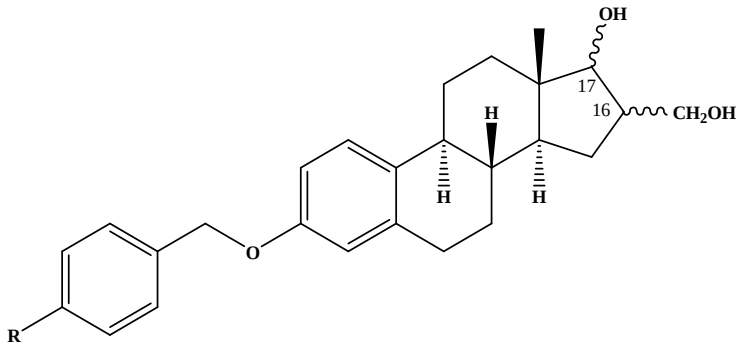

9	16β,17β
10	16α,17β
11	16β,17α
12	16α,17α
9a	16β,17β R=Cl
9b	16β,17β R=OMe
9c	16β,17β R=CN

Figure 2. *Chemical structures of the tested 3-benzyloxy-16-hydroxymethyl-estradiol analogs.*

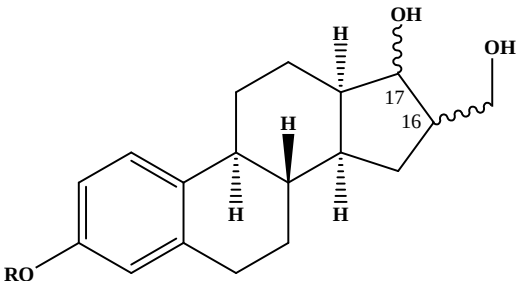

13	16α,17β R=Me
14	16β,17α R=Me
15	16α,17β R= Bn
16	16β,17α R=Bn
17	16α,17α R=Me
18	16β,17β R=Me
19	16α,17α R=Bn
20	16β,17β R=Bn

Figure 3. *Chemical structures of the tested of 16- hydroxymethyl-3-methoxy- and 16-hydroxymethyl-3-benzyloxy-13α-estradiols.*

3.2 Cell cultures

Human cancer cell lines HeLa, A2780, and A431 derived from cervical tumor, ovarian tumor, and epidermal carcinoma, respectively, breast cancer cell lines, including MCF7, T47D, MDA-MB-231, and MDA-MB-361, together with non-cancerous MRC-5 fibroblasts isolated from human fetal lung were obtained from the European Collection of Authenticated Cell Cultures (ECACC, Salisbury, UK). Minimal essential medium (MEM) supplemented with 10% fetal bovine serum, 1% non-essential amino acids and 1% antibiotic-antimycotic mixture was utilized to maintain each cell line. All the applied chemicals, if otherwise not specified were purchased from Lonza Group Ltd. (Basel, Switzerland) or Sigma-Aldrich Ltd. (Budapest, Hungary). For the storage of the cells, humidified atmosphere containing 5% CO_2 and temperature of 37 °C were provided.

3.3 Determination of antiproliferative activities

To assess the antiproliferative property of the test compounds against the above mentioned human cancer cell lines, an MTT (3-(4,5-dimethylthiazol-2-yl)-2,5-diphenyltetrazolium bromide) assay was performed. Cells were seeded into 96-well plates at a density of 5,000 cells/well (in the case of MDA-MB-361 10,000 cells/well), and after an

overnight growing period, 10 μM and 30 μM of the test compounds was added during the first screening. In case of the selected compounds, a treatment in increasing concentration (0.1–30.0 μM) was performed to determine their IC_{50} values. After incubation for 72 h under standard cell culture conditions, 5 mg/ml MTT solution was added into the plates for 4 h. As a result, formazan crystals were precipitated, and following solubilization in dimethyl sulfoxide, the measurement of absorbance was carried out at 545 nm with a microplate reader. Control samples were determined as wells containing untreated cells.[86]

According to the values of the assay, sigmoidal dose-response curves were fitted and IC_{50} values were calculated using GraphPad Prism 4.0 or 5.01 (GraphPad Software, San Diego, CA, USA). Cisplatin (Ebewe Pharma GmbH, Unterach, Austria) was used as positive control in the comparison of the growth-inhibitory effect of the tested compounds in the same concentration range. In order to characterize the selectivity of test compounds towards cancer, treatment on MRC-5 human fibroblasts was evaluated by the same method as well.

3.4 Cell cycle analysis by flow cytometry

Flow cytometry was implemented to assess the DNA content of cells. HeLa and MDA-MB-231 cells were seeded into 6-well plates at a density of 200,000 cells/well and 250,000–300,000 cells/well, respectively, and allowed to grow overnight. Following 24 h, and in case of HeLa cells 48 h incubation with test compounds, cells were washed with phosphate-buffered saline (PBS) and harvested by means of trypsin (Gibco BRL, Paisley, U.K.). Cells were centrifuged at 1,500 rpm for 10 min, additionally washed with PBS, centrifuged again, then fixed in 1 ml of –20 °C , 70% ethanol, for not less than 30 minutes. In the last step of the assay, the addition of dye solution (0.1 mg/ml PI, 0.003 μl/ml Triton-X, 0.02 mg/ml RNase A, and 1.0 mg/ml sodium citrate dissolved in distilled water) was performed into the samples for 1 h in the absence of light at room temperature. Partec CyFlow instrument (Partec GmbH, Münster, Germany) was utilized to carry out cell cycle analysis. 20,000 cells from each well were recorded in all measurements. The percentages of cells in different cell cycle phases (subG1, G1, S, and G2/M) were evaluated by ModFit LT software (Verity Software House, Topsham, ME, USA). The subG1 phase was regarded as apoptotic cell population.[87]

3.5 Hoechst 33258 – propidium iodide double staining

HeLa cells were seeded into 96-well plates (5000 cells/well) for overnight incubation. Cells were treated for 24 h with the test compound, and then final concentrations of 5 and 2

μg/ml of Hoechst 33258 (HO) and propidium iodide (PI) were added into the medium of cells, respectively. Following incubation with the dying mixture for 1 h at 37 °C in dark circumstances, cells were photographed by means of a Nikon ECLIPSE TS100 fluorescence microscope provided with the appropriate optical blocks for HO (excitation: 360/40 nm bandpass filter, emission: 460/50 nm bandpass filter and 400 nm dichromatic mirror) and PI (excitation: 500/20 nm bandpass filter, emission: 520 nm longpass filter and 515 nm dichromatic mirror) and a QCapture CCD camera. By means of the staining, intact, early-apoptotic, late-apoptotic, and necrotic cells could be identified based on the shaping of cell chromatin and damaging of cell membrane. HO permeates into all cells regardless of the state of membranes and stains the nuclei to blue. Programmed cell death was confirmed based on chromatin condensation and nuclear fragmentation of the nuclei. Red nuclei stained by PI proved the loss of cell membrane integrity, which is a marker of necrotic and late-apoptotic (secondary necrotic) cells.

3.6 Investigation of the activity of key caspases

3.6.1 Determination of in situ caspase-3 activity

The activity of caspase-3 enzyme was analyzed by using a commercially available colorimetric kit (Sigma–Aldrich, Budapest, Hungary). HeLa cells were seeded in tissue culture flasks (10^6 cells/flask), maintained under standard cell culture conditions for overnight incubation. On the basis of the antiproliferative properties of the test compound, cells were treated with two selected concentrations (3 and 10 μM) for 48 h. After this duration, scraping, counting and resuspending of cells in lysis buffer (10 ml for 10^6 cells) were performed. Samples were centrifuged, and then protein amounts of the supernatant were assessed in order to utilize equal amounts of protein content for the assay. Specific substrate (Ac-DEVD-*p*NA) of caspase-3 was incubated with the samples for 2 hours, which led to its cleavage by caspase-3. The absorbance of the released *p*-nitroaniline (*p*NA) was measured at 405 nm by means of a microplate reader. The comparison of the absorbance of the control and treated cells determines the fold increase of activity of caspase-3.

3.6.2 Determination of in situ caspase-8 activity

Colorimetric assay kit was utilized to evaluate the activity of caspase-8 (Sigma–Aldrich Ltd., Budapest, Hungary) with the addition of its specific substrate Ac-IETD-*p*NA. After incubation for 2 hours, the absorbance of the cleaved *p*NA was determined with a

microplate reader at 405 nm. The execution of the assay was identical to the above described caspase-3 assay.

3.6.3 Determination of in situ caspase-9 activity

Caspase-9 activity was assessed on the basis of the reaction with its specific substrate LEHD-*p*NA, provided by a commercially available colorimetric kit (Invitrogen, Carlsbad, CA, USA). The assay was carried out in accordance with the evaluation of the activity of caspase-3.

3.7 Wound healing assay

Wound healing assay was carried out to determine the action of selected test compounds from the series of 3-benzyloxy-16-hydroxymethyl-estradiols on cell migration, by utilizing specific wound healing assay chambers (ibidi GmbH, Martinsried, Germany). 25,000 MDA-MB-231 cells were seeded into each chamber of inserts, and then following an overnight incubation for sufficient cell attachment at 37 °C under 5% CO_2, inserts were removed. In order to remove non-adherent cells and debris a washing step with PBS was implemented. Test compounds were added in elevating concentrations to the cells in a medium containing 2% FBS for 24 h. Visualization of cell migration into the wound area was performed by a phase-contrast inverted microscope (Axiovert 40, Zeiss, Thornwood, NY, US). QCapture CCD camera was used to take images at previously designed intervals to observe wound closure. The rate of migration was calculated from the comparison of the ratio of wound closure in untreated control, and treated samples at 0 h and after 24 h of treatment.[88]

3.8 Boyden chamber assay

Examination of the invasion ability of MDA-MB-231 cells was performed by means of a BD BioCoat Matrigel Invasion Chamber (BD Biosciences, Bedford, MA, USA) provided with an 8 μm pore size PET membrane and a thin layer of matrigel basement matrix. Cells were suspended at a density of 50,000/insert in serum-free medium and placed into the top insert before the tested compounds were added in sub-antiproliferative concentrations. A medium containing 10% FBS was used as chemoattractant in the bottom well. The inserts were removed after incubation for 24 h at 37 °C under 5% CO_2 and the upper surface of the membrane was cleaned from non-invading cells with a cotton swab. After a washing step with PBS, the insert was fixed with cold 100% methanol, washed with PBS again, and stained with crystal violet solution. The invading and stained cells were counted under a phase-contrast

inverted microscope. To assess the rate of invasion, the number of treated cells and untreated controls were counted and compared to each other.

3.9 Gelatin zymography

In order to assess how the test compounds influence the activity of matrix metalloprotease-2 (MMP-2) and -9 (MMP-9), the gelatin zymography assay was performed.[89] In experimental dishes, MDA-MB-231 cells were seeded at approximately 80% confluency and maintained overnight under standard cell culture conditions. After the overnight incubation period, cells were washed with PBS, and treated with increasing concentration of test compounds in serum-free medium for 24 h. The supernatant comprising the secreted MMP-2 and MMP-9 enzymes was gathered from above the cells; afterward, it was centrifuged at 6,000 rpm at 4 °C for 2 minutes, and then collected again. Equal amounts of the samples mixed with bromophenol blue dye in 5:1 ratio were separated by SDS-PAGE containing 0.1% gelatin via electrophoresis at 120 V for 90 minutes. Major forms of MMPs were identified by Prism Ultra Protein Ladder molecular size marker (Abcam Cambridge, U.K.). After a cleaning step using 2.5% Triton X-100 solution, the reaction between the gel and a solution containing 50mM Tris-HCl (pH 7.5), 150 mM NaCl, and 5 mM $CaCl_2$ was performed. Following incubation for 24 h, the gel was stained with Coomassie brilliant blue G-250 (SimplyBlue^{TM} Safestain, Thermo Fisher Scientific, Waltham, MA, USA) for 60 minutes and washed with distilled water twice. At last, the gel was captured by a Luminescent Image Analyzer System (LAS 4000 mini, Fujifilm, Tokyo, Japan).

3.10 Western Blot assay

A Western Blot assay was carried out with the aim of assessing the influence of the tested compounds on the expression of focal adhesion kinase (FAK) and its phosphorylated form (pFAK) in MDA-MB-231 cells. In experimental dishes, approximately two million cells were seeded, and following an overnight incubation, medium containing increasing concentration of the examined compounds and 2% FBS was added into the dishes. Cells were detached from the dishes by a rubber scraper, centrifuged at 7,000 rpm, 4 °C for 2 minutes, washed with PBS, and then centrifuged again. In order to prepare whole-cell extracts (WCEs), cells were re-suspended in TEGN lysis buffer (10 mM Tris pH 7.5, 1 mM EDTA, 420 mM NaCl, 10% glycerol and 0.5% NP40) supplemented with 1 mM DTT and a cocktail of protease and phosphatase inhibitor (Roche Applied Science, Penzberg, Germany). Samples were maintained on ice for 10 minutes, centrifuged (13,000 rpm, 4 °C, 10 minutes), and then the

protein content of the supernatant was mixed with bromophenol blue dye in 2:1 ratio. Equal amounts of WCE per well were separated by SDS-PAGE via electrophoresis for 1 h at 160 V, and transferred from gels to nitrocellulose membranes for overnight at 20 V, 4 °C. After blocking of the samples, incubation with a primary antibody followed by appropriate secondary antibody was executed. The utilized antibodies were FAK pY397 (Becton Dickinson, Franklin Lakes, NJ, USA), FAK (Cell Signaling Technology, Danvers, MA, USA), β-actin (Santa Cruz Biotechnology, Santa Cruz, CA, USA), and GAPDH (Cell Signaling Technology). Visualization of the blots was performed by means of enhanced chemiluminescence (ECL-Plus, GE Healthcare Life Sciences, Little Chalfont, UK) implementing a Luminescent Image Analyzer System (LAS 4000 mini, Fujifilm, Tokyo, Japan).

3.11 Statistical analysis

GraphPad Prism 4.0 was implemented for the statistical evaluation of measured data in each experiment, with the exception of the analysis of 3-benzyloxy-16-hydroxymethyl-estradiol analogs, where the statistical evaluation was carried out by means of Graphpad Prism 5.01. One-way ANOVA with Dunnett post-test for comparison of multiple groups was carried out to assess statistical significance. A *p*-value of less than 0.05 was considered statistically significant.

4. Results

4.1 Antiproliferative activity of the tested compounds

Several examined estradiol analogs have shown significant antiproliferative property determined by MTT-assay. At first, screening of 16-triazolyl-13α-estradiol derivatives and their precursors on cell lines derived from different organs (HeLa, MCF7, A2780, and A431) (**Table 1.**) was performed. The precursor molecules (**1-5**) were proven to be modestly inhibiting cancer cell proliferation, since the most effective cell-growth inhibition after treatment with 10 μM was 39.0±1.0% (**5**). Compounds from the series of 16β,17α isomers (**7c-g**) that displayed the most potent cell-growth inhibition were selected for testing against a panel of breast cancer cell lines with different receptor status (T47D, MDA-MB-231, MDA-MB-361) (**Table 2**.). Based on the findings, 16β,17α isomers bearing *p*-alkyl substituents on the triazolyl-phenyl function showed the most significant antiproliferative potency (**7e**, **7f**). Selectivity towards cancer of the compound with the most effective IC_{50} value (**7e**) from the

series was tested by utilizing non-cancerous human fibroblast MRC-5 cell line. 22.2 ± 2.9% growth-inhibition of MRC-5 cells was assessed after treatment with 30 μM, the same concentration of the reference agent cisplatin caused a more considerable inhibition (70.7 ± 1.3%). Considering that **7e** did not influence the proliferation of MRC-5 cells significantly at 30 μM, and its calculated IC_{50} values on cancer cell lines were 2.4–6.5 μM, it can be declared as a cancer-selective agent. Based on the findings of the MTT-assay, **7e** was selected for further investigation from the 16-triazolyl-13α-estradiol series.

Regarding the 3-benzyloxy-16-hydroxymethyl-estradiol derivatives, MTT assay to determine their growth-inhibitory effects against breast cancer cell lines with distinct receptor status was carried out (T47D, MDA-MB-231, MCF-7 and MDA-MB-361) (**Table 3.**). Based on the results, the configuration of the substituent at positions 16 and 17 has a narrow influence on the antiproliferative feature of the compounds. However, certain substituents, especially the *p*-chloride group on the benzyl function at C-3 may increase the antiproliferative activity (**9a**, **9b**). Additionally, the examination of cancer-selectivity was performed against MRC-5 cells. Despite that the selectivity towards cancer could not be proved, the antiproliferative feature of test compounds was comparable to that of cisplatin. On the basis of the obtained data, the compound with the most potent IC_{50} value (**9a**) and its related, unsubstituted analog (**9**) were selected for additional examinations in order to characterize their mechanism of action.

In the set of 16- hydroxymethyl-3-methoxy- and 16-hydroxymethyl-3-benzyloxy-13α-estradiols, the 3-benzyl ethers (**15**, **16**, **19**, **20**) were demonstrated to be more potent compared to their 3-methyl ether counterparts (**13**, **14**, **17**, **18**). The calculated IC_{50} values of the mentioned 3-benzyl ethers were between 10 μM and 20 μM against breast cancer cell lines, while in the case of A2780 and HeLa cell lines, their antiproliferative activity was more notable. Compounds **20** and **15** were selected for the investigation of cancer selectivity by utilizing the MRC-5 human fibroblast cell line due to their potent antiproliferative feature against each examined cancer cell population. It was found that the proliferation of tumor cell lines was at least twice much inhibited by **20**, than that of the non-cancerous fibroblast cells. Regarding **15,** its calculated IC_{50} value against MRC-5 cells was similar to its action on breast cancer cells; nevertheless, in comparison with the results of A2780 and HeLa cells, a modest cancer selectivity could be assessed (**Table 4.**).

Table 1. *Antiproliferative properties of 16-triazolyl-13α-estradiol derivatives*

		Inhibition (%) ± SEM [calculated IC_{50} value[1] (μM)]			
Comp.	Conc. (μM)	**HeLa**	**MCF7**	**A2780**	**A431**
1	10	–[2]	–	–	–
	30	–	27.3 ± 1.6	24.6 ± 0.4	–
2	10	–	–	–	–
	30	28.9 ± 0.8	48.3 ± 1.2	36.3 ± 1.0	46.7 ± 1.1
3	10	–	–	–	–
	30	39.9 ± 1.4	48.8 ± 1.3	44.8 ± 0.6	68.8 ± 1.2
4	10	21.5 ± 0.7	36.2 ± 1.4	33.3 ±0.8	–
	30	98.3 ± 0.1	90.3 ± 0.4	96.4 ±0.2	97.7 ± 0.1
5	10	20.4 ± 0.5	34.6 ± 1.4	39.0 ±1.0	–
	30	96.0 ± 0.4	77.3 ± 1.3	96.0 ±0.4	82.3 ± 1.1
6a	10	64.7 ± 1.7	–	46.5 ±1.1	44.9 ± 0.9
	30	80.3 ± 0.4	–	50.7 ±2.0	36.1 ± 1.3
6b	10	23.9 ± 0.9	28.3 ± 1.0	38.9 ±0.2	–
	30	27.4 ± 1.0	30.0 ± 0.5	38.6 ±0.4	–
6c	10	57.3 ± 2.4	35.2 ± 2.0	46.9 ±0.8	–
	30	55.5 ± 1.0	37.6 ± 2.0	56.5 ±0.9	36.6 ± 0.4
6d	10	58.3 ± 1.0	42.9 ± 1.2	53.5 ±1.5	25.5 ± 2.6
	30	56.7 ± 1.2	43.6 ± 0.4	55.4 ±1.1	19.0 ± 4.4
6e	10	28.1 ± 1.4	30.4 ± 0.6	41.4 ±0.5	–
	30	24.1 ± 1.2	28.7 ± 2.3	40.5 ±0.3	–
6f	10	46.2 ± 2.4	36.4 ± 1.4	43.6 ±0.7	38.7 ± 0.4
	30	52.0 ± 2.4	39.6 ± 2.1	51.0 ±1.4	37.0 ± 1.1
6g	10	61.2 ± 2.7	22.9 ± 1.5	38.8 ± 0.98	18.5 ± 2.8
	30	65.1 ± 2.0 [2.0]	27.9 ± 1.0	39.8 ± 1.2	33.7 ± 2.1
6h	10	55.5 ± 1.0	22.3 ± 2.0	40.2 ± 2.2	13.1 ± 0.5
	30	62.8 ± 2.2	23.4 ± 0.8	36.8 ± 1.4	26.2 ± 2.8
7a	10	45.7 ± 2.7	–	33.3 ±1.6	–
	30	84.9 ± 0.5	74.7 ± 0.7	81.7 ±0.8	53.4 ± 0.4
7b	10	58.4 ± 0.1	41.5 ± 1.9	56.4 ±0.6	–
	30	79.3 ± 0.4	66.8 ± 1.5	82.9 ±1.0	–
7c	10	72.0 ± 2.0	82.0 ± 0.9	80.9 ±2.3	49.3 ± 1.3
	30	88.3 ± 1.3 [7.6]	93.6 ± 0.3 [6.0]	88.8 ±1.5 [6.0]	64.8 ± 2.4 [10.2]
7d	10	75.8 ± 1.0	67.7 ± 2.6	69.5 ±2.6	44.9 ± 0.5
	30	89.2 ± 0.9 [8.8]	94.3 ± 0.2 [9.3]	90.7 ±1.8 [7.5]	46.8 ± 1.1
7e	10	93.5 ± 0.2	83.3 ± 2.1	92.7 ±0.2	87.5 ± 0.7
	30	97.3 ± 0.1 [2.6]	89.5 ± 1.1 [2.4]	96.9 ±0.1 [2.6]	92.3 ± 0.6 [2.9]
7f	10	76.0 ± 0.8	73.5 ± 0.9	88.4 ±0.9	68.6 ± 0.6
	30	89.6 ± 0.5 [3.4]	84.8 ± 0.5 [2.9]	95.0 ±0.3 [2.9]	76.6 ± 0.3 [3.2]
7g	10	60.5 ± 1.1	35.1 ± 2.6	47.8 ± 1.0	31.2 ± 1.2
	30	86.3 ± 0.9 [8.5]	73.5 ± 1.2	58.5 ± 2.1	42.6 ± 1.4

		Inhibition (%) ± SEM [calculated IC_{50} value[1] (μM)]			
Comp.	Conc. (μM)	**HeLa**	**MCF7**	**A2780**	**A431**
7h	10	31.6 ± 2.4	18.4 ± 2.4	16.7 ± 2.4	4.3 ±1.4
	30	49.6 ± 0.4	34.2 ± 2.3	38.1 ± 1.7	12.8 ± 2.8
8	10	24.3 ± 1.6	8.8 ± 1.0	9.9 ± 0.9	4.6 ± 1.1
	30	24.5 ± 1.9	57.9 ± 0.9	39.0 ± 1.0	30.0 ± 1.3
Cisplatin	10	42.6 ± 2.3	53.0 ± 2.3	83.6 ± 1.2	88.6 ± 0.5
	30	99.9 ± 0.3	86.9 ± 1.3	95.0 ± 0.3	90.2 ± 1.8
		[12.4]	[9.6]	[1.3]	[2.8]

[1] Mean value from two independent experiments with five parallel wells; standard deviation <15%.

[2] Inhibition values <20% are not presented.

Table 2. *Antiproliferative properties of **7c–g**.*

		Inhibition (%) ± SEM [calculated IC_{50} value[3] (μM)]		
Comp.	Conc. (μM)	**T47D**	**MDA-MB-231**	**MDA-MB-361**
7c	10	85.9 ± 1.1	84.5 ± 1.01	83.6 ±_ 0.6
	30	92.0 ± 0.4	94.5 ± 0.5	89.2 ± 0.5
		[5.9]	[6.5]	[5.3]
7d	10	58.4 ± 0.9	41.8 ± 2.5	57.2 ± 1.8
	30	90.9 ± 0.5	82.2 ± 0.7	74.1 ± 1.2
		[9.7]	[10.3]	[9.7]
7e	10	85.6 ± 0.6	85.3 ± 1.8	74.1 ± 0.9
	30	92.0 ± 0.4	92.4 ± 0.9	83.6 ± 1.6
		[5.9]	[6.5]	[5.4]
7f	10	65.4 ± 0.8	57.0 ± 1.3	61.4 ± 0.3
	30	87.7 ± 0.6	84.5 ± 0.7	74.3 ± 1.2
		[6.2]	[8.3]	[6.6]
7g	10	56.5 ± 1.0	48.5 ± 1.5	56.0 ± 2.0
	30	81.1 ± 1.4	76.9 ± 1.9	73.7 ± 1.3
		[9.0]	[10.3]	[8.8]
Cisplatin	10	51.0 ± 2.0	20.08 ± 0.8	67.5 ± 1.0
	30	57.9 ± 1.4	71.7 ± 1.2	87.7 ± 1.1
		[9.8]	[19.1]	[3.7]

[3] Mean value from two independent determinations with five parallel wells; standard deviation <15%.

Table 3. *Antiproliferative properties of 3-benzyloxy-16-hydroxymethyl-estradiol derivatives*

Comp.	Conc. (μM)	Inhibition (%) ± SEM [calculated IC_{50} value[4] (μM)]				
		MDA-MB-231	**MCF7**	**T47D**	**MDA-MB-361**	**MRC-5**
9	10	31.5 ± 1.8	60.2 ± 1.6	54.5 ± 0.3	93.1 ± 0.5	78.0 ± 2.6
	30	94.9 ± 0.5	97.2 ± 0.4	90.0 ± 0.4	93.3 ± 1.1	96.5 ± 0.2
		[12.7]	[8.2]	[8.4]	[4.6]	[6.7]
10	10	93.8 ± 0.5	91.5 ± 0.6	82.7 ± 1.6	93.8 ± 0.7	94.8 ± 0.5
	30	96.2 ± 0.3	97.8 ± 0.2	82.1 ± 0.5	94.0± 0.3	96.9 ± 0.2
		[3.9]	[5.1]	[4.6]	[3.8]	[5.5]
11	10	76.4 ± 0.7	27.0 ± 1.3	38.8 ± 2.0	62.7 ± 2.2	39.1 ± 3.2
	30	92.2 ± 0.6	88.6 ± 1.2	90.3 ± 0.6	86.2 ± 0.9	92.6 ± 0.2
		[5.9]	[13.6]	[15.7]	[7.2]	[10.2]
12	10	84.3 ± 1.2	56.6 ± 2.2	47.5 ± 2.4	79.1 ± 2.7	53.7 ± 3.4
	30	92.8 ± 0.3	86.9 ± 0.9	94.6 ± 0.7	89.9 ± 1.0	76.8 ± 2.2
		[5.5]	[9.1]	[10.4]	[5.4]	[7.3]
9a	10	89.5 ± 0.8	96.5 ± 0.7	95.6 ± 0.3	81.1 ± 1.8	76.5 ± 2.3
	30	87.7 ± 0.3	96.7 ± 0.2	95.3 ± 0.9	87.0 ± 1.3	79.8 ± 1.0
		[4.6]	[3.5]	[2.8]	[1.3]	[6.7]
9b	10	61.1 ± 2.4	72.7 ± 0.8	80.2 ± 2.1	76.8 ± 1.2	61.0 ± 2.8
	30	82.8 ± 0.9	89.1 ± 0.9	87.0 ± 1.5	81.1 ± 1.7	78.1 ± 1.8
		[7.5]	[4.2]	[3.0]	[4.7]	[1.5]
9c	10	30.9 ± 2.4	39.3 ± 0.7	34.7 ± 1.4		
	30	68.8 ± 1.7	57.7 ± 0.8	52.7 ± 3.1	-[5]	-
		-	-	-		
Cisplatin	10	20.8 ± 0.8	53.0 ± 2.3	51.0 ± 2.0	67.5 ± 1.0	60.3 ± 3.3
	30	74.5 ± 1.2	87.0 ± 1.2	58.0 ± 1.5	87.8 ± 1.1	61.9 ± 1.0
		[19.1]	[5.8]	[9.8]	[3.7]	[6.2]

[4] IC_{50} values were calculated from two experiments with 5 parallel wells if the growth inhibition of the compound was >75% at 30 μM.

[5] Not determined.

Table 4. *Antiproliferative properties of 16-hydroxymethyl-3-methoxy- and 16-hydroxymethyl-3-benzyloxy-13α-estradiol derivatives*

		Inhibition (%) ± SEM [calculated IC_{50} value[6] μM]					
Comp.	Conc. (μM)	**MDA-MB-231**	**MCF7**	**T47D**	**MDA-MB-361**	**HeLa**	**A2780**
13	10	<10	<10	20.2 ± 1.7	22.9 ± 2.6	17.4 ± 2.0	23.6 ± 1.3
	30	32.1 ± 2.5	21.6 ± 2.3	36.7 ± 0.8	31.2 ± 2.9	58.6 ± 1.7	54.4 ± 2.0
		-[7]	-	-	-	[24.7]	[23.2]
14	10	10.1 ± 1.7	11.9 ± 2.1	31.7 ± 1.2	<10	55.4 ± 2.1	38.7 ± 0.7
	30	40.4 ± 1.2	43.2 ± 1.6	57.0 ± 1.8	26.0 ± 1.3	66.0 ± 0.9	71.4 ± 0.6
		-	-	[22.5]	-	[8.4]	[13.3]
15	10	18.2 ± 2.7	40.4 ± 1.7	46.3 ± 1.3	11.1 ± 1.9	50.9 ± 2.4	50.8 ± 0.8
	30	89.0 ± 1.5	96.7 ± 0.2	93.7 ± 0.3	96.5 ± 0.5	97.5 ± 0.1	94.9 ± 0.7
		[17.4]	[10.7]	[10.6]	[17.4]	[8.8]	[9.3]
16	10	20.6 ± 0.9	26.4 ± 1.6	29.7 ± 0.7	15.7 ± 2.9	76.7 ± 0.7	51.9 ± 1.4
	30	94.2 ± 0.6	93.6 ± 0.7	46.8 ± 1.4	75.2 ± 1.1	89.6 ± 0.5	75.3 ± 0.7
		[16.0]	[14.6]	-	[13.5]	[3.4]	[7.7]
17	10	27.1 ± 3.0	15.0 ± 2.2	28.0 ± 2.0	17.1 ± 1.3	56.5 ± 1.4	47.9 ± 1.9
	30	42.8 ± 2.1	31.3 ± 1.4	44.3 ± 2.1	39.3 ± 2.5	56.4 ± 1.5	63.7 ± 1.3
		-	-	-	-	[4.8]	[10.7]
18	10	<10	<10	16.7 ± 1.4	<10	47.5 ± 1.1	36.1 ± 0.9
	30	30.1 ± 1.0	26.8 ± 1.8	38.0 ± 0.7	17.8 ± 1.7	58.4 ± 1.5	55.2 ± 2.3
		-	-	-	-	[11.0]	[16.2]
19	10	22.3 ± 2.2	27.1 ± 2.0	44.3 ± 1.0	20.3 ± 2.8	55.3 ± 2.4	54.9 ± 1.9
	30	94.4 ± 0.7	95.4 ± 0.2	94.1 ± 0.9	88.1 ± 0.9	96.8 ± 0.5	93.7 ± 0.5
		[11.6]	[14.6]	[11.2]	[12.3]	[7.0]	[8.7]
20	10	24.4 ± 2.9	37.3 ± 1.5	44.3 ± 1.2	15.2 ± 2.3	70.5 ± 1.3	54.6 ± 1.3
	30	88.3 ± 1.4	97.4 ± 0.3	93.5 ± 0.5	93.7 ± 0.3	98.1 ± 0.2	94.5 ± 0.8
		[11.5]	[12.0]	[10.3]	[13.2]	[4.9]	[7.9]

		MRC-5			
20	10	<10	**15**	10	<10
	30	84.7 ± 0.1		30	86.9 ± 0.6
		[26.0]			[15.7]

[6] IC_{50} values were calculated from two experiments with 5 parallel wells if the growth inhibition of the compound at 30 μM was> 75%.

[7] Not determined.

4.2 Cell cycle analysis by flow cytometry

Flow cytometry was performed to specify the activity of the selected compounds on the cell cycle phase distributions. The utilized concentrations were selected based on the calculated IC_{50} value of the compounds. The analysis of **7e** was carried out after 24 and 48h incubation against HeLa cervical cancer cell line.

The reduction of cell population in the G1 phase along with the increase in the S and G2/M phase was found to be significant after treatment with 10 μM for 24 h. This result may indicate a blockage in the G2/M phase. A similar alteration of the cell cycle was assessed after 48 h; however, the hypodiploid subG1 population was significantly elevated, which shows the proapoptotic potency of the tested compound (**Fig. 4.**).

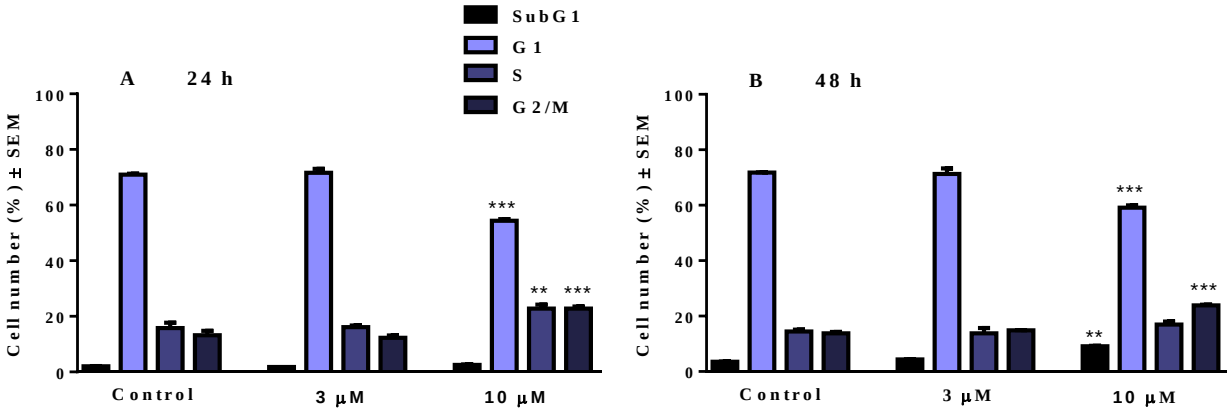

Figure 4. *Compound **7e** causes disturbance in the cell cycle distribution of HeLa cells after incubation for 24 or 48 h. Results are mean values ± SEM from two measurements. ** and *** indicate p <0.01 and p <0.001, respectively, as compared with the control cells.*

Compound **9** and **9a** induced a significant elevation of the cell population in G1 phase, with concomitant decrease in the G2/M phase. A remarkable effect on the cell cycle was observed by **9** even at 5 μM in spite of its relatively high IC_{50} value. The proapoptotic property of both compounds was demonstrated based on the significant but modest increase in the subG1 population, which was induced in all tested concentrations (**Fig. 5.**).

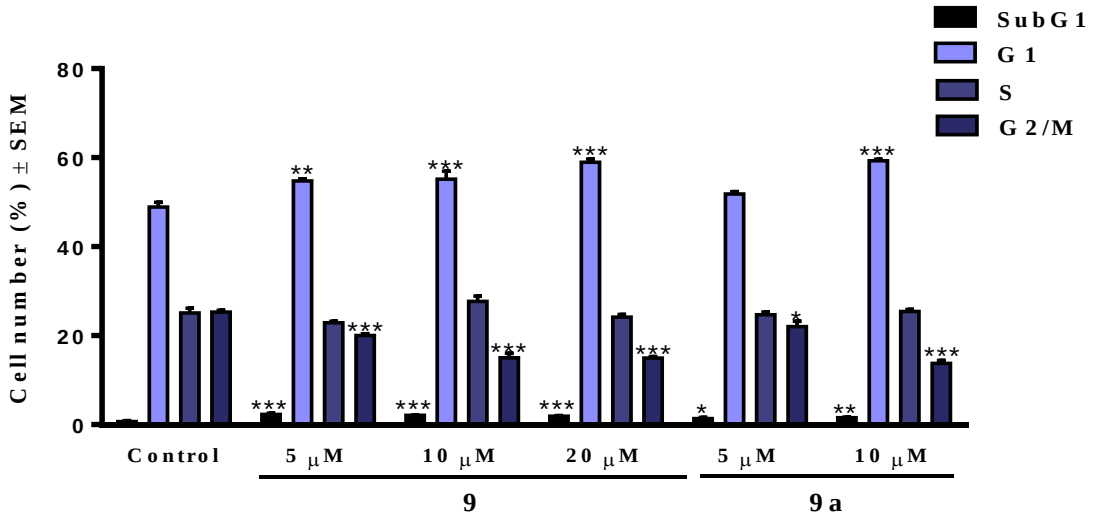

Figure 5. *Effects of compounds **9** and **9a** on the MDA-MB-231 cell cycle after incubation for 24 h. Results are mean values ± SEM from three measurements. *, ** and *** indicates p <0.05, p <0.01 and p <0.001 as compared with the control cells, respectively.*

4.3 Hoechst 33258 – propidium iodide double staining

Nuclear morphology and membrane integrity of the investigated cells were utilized as indicators of the presence of apoptosis or necrosis. Treatment of Hela cells was performed with **7e** for 24 or 48 h incubation period. Photographs were separated by the means of appropriate optical blocks for HO and PI. Chromatin condensation and nuclear fragmentation of nuclei were used as indicators for apoptosis, while the loss of membrane integrity proved necrosis (**Fig. 7.**).

Based on the quantitative results, exposure to 10 μM leads to the significant elevation of the ratio of early apoptotic and secondary necrotic cells after 24 h incubation. Treatment with the same concentration for 48 h resulted in a similar but more substantial alteration in the ratio of the cell populations (**Fig. 6.**).

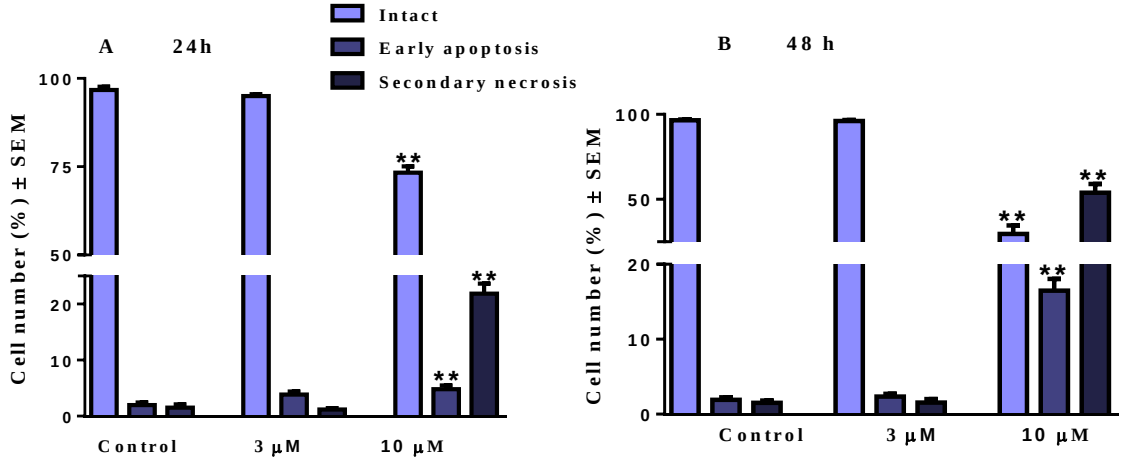

Figure 6. *Compound **7e** elicits apoptosis and necrosis in HeLa cells after incubation for 24 or 48 h. ** indicates p < 0.01 as compared with the control conditions.*

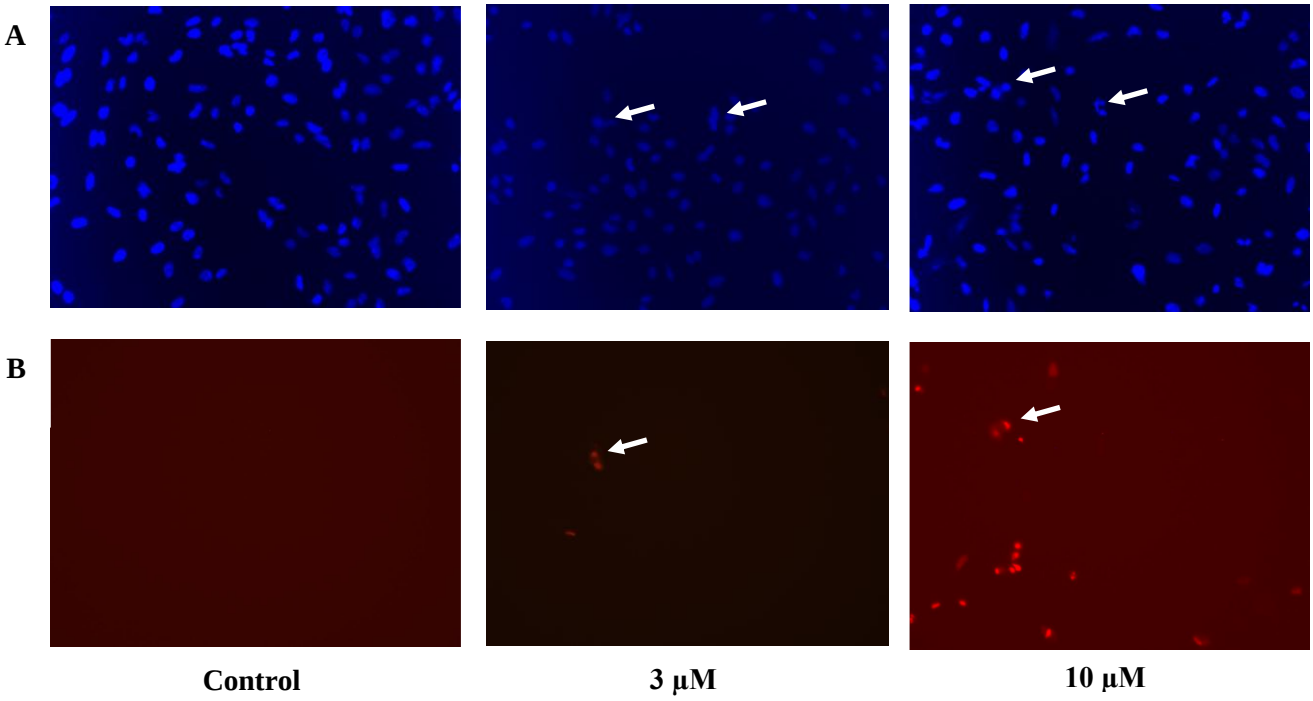

Figure 7. *Representative photographs utilized for the investigation of the effects of compound **7e** on HeLa cells after treatment with 3 µM and 10 µM for24 h. **A**: The cell population was stained by HO. **B**: The cell population was stained by PI. Chromatin condensation and nuclear fragmentation are indicated by white arrows on photographs stained by HO or PI.*

4.4 Determination of in situ caspase-3, caspase-8 and caspase-9 activity

The investigation of the activity of caspase-3 supported the proapoptotic potency of **7e.** HeLa cells were treated with 3 µM and 10 µM of **7e** for 48 h, which resulted in a significant concentration-dependent increase of caspase-3 activity. To determine the involvement of the mitochondrial pathway in the apoptotic process, the activity of caspase-9 was examined under the same conditions.

The significant increase in the concentration of caspase-9 indicates that mitochondrial damage may play a role in the mechanism of action of **7e.** The possible function of the death receptor pathway in the apoptotic property of **7e** was assessed as well via the determination of caspase-8 activity. Since there was no change in the activity of caspase-8, the extrinsic pathway may not be involved in the programmed cell death process induced by **7e** (**Fig. 8.**).

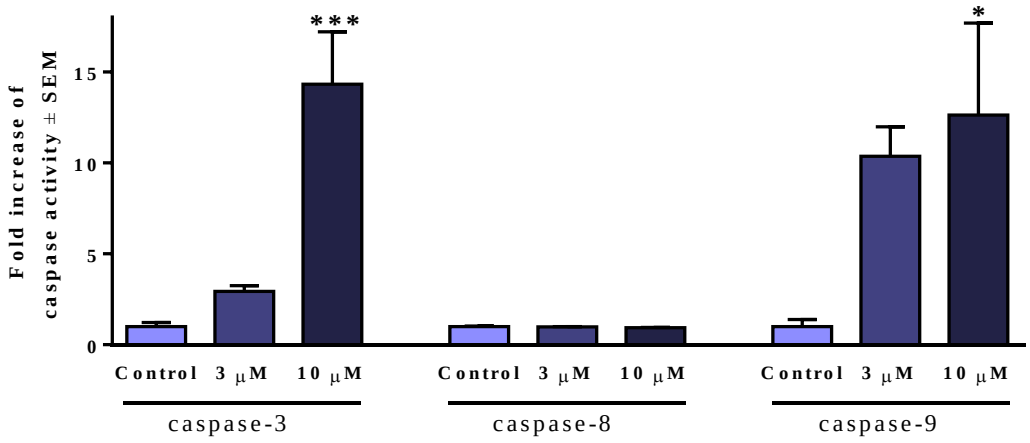

Figure 8. *Compound **7e** induces caspase-3 and caspase-9 but not caspase-8 activities after incubation for 48 h. The activities of the untreated cells were taken as one unit. * and *** indicate $p < 0.05$ and $p < 0.001$, respectively, as compared with the control cells.*

4.5 Wound healing assay

Inhibition of cell motility is another substantial segment of the anticancer activity of a potential drug candidate. Wound healing assay was utilized to assess the migration ability of MDA-MB-231 cells after treatment for 24 h with elevating concentrations of **9** and **9a**. Movement of untreated MDA-MB-231 cells within the wound of the chambers was considered as 100% in the statistics. A significant, concentration-dependent decrease was observed in the migration ability of MDA-MB-231 cells. It is considerable that sub-antiproliferative concentrations caused reduced cell migration as well (**Fig. 9-10.**).

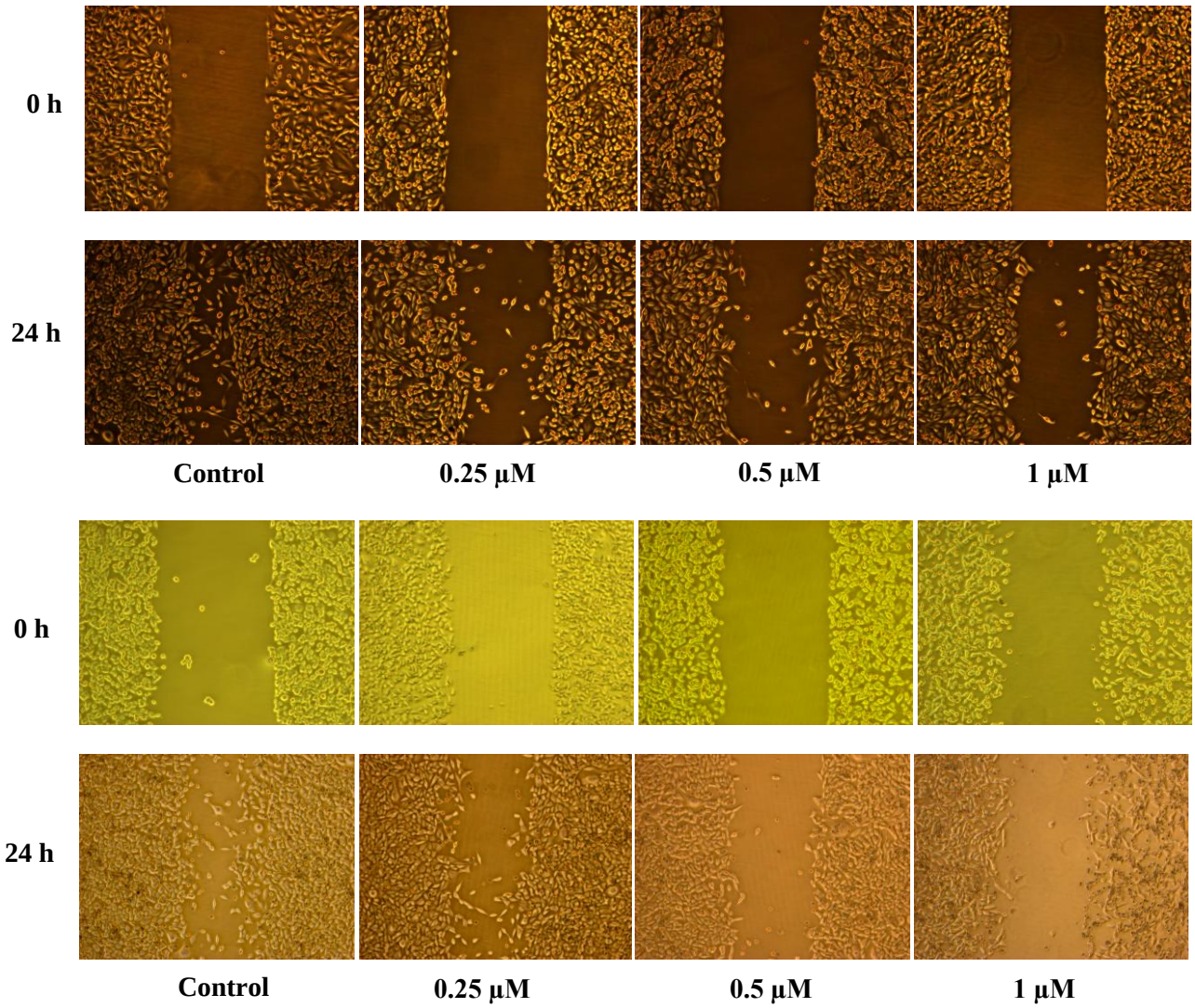

Figure 9. *Representative images of the migrating MDA-MB-231 cells in 0 hour and after 24 h treatment with* ***9*** *(upper panels) and* ***9a*** *(lower panels).*

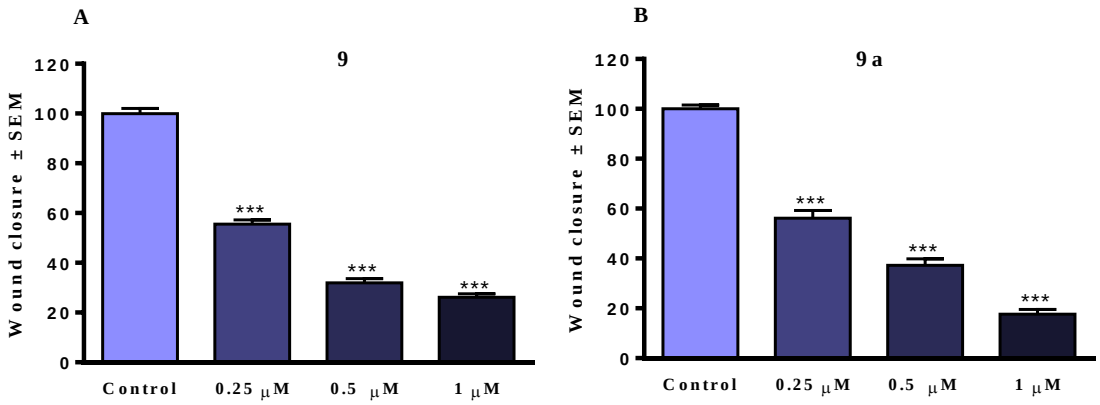

Figure 10. *Effect of* ***9 (A)*** *and* ***9a (B)*** *on the migration ability of MDA-MB-231 cells. The rates of the migration were evaluated after incubation for 24 h. Results are mean values ± SEM from three measurements.* *** *indicates* $p < 0.001$ *as compared with the untreated control samples .*

4.6 Boyden chamber assay

As another important aspect of the antimetastatic property, the influence of the tested compounds on the invasion ability of MDA-MB-231 cells was investigated by the means of Boyden chambers containing Matrigel Matrix-coated membrane (8.0 μm pore diameter). Invasive cells are capable of migrating through the membrane, while the crossing of non-invasive cells is blocked. After treatment with elevating concentrations for 24 h, the invasion of the examined cells was blocked by **9** and **9a** in a concentration-dependent manner (**Fig. 11-12.**).

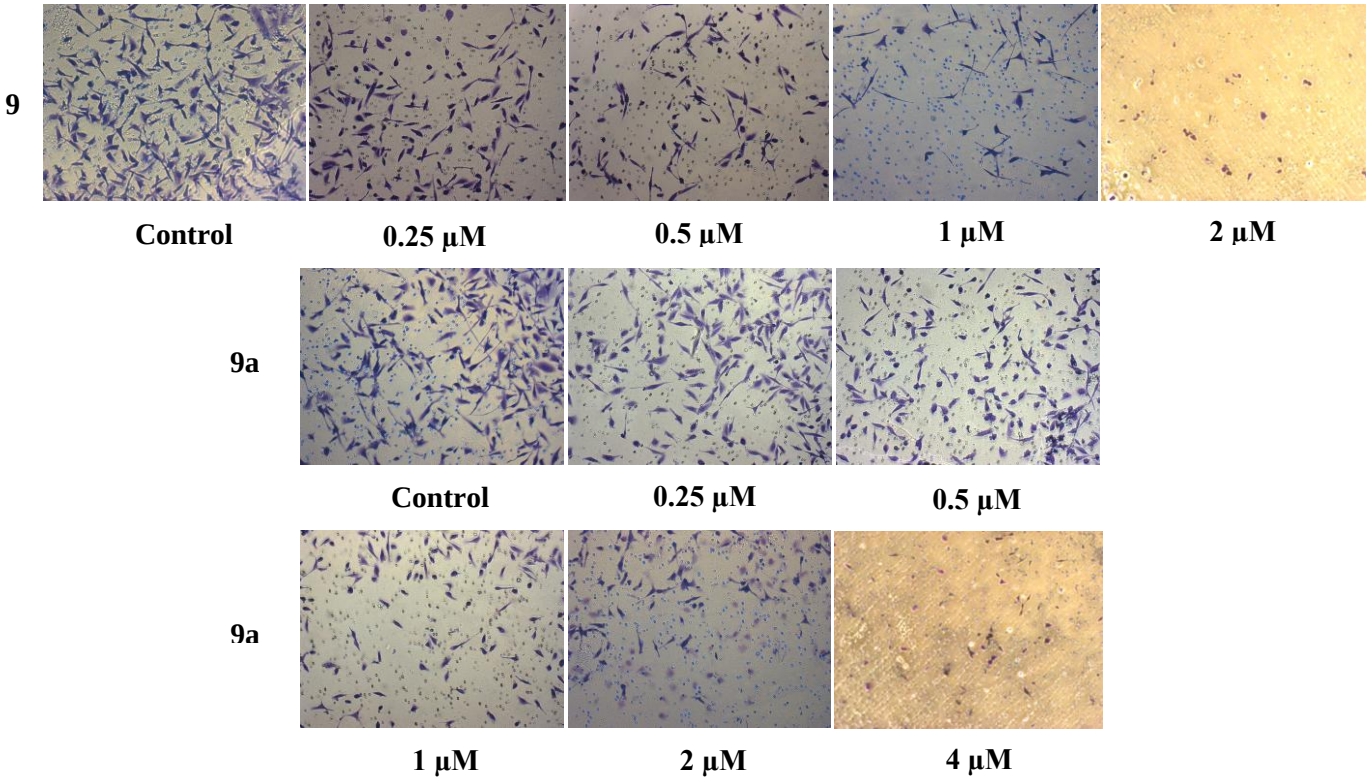

Figure 11. *Images from a visual field of one representative experiment that show the influence of compound **9** and **9a** on the invasion of MDA-MB-231 cells after 24 h treatment with increasing concentrations.*

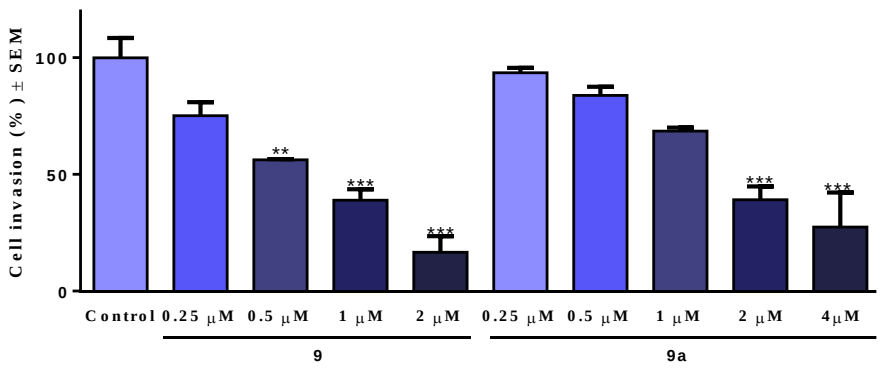

Figure 12. *Effects of compounds **9** and **9a** on the cell-invasion capacity of MDA-MB-231 cells. Statistical analyses of the percentage of invasive cells after incubation for 24 h with the test compounds. Results are mean values ± SEM from three measurements. ** and *** indicates $p<0.01$ and $p<0.001$ as compared with the untreated control samples, respectively.*

4.7 Gelatin zymography

To characterize the mechanism of the antimetastatic feature of **9** and **9a**, the activities of MMP-2 and MMP-9 released by MDA-MB-231 cells were assessed by a gelatin zymography assay. The base of the method that the active enzymes damage the gelatin and create a light patch on the blue staining. As a result, no significant inhibition was observed by the examined compounds on the activity of the enzymes even in 2 μM (**9a**) and 4 μM (**9**) concentrations indicating that MMP-2 and MMP-9 may not be involved in the antimetastatic property of **9** and **9a**. (**Fig. 13.**)

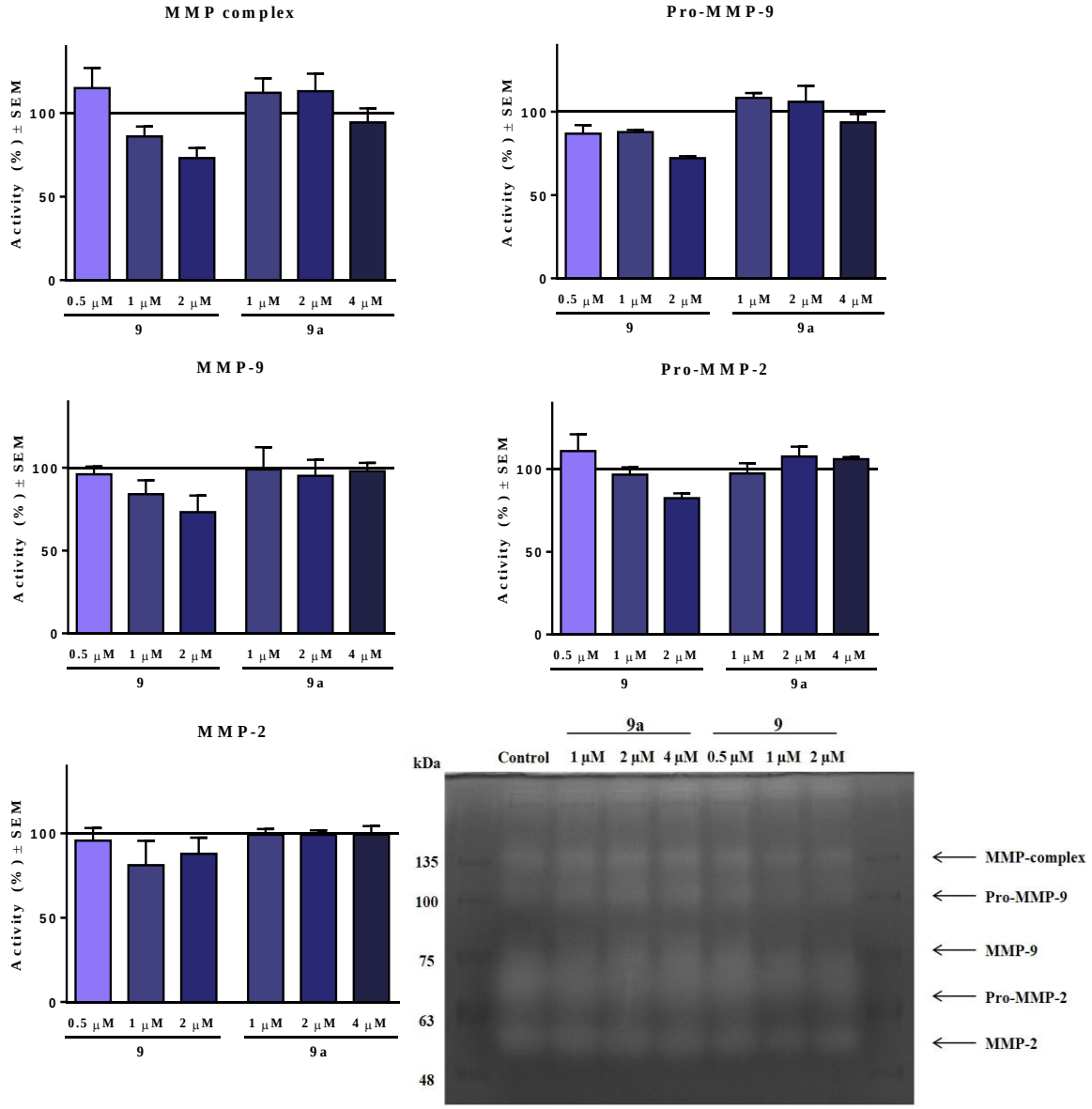

Figure 13. *Effects of compounds **9** and **9a** on the activities of MMP-9 (pro-MMP-9, MMP-9 and its complex form) and MMP-2 (pro-MMP-2, MMP-2). Results are mean values ± SEM from three measurements. The activities presented in graphs are expressed as the % of vehicle control group. None of the treatment-related differences are significant. A representative zymogram (right bottom panel).*

4.8 Western Blot assay

Since FAK and its phosphorylated form (pFAK) are possible targets for metastasis inhibition, the influence of the tested compounds on the expression of FAK and pFAK proteins was investigated. A significant concentration-dependent decrease was observed in the level of pFAK regarding both **9** (0.5–2 μM) and **9a** (1–4 μM), while the total amount of FAK was not altered. These findings demonstrate that **9** and **9a** inhibited the phosphorylation of FAK protein. (**Fig.14.**)

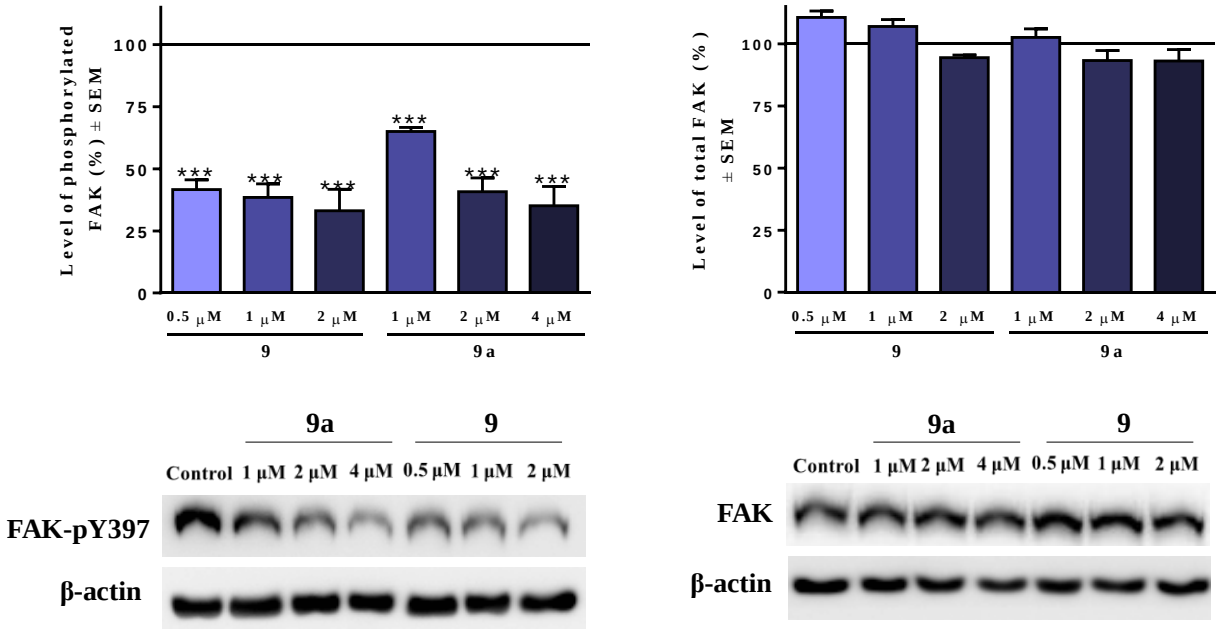

Figure 14. *Effects of compounds **9** and **9a** on the expression of phosphorylated and total FAK protein in MDA-MB-231 cells (upper panels). Results are mean values ± SEM from three measurements. *** indicates $p<0.001$ as compared with the untreated control samples. Representative results of the Western blot analysis (lower panels).*

5. Discussion

The first reported estrogen analog possessing considerable antiproliferative property with the lack of the binding ability to the ER was 2-methoxyestradiol (2-ME), an endogenous metabolite of 17β-estradiol.[90] The pharmacology of 2-ME has been extensively investigated in several studies proving its antiproliferative, pro-apoptotic, antiangiogenic, antitubulin and antimetastatic effects.[90–101] The mechanism of action of 2-ME comprises several actions, including the inhibition of microtubule disruption and neoangiogenesis; furthermore, upregulation of the extrinsic and intrinsic apoptotic pathways. 2-ME has exerted growth-inhibition on numerous human cancer cell lines, notably against breast tumor (MCF7, MDA-

MB-231, MDA-MB-435, ZR-75, T47D), lung cancer (A549, H460, HOP64), ovarian cancer (OVCAR-3), prostate cancer (LNCaP, DU-145), cervical malignancy (HeLa, HeLaS3), pancreatic cancer (PaTu8902, PaTu8988s, PaTu8988t), stomach tumor (SC-MI, NUGC-3), and several others.[102] Breast cancer was reported to be the most sensitive for 2-ME considering its concentration-dependent antiproliferative effect against both ER negative (MDA-MB-231 and MDA-MB-435) and ER-positive (MCF7 and T47D) cells.[102,103]

Inducing blockade and arresting the cell cycle in the G2/M phase by inhibiting tubulin polymerisation through binding to colchicine binding site of the tubulin is one of the most important segments of the antiproliferative property of 2-ME.[95,104,105] Marked early up-regulation of cyclin B1 and Cdc2 proteins together with rapid nuclear accumulation of these two proteins; moreover, the development of nuclear chromosomal condensation and segregation were described in both ER-positive and negative breast cancer cells following exposure to 2-ME, which indicate a mitotic arrest in prometaphase. A close correlation was found between the time-dependent alterations in 2-ME-induced prometaphase arrest and the level of the G2/M population. These results suggest that besides the potent antitubulin activity of 2-ME, this effect is independent of the presence of estrogen receptors.[106] This coincides with the fact, that the relative affinity of 2-ME for ER is very low.[90] The protection against ovariectomy-induced bone loss of 2-ME is not suppressed by competitive inhibitors of ER, supporting that the activity of the compound is not influenced by ER.[107] In clinical trials, 2-ME was well-tolerated both as monotherapy and in combination with other anticancer agents; however, the exhibited activity was modest even in a NanoCrystal Dispersion (NCD) formulation due to its not sufficient bioavailability.[108–110]

As a result of the extensive experiments on the anticancer activity, selectivity, and toxicity of 2-ME with promising findings, drug candidates with estrone skeleton became a new focus of the research and development of agents for the treatment of malignant diseases, such as 2-substituted 17β-hydroxy/17-methylene estratrienes, 16-modified 2-ME analogs, 2-alkoxy and 2-benzyloxy analogues of estradiol, and antitumor pharmacophores combined with 2-ME.[111–114] The structure of 2-ME was utilized for designing quinazolinone-based anticancer agents that were proven to be potent microtubule disruptors with promising *in vivo* findings.[115]

It was described that natural 17β-estradiol is able to bind DNA directly not only through the estrogen response element (ERE), but influencing random DNA sequences. By forming aromatic interactions with the base pairs 17β-estradiol intercalates between them.[116] These results may be related to the hormonal receptor-independent activity of the estrogen-

based molecules with possible antitumor activity, comprising the examined compounds of the present thesis.

The criteria of binding to ER are known and well-founded, thus the structural modifications to develop molecules with low receptor binding affinities (RBA) are stated as well. A methyl substituent at C-3 is enough by itself to lose estrogenic property[72], inversion of configuration at C-13 of estradiol leads to a low binding ability to the ER and no uterotropic action in mice [73]; furthermore, hydrophilic functional groups attached to ring D also results in molecules with low RBA.

Our present analogs can be selected into three groups based on their structural modifications. The set of 16-triazolyl-13α-estradiol analogs and their precursors were designed by inverting the configuration at C-13 and with a benzyloxy function at C-3, the 3-benzyloxy-16-hydroxymethyl-estradiol derivatives were synthesized with a benzyloxy substituent at C-3, and a hydrophilic function at C-16. The four possible isomers of 16-hydroxymethyl-3-methoxy- and 16-hydroxymethyl-3-benzyloxy-13α-estradiols also contain inverted configuration at C-13; moreover, a hydrophilic group at C-16, and a methoxy or benzyloxy substituent at C-3. Considering these alterations in the estrane skeleton, the loss of estrogenic activity can be expected. The lacking hormonal property of 16-hydroxymethyl-3,17-estradiol analogs was demonstrated through radioligand-binding assays.[85] Our research group reported the antiproliferative activity of compounds with the previously described modifications of the estrange skeleton in several studies.[66,79,83,84] Based on these results, we have continued the investigation of the antitumor activity of A- and D-ring modified estradiol analogs against numerous gynecological cancer cell lines.

In the set of 16-triazolyl-13α-estradiols and their precursors, the latter molecules (**1-5**) merely exerted a modest cell-growth inhibition considering that at 10 μM the maximum inhibition of the cell proliferation was 39.0±1.0% (**5**). On the other hand, compounds containing triazolyl function displayed more robust antiproliferative activity (**6-7**). The influence of the configuration of substituents at C-16 and C-17 was notable, 16β,17α (**7**) isomers generally showed more potent activity in comparison with their 16α,17β counterparts, with the exception of halogenated analogs (**6g**, **6h**)**.** The important role of benzyloxy function at C-3 was demonstrated, since compound **8** with a hydroxyl group at C-3 did not show any significant antiproliferative property. The most active molecules were additionally investigated against a panel of breast cancer cell lines differing in receptorial status (MDA-MB-231 triple-negative cells, MDA-MB-361 cells expressing ER and HER2, and T47D cells bearing ER, PR, and AR). Only a modest difference between the activities of the molecules

was observed regarding the various cell lines. Compounds containing *p*-alkyl function, especially ethyl and *tert*-butyl on the triazolyl-phenyl substituent were demonstrated the most potent antitumor activities (**7e**, **7f**). Bearing alkyl group, such as ethyl, propyl, or *tert*-butyl function on the triazolyl-phenyl ring of the estradiol skeleton was reported previously to increase the antiproliferative effect, and our result correlates with this finding.[83] Cancer selectivity of compound **7e** with *p*-ethyl substituent on its triazolyl-phenyl ring was assessed based on its lowest IC_{50} value from the series. Since the proliferation of MRC-5 cell population was not interfered significantly even after exposure to 30 μM of **7e**; moreover, its growth-inhibitory value at 30 μM was at least 3.5 times higher against all types of the examined cancerous cells, it can be considered as a cancer-selective molecule.

Regarding the 3-benzyloxy-16-hydroxymethyl-estrane derivatives, we determined the antiproliferative activity of the molecules against breast cancer cell lines with distinct receptor status in order to investigate their potential selectivity. Most compounds of the series (**9**, **10**, **12**, **9a**, **9b**) generally induced notable inhibition of proliferation of breast tumor cells indicating no significant selectivity between the examined cell lines. Configuration of substituents at C-16 and C-17 displayed a limited affection on the antiproliferative potency; nevertheless, 16β,17β isomers were more outstanding in the series, except for compound **10**. Certain *p*-substituents on the benzyl ether function at C-3 were shown to increase the antiproliferative potency (**9a**, **9b**). Compound **9a** containing *p*-chloride substituent on the benzyloxy group at C-3 was demonstrated to be the most potent from the series considering its antiproliferative activity on the examined cancerous cells.

The antiproliferative activity of 3-benzyloxy-13α-estradiols was found to be more pronounced compared to their 3-methyl ether counterparts considering the results of all examined cancer cell lines. All benzyl ethers displayed notable activity on HeLa and A2780 cells, the 16β,17β-isomer (**20**) was the most potent against breast cancer cells based on its IC_{50} values regarding each four cell lines. The 16β,17α-isomer (**16**) was proven to be the most effective and selective towards HeLa and A2780 cell lines. Cancer-selectivity of compound **20** and **15** (16β,17β) was detemined due to their generally potent antiproliferative characteristic on all investigated tumorous cell lines by using MRC-5 cells. Both compounds exterted a dose-dependent activity, **20** inhibited the proliferation of MRC-5 cells at least 2 times lesser compared to its activity on cancer cell lines. **15** showed a modest selectivity on HeLa and A2780 cells; however, regarding breast cancer cell lines, the IC_{50} value of the compound was similar to its activity against non-cancerous cells.

In summary of structure-activity relationships of all three groups of the examined compounds, benzyl ether function at C-3 enhanced the antiproliferative potency, the configuration of substituents at C-16 and C-17 exerted a varying influence on the activity of the molecules; 16β,17β and 16β,17α isomers were proven to be the most potent estradiol analogs in general. The activity of the most potent compounds (**7e**, **7f**, **9**, **9a**, **9b, 10, 20**) was comparable with cisplatin that is currently used in gynecological cancer therapy protocols, such as cervix and breast cancer protocols.[117–119]

To characterize the antiproliferative activity of the selected compounds on cell cycle distributon, flow cytometry analysis was performed. The effect of **7e** was examined after a 24 h and 48 h treatment on HeLa cervical tumor cells due to its potent activity against this type of cancer cell line. Exposure for 24 h to 10 μM **7e** generated a marked elevation in the ratio of cells in S and G2/M phases while the ratio of cells in the G1 phase was decreased. Treatment for 48 h led to the elevation of G2/M cells at the expense of the G1 population again; furthermore, the significant increase of the subG1 population indicating a blockade of the cell cycle at the G2/M phase and the induction of programmed cell death. The blockage in the G2/M phase induced by **7e** was additionally supported based on the measurement of the mRNA levels of p21, one of the key regulators of a G2/M arrest by QPCR. The induction of p21 was determined after 24 and 48 h treatment with **7e**. G2/M phase arrest was also reported regarding other structurally modified estradiol analogs *i.e.* D-secoestrone-triazole [88] and D-homoestrone.[120]

G1 cell population was significantly elevated together with the decrease of the ratio of cells in the G2/M phase after treatment with the increasing concentrations of compound **9** for 24h in MDA-MB-231 cancer cells. An increase in the percentage of subdiploid cells was detected, even at 5 μM concenration. This tendency was observed regarding **9a** as well**;** however, the alterations were less pronounced. These findings correlate with previously described G1 phase arrests induced by estrone analogs, such as unsubstituted 16-oxime-estrone molecules and oxadiazole derivatives of estrone.[79,121]

Hoechst 33258 – propidium iodide double staining was performed utilizing the HeLa cell line to confirm the presence of apoptotic cells following exposure to **7e**. The treatment induced the siginificant elevation of the ratio of early apoptotic and secondary necrotic cells, while a decrease was observed in the population of intact cells. During the development of anticancer agents, apoptosis-inducing molecules are preferred[122], since mainly there is no inflammatory reaction in connection with the apoptotic process or the removal of the apoptotic cells.[123,124] On the other hand, the loss of membrane integrity of necrotic cells

results in the release of the cytoplasmic constituents into the surrounding interstitial tissue and subsequent inflammation.[125] Secondary necrosis is the outcome when *in vitro* cultured non-phagocytic cells undergo programmed cell death.[29,126] Treatment with **7e** led to both early apoptotic and secondary necrotic cells according to our results.

The apoptosis-inducing property of **7e** against HeLa cervical cancer cells was additionally supported by the findings of the investigation of the activity of caspase-3, the execution enzyme of the programmed cell death. A significant elevation of caspase-3 concentration was observed in a dose-dependent manner after exposure to the test compound. The involvement of the intrinsic pathway of the apoptotic process was revealed through the increased activity of caspase-9, while the unaltered concentration of caspase-8 indicates that the extrinsic pathway does not play a role in the activity of **7e**.

Metastasis is the major cause of malignancy-related deaths; it can be connected with approximately 90% of the fatal cases.[3] Consequently, developing innovative agents with anti-metastatic potency is a huge need to control cancer-related mortality. The metastatic process involves several steps, such as the local migration and invasion of cancer cells into adjacent tissue, infiltrating into the vasculature, surviving and seceding from the circulation system, and then the following proliferation in distant organs that results in colonization.[127] Triple-negative breast cancer is characterized by higher chance of recurrence, shorter median time to death and worse overall survival compared to other breast cancer subtypes.[9,12] The high risk of developing visceral metastases in a short time after the diagnosis of patients with TNBC is responsible in a large part for the poorer prognosis in connection with the phenotype.[128]

Compounds **9** and **9a** were additionally investigated regarding their activity on triple-negative MDA-MB-231 cell migration and invasion, the intitial steps of metastatic spread. Significant inhibiton of cell migration was observed at even 0.25 μM, indicating the potency of the compounds in sub-antiproliferative concentration. The inhibitory action of compound **9** on cell invasion capacity was demonstrated to be more pronounced as evaluated by the Boyden chamber assay.

Degradation and subsequent rearrangement of ECM induced by matrix metalloproteinases participate in multiple steps of the processes of metastasis, including invasion of the basement membrane at primary and metastatic sites, invasion through the stroma; moreover, intra- and extravasation.[129] The significantly elevated activity of the latent and active forms of MMP-2 and MMP-9 in breast tumoral tissues was demonstrated as compared to the non-tumoral adjacent tissues. Evaluation by distant metastasis-free survival in the Kaplan-Meier plotter database showed that overexpression of MMP-2 and MMP-9

mRNA are correlated with poor outcome.[130] The increased expression of MMP-2 and MMP-9 at the mRNA level was reported in MDA-MB-231 cells compared to non-cancerous HS578Bst breast cells. A close correlation between overexpression of the two mentioned metalloproteinases and lymph node metastasis; moreover, tumor staging was assessed from the examination of breast cancer tissues derived from patients with clinically diagnosed breast tumors.[131]

After the treatment of triple-negative MDA-MB-231 cells for 24 h, we found that compound **9** and **9a** did not exhibit a notable influence on the level of MMP-2 and MPP-9, demonstrating that these enzymes do not play a crucial part in the mechanism of action of the examined estradiol analogs.

Most types of cells and tissues express focal adhesion kinase that is involved in the processes of cell spreading, differentation, cell cycle, cell migration, and cell death; therefore, it is an enzyme with a notably extensive function. The activation of FAK is mainly based on the autophosphorylation on tyrosine Y397 executed by the clustering of integrins.[132] The role of the enzyme in the process of cell migration was reported in several studies; moreover, its elevated activity was demonstrated in several tumor types, such as breast cancer. In addition, the rate of its upregulation was associated with a poorer prognosis and metastatic spread.[133,134]

Another important finding that overexpression of FAK occurred in the early stage of tumorigenesis, even before cell invasion in ductal carcinoma in situ.[135] Overexpression of the enzyme enhanced the migration of Chinese hamster ovary (CHO) cells, while downregulation of FAK led to weak cell migration in response to chemotactic and haptotactic signals.[136] Several studies reported that FAK contributes to the development and progression of various cancer types, including breast cancer; moreover, the deletion of FAK suppressed tumor formation and progression in mouse models of breast cancer. It was demonstrated that FAK plays a role in the intercellular communication between cancer-associated fibroblasts in the tumor microenvironment and mammary tumor cells important for cancer cell migration and metastasis development. The deletion of FAK led to the suppressed ability of cancer-associated fibroblasts to promote tumor cell migration.[137]

A dose-dependent decrease was observed in the level of pFAK Y397 in MDA-MB-231 cells after treatment with **9** and **9a** in sub-antiproliferative concentrations. The expression of total FAK was not influenced by the treatment indicating that the compounds inhibited the phosphorylation of the enzyme.

6. Summary

In summary, the present work revealed that numerous compounds from the set of 16-triazolyl-13α-estradiols, 3-benzyloxy-16-hydroxymethyl-estradiols, and 16-hydroxymethyl-3-benzyloxy-13α-estradiols are potent antiproliferative agents against gynecological cancer cell lines, especially breast and cervical tumors.

Apoptosis-induction was observed in cervical cancer cells bearing HPV 18 DNA by 16-triazolyl-13α-estradiol **7e** through G2/M phase blockage and involving the mitochondrial apoptotic pathway, while showing a beneficial cancer-selectivity. **9** and **9a** 3-benzyloxy-16-hydroxymethyl-estradiols caused programmed cell death and G1 phase increase in TNBC cells.

TNBC cell line was utilized for the investigation of the antimetastatic capacity of test compounds due to the unmet medical need of the subtype. **9** and **9a** exerted substantial dose-dependent inhibition on cell migration and invasion; furthermore, on the phosphorylation of focal adhesion kinase, an important target in antimetastatic research. The treatment proved to be potent in sub-antiproliferative concentrations that indicates the advantageous cancer selectivity of the compounds.

Our findings demonstrate that molecules with modified estradiol structure can be regarded as promising candidates in the development of new anticancer agents exerting antiproliferative and antimetastatic properties.

7. References

(1) Bray, F.; Ferlay, J.; Soerjomataram, I.; Siegel, R. L.; Torre, L. A.; Jemal, A. Global Cancer Statistics 2018: GLOBOCAN Estimates of Incidence and Mortality Worldwide for 36 Cancers in 185 Countries. *CA. Cancer J. Clin.* **2018**, *68* (6), 394–424. https://doi.org/10.3322/caac.21492.

(2) Torre, L. A.; Bray, F.; Siegel, R. L.; Ferlay, J.; Lortet-Tieulent, J.; Jemal, A. Global Cancer Statistics, 2012: Global Cancer Statistics, 2012. *CA. Cancer J. Clin.* **2015**, *65* (2), 87–108. https://doi.org/10.3322/caac.21262.

(3) Mehlen, P.; Puisieux, A. Metastasis: A Question of Life or Death. *Nat. Rev. Cancer* **2006**, *6* (6), 449–458. https://doi.org/10.1038/nrc1886.

(4) Steeg, P. S. Targeting Metastasis. *Nat. Rev. Cancer* **2016**, *16* (4), 201–218. https://doi.org/10.1038/nrc.2016.25.

(5) Tevaarwerk, A. J.; Gray, R. J.; Schneider, B. P.; Smith, M. L.; Wagner, L. I.; Fetting, J. H.; Davidson, N.; Goldstein, L. J.; Miller, K. D.; Sparano, J. A. Survival in Patients with Metastatic Recurrent Breast Cancer after Adjuvant Chemotherapy: Little Evidence of Improvement over the Past 30 Years. *Cancer* **2013**, *119* (6), 1140–1148. https://doi.org/10.1002/cncr.27819.

(6) Cheang, M. C. U.; Martin, M.; Nielsen, T. O.; Prat, A.; Voduc, D.; Rodriguez-Lescure, A.; Ruiz, A.; Chia, S.; Shepherd, L.; Ruiz-Borrego, M.; Calvo, L.; Alba, E.; Carrasco, E.; Caballero, R.; Tu, D.; Pritchard, K. I.; Levine, M. N.; Bramwell, V. H.; Parker, J.; Bernard, P. S.; Ellis, M. J.; Perou, C. M.; Di Leo, A.; Carey, L. A. Defining Breast Cancer Intrinsic Subtypes by Quantitative Receptor Expression. *The Oncologist* **2015**, *20* (5), 474–482. https://doi.org/10.1634/theoncologist.2014-0372.

(7) Perou, C. M.; Sørlie, T.; Eisen, M. B.; van de Rijn, M.; Jeffrey, S. S.; Rees, C. A.; Pollack, J. R.; Ross, D. T.; Johnsen, H.; Akslen, L. A.; Fluge, Ø.; Pergamenschikov, A.; Williams, C.; Zhu, S. X.; Lønning, P. E.; Børresen-Dale, A.-L.; Brown, P. O.; Botstein, D. Molecular Portraits of Human Breast Tumours. *Nature* **2000**, *406* (6797), 747–752. https://doi.org/10.1038/35021093.

(8) Brenton, J. D.; Carey, L. A.; Ahmed, A. A.; Caldas, C. Molecular Classification and Molecular Forecasting of Breast Cancer: Ready for Clinical Application? *J. Clin. Oncol.* **2005**, *23* (29), 7350–7360. https://doi.org/10.1200/JCO.2005.03.3845.

(9) Lee, A.; Djamgoz, M. B. A. Triple Negative Breast Cancer: Emerging Therapeutic Modalities and Novel Combination Therapies. *Cancer Treat. Rev.* **2018**, *62*, 110–122. https://doi.org/10.1016/j.ctrv.2017.11.003.

(10) Alluri, P.; Newman, L. A. Basal-Like and Triple-Negative Breast Cancers. *Surg. Oncol. Clin. N. Am.* **2014**, *23* (3), 567–577. https://doi.org/10.1016/j.soc.2014.03.003.

(11) Bianchini, G.; Balko, J. M.; Mayer, I. A.; Sanders, M. E.; Gianni, L. Triple-Negative Breast Cancer: Challenges and Opportunities of a Heterogeneous Disease. *Nat. Rev. Clin. Oncol.* **2016**, *13* (11), 674–690. https://doi.org/10.1038/nrclinonc.2016.66.

(12) Dent, R.; Trudeau, M.; Pritchard, K. I.; Hanna, W. M.; Kahn, H. K.; Sawka, C. A.; Lickley, L. A.; Rawlinson, E.; Sun, P.; Narod, S. A. Triple-Negative Breast Cancer: Clinical Features and Patterns of Recurrence. *Clin. Cancer Res.* **2007**, *13* (15), 4429–4434. https://doi.org/10.1158/1078-0432.CCR-06-3045.

(13) Lin, N. U.; Claus, E.; Sohl, J.; Razzak, A. R.; Arnaout, A.; Winer, E. P. Sites of Distant Recurrence and Clinical Outcomes in Patients with Metastatic Triple-Negative Breast Cancer: High Incidence of Central Nervous System Metastases. *Cancer* **2008**, *113* (10), 2638–2645. https://doi.org/10.1002/cncr.23930.

(14) Newman, L. A.; Reis-Filho, J. S.; Morrow, M.; Carey, L. A.; King, T. A. The 2014 Society of Surgical Oncology Susan G. Komen for the Cure Symposium: Triple-Negative Breast Cancer. *Ann. Surg. Oncol.* **2015**, *22* (3), 874–882. https://doi.org/10.1245/s10434-014-4279-0.

(15) Lehmann, B. D.; Bauer, J. A.; Chen, X.; Sanders, M. E.; Chakravarthy, A. B.; Shyr, Y.; Pietenpol, J. A. Identification of Human Triple-Negative Breast Cancer Subtypes and Preclinical Models for Selection of Targeted Therapies. *J. Clin. Invest.* **2011**, *121* (7), 2750–2767. https://doi.org/10.1172/JCI45014.

(16) Lehmann, B. D.; Jovanović, B.; Chen, X.; Estrada, M. V.; Johnson, K. N.; Shyr, Y.; Moses, H. L.; Sanders, M. E.; Pietenpol, J. A. Refinement of Triple-Negative Breast Cancer Molecular Subtypes: Implications for Neoadjuvant Chemotherapy Selection. *PLOS ONE* **2016**, *11* (6), e0157368. https://doi.org/10.1371/journal.pone.0157368.

(17) Shah, S. P.; Roth, A.; Goya, R.; Oloumi, A.; Ha, G.; Zhao, Y.; Turashvili, G.; Ding, J.; Tse, K.; Haffari, G.; Bashashati, A.; Prentice, L. M.; Khattra, J.; Burleigh, A.; Yap, D.; Bernard, V.; McPherson, A.; Shumansky, K.; Crisan, A.; Giuliany, R.; Heravi-Moussavi, A.; Rosner, J.; Lai, D.; Birol, I.; Varhol, R.; Tam, A.; Dhalla, N.; Zeng, T.; Ma, K.; Chan, S. K.; Griffith, M.; Moradian, A.; Cheng, S.-W. G.; Morin, G. B.; Watson, P.; Gelmon, K.; Chia, S.; Chin, S.-F.; Curtis, C.; Rueda, O. M.; Pharoah, P. D.;

Damaraju, S.; Mackey, J.; Hoon, K.; Harkins, T.; Tadigotla, V.; Sigaroudinia, M.; Gascard, P.; Tlsty, T.; Costello, J. F.; Meyer, I. M.; Eaves, C. J.; Wasserman, W. W.; Jones, S.; Huntsman, D.; Hirst, M.; Caldas, C.; Marra, M. A.; Aparicio, S. The Clonal and Mutational Evolution Spectrum of Primary Triple-Negative Breast Cancers. *Nature* **2012**, *486* (7403), 395–399. https://doi.org/10.1038/nature10933.

(18) Burstein, M. D.; Tsimelzon, A.; Poage, G. M.; Covington, K. R.; Contreras, A.; Fuqua, S. A. W.; Savage, M. I.; Osborne, C. K.; Hilsenbeck, S. G.; Chang, J. C.; Mills, G. B.; Lau, C. C.; Brown, P. H. Comprehensive Genomic Analysis Identifies Novel Subtypes and Targets of Triple-Negative Breast Cancer. *Clin. Cancer Res.* **2015**, *21* (7), 1688–1698. https://doi.org/10.1158/1078-0432.CCR-14-0432.

(19) Jézéquel, P.; Loussouarn, D.; Guérin-Charbonnel, C.; Campion, L.; Vanier, A.; Gouraud, W.; Lasla, H.; Guette, C.; Valo, I.; Verrièle, V.; Campone, M. Gene-Expression Molecular Subtyping of Triple-Negative Breast Cancer Tumours: Importance of Immune Response. *Breast Cancer Res.* **2015**, *17* (1), 43. https://doi.org/10.1186/s13058-015-0550-y.

(20) Masuda, H.; Baggerly, K. A.; Wang, Y.; Zhang, Y.; Gonzalez-Angulo, A. M.; Meric-Bernstam, F.; Valero, V.; Lehmann, B. D.; Pietenpol, J. A.; Hortobagyi, G. N.; Symmans, W. F.; Ueno, N. T. Differential Response to Neoadjuvant Chemotherapy Among 7 Triple-Negative Breast Cancer Molecular Subtypes. *Clin. Cancer Res.* **2013**, *19* (19), 5533–5540. https://doi.org/10.1158/1078-0432.CCR-13-0799.

(21) Fang, J.; Zhang, H.; Jin, S. Epigenetics and Cervical Cancer: From Pathogenesis to Therapy. *Tumor Biol.* **2014**, *35* (6), 5083–5093. https://doi.org/10.1007/s13277-014-1737-z.

(22) Saavedra, K. P.; Brebi, P. M.; Roa, J. C. S. Epigenetic Alterations in Preneoplastic and Neoplastic Lesions of the Cervix. *Clin. Epigenetics* **2012**, *4* (1), 13. https://doi.org/10.1186/1868-7083-4-13.

(23) Das, P.; Thomas, A.; Kannan, S.; Deodhar, K.; Shrivastava, S.; Mahantshetty, U.; Mulherkar, R. Human Papillomavirus (HPV) Genome Status & Cervical Cancer Outcome - A Retrospective Study. *Indian J. Med. Res.* **2015**, *142* (5), 525. https://doi.org/10.4103/0971-5916.171276.

(24) Mahantshetty, U.; Teni, T.; Naga, P.; Hotwani, C.; Umesh, S.; Kannan, S.; Hande, V.; Pawar, S.; Engineer, R.; Chopra, S.; Deodhar, K.; Maheshwari, A.; Gurram, L.; Gupta, S.; Shrivastava, S. K. Impact of HPV 16/18 Infection on Clinical Outcomes in Locally Advanced Cervical Cancers Treated with Radical Radio (Chemo) Therapy - A Prospective Observational Study. *Gynecol. Oncol.* **2018**, *148* (2), 299–304. https://doi.org/10.1016/j.ygyno.2017.11.034.

(25) Saranath, D.; Khan, Z.; Tandle, A. T.; Dedhia, P.; Sharma, B.; Contractor, R.; Shrivastava, S.; Dinshaw, K. HPV16/18 Prevalence in Cervical Lesions/Cancers and P53 Genotypes in Cervical Cancer Patients from India. *Gynecol. Oncol.* **2002**, *86* (2), 157–162. https://doi.org/10.1006/gyno.2002.6735.

(26) Vinokurova, S.; Wentzensen, N.; Kraus, I.; Klaes, R.; Driesch, C.; Melsheimer, P.; Kisseljov, F.; Durst, M.; Schneider, A.; von Knebel Doeberitz, M. Type-Dependent Integration Frequency of Human Papillomavirus Genomes in Cervical Lesions. *Cancer Res.* **2008**, *68* (1), 307–313. https://doi.org/10.1158/0008-5472.CAN-07-2754.

(27) Landry, J. J. M.; Pyl, P. T.; Rausch, T.; Zichner, T.; Tekkedil, M. M.; Stütz, A. M.; Jauch, A.; Aiyar, R. S.; Pau, G.; Delhomme, N.; Gagneur, J.; Korbel, J. O.; Huber, W.; Steinmetz, L. M. The Genomic and Transcriptomic Landscape of a HeLa Cell Line. *G3 GenesGenomesGenetics* **2013**, *3* (8), 1213–1224. https://doi.org/10.1534/g3.113.005777.

(28) Boshart, M.; Gissmann, L.; Ikenberg, H.; Kleinheinz, A.; Scheurlen, W.; zur Hausen, H. A New Type of Papillomavirus DNA, Its Presence in Genital Cancer Biopsies and in Cell Lines Derived from Cervical Cancer. *EMBO J.* **1984**, *3* (5), 1151–1157. https://doi.org/10.1002/j.1460-2075.1984.tb01944.x.

(29) Elmore, S. Apoptosis: A Review of Programmed Cell Death. *Toxicol. Pathol.* **2007**, *35* (4), 495–516. https://doi.org/10.1080/01926230701320337.

(30) Hassan, M.; Watari, H.; AbuAlmaaty, A.; Ohba, Y.; Sakuragi, N. Apoptosis and Molecular Targeting Therapy in Cancer. *BioMed Res. Int.* **2014**, *2014*, 1–23. https://doi.org/10.1155/2014/150845.

(31) D'Arcy, M. S. Cell Death: A Review of the Major Forms of Apoptosis, Necrosis and Autophagy. *Cell Biol. Int.* **2019**, *43* (6), 582–592. https://doi.org/10.1002/cbin.11137.

(32) Lockshin, R. A.; Zakeri, Z. Apoptosis, Autophagy, and More. *Int. J. Biochem. Cell Biol.* **2004**, *36* (12), 2405–2419. https://doi.org/10.1016/j.biocel.2004.04.011.

(33) Nair, P.; Lu, M.; Petersen, S.; Ashkenazi, A. Apoptosis Initiation Through the Cell-Extrinsic Pathway. In *Methods in Enzymology*; Elsevier, 2014; Vol. 544, pp 99–128. https://doi.org/10.1016/B978-0-12-417158-9.00005-4.

(34) Samraj, A. K.; Keil, E.; Ueffing, N.; Schulze-Osthoff, K.; Schmitz, I. Loss of Caspase-9 Provides Genetic Evidence for the Type I/II Concept of CD95-Mediated Apoptosis. *J. Biol. Chem.* **2006**, *281* (40), 29652–29659. https://doi.org/10.1074/jbc.M603487200.

(35) Spencer, S. L.; Gaudet, S.; Albeck, J. G.; Burke, J. M.; Sorger, P. K. Non-Genetic Origins of Cell-to-Cell Variability in TRAIL-Induced Apoptosis. *Nature* **2009**, *459* (7245), 428–432. https://doi.org/10.1038/nature08012.

(36) Lintz, M.; Muñoz, A.; Reinhart-King, C. A. The Mechanics of Single Cell and Collective Migration of Tumor Cells. *J. Biomech. Eng.* **2017**, *139* (2), 021005. https://doi.org/10.1115/1.4035121.

(37) Kapoor, C.; Vaidya, S.; Wadhwan, V.; Hitesh; Kaur, G.; Pathak, A. Seesaw of Matrix Metalloproteinases (MMPs). *J. Cancer Res. Ther.* **2016**, *12* (1), 28. https://doi.org/10.4103/0973-1482.157337.

(38) Egeblad, M.; Werb, Z. New Functions for the Matrix Metalloproteinases in Cancer Progression. *Nat. Rev. Cancer* **2002**, *2* (3), 161–174. https://doi.org/10.1038/nrc745.

(39) Isaacson, K. J.; Martin Jensen, M.; Subrahmanyam, N. B.; Ghandehari, H. Matrix-Metalloproteinases as Targets for Controlled Delivery in Cancer: An Analysis of Upregulation and Expression. *J. Controlled Release* **2017**, *259*, 62–75. https://doi.org/10.1016/j.jconrel.2017.01.034.

(40) Deryugina, E. I.; Quigley, J. P. Matrix Metalloproteinases and Tumor Metastasis. *Cancer Metastasis Rev.* **2006**, *25* (1), 9–34. https://doi.org/10.1007/s10555-006-7886-9.

(41) Fields, G. B. The Rebirth of Matrix Metalloproteinase Inhibitors: Moving Beyond the Dogma. *Cells* **2019**, *8* (9), 984. https://doi.org/10.3390/cells8090984.

(42) Shah, M. A.; Starodub, A.; Sharma, S.; Berlin, J.; Patel, M.; Wainberg, Z. A.; Chaves, J.; Gordon, M.; Windsor, K.; Brachmann, C. B.; Huang, X.; Vosganian, G.; Maltzman, J. D.; Smith, V.; Silverman, J. A.; Lenz, H.-J.; Bendell, J. C. Andecaliximab/GS-5745 Alone and Combined with MFOLFOX6 in Advanced Gastric and Gastroesophageal Junction Adenocarcinoma: Results from a Phase I Study. *Clin. Cancer Res.* **2018**, *24* (16), 3829–3837. https://doi.org/10.1158/1078-0432.CCR-17-2469.

(43) Vandenbroucke, R. E.; Libert, C. Is There New Hope for Therapeutic Matrix Metalloproteinase Inhibition? *Nat. Rev. Drug Discov.* **2014**, *13* (12), 904–927. https://doi.org/10.1038/nrd4390.

(44) Sulzmaier, F. J.; Jean, C.; Schlaepfer, D. D. FAK in Cancer: Mechanistic Findings and Clinical Applications. *Nat. Rev. Cancer* **2014**, *14* (9), 598–610. https://doi.org/10.1038/nrc3792.

(45) Sieg, D. J.; Hauck, C. R.; Ilic, D.; Klingbeil, C. K.; Schaefer, E.; Damsky, C. H.; Schlaepfer, D. D. FAK Integrates Growth-Factor and Integrin Signals to Promote Cell Migration. *Nat. Cell Biol.* **2000**, *2* (5), 249–256. https://doi.org/10.1038/35010517.

(46) Alexopoulou, A. N.; Lees, D. M.; Bodrug, N.; Lechertier, T.; Fernandez, I.; D'Amico, G.; Dukinfield, M.; Batista, S.; Tavora, B.; Serrels, B.; Hodivala-Dilke, K. Focal Adhesion Kinase (FAK) Tyrosine 397E Mutation Restores the Vascular Leakage Defect in Endothelium-Specific FAK-Kinase Dead Mice: Endothelial FAKY397E Mutation and Tumour Vascular Leakage. *J. Pathol.* **2017**, *242* (3), 358–370. https://doi.org/10.1002/path.4911.

(47) Zhou, J.; Yi, Q.; Tang, L. The Roles of Nuclear Focal Adhesion Kinase (FAK) on Cancer: A Focused Review. *J. Exp. Clin. Cancer Res.* **2019**, *38* (1), 250. https://doi.org/10.1186/s13046-019-1265-1.

(48) Agochiya, M.; Brunton, V. G.; Owens, D. W.; Parkinson, E. K.; Paraskeva, C.; Keith, W. N.; Frame, M. C. Increased Dosage and Amplification of the Focal Adhesion Kinase Gene in Human Cancer Cells. *Oncogene* **1999**, *18* (41), 5646–5653. https://doi.org/10.1038/sj.onc.1202957.

(49) Owens, L. V.; Xu, L.; Marston, W. A.; Yang, X.; Farber, M. A.; Iacocca, M. V.; Cance, W. G.; Keagy, B. A. Overexpression of the Focal Adhesion Kinase (P125FAK) in the Vascular Smooth Muscle Cells of Intimal Hyperplasia. *J. Vasc. Surg.* **2001**, *34* (2), 344–349. https://doi.org/10.1067/mva.2001.114814.

(50) Cance, W. G.; Harris, J. E.; Iacocca, M. V.; Roche, E.; Yang, X.; Chang, J.; Simkins, S.; Xu, L. Immunohistochemical Analyses of Focal Adhesion Kinase Expression in Benign and Malignant Human Breast and Colon Tissues: Correlation with Preinvasive and Invasive Phenotypes. *Clin. Cancer Res. Off. J. Am. Assoc. Cancer Res.* **2000**, *6* (6), 2417–2423.

(51) Zhao, J.; Guan, J.-L. Signal Transduction by Focal Adhesion Kinase in Cancer. *Cancer Metastasis Rev.* **2009**, *28* (1–2), 35–49. https://doi.org/10.1007/s10555-008-9165-4.

(52) Soria, J. C.; Gan, H. K.; Blagden, S. P.; Plummer, R.; Arkenau, H. T.; Ranson, M.; Evans, T. R. J.; Zalcman, G.; Bahleda, R.; Hollebecque, A.; Lemech, C.; Dean, E.; Brown, J.; Gibson, D.; Peddareddigari, V.; Murray, S.; Nebot, N.; Mazumdar, J.; Swartz, L.; Auger, K. R.; Fleming, R. A.; Singh, R.; Millward, M. A Phase I, Pharmacokinetic and Pharmacodynamic Study of GSK2256098, a Focal Adhesion Kinase Inhibitor, in Patients with Advanced Solid Tumors. *Ann. Oncol.* **2016**, *27* (12), 2268–2274. https://doi.org/10.1093/annonc/mdw427.

(53) Doi, T.; Yang, J. C.-H.; Shitara, K.; Naito, Y.; Cheng, A.-L.; Sarashina, A.; Pronk, L. C.; Takeuchi, Y.; Lin, C.-C. Phase I Study of the Focal Adhesion Kinase Inhibitor BI 853520 in Japanese and Taiwanese Patients with Advanced or Metastatic Solid Tumors. *Target. Oncol.* **2019**, *14* (1), 57–65. https://doi.org/10.1007/s11523-019-00620-0.

(54) Brown, N. F.; Williams, M.; Arkenau, H.-T.; Fleming, R. A.; Tolson, J.; Yan, L.; Zhang, J.; Singh, R.; Auger, K. R.; Lenox, L.; Cox, D.; Lewis, Y.; Plisson, C.; Searle, G.; Saleem, A.; Blagden, S.;

Mulholland, P. A Study of the Focal Adhesion Kinase Inhibitor GSK2256098 in Patients with Recurrent Glioblastoma with Evaluation of Tumor Penetration of [11C]GSK2256098. *Neuro-Oncol.* **2018**, *20* (12), 1634–1642. https://doi.org/10.1093/neuonc/noy078.

(55) Gerber, D. E.; Camidge, D. R.; Morgensztern, D.; Cetnar, J.; Kelly, R. J.; Ramalingam, S. S.; Spigel, D. R.; Jeong, W.; Scaglioni, P. P.; Zhang, S.; Li, M.; Weaver, D. T.; Vaikus, L.; Keegan, M.; Horobin, J. C.; Burns, T. F. Phase 2 Study of the Focal Adhesion Kinase Inhibitor Defactinib (VS-6063) in Previously Treated Advanced KRAS Mutant Non-Small Cell Lung Cancer. *Lung Cancer* **2020**, *139*, 60–67. https://doi.org/10.1016/j.lungcan.2019.10.033.

(56) de Jonge, M. J. A.; Steeghs, N.; Lolkema, M. P.; Hotte, S. J.; Hirte, H. W.; van der Biessen, D. A. J.; Abdul Razak, A. R.; De Vos, F. Y. F. L.; Verheijen, R. B.; Schnell, D.; Pronk, L. C.; Jansen, M.; Siu, L. L. Phase I Study of BI 853520, an Inhibitor of Focal Adhesion Kinase, in Patients with Advanced or Metastatic Nonhematologic Malignancies. *Target. Oncol.* **2019**, *14* (1), 43–55. https://doi.org/10.1007/s11523-018-00617-1.

(57) Ascenzi, P.; Bocedi, A.; Marino, M. Structure–Function Relationship of Estrogen Receptor α and β: Impact on Human Health. *Mol. Aspects Med.* **2006**, *27* (4), 299–402. https://doi.org/10.1016/j.mam.2006.07.001.

(58) Chen, G. G.; Zeng, Q.; Tse, G. M. Estrogen and Its Receptors in Cancer. *Med. Res. Rev.* **2008**, *28* (6), 954–974. https://doi.org/10.1002/med.20131.

(59) Nelles, J. L.; Hu, W.-Y.; Prins, G. S. Estrogen Action and Prostate Cancer. *Expert Rev. Endocrinol. Metab.* **2011**, *6* (3), 437–451. https://doi.org/10.1586/eem.11.20.

(60) Pearce, S. T.; Jordan, V. C. The Biological Role of Estrogen Receptors α and β in Cancer. *Crit. Rev. Oncol. Hematol.* **2004**, *50* (1), 3–22. https://doi.org/10.1016/j.critrevonc.2003.09.003.

(61) Cushman, M.; He, H.-M.; Katzenellenbogen, J. A.; Varma, R. K.; Hamel, E.; Lin, C. M.; Ram, S.; Sachdeva, Y. P. Synthesis of Analogs of 2-Methoxyestradiol with Enhanced Inhibitory Effects on Tubulin Polymerization and Cancer Cell Growth. *J. Med. Chem.* **1997**, *40* (15), 2323–2334. https://doi.org/10.1021/jm9700833.

(62) Wang, Z.; Yang, D.; Mohanakrishnan, A. K.; Fanwick, P. E.; Nampoothiri, P.; Hamel, E.; Cushman, M. Synthesis of B-Ring Homologated Estradiol Analogues That Modulate Tubulin Polymerization and Microtubule Stability. *J. Med. Chem.* **2000**, *43* (12), 2419–2429. https://doi.org/10.1021/jm0001119.

(63) Bodnár, B.; Mernyák, E.; Wölfling, J.; Schneider, G.; Herman, B.; Szécsi, M.; Sinka, I.; Zupkó, I.; Kupihár, Z.; Kovács, L. Synthesis and Biological Evaluation of Triazolyl 13α-Estrone–Nucleoside Bioconjugates. *Molecules* **2016**, *21* (9), 1212. https://doi.org/10.3390/molecules21091212.

(64) Cadot, C.; Laplante, Y.; Kamal, F.; Luu-The, V.; Poirier, D. C6-(N,N-Butyl-Methyl-Heptanamide) Derivatives of Estrone and Estradiol as Inhibitors of Type 1 17β-Hydroxysteroid Dehydrogenase: Chemical Synthesis and Biological Evaluation. *Bioorg. Med. Chem.* **2007**, *15* (2), 714–726. https://doi.org/10.1016/j.bmc.2006.10.055.

(65) Jourdan, F.; Leese, M. P.; Dohle, W.; Ferrandis, E.; Newman, S. P.; Chander, S.; Purohit, A.; Potter, B. V. L. Structure–Activity Relationships of C-17-Substituted Estratriene-3- *O* -Sulfamates as Anticancer Agents. *J. Med. Chem.* **2011**, *54* (13), 4863–4879. https://doi.org/10.1021/jm200483x.

(66) Mernyák, E.; Fiser, G.; Szabó, J.; Bodnár, B.; Schneider, G.; Kovács, I.; Ocsovszki, I.; Zupkó, I.; Wölfling, J. Synthesis and in Vitro Antiproliferative Evaluation of D-Secooxime Derivatives of 13β- and 13α-Estrone. *Steroids* **2014**, *89*, 47–55. https://doi.org/10.1016/j.steroids.2014.08.015.

(67) Möller, G.; Deluca, D.; Gege, C.; Rosinus, A.; Kowalik, D.; Peters, O.; Droescher, P.; Elger, W.; Adamski, J.; Hillisch, A. Structure-Based Design, Synthesis and in Vitro Characterization of Potent 17β-Hydroxysteroid Dehydrogenase Type 1 Inhibitors Based on 2-Substitutions of Estrone and D-Homo-Estrone. *Bioorg. Med. Chem. Lett.* **2009**, *19* (23), 6740–6744. https://doi.org/10.1016/j.bmcl.2009.09.113.

(68) Szabó, J.; Pataki, Z.; Wölfling, J.; Schneider, G.; Bózsity, N.; Minorics, R.; Zupkó, I.; Mernyák, E. Synthesis and Biological Evaluation of 13α-Estrone Derivatives as Potential Antiproliferative Agents. *Steroids* **2016**, *113*, 14–21. https://doi.org/10.1016/j.steroids.2016.05.010.

(69) Bacsa, I.; Herman, B. E.; Jójárt, R.; Herman, K. S.; Wölfling, J.; Schneider, G.; Varga, M.; Tömböly, C.; Rižner, T. L.; Szécsi, M.; Mernyák, E. Synthesis and Structure–Activity Relationships of 2- and/or 4-Halogenated 13 $\boldsymbol{\beta}$ - and 13α-Estrone Derivatives as Enzyme Inhibitors of Estrogen Biosynthesis. *J. Enzyme Inhib. Med. Chem.* **2018**, *33* (1), 1271–1282. https://doi.org/10.1080/14756366.2018.1490731.

(70) Kiss, A.; Wölfling, J.; Mernyák, E.; Frank, É.; Benke, Z.; Ashkan Senobar Tahaei, S.; Zupkó, I.; Mahó, S.; Schneider, G. Stereocontrolled Synthesis of the Four Possible 3-Methoxy and 3-Benzyloxy-16-Triazolyl-Methyl-Estra-17-Ol Hybrids and Their Antiproliferative Activities. *Steroids* **2019**, *152*, 108500. https://doi.org/10.1016/j.steroids.2019.108500.

(71) Herman, B. E.; Kiss, A.; Wölfling, J.; Mernyák, E.; Szécsi, M.; Schneider, G. Synthesis of Substituted 15β-Alkoxy Estrone Derivatives and Their Cofactor-Dependent Inhibitory Effect on 17β-HSD1. *J. Enzyme Inhib. Med. Chem.* **2019**, *34* (1), 1271–1286. https://doi.org/10.1080/14756366.2019.1634064.

(72) Anstead, G. M.; Carlson, K. E.; Katzenellenbogen, J. A. The Estradiol Pharmacophore: Ligand Structure-Estrogen Receptor Binding Affinity Relationships and a Model for the Receptor Binding Site. *Steroids* **1997**, *62* (3), 268–303. https://doi.org/10.1016/S0039-128X(96)00242-5.

(73) Wölfling, J.; Mernyák, E; Frank, É; Falkay, G.; Márki, Á.; Minorics, R.; Schneider, G. Synthesis and Receptor-Binding Examinations of the Normal and 13-Epi-D-Homoestrones and Their 3-Methyl Ethers. *Steroids* **2003**, *68* (3), 277–288. https://doi.org/10.1016/S0039-128X(02)00181-2.

(74) Jovanović-Šanta, S.; Petrović, J.; Andrić, S.; Kovačević, R.; Đurendić, E.; Sakač, M.; Lazar, D.; Stanković, S. Synthesis, Structure, and Screening of Estrogenic and Antiestrogenic Activity of New 3,17-Substituted-16,17-Seco-Estratriene Derivatives. *Bioorganic Chem.* **2003**, *31* (6), 475–484. https://doi.org/10.1016/S0045-2068(03)00101-9.

(75) Jovanović-Šanta, S. S.; Petri, E. T.; Klisurić, O. R.; Szécsi, M.; Kovačević, R.; Petrović, J. A. Antihormonal Potential of Selected D-Homo and D-Seco Estratriene Derivatives. *Steroids* **2015**, *97*, 45–53. https://doi.org/10.1016/j.steroids.2014.08.026.

(76) Trifunović, J.; Borčić, V.; Vukmirović, S.; Mikov, M. Structural Insights into Anticancer Activity of D-Ring Modified Estrone Derivatives Using Their Lipophilicity in Estimation of SAR and Molecular Docking Studies: Evaluation of Use HPTLC in Drug Discovery. *Drug Test. Anal.* **2017**, *9* (10), 1542–1548. https://doi.org/10.1002/dta.2172.

(77) Ayan, D.; Roy, J.; Maltais, R.; Poirier, D. Impact of Estradiol Structural Modifications (18-Methyl and/or 17-Hydroxy Inversion of Configuration) on the in Vitro and in Vivo Estrogenic Activity. *J. Steroid Biochem. Mol. Biol.* **2011**, *127* (3–5), 324–330. https://doi.org/10.1016/j.jsbmb.2011.07.009.

(78) Schönecker, B.; Lange, C.; Kötteritzsch, M.; Günther, W.; Weston, J.; Anders, E.; Görls, H. Conformational Design for 13α-Steroids. *J. Org. Chem.* **2000**, *65* (18), 5487–5497. https://doi.org/10.1021/jo000108x.

(79) Berényi, Á.; Minorics, R.; Iványi, Z.; Ocsovszki, I.; Ducza, E.; Thole, H.; Messinger, J.; Wölfling, J.; Mótyán, G.; Mernyák, E.; Frank, É.; Schneider, G.; Zupkó, I. Synthesis and Investigation of the Anticancer Effects of Estrone-16-Oxime Ethers in Vitro. *Steroids* **2013**, *78* (1), 69–78. https://doi.org/10.1016/j.steroids.2012.10.009.

(80) Kádár, Z.; Baji, Á.; Zupkó, I.; Bartók, T.; Wölfling, J.; Frank, É. Efficient Approach to Novel 1α-Triazolyl-5α-Androstane Derivatives as Potent Antiproliferative Agents. *Org. Biomol. Chem.* **2011**, *9* (23), 8051. https://doi.org/10.1039/c1ob06086d.

(81) Kádár, Z; Frank, É; Schneider, Gy; Molnár, J; Zupkó, I; Kóti, J; Schönecker, B; Wölfling, J. Efficient Synthesis of Novel A-Ring-Substituted 1,2,3-Triazolylcholestane Derivatives via Catalytic Azide-Alkyne Cycloaddition. *Arkivoc* **2012**, *2012* (3), 279. https://doi.org/10.3998/ark.5550190.0013.320.

(82) Kádár, Z.; Molnár, J.; Schneider, G.; Zupkó, I.; Frank, É. A Facile 'Click' Approach to Novel 15β-Triazolyl-5α-Androstane Derivatives, and an Evaluation of Their Antiproliferative Activities in Vitro. *Bioorg. Med. Chem.* **2012**, *20* (4), 1396–1402. https://doi.org/10.1016/j.bmc.2012.01.008.

(83) Molnár, J.; Frank, É.; Minorics, R.; Kádár, Z.; Ocsovszki, I.; Schönecker, B.; Wölfling, J.; Zupkó, I. A Click Approach to Novel D-Ring-Substituted 16α-Triazolylestrone Derivatives and Characterization of Their Antiproliferative Properties. *PLOS ONE* **2015**, *10* (2), e0118104. https://doi.org/10.1371/journal.pone.0118104.

(84) Frank, É.; Molnár, J.; Zupkó, I.; Kádár, Z.; Wölfling, J. Synthesis of Novel Steroidal 17α-Triazolyl Derivatives via Cu(I)-Catalyzed Azide-Alkyne Cycloaddition, and an Evaluation of Their Cytotoxic Activity in Vitro. *Steroids* **2011**, *76* (10–11), 1141–1148. https://doi.org/10.1016/j.steroids.2011.05.002.

(85) Tapolcsányi, P.; Wölfling, J.; Falkay, G.; Márki, Á.; Minorics, R.; Schneider, G. Synthesis and Receptor-Binding Examination of 16-Hydroxymethyl-3,17-Estradiol Stereoisomers. *Steroids* **2002**, *67* (5), 371–377. https://doi.org/10.1016/S0039-128X(01)00191-X.

(86) Mosmann, T. Rapid Colorimetric Assay for Cellular Growth and Survival: Application to Proliferation and Cytotoxicity Assays. *J. Immunol. Methods* **1983**, *65* (1–2), 55–63. https://doi.org/10.1016/0022-1759(83)90303-4.

(87) Vermes, I.; Haanen, C.; Reutelingsperger, C. Flow Cytometry of Apoptotic Cell Death. *J. Immunol. Methods* **2000**, *243* (1–2), 167–190. https://doi.org/10.1016/S0022-1759(00)00233-7.

(88) Bózsity, N.; Minorics, R.; Szabó, J.; Mernyák, E.; Schneider, G.; Wölfling, J.; Wang, H.-C.; Wu, C.-C.; Ocsovszki, I.; Zupkó, I. Mechanism of Antiproliferative Action of a New d -Secoestrone-Triazole Derivative in Cervical Cancer Cells and Its Effect on Cancer Cell Motility. *J. Steroid Biochem. Mol. Biol.* **2017**, *165*, 247–257. https://doi.org/10.1016/j.jsbmb.2016.06.013.

(89) Snoek-van Beurden, P. A. M.; Von den Hoff, J. W. Zymographic Techniques for the Analysis of Matrix Metalloproteinases and Their Inhibitors. *BioTechniques* **2005**, *38* (1), 73–83. https://doi.org/10.2144/05381RV01.

(90) LaVallee, T. M.; Zhan, X. H.; Herbstritt, C. J.; Kough, E. C.; Green, S. J.; Pribluda, V. S. 2-Methoxyestradiol Inhibits Proliferation and Induces Apoptosis Independently of Estrogen Receptors Alpha and Beta. *Cancer Res.* **2002**, *62* (13), 3691–3697.

(91) Mabjeesh, N. J.; Escuin, D.; LaVallee, T. M.; Pribluda, V. S.; Swartz, G. M.; Johnson, M. S.; Willard, M. T.; Zhong, H.; Simons, J. W.; Giannakakou, P. 2ME2 Inhibits Tumor Growth and Angiogenesis by Disrupting Microtubules and Dysregulating HIF. *Cancer Cell* **2003**, *3* (4), 363–375. https://doi.org/10.1016/S1535-6108(03)00077-1.

(92) Lin, H.-L.; Yang, M.-H.; Wu, C.-W.; Chen, P.-M.; Yang, Y.-P.; Chu, Y.-R.; Kao, C.-L.; Ku, H.-H.; Lo, J.-F.; Liou, J.-P.; Chi, C.-W.; Chiou, S.-H. 2-Methoxyestradiol Attenuates Phosphatidylinositol 3-Kinase/Akt Pathway-Mediated Metastasis of Gastric Cancer. *Int. J. Cancer* **2007**, *121* (11), 2547–2555. https://doi.org/10.1002/ijc.22963.

(93) Schumacher, G.; Kataoka, M.; Roth, J. A.; Mukhopadhyay, T. Potent Antitumor Activity of 2-Methoxyestradiol in Human Pancreatic Cancer Cell Lines. *Clin. Cancer Res. Off. J. Am. Assoc. Cancer Res.* **1999**, *5* (3), 493–499.

(94) Reiser, F.; Way, D.; Bernas, M.; Witte, M.; Witte, C. Inhibition of Normal and Experimental Angiotumor Endothelial Cell Proliferation and Cell Cycle Progression by 2-Methoxyestradiol. *Exp. Biol. Med.* **1998**, *219* (3), 211–216. https://doi.org/10.3181/00379727-219-44334.

(95) Li, L.; Bu, S.; Bäckström, T.; Landström, M.; Ulmsten, U.; Fu, X. Induction of Apoptosis and G2/M Arrest by 2-Methoxyestradiol in Human Cervical Cancer HeLaS3 Cells. *Anticancer Res.* **2004**, *24 (2B)*, 873–880.

(96) Joubert, A.; Maritz, C.; Joubert, F. Influence of Prostaglandin A2 and 2-Methoxyestradiol on Bax and Bcl-2 Expression Levels in Cervical Carcinoma Cells. *Biomed. Res.* **2005**, *26* (2), 87–90. https://doi.org/10.2220/biomedres.26.87.

(97) Montgomery, R. B.; Bonham, M.; Nelson, P. S.; Grim, J.; Makary, E.; Vessella, R.; Stahl, W. L. Estrogen Effects on Tubulin Expression and Taxane Mediated Cytotoxicity in Prostate Cancer Cells. *Prostate* **2005**, *65* (2), 141–150. https://doi.org/10.1002/pros.20246.

(98) Bu, S.; Blaukat, A.; Fu, X.; Heldin, N.-E.; Landström, M. Mechanisms for 2-Methoxyestradiol-Induced Apoptosis of Prostate Cancer Cells. *FEBS Lett.* **2002**, *531* (2), 141–151. https://doi.org/10.1016/S0014-5793(02)03478-6.

(99) Kinuya, S.; Kawashima, A.; Yokoyama, K.; Kudo, M.; Kasahara, Y.; Watanabe, N.; Shuke, N.; Bunko, H.; Michigishi, T.; Tonami, N. Anti-Angiogenic Therapy and Radioimmunotherapy in Colon Cancer Xenografts. *Eur. J. Nucl. Med.* **2001**, *28* (9), 1306–1312. https://doi.org/10.1007/s002590100585.

(100) Fotsis, T.; Zhang, Y.; Pepper, M. S.; Adlercreutz, H.; Montesano, R.; Nawroth, P. P.; Schweigerer, L. The Endogenous Oestrogen Metabolite 2-Methoxyoestradiol Inhibits Angiogenesis and Suppresses Tumour Growth. *Nature* **1994**, *368* (6468), 237–239. https://doi.org/10.1038/368237a0.

(101) Yue, T.-L.; Wang, X.; Louden, C. S.; Gupta, S.; Pillarisetti, K.; Gu, J.-L.; Hart, T. K.; Lysko, P. G.; Feuerstein, G. Z. 2-Methoxyestradiol, an Endogenous Estrogen Metabolite, Induces Apoptosis in Endothelial Cells and Inhibits Angiogenesis: Possible Role for Stress-Activated Protein Kinase Signaling Pathway and Fas Expression. *Mol. Pharmacol.* **1997**, *51* (6), 951–962. https://doi.org/10.1124/mol.51.6.951.

(102) Kumar, B. S.; Raghuvanshi, D. S.; Hasanain, M.; Alam, S.; Sarkar, J.; Mitra, K.; Khan, F.; Negi, A. S. Recent Advances in Chemistry and Pharmacology of 2-Methoxyestradiol: An Anticancer Investigational Drug. *Steroids* **2016**, *110*, 9–34. https://doi.org/10.1016/j.steroids.2016.03.017.

(103) Mueck, A. O.; Seeger, H. 2-Methoxyestradiol—Biology and Mechanism of Action. *Steroids* **2010**, *75* (10), 625–631. https://doi.org/10.1016/j.steroids.2010.02.016.

(104) Qadan, L. R.; Perez-Stable, C. M.; Anderson, C.; D'Ippolito, G.; Herron, A.; Howard, G. A.; Roos, B. A. 2-Methoxyestradiol Induces G2/M Arrest and Apoptosis in Prostate Cancer. *Biochem. Biophys. Res. Commun.* **2001**, *285* (5), 1259–1266. https://doi.org/10.1006/bbrc.2001.5320.

(105) D'Amato, R. J.; Lin, C. M.; Flynn, E.; Folkman, J.; Hamel, E. 2-Methoxyestradiol, an Endogenous Mammalian Metabolite, Inhibits Tubulin Polymerization by Interacting at the Colchicine Site. *Proc. Natl. Acad. Sci.* **1994**, *91* (9), 3964–3968. https://doi.org/10.1073/pnas.91.9.3964.

(106) Choi, H. J.; Zhu, B. T. Critical Role of Cyclin B1/Cdc2 up-Regulation in the Induction of Mitotic Prometaphase Arrest in Human Breast Cancer Cells Treated with 2-Methoxyestradiol. *Biochim. Biophys. Acta BBA - Mol. Cell Res.* **2012**, *1823* (8), 1306–1315. https://doi.org/10.1016/j.bbamcr.2012.05.003.

(107) Sibonga, J. D.; Lotinun, S.; Evans, G. L.; Pribluda, V. S.; Green, S. J.; Turner, R. T. Dose-Response Effects of 2-Methoxyestradiol on Estrogen Target Tissues in the Ovariectomized Rat. *Endocrinology* **2003**, *144* (3), 785–792. https://doi.org/10.1210/en.2002-220632.

(108) Harrison, M. R.; Hahn, N. M.; Pili, R.; Oh, W. K.; Hammers, H.; Sweeney, C.; Kim, K.; Perlman, S.; Arnott, J.; Sidor, C.; Wilding, G.; Liu, G. A Phase II Study of 2-Methoxyestradiol (2ME2) NanoCrystal® Dispersion (NCD) in Patients with Taxane-Refractory, Metastatic Castrate-Resistant Prostate Cancer (CRPC). *Invest. New Drugs* **2011**, *29* (6), 1465–1474. https://doi.org/10.1007/s10637-010-9455-x.

(109) Rajkumar, S. V.; Richardson, P. G.; Lacy, M. Q.; Dispenzieri, A.; Greipp, P. R.; Witzig, T. E.; Schlossman, R.; Sidor, C. F.; Anderson, K. C.; Gertz, M. A. Novel Therapy with 2-Methoxyestradiol for the Treatment of Relapsed and Plateau Phase Multiple Myeloma. *Clin. Cancer Res.* **2007**, *13* (20), 6162–6167. https://doi.org/10.1158/1078-0432.CCR-07-0807.

(110) Matei, D.; Schilder, J.; Sutton, G.; Perkins, S.; Breen, T.; Quon, C.; Sidor, C. Activity of 2 Methoxyestradiol (Panzem ® NCD) in Advanced, Platinum-Resistant Ovarian Cancer and Primary Peritoneal Carcinomatosis: A Hoosier Oncology Group Trial. *Gynecol. Oncol.* **2009**, *115* (1), 90–96. https://doi.org/10.1016/j.ygyno.2009.05.042.

(111) Panchapakesan, G.; Dhayalan, V.; Dhatchana Moorthy, N.; Saranya, N.; Mohanakrishnan, A. K. Synthesis of 2-Substituted 17β-Hydroxy/17-Methylene Estratrienes and Their in Vitro Cytotoxicity in Human Cancer Cell Cultures. *Steroids* **2011**, *76* (13), 1491–1504. https://doi.org/10.1016/j.steroids.2011.08.004.

(112) Agoston, G. E.; Shah, J. H.; LaVallee, T. M.; Zhan, X.; Pribluda, V. S.; Treston, A. M. Synthesis and Structure–Activity Relationships of 16-Modified Analogs of 2-Methoxyestradiol. *Bioorg. Med. Chem.* **2007**, *15* (24), 7524–7537. https://doi.org/10.1016/j.bmc.2007.09.011.

(113) Sathish Kumar, B.; Kumar, A.; Singh, J.; Hasanain, M.; Singh, A.; Fatima, K.; Yadav, D. K.; Shukla, V.; Luqman, S.; Khan, F.; Chanda, D.; Sarkar, J.; Konwar, R.; Dwivedi, A.; Negi, A. S. Synthesis of 2-Alkoxy and 2-Benzyloxy Analogues of Estradiol as Anti-Breast Cancer Agents through Microtubule Stabilization. *Eur. J. Med. Chem.* **2014**, *86*, 740–751. https://doi.org/10.1016/j.ejmech.2014.09.033.

(114) Sheng, L.-X.; Zhang, J.-Y.; Li, L.; Xie, X.; Wen, X.-A.; Cheng, K.-G. Design, Synthesis, and Evaluation of Novel 2-Methoxyestradiol Derivatives as Apoptotic Inducers through an Intrinsic Apoptosis Pathway. *Biomolecules* **2020**, *10* (1), 123. https://doi.org/10.3390/biom10010123.

(115) Dohle, W.; Jourdan, F. L.; Menchon, G.; Prota, A. E.; Foster, P. A.; Mannion, P.; Hamel, E.; Thomas, M. P.; Kasprzyk, P. G.; Ferrandis, E.; Steinmetz, M. O.; Leese, M. P.; Potter, B. V. L. Quinazolinone-Based Anticancer Agents: Synthesis, Antiproliferative SAR, Antitubulin Activity, and Tubulin Co-Crystal Structure. *J. Med. Chem.* **2018**, *61* (3), 1031–1044. https://doi.org/10.1021/acs.jmedchem.7b01474.

(116) Hilder, T. A.; Hodgkiss, J. M. Molecular Mechanism of Binding between 17β-Estradiol and DNA. *Comput. Struct. Biotechnol. J.* **2017**, *15*, 91–97. https://doi.org/10.1016/j.csbj.2016.12.001.

(117) Carey, L. Old Drugs, New Tricks for Triple-Negative Breast Cancer. *Lancet Oncol.* **2015**, *16* (4), 357–359. https://doi.org/10.1016/S1470-2045(15)70108-7.

(118) Koh, W.-J.; Abu-Rustum, N. R.; Bean, S.; Bradley, K.; Campos, S. M.; Cho, K. R.; Chon, H. S.; Chu, C.; Clark, R.; Cohn, D.; Crispens, M. A.; Damast, S.; Dorigo, O.; Eifel, P. J.; Fisher, C. M.; Frederick, P.; Gaffney, D. K.; Han, E.; Huh, W. K.; Lurain, J. R.; Mariani, A.; Mutch, D.; Nagel, C.; Nekhlyudov, L.; Fader, A. N.; Remmenga, S. W.; Reynolds, R. K.; Tillmanns, T.; Ueda, S.; Wyse, E.; Yashar, C. M.; McMillian, N. R.; Scavone, J. L. Cervical Cancer, Version 3.2019, NCCN Clinical Practice Guidelines in Oncology. *J. Natl. Compr. Canc. Netw.* **2019**, *17* (1), 64–84. https://doi.org/10.6004/jnccn.2019.0001.

(119) Hu, X.-C.; Zhang, J.; Xu, B.-H.; Cai, L.; Ragaz, J.; Wang, Z.-H.; Wang, B.-Y.; Teng, Y.-E.; Tong, Z.-S.; Pan, Y.-Y.; Yin, Y.-M.; Wu, C.-P.; Jiang, Z.-F.; Wang, X.-J.; Lou, G.-Y.; Liu, D.-G.; Feng, J.-F.; Luo, J.-F.; Sun, K.; Gu, Y.-J.; Wu, J.; Shao, Z.-M. Cisplatin plus Gemcitabine versus Paclitaxel plus Gemcitabine as First-Line Therapy for Metastatic Triple-Negative Breast Cancer (CBCSG006): A Randomised, Open-Label, Multicentre, Phase 3 Trial. *Lancet Oncol.* **2015**, *16* (4), 436–446. https://doi.org/10.1016/S1470-2045(15)70064-1.

(120) Minorics, R.; Bózsity, N.; Molnár, J.; Wölfling, J.; Mernyák, E.; Schneider, G.; Ocsovszki, I.; Zupkó, I. A Molecular Understanding of D -Homoestrone-Induced G2/M Cell Cycle Arrest in HeLa Human Cervical Carcinoma Cells. *J. Cell. Mol. Med.* **2015**, *19* (10), 2365–2374. https://doi.org/10.1111/jcmm.12587.

(121) Mernyák, E.; Huber, J.; Szabó, J.; Schneider, G.; Hetényi, A.; Márk, L.; Maász, G.; Berényi, Á.; Kovács, I.; Minorics, R.; Zupkó, I.; Wölfling, J. Cycloaddition of Steroidal Cyclic Nitrones to CN Dipolarophiles: Stereoselective Synthesis and Antiproliferative Effects of Oxadiazolidinones in the Estrone Series. *Steroids* **2013**, *78* (10), 1021–1028. https://doi.org/10.1016/j.steroids.2013.06.009.

(122) Pistritto, G.; Trisciuoglio, D.; Ceci, C.; Garufi, A.; D'Orazi, G. Apoptosis as Anticancer Mechanism: Function and Dysfunction of Its Modulators and Targeted Therapeutic Strategies. *Aging* **2016**, *8* (4), 603–619. https://doi.org/10.18632/aging.100934.

(123) Savill, J.; Fadok, V. Corpse Clearance Defines the Meaning of Cell Death. *Nature* **2000**, *407* (6805), 784–788. https://doi.org/10.1038/35037722.

(124) Kurosaka, K.; Takahashi, M.; Watanabe, N.; Kobayashi, Y. Silent Cleanup of Very Early Apoptotic Cells by Macrophages. *J. Immunol.* **2003**, *171* (9), 4672–4679. https://doi.org/10.4049/jimmunol.171.9.4672.

(125) Scaffidi, P.; Misteli, T.; Bianchi, M. E. Release of Chromatin Protein HMGB1 by Necrotic Cells Triggers Inflammation. *Nature* **2002**, *418* (6894), 191–195. https://doi.org/10.1038/nature00858.

(126) Silva, M. T. Secondary Necrosis: The Natural Outcome of the Complete Apoptotic Program. *FEBS Lett.* **2010**, *584* (22), 4491–4499. https://doi.org/10.1016/j.febslet.2010.10.046.

(127) Eger, A.; Mikulits, W. Models of Epithelial–Mesenchymal Transition. *Drug Discov. Today Dis. Models* **2005**, *2* (1), 57–63. https://doi.org/10.1016/j.ddmod.2005.04.001.

(128) Dent, R.; Hanna, W. M.; Trudeau, M.; Rawlinson, E.; Sun, P.; Narod, S. A. Pattern of Metastatic Spread in Triple-Negative Breast Cancer. *Breast Cancer Res. Treat.* **2009**, *115* (2), 423–428. https://doi.org/10.1007/s10549-008-0086-2.

(129) Nabeshima, K.; Inoue, T.; Shimao, Y.; Sameshima, T. Matrix Metalloproteinases in Tumor Invasion: Role for Cell Migration. *Pathol. Int.* **2002**, *52* (4), 255–264. https://doi.org/10.1046/j.1440-1827.2002.01343.x.

(130) Cancemi, P.; Buttacavoli, M.; Roz, E.; Feo, S. Expression of Alpha-Enolase (ENO1), Myc Promoter-Binding Protein-1 (MBP-1) and Matrix Metalloproteinases (MMP-2 and MMP-9) Reflect the Nature and Aggressiveness of Breast Tumors. *Int. J. Mol. Sci.* **2019**, *20* (16), 3952. https://doi.org/10.3390/ijms20163952.

(131) Li, H.; Qiu, Z.; Li, F.; Wang, C. The Relationship between MMP-2 and MMP-9 Expression Levels with Breast Cancer Incidence and Prognosis. *Oncol. Lett.* **2017**. https://doi.org/10.3892/ol.2017.6924.

(132) McLean, G. W.; Carragher, N. O.; Avizienyte, E.; Evans, J.; Brunton, V. G.; Frame, M. C. The Role of Focal-Adhesion Kinase in Cancer — a New Therapeutic Opportunity. *Nat. Rev. Cancer* **2005**, *5* (7), 505–515. https://doi.org/10.1038/nrc1647.

(133) Miyazaki, T.; Kato, H.; Nakajima, M.; Sohda, M.; Fukai, Y.; Masuda, N.; Manda, R.; Fukuchi, M.; Tsukada, K.; Kuwano, H. FAK Overexpression Is Correlated with Tumour Invasiveness and Lymph Node Metastasis in Oesophageal Squamous Cell Carcinoma. *Br. J. Cancer* **2003**, *89* (1), 140–145. https://doi.org/10.1038/sj.bjc.6601050.

(134) Recher, C.; Ysebaert, L.; Beyne-Rauzy, O.; Mansat-De Mas, V.; Ruidavets, J.-B.; Cariven, P.; Demur, C.; Payrastre, B.; Laurent, G.; Racaud-Sultan, C. Expression of Focal Adhesion Kinase in Acute Myeloid Leukemia Is Associated with Enhanced Blast Migration, Increased Cellularity, and Poor Prognosis. *Cancer Res.* **2004**, *64* (9), 3191–3197. https://doi.org/10.1158/0008-5472.CAN-03-3005.

(135) Lightfoot, H. M.; Lark, A.; Livasy, C. A.; Moore, D. T.; Cowan, D.; Dressler, L.; Craven, R. J.; Cance, W. G. Upregulation of Focal Adhesion Kinase (FAK) Expression in Ductal Carcinoma in Situ (DCIS) Is an Early Event in Breast Tumorigenesis. *Breast Cancer Res. Treat.* **2004**, *88* (2), 109–116. https://doi.org/10.1007/s10549-004-1022-8.

(136) Parsons, J. T.; Martin, K. H.; Slack, J. K.; Taylor, J. M.; Weed, S. A. Focal Adhesion Kinase: A Regulator of Focal Adhesion Dynamics and Cell Movement. *Oncogene* **2000**, *19* (49), 5606–5613. https://doi.org/10.1038/sj.onc.1203877.

(137) Wu, H.-J.; Hao, M.; Yeo, S. K.; Guan, J.-L. FAK Signaling in Cancer-Associated Fibroblasts Promotes Breast Cancer Cell Migration and Metastasis by Exosomal MiRNAs-Mediated Intercellular Communication. *Oncogene* **2020**, *39* (12), 2539–2549. https://doi.org/10.1038/s41388-020-1162-2.

8. Acknowledgements

I would like to express my special thanks to my supervisor István Zupkó D.Sc., who helped and supported my work since the start of my student researcher years in 2013. I am very grateful to Professor Hui-Chun Wang, who aided my research for six months at the Graduate Institute of Natural Products in Taiwan.

I would like to offer my thanks for all the help of my former colleagues at the Institute of Pharmacodynamics and Biopharmacy of Szeged, and at the Graduate Institute of Natural Products of Kaohsiung. My sincere thanks to Imre Ocsovszki for performing flow cytometry analysis; moreover, to the Department of Organic Chemistry of Szeged, especially to Professor Gyula Schneider, Erzsébet Mernyák Ph.D., and Anita Kiss Ph.D. for designing and synthesizing the examined molecules of my work.

I gratefully acknowlege the financial support from the Economic Development and Innovation Operative Programs, Taiwan Ministry of Science and Technology Grant, and Campus Mundi Scholarship which made the opportunity to spend six months at Kaohsiung Medical University, Taiwan.

Last, but not least, I am extremely grateful to my family and friends for their understanding and support through the years of my Ph.D. studies.

Appendix

I.

European Journal of Pharmaceutical Sciences 123 (2018) 362–370

Contents lists available at ScienceDirect

European Journal of Pharmaceutical Sciences

journal homepage: www.elsevier.com/locate/ejps

Antiproliferative and antimetastatic properties of 3-benzyloxy-16-hydroxymethylene-estradiol analogs against breast cancer cell lines

Izabella Sinka[a], Anita Kiss[b], Erzsébet Mernyák[b], János Wölfling[b], Gyula Schneider[b], Imre Ocsovszki[c], Ching-Ying Kuo[d], Hui-Chun Wang[d], István Zupkó[a,e,*]

[a] Department of Pharmacodynamics and Biopharmacy, University of Szeged, Szeged, Hungary
[b] Department of Organic Chemistry, University of Szeged, Szeged, Hungary
[c] Department of Biochemistry, University of Szeged, Szeged, Hungary
[d] Graduate Institute of Natural Products, Kaohsiung Medical University, Kaohsiung City, Taiwan
[e] Interdisciplinary Centre for Natural Products, University of Szeged, Szeged, Hungary

ARTICLE INFO

Keywords:
Breast cancer cells
Estradiol analog
Anticancer action
Antimetastatic action
Focal adhesion kinase

ABSTRACT

Despite emerging new therapeutic opportunities, cancer is still a major health problem and a leading cause of death worldwide. Breast tumors are the most frequently diagnosed female malignancies, and the triple-negative subtype is associated with poorer prognosis and lower survival rates than other breast cancer types. The aims of the present study were to determine the anticancer potency of a set of C-3 and C-16 modified estradiol-derivatives against a panel of breast cancer cell lines, and to characterize the mechanism of action of two selected compounds (**1** and **5**) against the MDA-MB-231 triple-negative breast cancer cell line. Growth-inhibitory properties were investigated by an MTT-assay. Cell cycle analysis by flow cytometry has revealed G1 phase accumulation and indicated the proapoptotic effect of **1** and **5** through the elevation of the apoptotic subG1 phase on MDA-MB-231 cells after 24 h treatment. The antimetastatic activities of these compounds were examined by wound healing and Boyden chamber assays, and both compounds were shown to significantly inhibit the migration and invasion of MDA-MB-231 cells at sub-antiproliferative concentrations. Gelatin zymography assay has indicated that matrix metalloproteinase-2 and -9 are not involved in the antimetastatic action of the molecules. Western blot analysis was performed with 24 h incubation to examine the possible changes in the level of focal adhesion kinase (FAK), and both compounds were found to inhibit the phosphorylation of FAK in a concentration-dependent manner in MDA-MB-231 cells. The results of this study demonstrate that C-3 and C-16 modified estradiol derivatives are potent antiproliferative and antimetastatic compounds against a triple-negative breast cancer cell line with a mechanism of action involving the inhibition of FAK, a novel anticancer therapeutic target. Therefore, these findings can be utilized in the development of promising anticancer agents with steroid skeleton.

1. Introduction

Cancer is a crucial cause of morbidity and mortality worldwide, with the incidence of malignant diseases rising both in highly developed and less developed countries. In 2012, 14.1 million new patients and 8.2 million cancer-related deaths were estimated globally, and > 3.14 million new cancer cases were diagnosed in Europe. Amongst women, the most common cancer type is breast cancer, characterized by the highest incidence and mortality rates, comprising 25% of all diagnosed cancer cases and causing 15% of all cancer-related deaths (Steliarova-Foucher et al., 2015; Torre et al., 2015).

Triple-negative breast cancer (TNBC) is a subtype of breast tumors described by the downregulation of estrogen receptor (ER), progesterone receptor (PR) and human epidermal growth factor receptor 2 (HER2). Approximately 15–20% of all breast cancers are triple-negative tumors, and this subtype is responsible for 25% of breast cancer-related deaths (Lee and Djamgoz, 2018). TNBC patients are typically 5–10 years younger than other breast cancer patients at the time of diagnosis (Newman et al., 2015). Indicators for the aggressive behavior of TNBC include a high recurrence rate and faster metastatic spread, leading to poorer prognosis amongst all breast cancer subtypes. Regarding recurrence, the secondary tumor usually occurs within 5 years from the initial diagnosis, with the brain and viscera being affected more often than in case of non-TNBC primaries which usually cause

* Corresponding author at: Department of Pharmacodynamics and Biopharmacy, University of Szeged, Szeged, Eötvös u. 6, Szeged H-6720, Hungary.
E-mail address: zupko@pharm.u-szeged.hu (I. Zupkó).

https://doi.org/10.1016/j.ejps.2018.07.029
Received 20 March 2018; Received in revised form 22 May 2018; Accepted 12 July 2018
0928-0987/ © 2018 Elsevier B.V. All rights reserved.

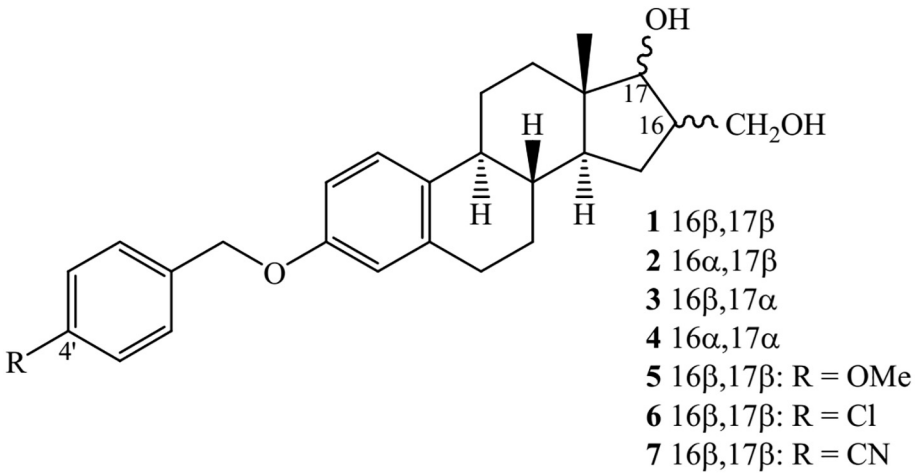

Fig. 1. Chemical structures of the synthesized and investigated estradiol analogs.

metastasis to bone. Compared to other subtypes, TNBC has a shorter median time to death (4.2 vs. 6 years) and worse overall survival. Both of these basic triple-negative features and the possible molecular diversity within TNBCs hamper the development of targeted therapies. Although several novel pharmacological groups of drugs, like poly (ADP-ribose) polymerase inhibitors and immunotherapeutic agents have shown promising results in clinical trials, developing specified treatment for TNBC is still an urgent unmet medical need (Lee and Djamgoz, 2018; Lin et al., 2008).

Estrogens have an essential influence on the evolution of reproductive processes. Furthermore, they play a role in the development of hormone-dependent tumors of the reproductive organs, such as breast, ovarian, endometrial, uterine and prostate cancers (Ascenzi et al., 2006; Chen et al., 2008; Nelles et al., 2011; Pearce and Jordan, 2004). Although the proliferation-stimulating activity of 17β-estradiol is well-established, numerous studies have also investigated the anticancer potential of structurally modified estrogen derivatives (Bodnár et al., 2016; Cadot et al., 2007; Cushman et al., 1997; Jourdan et al., 2011; Mernyák et al., 2014; Mernyák et al., 2015; Möller et al., 2009; Szabó et al., 2016).

A fundamental requirement for estrane-based anticancer drug candidates is the lack of their hormonal activity. Certain structural modifications, such as substitution at C-2 or C-3 of the estrane skeleton lead to the loss of the estrogenic properties of the compounds (Anstead et al., 1997; Cushman et al., 1997; Wölfling et al., 2003). Additionally, modification of the D-ring of the estrange skeleton leading to D-homo and D-seco derivatives results complete loss of estrogenic activity (Jovanovic-Santa et al., 2003; Jovanovic-Santa et al., 2015). Moreover, some of such agents may additionally interact with the enzyme aromatase (CYP1A19) indicating a secondary way of intervention in the estrogen-dependent proliferative disorders including gynecological cancers, endometriosis (Trifunovic et al., 2017).

In a previous study, the binding abilities of possible isomers of 16-hydroxymethyl-3,17-estradiol to estrogen receptor were investigated by radioligand-binding assay, utilizing receptor protein prepared from rabbit uteri. The relative binding affinities (RBA) of each estradiol derivative was lower than 2.0% of that of estradiol, indicating that the introduction of a 16-hydroxymethyl group abolishes the affinity independently of its configuration (Tapolcsányi et al., 2002). Consequently, the presence of a hydroxymethylene group at C-16 is detrimental concerning the estrogenic activity of the tested compounds. Based on these preliminary findings, it can be stated that the 16-hydroxymethylene-3,17-estradiol core might be suitable for the design of biologically active estrone derivatives lacking hormonal activity.

We have recently reported that the presence of a 3-benzyl ether function on the estrane core may enhance the antiproliferative potential of the steroid (Mernyák et al., 2014; Mernyák et al., 2015). In order to combine the structural moieties responsible for an increase in the antiproliferative and a decrease in the estrogenic actions, here we have synthesized additional 3-benzyl ethers bearing electronically different substituents at the 4′-position.

The aim of the current investigation was to characterize the anticancer properties of these 16-hydroxymethyl-estradiol analogs on a panel of breast cancer cell lines in vitro. The most promising agents were selected for further analyses in order to describe the mechanism of the action against the MDA-MB-231 triple-negative breast cancer cell line. Although the hormonal receptor status of the utilized cell lines was different we aimed to describe hormone-independent antiproliferative properties. The effects of the selected molecules on cancer cell migration were also evaluated.

2. Materials and methods

2.1. Chemicals

The four possible stereoisomers of 3-benzyloxy-16-hydroxymethylene-estra-1,3,5(10)-trien-17-ol (**1**–**4**) were synthesized and characterized as reported previously (Tapolcsányi et al., 2002). Three further analogs with a substituted benzyl function at C-3 have also been prepared (**5**–**7**). The synthesis and chemical characterization of the molecules are available as Supplementary material (Fig. 1).

2.2. Cell cultures

Human breast cancer cell lines, including MCF7, T47D, MDA-MB-231 and MDA-MB-361, as well as non-cancerous fibroblasts (MRC-5) were purchased from the European Collection of Authenticated Cell Cultures (ECACC, Salisbury, UK). All cell lines were maintained in minimal essential medium (MEM) supplemented with 10% fetal bovine serum, 1% non-essential amino acids and 1% antibiotic-antimycotic mixture, and were stored in humidified air containing 5% CO_2 at 37 °C. All utilized components were obtained from Lonza Group Ltd. (Basel, Switzerland).

2.3. Determination of antiproliferative activities

To determine the antiproliferative action of the tested compounds against four malignant breast cancer cell lines (MCF-7, T47D, MDA-MB-231 and MDA-MB-361), an MTT (3-(4,5-dimethylthiazol-2-yl)-2,5-diphenyltetrazolium bromide) assay was carried out. Cells were seeded at a density of 5000 cells/well into 96-well plates (in the case of MDA-MB-361 10,000 cells/well), treated with increasing concentrations of 16-

hydroxymethyl-estranes (0.1–30.0 μM) under cell culturing conditions for 72 h. At the end of incubation, 5 mg/ml MTT solution was added to the samples. Precipitated formazan crystals were solubilized in dimethyl sulfoxide and absorbance was measured at 545 nm with a microplate reader. Wells containing untreated cells were used as control (Mosmann, 1983).

Based on these results, sigmoidal dose-response curves were fitted and IC_{50} values were calculated using GraphPad Prism 5.01 (GraphPad Software, San Diego, CA, USA). The growth-inhibitory effects of the tested compounds were compared to cisplatin (Ebewe Pharma GmbH, Unterach, Austria) in the same concentration range. MRC-5 human fibroblasts were also examined by the same method to verify the selectivity of the test compounds towards cancer.

2.4. Cell cycle analysis by flow cytometry

Cellular DNA content was determined by flow cytometry. MDA-MB-231 cells were seeded into 6-well plates at a density of 250,000–300,000 cells/well. After 24 h incubation cells were washed with phosphate-buffered saline (PBS) and gathered with trypsin. The samples were centrifuged at 1500 rpm for 10 min, additionally washed and centrifuged again, and fixed in 1 ml of 70% ethanol, −20 °C, for at least 30 min. The dye solution (0.1 mg/ml PI, 0.003 μl/ml Triton-X, 0.02 mg/ml RNase A, and 1.0 mg/ml sodium citrate dissolved in distilled water) was then added to the samples for 60 min. The cell cycle analysis was carried out by a Partec CyFlow instrument (Partec GmbH, Münster, Germany). In all measurements, 20,000 cells were analyzed. The percentages of cells in different cell cycle phases (subG1, G1, S and G2/M) were determined by the ModFit LT software (Verity Software House, Topsham, ME, USA). The subG1 fraction was considered as the apoptotic cell population (Vermes et al., 2000).

2.5. Wound healing assay

The action of the selected compounds on cell migration was assessed by a wound healing assay. The assay was performed with specific wound assay chambers (ibidi GmbH, Martinsried, Germany). MDA-MB-231 cells were trypsinized and 25,000 cells were seeded into each chamber of the inserts. After an overnight incubation for appropriate cell attachment at 37 °C under 5% CO_2, the culture insert was removed. A washing step with PBS was performed to remove non-adherent cells and debris. Cells were treated with increasing concentrations of each test compound in a medium containing 2% FBS for 24 h. Migration of the cells to the wound site was visualized by a phase-contrast inverted microscope (Axiovert 40, Zeiss, Thornwood, NY, US). Images were taken by a CCD camera at planned intervals to assess wound closure. The rate of migration was calculated as the ratio of wound closure in treated samples after 24 h and 0 h, respectively, as compared with the ratio of the wound closure in untreated control samples after 24 h and 0 h, respectively (Bózsity et al., 2017).

2.6. Boyden chamber assay

Invasion ability of MDA-MB-231 cells was investigated by a BD BioCoat Matrigel Invasion Chamber (BD Biosciences, Bedford, MA, USA) containing an 8 μm pore size PET membrane and a thin layer of matrigel basement matrix. Fifty thousand cells were suspended in serum-free medium and were injected into the top insert before the tested compounds were added in sub-antiproliferative concentrations. A medium containing 10% FBS was used as chemoattractant in the bottom well. The inserts were removed after incubation for 24 h at 37 °C under 5% CO_2 and the upper surface of the membrane was cleaned from non-invading cells with a cotton swab. After a washing step with PBS, the insert was fixed with cold 100% methanol, washed with PBS again and stained with crystal violet solution. The invading and stained cells were counted under a phase-contrast inverted microscope. To determine the rate of invasion, the number of treated samples and untreated controls were counted and compared to each other.

2.7. Gelatin zymography assay

A gelatin zymography assay was utilized to determine how the test compounds affect the activities of matrix metalloprotease-2 (MMP-2) and −9 (Snoek-van Beurden and Von den Hoff, 2005). MDA-MB-231 cells were seeded in experimental dishes at approximately 80% confluency and were allowed to grow overnight. After a washing step with PBS the test compounds were added in serum-free medium and incubated for 24 h. Then the supernatant containing the secreted MMP-2 and MMP-9 enzymes were collected from above the cells and was centrifuged at 6000 rpm at 4 °C for 2 min, then collected again. Equal amounts of the samples mixed with bromophenol blue dye in 5:1 ratio were separated by SDS-PAGE containing 0.1% gelatin via electrophoresis at 120 V for 90 min. Major forms of MMPs were identified by Prism Ultra Protein Ladder molecular size marker (Abcam Cambridge, U.K.). The gel was washed twice by 2.5% Triton X-100 solution, then treated with the reaction solution containing 50 mM Tris-HCl (pH 7.5), 150 mM NaCl and 5 mM $CaCl_2$. After incubation for 24 h the gel was stained with Coomassie brilliant blue G-250 (SimplyBlue™ Safestain, Thermo Fisher Scientific, Waltham, MA, USA) for 60 min and washed by distilled water twice. Finally, the gel was captured by a Luminescent Image Analyzer System (LAS 4000 mini, Fujifilm, Tokyo, Japan).

2.8. Western blot assay

A Western Blot assay was performed to evaluate the antimetastatic properties of the examined compounds. Two million cells were seeded in small experimental dishes, and the tested compounds were added in medium containing 2% FBS the next day. Cells were detached from the dishes by a rubber policeman and centrifuged at 7000 rpm, 4 °C for 2 min, washed with PBS and centrifuged again. Whole cell extracts (WCEs) were prepared by re-suspending cells in TEGN lysis buffer (10 mM Tris pH 7.5, 1 mM EDTA, 420 mM NaCl, 10% glycerol and 0.5% NP40) supplemented with 1 mM DTT and a cocktail of protease and phosphatase inhibitor (Roche Applied Science, Penzberg, Germany). After 10 min on ice and centrifugation (13,000 rpm, 4 °C, 10 min) the protein content of the supernatant was mixed with bromophenol blue dye in 2:1 ratio. Equal amounts of WCEs were first separated by SDS-PAGE with electrophoresis for 1 h at 160 V, transferred onto nitrocellulose membranes for overnight at 20 V, 4 °C. Afterwards, the samples were blocked and incubated with a primary antibody followed by an appropriate secondary antibody. The antibodies utilized were FAK pY397 (Becton Dickinson, Franklin Lakes, NJ, USA), FAK (Cell Signaling Technology, Danvers, MA, USA), β-actin (Santa Cruz Biotechnology, Santa Cruz, CA, USA) and GAPDH (Cell Signaling Technology). Blots were visualized by enhanced chemiluminescence (ECL-Plus, GE Healthcare Life Sciences, Little Chalfont, UK) using a Luminescent Image Analyzer System.

2.9. Statistical analysis

GraphPad Prism 5.01 was used for the statistical evaluation of measured data in each experiment. To determine statistical significance, one-way ANOVA with Dunnett post-test for comparison of multiple groups was utilized. A p value < 0.05 was regarded as statistically significant.

3. Results

3.1. Antiproliferative activity of the tested compounds

Several 16-hydroxymethyl-estranes proved to be potent

Table 1
Antiproliferative effects of the tested compounds (**1–7**) on human breast cancer cell lines and MRC-5.

		Growth inhibition (%) ± SEM [calculated IC_{50} value (μM)[a]]				
		MDA-MB-231	MCF7	T47D	MDA-MB-361	MRC-5
1	10 μM	31.52 ± 1.82	60.16 ± 1.56	54.49 ± 0.27	93.07 ± 0.52	78.02 ± 2.63
	30 μM	94.90 ± 0.46	97.20 ± 0.41	89.95 ± 043	93.25 ± 1.09	96.50 ± 0.20
	IC_{50} (μM)	12.70	8.15	8.41	4.60	6.73
2	10 μM	93.82 ± 0.49	91.54 ± 0.56	82.73 ± 1.63	93.80 ± 0.70	94.78 ± 0.49
	30 μM	96.21 ± 0.34	97.83 ± 0.24	82.10 ± 0.50	93.98 ± 0.26	96.88 ± 0.21
	IC_{50} (μM)	3.91	5.05	4.58	3.81	5.53
3	10 μM	76.41 ± 0.65	27.02 ± 1.28	38.76 ± 2.02	62.73 ± 2.20	39.10 ± 3.23
	30 μM	92.17 ± 0.59	88.57 ± 1.23	90.29 ± 0.58	86.15 ± 0.93	92.63 ± 0.15
	IC_{50} (μM)	5.93	13.57	15.73	7.21	10.20
4	10 μM	84.34 ± 1.22	56.64 ± 2.23	47.49 ± 2.41	79.06 ± 2.70	53.67 ± 3.39
	30 μM	92.79 ± 0.26	86.85 ± 0.89	94.56 ± 0.73	89.85 ± 1.02	76.84 ± 2.19
	IC_{50} (μM)	5.47	9.05	10.44	5.38	7.33
5	10 μM	89.54 ± 0.82	96.46 ± 0.65	95.58 ± 0.26	81.08 ± 1.77	76.50 ± 2.28
	30 μM	87.73 ± 0.32	96.68 ± 0.17	95.26 ± 0.90	86.97 ± 1.26	79.75 ± 0.95
	IC_{50} (μM)	4.59	3.45	2.75	1.26	6.67
6	10 μM	61.13 ± 2.35	72.68 ± 0.79	80.22 ± 2.10	76.84 ± 1.24	61.03 ± 2.82
	30 μM	82.84 ± 0.92	89.08 ± 0.94	87.03 ± 1.45	81.08 ± 1.72	78.09 ± 1.79
	IC_{50} (μM)	7.48	4.24	2.98	4.65	1.46
7	10 μM	30.94 ± 2.42	39.34 ± 0.86	34.70 ± 1.42	n.d.	n.d.
	30 μM	68.82 ± 1.68	57.70 ± 0.75	52.69 ± 3.13		
	IC_{50} (μM)	n.d.	n.d.	n.d.		
Cisplatin	10 μM	20.84 ± 0.81	53.03 ± 2.29	51.00 ± 2.02	67.51 ± 1.01	60.25 ± 3.31
	30 μM	74.47 ± 1.20	86.90 ± 1.24	57.95 ± 1.45	87.75 ± 1.10	61.92 ± 1.01
	IC_{50} (μM)	19.13	5.78	9.78	3.74	6.19

n.d.: not determined.
[a] IC_{50} values were calculated from two experiments with 5 parallel wells if the growth inhibition of the compound was > 75% at 30 μM.

antiproliferative agents against various breast cancer cell lines. The calculated IC_{50} values representing their growth-inhibitory effects are presented in Table 1. As shown by our results, the configuration of the substituents at positions 16 and 17 play a limited role in the agents' antiproliferative properties. On the other hand, substituents, especially the *p*-methoxy group on the benzyl function at C-3 may enhance the anticancer potency. The compounds were additionally tested against the non-cancerous MRC-5 cells in order to obtain data concerning their selectivity towards cancer. In this regard, our compounds were not selective towards cancer cells but they were comparable to the reference agent cisplatin. Based on these results the analog with the lowest IC_{50} value (**5**) and its related, unsubstituted analog (**1**) were selected for additional investigations.

3.2. Cell cycle analysis by flow cytometry

In order to characterize the mechanism of action of the selected compounds against the MDA-MB-231 cell line, flow cytometry was carried out and the cell cycle phase distributions were analyzed after 24 h of incubation. The applied concentrations were determined based on the calculated IC_{50} values. Both compounds elicited a significant and concentration-dependent increase of the cell population in the G1 phase, on the expense of the reduction of those in the G2/M phase (Fig. 2). In spite of its substantially higher calculated IC_{50} **1** elicited remarkable cell cycle disturbance even at 5 μM. Additionally, **1** and **5** induced a modest but significant elevation of the hypodiploid (subG1) cell population at all the applied concentrations indicating the proapoptotic potential of these compounds.

3.3. Wound healing assay

As another means of investigating the anticancer activity of the tested estradiol derivatives, the possible motility inhibiting properties were examined by a wound healing assay. Migration of untreated MDA-MB-231 cells within the wound of the chambers was considered as 100% after 24 h incubation. Treatment with **1** and **5** significantly reduced the movement ability of MDA-MB-231 cells even at sub-antiproliferative concentrations (Fig. 3).

3.4. Boyden chamber assay

Besides the anti-migratory effect, the influence on the invasion

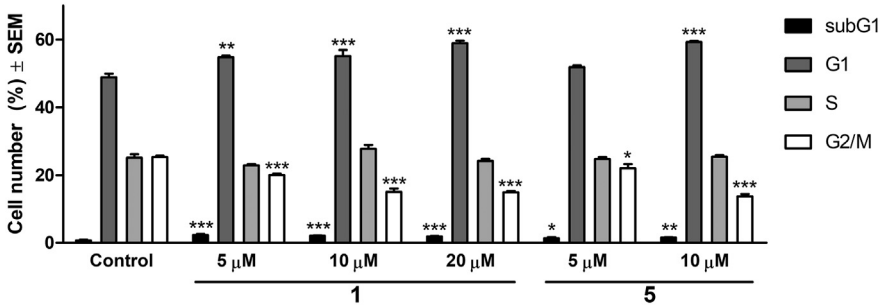

Fig. 2. Effects of compounds **1** and **5** on the MDA-MB-231 cell cycle after incubation for 24 h. Results are mean values ± SEM from three measurements. *, ** and *** indicates $p < 0.05$, $p < 0.01$ and $p < 0.001$ as compared t with the control cells, respectively.

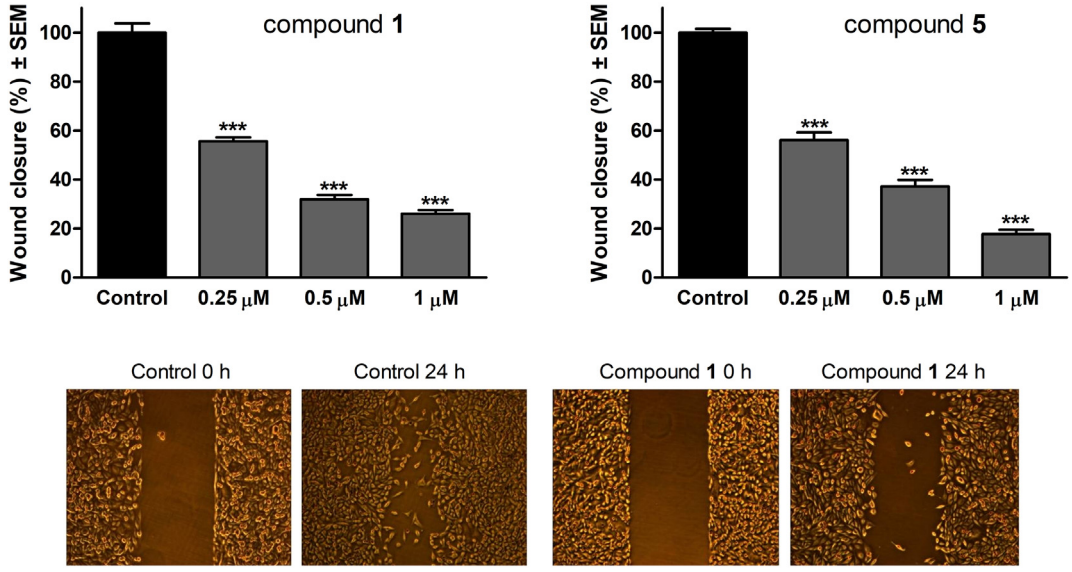

Fig. 3. Effects of compounds **1** and **5** on the migratory capacity of MDA-MB-231 cells (upper panels). The rates of the migration were evaluated after incubation for 24 h. Results are mean values ± SEM from three measurements *** indicates $p < 0.001$ as compared with the untreated control samples. Representative images of the migrating cells in 0 and 24 h (lower panels).

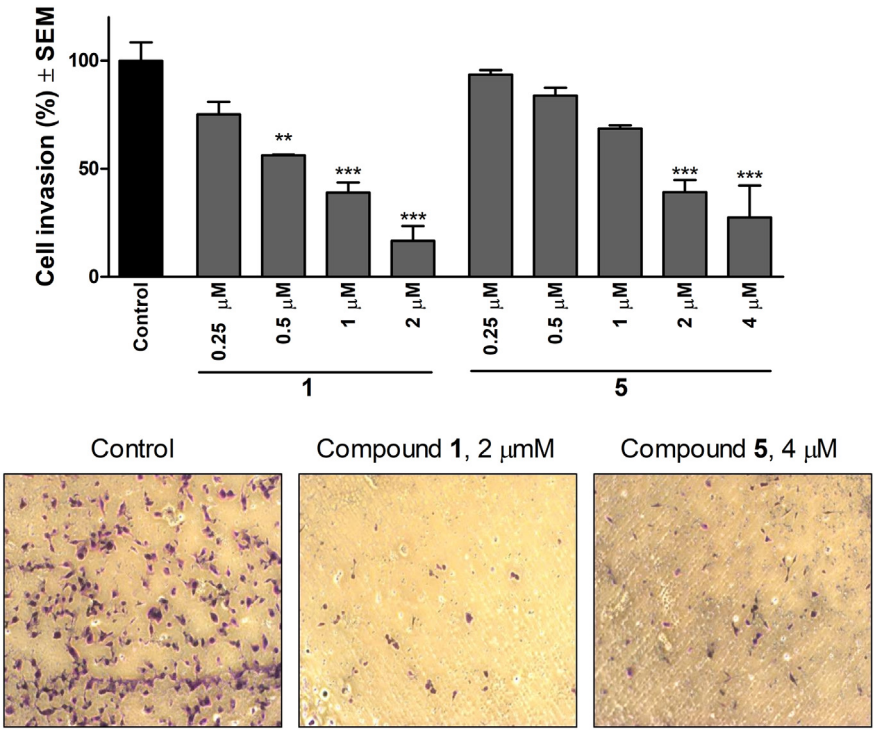

Fig. 4. Effects of compounds **1** and **5** on the cell-invasion capacity of MDA-MB-231 cells (upper panels). Statistical analyses of the percentage of invasive cells after incubation for 24 h with the test compounds. Results are mean values ± SEM from three measurements. *, ** and *** indicates $p < 0.05$, $p < 0.01$ and $p < 0.001$ as compared with the untreated control samples, respectively. Images from a visual field of one representative experiment (lower panels).

capacity of tumor cells is another important descriptor of the anti-metastatic property. The Matrigel Matrix-coated membrane (8.0 μm pore diameter) in Boyden chambers allows invasive cells to cross the membrane while it blocks the migration of non-invading cells. The invasion of MDA-MB-231 cells was found to be blocked by the compounds tested, in a concentration as low as 0.5 μM of **1** and 2 μM of **5**, and the effect size increased with higher concentrations (Fig. 4).

3.5. Gelatin zymography assay

In order to find a possible explanation for the metastasis-inhibitory effect of compounds **1** and **5**, the activities of released MMP-2 and MMP-9 were determined by a gelatin zymography assay. The active enzymes break down gelatin leaving a light patch on the blue background. None of our compounds exerted a significant influence on the activity of either MMP-2 or MMP-9 up to the concentrations of 2 μM (**1**) or 4 μM (**5**), suggesting that the antimetastatic activity of the tested compounds are independent of these enzymes (Fig. 5).

3.6. Western blot assay

The inhibition of focal adhesion kinase (FAK) and its phosphorylated form (pFAK) is another possible mechanism to block metastatic processes. Therefore the changes elicited by the tested compounds in the levels of proteins FAK and pFAK proteins were determined. Both compounds **1** (0.5–2 μM) and **5** (1–4 μM) reduced the level of phospho-

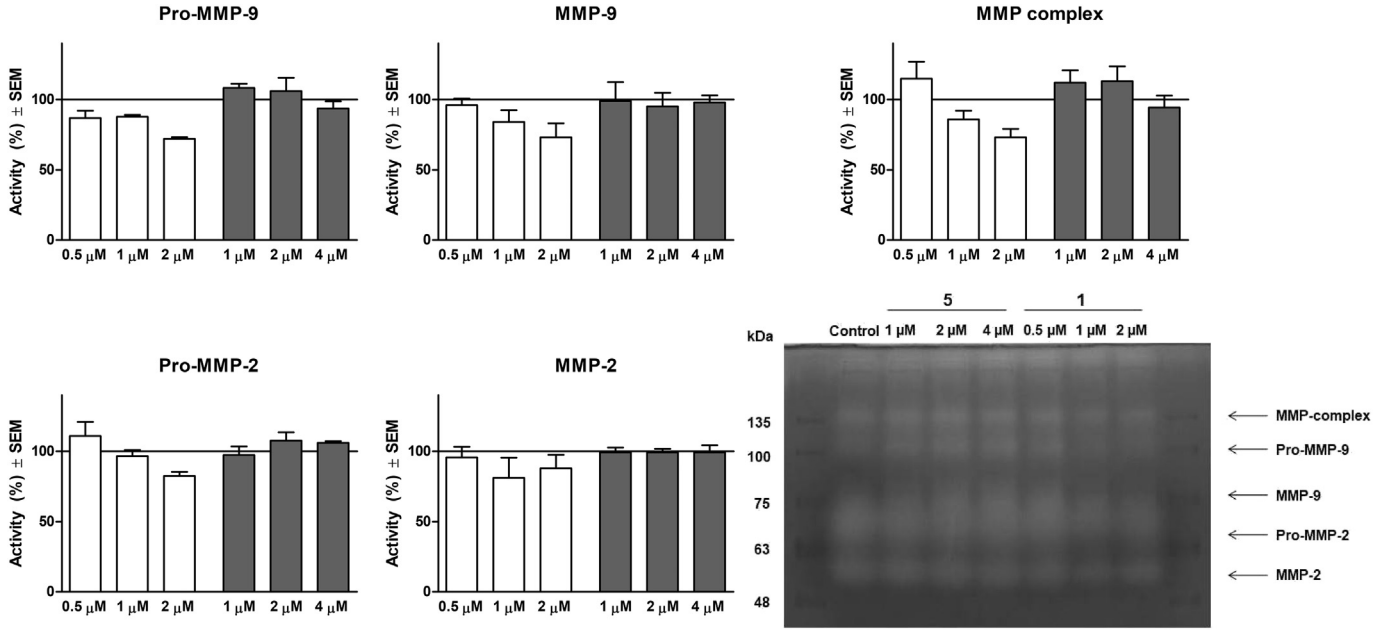

Fig. 5. Effects of compounds **1** and **5** on the activities of MMP-9 (pro-MMP-9, MMP-9 and its complex form) and MMP-2 (pro-MMP-2, MMP-2). Results are mean values ± SEM from three measurements. The activities presented in graphs are expressed as the % of vehicle control group. None of the treatment-related differences are significant. A representative zymogram (right bottom panel).

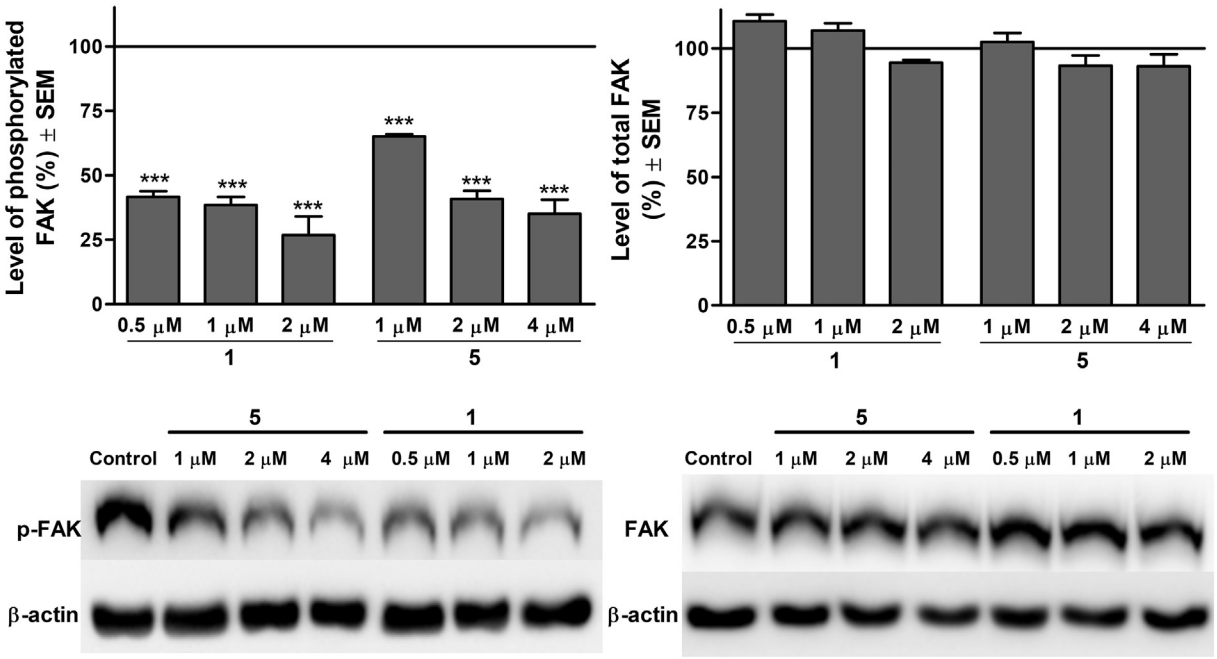

Fig. 6. Effects of compounds **1** and **5** on the expression of phosphorylated and total FAK protein in MDA-MB-231 cells (upper panels). Results are mean values ± SEM from three measurements. *** indicates $p < 0.001$ as compared with the untreated control samples. Representative results of the Western blot analysis (lower panels).

FAK in a concentration-dependent manner, without exerting any action on the total amount of FAK, indicating that the phosphorylation of FAK protein is inhibited by the compounds tested (Fig. 6).

4. Discussion

An endogenous derivative of 17β-estradiol (E2), 2-methoxyestradiol (2-ME) was discovered as the first estrane analog with potent growth-inhibitory effect, but without binding to the estrogen receptor (ER) (LaVallee et al., 2002). Since the possible mechanism of action, pharmacokinetic properties, selectivity and toxicity of 2-ME have been widely investigated, potential antiproliferative agents with an estrane skeleton are a new focus of the research and development of anticancer drug candidates (Kumar et al., 2016). Several studies have demonstrated that the antitumor mechanism of action of 2-ME comprises antiproliferative, antitubulin, antiangiogenic, antimetastatic and proapoptotic effects (Minorics and Zupkó, 2018; Pribluda et al., 2000; Zhu and Conney, 1998). Growth inhibition induced by 2-ME treatment in numerous malignant cell lines, including lung, colon, breast, prostate, eye, kidney, esophagus, stomach and pancreas cancers, as well as

tumors of the nervous system, melanoma, gynecologic malignancies, angiosarcoma and carcinoma of the musculature, was confirmed. Amongst the examined cell lines, breast carcinoma was found to be the most sensitive against 2-ME (Mueck and Seeger, 2010). It has been reported that its antiproliferative action against various cancer cell lines is mainly based on inducing blockade in the G2/M phase of cell cycle in various cancer cell lines (Carothers et al., 2002; Li et al., 2004; Pribluda et al., 2000; Qadan et al., 2001).

Treatment with 2-ME resulted in mitotic arrest in the prometaphase through the intense early up-regulation of cyclin B1 and Cdc2 proteins in both ER-positive and negative breast cancer cell lines. A close correlation was observed between the time-dependent variations of the prometaphase arrest and the level of the G2/M population. These results suggest not only the potent anti-microtubule effect of 2-ME but also demonstrate that this action is not influenced by the presence of estrogen receptor (Choi and Zhu, 2012). Despite 2-ME was well-tolerated in clinical trials, both as monotherapy and in combination with other anticancer agents, its activity was modest, even in a NanoCrystal Dispersion (NCD) formulation possessing more advantageous bioavailability (Harrison et al., 2011; Kumar et al., 2016; Matei et al., 2009). Despite this failure these studies showed that the modification of the estrane skeleton may yield promising anticancer agents. The structure of 2-ME has been recently utilized to design and synthesize a set of quinazolinone-based microtubule disruptors indicating the unexploited potency of the estrange skeleton as a base for innovative anticancer agents (Dohle et al., 2018).

Natural 17β-estradiol has been recently demonstrated to bind to DNA directly and that binding is not limited to the estrogen response element but it can affect random DNA sequences. This binding involves the intercalation of the steroid between base pairs of DNA, forming aromatic interactions with these base pairs (Hilder and Hodgkiss, 2017). These findings may serve as an explanation for the hormonal receptor independent character of a wide range of estrogen-related potential antiproliferative molecules including our present analogs.

Since the requirements of binding to the estrogen receptors are well-established, it is also known that a methlyl substitution at C-3 by itself is sufficient for the loss of the estrogenic activity (Anstead et al., 1997). Another opportunity to configure estrogen derivatives with low receptor binding affinities (RBA) is the specific substitution at C-16 with a polar or large group, such as hydroxymethyl. The compounds we examined contain a benzyloxy function at C-3 and a hydroxymethyl at C-16, therefore the lack of hormonal activity can be expected. This feature of the isomers of 16-hydroxymethyl-3,17-estradiol analogs was confirmed by radioligand-binding assays (Tapolcsányi et al., 2002). Previously we have reported on the antiproliferative action of estradiol-based compounds containing several distinct modifications at C-3 and C-16. The 16-triazole compounds of the 13α-estrone series were found to be effective against seven different cancer cell lines (Mernyák et al., 2015). Furthermore, a set of 16-hydroxymethyl-3-methoxy- and 16-hydroxymethyl-3-benzyloxy-13α-estradiol derivatives were demonstrated to exert potent anticancer activity against several gynecological cell lines (Kiss et al., 2018).

These previous accomplishments have encouraged us to continue the experiments with estradiol-derivatives, leading to the examination of the growth-inhibitory potential of a set of 16-hydroxymethyl-estradiols against various human adherent breast cancer cell lines.

Based on our data, the configurations of the substituents at positions 16–17 have a limited role in the agents' antiproliferative potency, while the benzyloxy function with *p*-substituent at position C-3 enhance the antiproliferative effect. Concerning the antiproliferative activities of the tested agents compound **5** proved to be the most potent and in terms of acting on non-cancerous cells it was comparable with cisplatin, which is currently used in breast cancer therapy protocols (Carey, 2015).

Although **5** and its precursor molecule **1** showed appreciable growth-inhibitory effects against all of the cell lines examined (MCF-7, MDA-MB-231, MDA-MB-361, T47D), our primary purpose was to characterize its effects and mechanism of action against MDA-MB-231, a triple-negative breast tumor cell line. In spite of the different receptorial status of the utilized cancer cell lines the IC_{50} values determined for a given agent were not crucially different. The aim of our study was to describe antiproliferative actions which are unrelated to receptorial status and our experimental system was optimized for this purpose. The medium contained phenol red which has some estrogenic action and it was also supplemented with usual fetal bovine serum instead of charcoal stripped fetal bovine serum which contains no residual steroids.

Performing cell cycle analyses by flow cytometry revealed that treatment with these agents caused G1 phase accumulation with significantly elevated apoptotic cell population. These results are in line with previously described G1 blockades by estradiol-related compounds such as two unsubstituted 16-oxime estrone analogues and oxadiazole derivatives of estrone (Berényi et al., 2013; Mernyák et al., 2013).

Approximately 90% of human cancer deaths are related to cancer metastases (Mehlen and Puisieux, 2006). This multi-step process involves local migration and invasion of tumor cells into adjacent tissues, entering into the vasculature, surviving and leaving the circulation system, with subsequent proliferation in distant organs that leads to colonization (Eger and Mikulits, 2005). Therefore, besides the cytotoxic and apoptosis-inducing approaches currently utilized in oncotherapy, innovative drugs with an antimetastatic capacity are eagerly needed to control cancer-related mortality. Besides their antiproliferative activity, the compounds tested in our experiments also inhibited cell migration and invasion, the initial steps of metastatic spread. Moreover, this significant reduction in cell migration was observed at a sub-antiproliferative concentration as low as 0.25 μM, after treatment for 24 h. The inhibitory action of compound **1** on cell invasion capacity proved to be more pronounced as determined by the Boyden chamber assay.

The role of matrix metalloproteinases (MMPs), a family of zinc-dependent endopeptidases have been extensively investigated, since their expression and activity are increased in almost all human cancer compared with normal tissue (Egeblad and Werb, 2002). The increased expression of MMP-2 and MMP-9 at the mRNA level was demonstrated in MDA-MB-231 cells compared to normal HS578Bst breast cells. Moreover, high expression of MMP-2 and MMP-9 in cancerous breast tissues has a close correlation with lymph node metastasis and tumor staging (Li et al., 2017). Based on our results of the gelatin zymography assay, none of the examined compounds influenced substantially the level of MMP-2 and MMP-9, indicating that these metalloproteinases are not crucially involved in the mechanism of action of **1** and **5**.

Focal adhesion kinase (FAK) is expressed in most cell types and tissues and has a complex function in various processes including cell spreading, differentiation, cell cycle, migration and cell death. The activation of FAK principally occurs via autophosphorylation on tyrosine 397 by clustering of integrins (McLean et al., 2005). Several studies have demonstrated its role in the regulation of cell migration. The up-regulation of FAK was reported in various cancer types, including malignancy of the breast, and its elevated activity correlates with metastatic spread and poor prognosis of the disease (Miyazaki et al., 2003; Recher et al., 2004). In breast cancer, FAK overexpression is regarded as an early event in tumorigenesis which precedes cell invasion and metastasis in ductal carcinoma in situ (DCIS) (Lightfoot Jr. et al., 2004). On the contrary, the lack of FAK-activity is reported to result in poor cell migration in response to chemotactic and haptotactic signals, while overexpression of FAK increases cell migration in Chinese hamster ovary (CHO) cells (Parsons et al., 2000). Our present compounds decreased the level of pFAK (Y397) in a concentration-dependent manner, whereas total FAK level was unaffected, demonstrating that the phosphorylation of the kinase enzyme was inhibited. These are the first reported estrogen-related compounds which proved to be effective in the inhibition of FAK phosphorylation.

In summary, our study revealed that 3-substituted C16-hydroxymethyl-estradiols are potent antiproliferative agents against breast

cancer cell lines. In MDA-MB-231 triple-negative cell lines 2 test compounds caused programmed cell death and G1 phase elevation. Furthermore, the molecules significantly and concentration-dependently inhibited cell migration and invasion, as well as the phosphorylation of focal adhesion kinase in sub-antiproliferative concentration. These results indicate that modified estradiol-derivatives can be regarded as promising candidates in the design of new anticancer agents.

Conflict of interest

The authors have no conflict of interest to declare.

Acknowledgments

The authors are grateful for financial support from the Hungarian Scientific Research Fund (OTKA K109293 and K113150). Financial support from the Economic Development and Innovation Operative Programs (GINOP-2.3.2-15-2016-00012 and GINOP-2.3.2-15-2016-00038) and Taiwan Ministry of Science and Technology Grant (MOST106-2911-I-037-504) is gratefully acknowledged.

Appendix A. Supplementary data

Supplementary data to this article can be found online at https://doi.org/10.1016/j.ejps.2018.07.029.

References

Anstead, G.M., Carlson, K.E., Katzenellenbogen, J.A., 1997. The estradiol pharmacophore: ligand structure-estrogen receptor binding affinity relationships and a model for the receptor binding site. Steroids 62, 268–303.
Ascenzi, P., Bocedi, A., Marino, M., 2006. Structure-function relationship of estrogen receptor alpha and beta: impact on human health. Mol. Asp. Med. 27, 299–402.
Berényi, A., Minorics, R., Iványi, Z., Ocsovszki, I., Ducza, E., Thole, H., Messinger, J., Wölfling, J., Mótyan, G., Mernyák, E., Frank, E., Schneider, G., Zupkó, I., 2013. Synthesis and investigation of the anticancer effects of estrone-16-oxime ethers in vitro. Steroids 78, 69–78.
Bodnár, B., Mernyák, E., Wölfling, J., Schneider, G., Herman, E.B., Szécsi, M., Sinka, I., Zupkó, I., Kupihár, Z., Kovács, L., 2016. Synthesis and biological evaluation of triazolyl 13α-estrone-nucleoside bioconjugates. Molecules 21, 1212.
Bózsity, N., Minorics, R., Szabó, J., Mernyák, E., Schneider, G., Wölfling, J., Wang, H.C., Wu, C.C., Ocsovszki, I., Zupkó, I., 2017. Mechanism of antiproliferative action of a new d-secoestrone-triazole derivative in cervical cancer cells and its effect on cancer cell motility. J. Steroid Biochem. Mol. Biol. 165, 247–257.
Cadot, C., Laplante, Y., Kamal, F., Luu-The, V., Poirier, D., 2007. C6-(N,N-butyl-methyl-heptanamide) derivatives of estrone and estradiol as inhibitors of type 1 17beta-hydroxysteroid dehydrogenase: chemical synthesis and biological evaluation. Bioorg. Med. Chem. 15, 714–726.
Carey, L., 2015. Old drugs, new tricks for triple-negative breast cancer. Lancet Oncol. 16, 357–359.
Carothers, A.M., Hughes, S.A., Ortega, D., Bertagnolli, M.M., 2002. 2-Methoxyestradiol induces p53-associated apoptosis of colorectal cancer cells. Cancer Lett. 187, 77–86.
Chen, G.G., Zeng, Q., Tse, G.M., 2008. Estrogen and its receptors in cancer. Med. Res. Rev. 28, 954–974.
Choi, H.J., Zhu, B.T., 2012. Critical role of cyclin B1/Cdc2 up-regulation in the induction of mitotic prometaphase arrest in human breast cancer cells treated with 2-methoxyestradiol. Biochim. Biophys. Acta 1823, 1306–1315.
Cushman, M., He, H.M., Katzenellenbogen, J.A., Varma, R.K., Hamel, E., Lin, C.M., Ram, S., Sachdeva, Y.P., 1997. Synthesis of analogs of 2-methoxyestradiol with enhanced inhibitory effects on tubulin polymerization and cancer cell growth. J. Med. Chem. 40, 2323–2334.
Dohle, W., Jourdan, F.L., Menchon, G., Prota, A.E., Foster, P.A., Mannion, P., Hamel, E., Thomas, M.P., Kasprzyk, P.G., Ferrandis, E., Steinmetz, M.O., Leese, M.P., Potter, B.V.L., 2018. Quinazolinone-based anticancer agents: synthesis, antiproliferative SAR, antitubulin activity, and tubulin co-crystal structure. J. Med. Chem. 61, 1031–1044.
Egeblad, M., Werb, Z., 2002. New functions for the matrix metalloproteinases in cancer progression. Nat. Rev. Cancer 2, 161–174.
Eger, A., Mikulits, W., 2005. Models of epithelial-mesenchymal transition. Drug Discov. Today Dis. Model. 2, 57–63.
Harrison, M.R., Hahn, N.M., Pili, R., Oh, W.K., Hammers, H., Sweeney, C., Kim, K., Perlman, S., Arnott, J., Sidor, C., Wilding, G., Liu, G., 2011. A phase II study of 2-methoxyestradiol (2ME2) NanoCrystal® dispersion (NCD) in patients with taxane-refractory, metastatic castrate-resistant prostate cancer (CRPC). Investig. New Drugs 29, 1465–1474.
Hilder, T.A., Hodgkiss, J.M., 2017. Molecular mechanism of binding between 17β-estradiol and DNA. Comput. Struct. Biotechnol. J. 15, 91–97.
Jourdan, F., Leese, M.P., Dohle, W., Ferrandis, E., Newman, S.P., Chander, S., Purohit, A., Potter, B.V., 2011. Structure-activity relationships of C-17-substituted estratriene-3-O-sulfamates as anticancer agents. J. Med. Chem. 54, 4863–4879.
Jovanovic-Santa, S., Petrovic, J., Andric, S., Kovacevic, R., Durendic, E., Sakac, M., Lazar, D., Stankovic, S., 2003. Synthesis, structure, and screening of estrogenic and anti-estrogenic activity of new 3,17-substituted-16,17-seco-estratriene derivatives. Bioorg. Chem. 31, 475–484.
Jovanovic-Santa, S.S., Petri, E.T., Klisuric, O.R., Szécsi, M., Kovacevic, R., Petrovic, J.A., 2015. Antihormonal potential of selected D-homo and D-seco estratriene derivatives. Steroids 97, 45–53.
Kiss, A., Mernyák, E., Wölfling, J., Sinka, I., Zupkó, I., Schneider, G., 2018. Stereoselective synthesis of the four 16-hydroxymethyl-3-methoxy- and 16-hydroxymethyl-3-benzyloxy-13α-estra-1,3,5(10)-trien-17-ol isomers and their antiproliferative activities. Steroids 134, 67–77.
Kumar, B.S., Raghuvanshi, D.S., Hasanain, M., Alam, S., Sarkar, J., Mitra, K., Khan, F., Negi, A.S., 2016. Recent advances in chemistry and pharmacology of 2-methoxyestradiol: an anticancer investigational drug. Steroids 110, 9–34.
LaVallee, T.M., Zhan, X.H., Herbstritt, C.J., Kough, E.C., Green, S.J., Pribluda, V.S., 2002. 2-Methoxyestradiol inhibits proliferation and induces apoptosis independently of estrogen receptors alpha and beta. Cancer Res. 62, 3691–3697.
Lee, A., Djamgoz, M.B.A., 2018. Triple negative breast cancer: emerging therapeutic modalities and novel combination therapies. Cancer Treat. Rev. 62, 110–122.
Li, L., Bu, S., Backstrom, T., Landstrom, M., Ulmsten, U., Fu, X., 2004. Induction of apoptosis and G2/M arrest by 2-methoxyestradiol in human cervical cancer HeLaS3 cells. Anticancer Res. 24, 873–880.
Li, H., Qiu, Z., Li, F., Wang, C., 2017. The relationship between MMP-2 and MMP-9 expression levels with breast cancer incidence and prognosis. Oncol. Lett. 14, 5865–5870.
Lightfoot Jr., H.M., Lark, A., Livasy, C.A., Moore, D.T., Cowan, D., Dressler, L., Craven, R.J., Cance, W.G., 2004. Upregulation of focal adhesion kinase (FAK) expression in ductal carcinoma in situ (DCIS) is an early event in breast tumorigenesis. Breast Cancer Res. Treat. 88, 109–116.
Lin, N.U., Claus, E., Sohl, J., Razzak, A.R., Arnaout, A., Winer, E.P., 2008. Sites of distant recurrence and clinical outcomes in patients with metastatic triple-negative breast cancer: high incidence of central nervous system metastases. Cancer 113, 2638–2645.
Matei, D., Schilder, J., Sutton, G., Perkins, S., Breen, T., Quon, C., Sidor, C., 2009. Activity of 2 methoxyestradiol (Panzem NCD) in advanced, platinum-resistant ovarian cancer and primary peritoneal carcinomatosis: a Hoosier Oncology Group trial. Gynecol. Oncol. 115, 90–96.
McLean, G.W., Carragher, N.O., Avizienyte, E., Evans, J., Brunton, V.G., Frame, M.C., 2005. The role of focal-adhesion kinase in cancer - a new therapeutic opportunity. Nat. Rev. Cancer 5, 505–515.
Mehlen, P., Puisieux, A., 2006. Metastasis: a question of life or death. Nat. Rev. Cancer 6, 449–458.
Mernyák, E., Huber, J., Szabó, J., Schneider, G., Hetényi, A., Márk, L., Maász, G., Berényi, Á., Kovács, I., Minorics, R., Zupkó, I., Wölfling, J., 2013. Cycloaddition of steroidal cyclic nitrones to C=N dipolarophiles: Stereoselective synthesis and antiproliferative effects of oxadiazolidinones in the estrone series. Steroids 78, 1021–1028.
Mernyák, E., Fiser, G., Szabó, J., Bodnár, B., Schneider, G., Kovács, I., Ocsovszki, I., Zupkó, I., Wölfling, J., 2014. Synthesis and in vitro antiproliferative evaluation of d-secooxime derivatives of 13β- and 13α-estrone. Steroids 89, 47–55.
Mernyák, E., Kovács, I., Minorics, R., Sere, P., Czégány, D., Sinka, I., Wölfling, J., Schneider, G., Újfaludi, Z., Boros, I., Ocsovszki, I., Varga, M., Zupkó, I., 2015. Synthesis of trans-16-triazolyl-13α-methyl-17-estradiol diastereomers and the effects of structural modifications on their in vitro antiproliferative activities. J. Steroid Biochem. Mol. Biol. 150, 123–134.
Minorics, R., Zupkó, I., 2018. Steroidal anticancer agents: an overview of estradiol-related compounds. Anti Cancer Agents Med. Chem (In Press). https://doi.org/10.2174/1871520617666171114111721.
Miyazaki, T., Kato, H., Nakajima, M., Sohda, M., Fukai, Y., Masuda, N., Manda, R., Fukuchi, M., Tsukada, K., Kuwano, H., 2003. FAK overexpression is correlated with tumour invasiveness and lymph node metastasis in oesophageal squamous cell carcinoma. Br. J. Cancer 89, 140–145.
Möller, G., Deluca, D., Gege, C., Rosinus, A., Kowalik, D., Peters, O., Droescher, P., Elger, W., Adamski, J., Hillisch, A., 2009. Structure-based design, synthesis and in vitro characterization of potent 17beta-hydroxysteroid dehydrogenase type 1 inhibitors based on 2-substitutions of estrone and D-homo-estrone. Bioorg. Med. Chem. Lett. 19, 6740–6744.
Mosmann, T., 1983. Rapid colorimetric assay for cellular growth and survival: application to proliferation and cytotoxicity assays. J. Immunol. Methods 65, 55–63.
Mueck, A.O., Seeger, H., 2010. 2-Methoxyestradiol - biology and mechanism of action. Steroids 75, 625–631.
Nelles, J.L., Hu, W.Y., Prins, G.S., 2011. Estrogen action and prostate cancer. Expert. Rev. Endocrinol. Metab. 6, 437–451.
Newman, L.A., Reis-Filho, J.S., Morrow, M., Carey, L.A., King, T.A., 2015. The 2014 Society of Surgical Oncology Susan G. Komen for the Cure Symposium: triple-negative breast cancer. Ann. Surg. Oncol. 22, 874–882.
Parsons, J.T., Martin, K.H., Slack, J.K., Taylor, J.M., Weed, S.A., 2000. Focal adhesion kinase: a regulator of focal adhesion dynamics and cell movement. Oncogene 19, 5606–5613.
Pearce, S.T., Jordan, V.C., 2004. The biological role of estrogen receptors alpha and beta in cancer. Crit. Rev. Oncol. Hematol. 50, 3–22.
Pribluda, V.S., Gubish Jr., E.R., Lavallee, T.M., Treston, A., Swartz, G.M., Green, S.J., 2000. 2-Methoxyestradiol: an endogenous antiangiogenic and antiproliferative drug candidate. Cancer Metastasis Rev. 19, 173–179.
Qadan, L.R., Perez-Stable, C.M., Anderson, C., D'Ippolito, G., Herron, A., Howard, G.A.,

Roos, B.A., 2001. 2-Methoxyestradiol induces G2/M arrest and apoptosis in prostate cancer. Biochem. Biophys. Res. Commun. 285, 1259–1266.
Recher, C., Ysebaert, L., Beyne-Rauzy, O., Mansat-De Mas, V., Ruidavets, J.B., Cariven, P., Demur, C., Payrastre, B., Laurent, G., Racaud-Sultan, C., 2004. Expression of focal adhesion kinase in acute myeloid leukemia is associated with enhanced blast migration, increased cellularity, and poor prognosis. Cancer Res. 64, 3191–3197.
Snoek-van Beurden, P.A., Von den Hoff, J.W., 2005. Zymographic techniques for the analysis of matrix metalloproteinases and their inhibitors. BioTechniques 38, 73–83.
Steliarova-Foucher, E., O'Callaghan, M., Ferlay, J., Masuyer, E., Rosso, S., Forman, D., Bray, F., Comber, H., 2015. The European Cancer Observatory: a new data resource. Eur. J. Cancer 51, 1131–1143.
Szabó, J., Pataki, Z., Wölfling, J., Schneider, G., Bózsity, N., Minorics, R., Zupkó, I., Mernyák, E., 2016. Synthesis and biological evaluation of 13α-estrone derivatives as potential antiproliferative agents. Steroids 113, 14–21.
Tapolcsányi, P., Wölfling, J., Falkay, G., Márki, A., Minorics, R., Schneider, G., 2002. Synthesis and receptor-binding examination of 16-hydroxymethyl-3,17-estradiol stereoisomers. Steroids 67, 671–678.
Torre, L.A., Bray, F., Siegel, R.L., Ferlay, J., Lortet-Tieulent, J., Jemal, A., 2015. Global cancer statistics, 2012. CA Cancer J. Clin. 65, 87–108.
Trifunovic, J., Borcic, V., Vukmirovic, S., Mikov, M., 2017. Structural insights into anticancer activity of D-ring modified estrone derivatives using their lipophilicity in estimation of SAR and molecular docking studies. Drug Test. Anal. 9, 1542–1548.
Vermes, I., Haanen, C., Reutelingsperger, C., 2000. Flow cytometry of apoptotic cell death. J. Immunol. Methods 243, 167–190.
Wölfling, J., Mernyák, E., Frank, E., Falkay, G., Marki, A., Minorics, R., Schneider, G., 2003. Synthesis and receptor-binding examinations of the normal and 13-epi-D-homoestrones and their 3-methyl ethers. Steroids 68, 277–288.
Zhu, B.T., Conney, A.H., 1998. Is 2-methoxyestradiol an endogenous estrogen metabolite that inhibits mammary carcinogenesis? Cancer Res. 58, 2269–2277.

II.

Steroids 134 (2018) 67–77

Contents lists available at ScienceDirect

Steroids

journal homepage: www.elsevier.com/locate/steroids

Stereoselective synthesis of the four 16-hydroxymethyl-3-methoxy- and 16-hydroxymethyl-3-benzyloxy-13α-estra-1,3,5(10)-trien-17-ol isomers and their antiproliferative activities

Anita Kiss[a], Erzsébet Mernyák[a], János Wölfling[a], Izabella Sinka[b], István Zupkó[b], Gyula Schneider[a,*]

[a] Department of Organic Chemistry, University of Szeged, Dóm tér 8, H-6720 Szeged, Hungary
[b] Department of Pharmacodynamics and Biopharmacy, University of Szeged, Eötvös u. 6, H-6720, Hungary

ARTICLE INFO

Keywords:
13α-Estrone
Stereocontrolled synthesis
Stereoisomers
Antiproliferative activity

ABSTRACT

The reduction of 16-hydroxymethylene-3-methoxy-13α-estra-1,3,5(10)-trien-17-one (**14**) and 16-hydroxymethylene-3-benzyloxy-13α-estra-1,3,5(10)-trien-17-one (**16**) yielded a mixture of two diastereomeric diols, the 16α-hydroxymethyl,17β-hydroxy and 16β-hydroxymethyl,17α-hydroxy isomers (**17a-20a**) in a ratio of 6:1. We describe a straightforward synthetic route to transform the isomers with *trans* functional groups attached to ring D (**17a-20a**) into isomers with *cis* functional groups (**25a-28a**).

We determined the *in vitro* antiproliferative activities of compounds **17a–20a** and **25a–28a** by means of MTT assays against a panel of human adherent cancer cell lines HeLa, A2780, MCF-7, T47D, MDA-MB-231 and MDA-MB-361.

1. Introduction

Breast cancer is the most frequently diagnosed cancer in women worldwide [1]. Since estrogens are known to play a role in the development of many breast cancers, a logical approach to the treatment of estrogen-sensitive breast cancer is the use of anti-estrogens that block the interaction of estrogens with their specific receptor. The literature provides evidence that inversion of the configuration of estra-1,3,5(10)-trien-17-one at C-13 may lead to the loss of estrogenic activity [2,3]. These investigations revealed that the C-13 epimers of estradiols possess low affinity for the estrogen receptor, with no uterotropic activity when tested on mice. The probable explanation of the negligible receptor binding ability of the 13-*epi*-estradiols of ring C and D [4]. 13α-Estrone is readily available from natural estrone by the epimerization method developed by Yaramenko and Khvat, using 1,2-phenylenediamine and acetic acid [5]. As 13α-estradiols possess low affinity for the estrogen receptor and are readily available, we have chosen these compounds as scaffolds for the design of 13α-estrone derivatives as potential antitumor agents.

Hydrophilic functional groups attached to ring D in the steroid skeleton have strong effect on biological properties of these compounds. Earlier we reported preparation and configuration determinations of the four possible isomers of 16-hydroxymethyl-estra-1,3,5(10)-trien-3,17-diol [6], and their 3-methyl [7,8] and 3-benzyl ethers [6].

We describe here the preparation of four possible isomers of 16-hydroxymethyl-3-methoxy- and 16-hydroxymethyl-3-benzyloxy-13α-estra-1,3,5(10)-trien-17-ols (**17a-20a** and **25a-28a**).

The reduction of 16-hydroxymethylene-3-methoxy-13α-estra-1,3,5(10)-trien-17-one (**14**) and 16-hydroxymethylene-3-benzyloxy-13α-estra-1,3,5(10)-trien-17-one (**16**) with $NaBH_4$ in ethanol yielded a mixture of two diastereomeric diols **17a-20a** in a 6:1 ratio. The simultaneous development of the two chiral centers permits formation of the four isomers (**17a-20a** and **25a-28a**). However, only two isomers (**17a-20a**) were detected by thin-layer chromatography [9,10].

Here, we describe a straightforward synthetic route to transform the isomers with *trans* functional groups attached to ring D (**17a-20a**) into isomers with *cis* functional groups (**25a-28a**).

We set out to obtain answers to the following questions: (1) how the antiproliferative activities in the 16-hydroxymethyl-13α-estrane-3-methoxy- and 16-hydroxymethyl-3-benzyloxy series differ, and (2) how the antiproliferative activities are influenced by the relative steric positions of the 16-hydroxymethyl and 17-hydroxy groups.

* Corresponding author.
E-mail address: schneider@chem.u-szeged.hu (G. Schneider).

https://doi.org/10.1016/j.steroids.2018.02.008
Received 1 December 2017; Received in revised form 12 February 2018; Accepted 22 February 2018
Available online 01 March 2018
0039-128X/ © 2018 Elsevier Inc. All rights reserved.

2. Experimental

2.1. General

Melting points (mp) were determined on Kofler block and are uncorrected. Specific rotations were measured in $CHCl_3$ (*c* 1 in $CHCl_3$) at 20 °C with a POLAMAT-A (Zeiss-Jena) polarimeter and are given in units of 10^{-1} deg cm^2 g^{-1}. Elementary analysis data were determined with PerkinElmer CHN analyzer model 2400. The reactions were monitored by TLC on Kieselgel (Merck Si 254 F) layers (0.25 mm thick); solvent system: (A) acetone/toluene/hexane (30:35:35 v/v), (B) diisopropyl ether. The spots were detected by spraying with 5% phosphomolybdic acid in 50% aqueous H_3PO_4. The R_f values were determined for the spots observed by illumination at 254 and 365 nm. Flash chromatography: silica gel 60, 40–63 μm. All solvents were freshly distilled prior to use. NMR spectra were recorded on a Bruker DRX 500 instrument at 500 (^{1}H NMR) or 125 MHz (^{13}C NMR). Chemical shifts are reported in ppm (δ scale), and coupling constants (*J*) are in Hz. For the determination of multiplicities, the *J*-MOD pulse sequence was used.

2.2. 3-Methoxy-13α-estra-1,3,5(10)-trien-17-one (13)

A mixture of compound **1** (25 g, 87.9 mmol) in acetic acid (250 ml) and *o*-phenylenediamine (13.5 g, 125 mmol) was treated at reflux temperature for 3 h. After cooling, the mixture was slowly poured onto ice and the resulting precipitate was filtered off, washed with water and dried. The solid was dissolved in CH_2Cl_2 (300 ml), the solution was washed with water (3 × 250 ml), dried (Na_2SO_4) and the solvent evaporated. The crude product was dissolved in methanol (200 ml) and Girard-P reagent (18.8 g, 100 mmol) and acetic acid (20 ml) were added to the solution. The reaction mixture was heated at reflux for 3 h, and then allowed to stand at room temperature overnight. After white crystals formed, the mixture was neutralized with a dilute Na_2CO_3 solution. The precipitate was filtered off and dissolved in CH_2Cl_2 (250 ml), the solution was washed with water (3 × 250 ml), dried (Na_2SO_4) and the solvent evaporated Yield of pure **13**: 23.7 g (95%). It is identical with the compound described in ref. [9].

2.3. 16-Hydroxymethylidene-3-methoxy-13α-estra-1,3,5(10)-trien-17-one (14)

Compound **13** (25 g, 88 mmol) was dissolved in anhydrous toluene (200 ml), then NaOMe (9.5 g, 0.18 mmol) and freshly distilled ethyl formate (100 ml, 1.3 mol) were added to the solution. The mixture was stirred for 6 h at 50 °C and allowed to stand overnight at room temperature. It was then diluted with water (1000 ml) and carefully poured onto a mixture of ice (100 g) and concentrated HCl (25 ml). The white precipitate separating out was filtered off, washed thoroughly with water and dried. Recrystallization from CH_2Cl_2/hexane gave **14** (25.2 g, 90%). Mp: 103–107 °C; R_f = 0.70 (ss A); $[\alpha]_D^{25}$ = +72 (*c* 1 in $CHCl_3$). (Found: C, 76.93; H, 7.52. $C_{20}H_{24}O_3$ (312.17) requires: C, 76.89; H, 7.74%). ^{1}H NMR (δ, ppm, $CDCl_3$): 1.12 (s, 3H, 18-H_3), 2.82 (m, 2H, 6-H_2), 3.76 (s, 3H, 3-OCH_3), 6.60 (s, 1H, 4-H), 6.70 (d, 1H, *J* = 8.5 Hz, 2-H), 7.10 (s, 1H, 16-CH), 7.19 (d, 1H, *J* = 8.5 Hz, 1-H). ^{13}C NMR (δ, ppm, $CDCl_3$): 25.3 (C-18), 25.7, 28.2, 28.6, 30.4, 31.6, 41.2, 41.9, 48.9, 50.8 (C-13), 55.2 (3-OCH_3), 62.1, 111.1 (C-16), 111.7 (C-2), 113.5 (C-4), 126.8 (C-1), 131.9 (C-10), 138.0 (C-5),157.5 (C-3), 159.3 (16-CH), 213.9 (C-17).

2.4. 16α-Hydroxymethyl-3-methoxy-13α-estra-1,3,5(10)-trien-17β-ol (17a) and 16β-hydroxymethyl-3-methoxy-13α-estra-1,3,5(10)-trien-17α-ol (18a)

Compound **14** (15 g, 48 mmol) was suspended in MeOH (300 ml) and then KBH_4 (13 g, 240 mmol) was added in small portions at room temperature. The mixture was allowed to stand for 6 h, then poured onto ice (1000 g) and acidified with dilute HCl to pH 3. The precipitate separating out was filtered off, washed until free from acid and dried. The mixture obtained consisted of diols **17a** and **18a** in a ratio of 6:1 (yield 15 g, 98%) [9].

2.5. 17β-Hydroxy-3-methoxy-13α-estra-1,3,5(10)-trien-16α-ylmethyl acetate (17b) and 17α-hydroxy-3-methoxy-13α-estra-1,3,5(10)-trien-16β-ylmethyl acetate (18b)

A mixture of **17a** and **18a** (10 g, 31.6 mmol) was dissolved in pyridine (40 ml) and a solution of Ac_2O (3.2 ml, 32 mmol) in pyridine (60 ml) was added dropwise with cooling in salt-ice bath. The mixture was allowed to stand for 5 h at room temperature, and then poured onto a mixture of ice (400 g) and concentrated H_2SO_4 (40 ml). The precipitate separating out was filtered off and dissolved in CH_2Cl_2 (60 ml). The solution was washed with water, dried over Na_2SO_4 and evaporated *in vacuo*. The residue obtained was subjected to chromatographic separation (silica gel, hexane/CH_2Cl_2 (75:25, v/v)) to give **17c** and **18c** as oil (2.4 g, 18.8%). Continued elution with CH_2Cl_2 and CH_2Cl_2/ethyl acetate (95:5, v/v) resulted in **17b** as a white powder (5.6 g, 50%), **18b** as an oil (1.1 g, 10%), and a residual mixture of **17a** and **18a** (2.0 g, 20%). After alkaline methanolysis of the mixture of diacetates (**17c** and **18c**), the resulting mixture of diols (**17a** and **18a**) was recycled.

17b: Mp: 104–105 °C; R_f = 0.45 (ss A); $[\alpha]_D^{25}$ = +91 (*c* 1 in $CHCl_3$). (Found: C, 73.86; H, 8.32. $C_{22}H_{30}O_4$ (358.48) requires: C, 73.71; H, 8.44%). ^{1}H NMR (δ, ppm, $CDCl_3$): 1.08 (s, 3H, 18-H_3), 2.08 (s, 3H, Ac-H_3), 2.78 (m, 2H, 6-H_2), 3.77 (s, 3H, 3-OCH_3), 4.17 (m, 2H, 16a-H_2), 6.60 (s, 1H, 4H); 6.72 (t, 1H, *J* = 6.0 Hz, 2-H), 7.16 (d, 1H, *J* = 8.5 Hz, 1-H). ^{13}C NMR (δ, ppm, $CDCl_3$): 21.0 (C-18), 27.9, 28.8, 29.0, 29.3 (Ac-CH_3), 30.4, 38.5, 40.8, 43.5 (C-13), 44.9, 50.2, 55.2 (3-OCH_3), 66.9 (C-16a), 84.6 (C-17), 112.0 (C-2), 113.2 (C-4), 127.5 (C-1), 133.6 (C-10), 137.9 (C-5), 157.2 (C-3), 171.3 (Ac-C = O). **18b**: Oil; R_f = 0.40 (ss A); $[\alpha]_D^{25}$ = +19 (*c* 1 in $CHCl_3$). (Found: C, 73.92; H, 8.25. $C_{22}H_{30}O_4$ (358.48) requires: C, 73.71; H, 8.44%). ^{1}H NMR (δ, ppm, $CDCl_3$): 0.98 (s, 3H, 18-H_3), 2.03 (s, 3H, Ac-H_3), 2.79 (m, 2H, 6-H_2), 3.78 (s, 3H, 3-OCH_3), 3.94 (m, 1H, 17-H), 4.10 (dd, 1H, *J* = 10.9 Hz, *J* = 6.1 Hz, 16a-H_2), 4.20 (dd, 1H, *J* = 10.9 Hz, *J* = 5.5 Hz, 16-H_2), 6.62 (d, 1H, *J* = 2.7 Hz, 4-H), 6.73 (dd, 1H, *J* = 8.6 Hz, *J* = 2.7 Hz, 2-H), 7.23 (d, 1H, *J* = 8.6 Hz, 1-H). ^{13}C NMR (δ, ppm, $CDCl_3$): 20.8 (Ac-CH_3), 22.9 (C-18), 26.5, 28.1, 28.3, 30.4, 33.0, 42.1, 42.3, 43.2, 43.8 (C-13). 48.7, 55.0 (3-OCH_3), 67.5 (C-16a), 75.8 (C-17), 111.7 (C-2), 113.5 (C-4), 126.8 (C-1), 132.1 (C-10), 137.9 (C-5), 171.1 (Ac-C = O).

2.6. 3-Methoxy-17-oxo-13α-estra-1,3,5(10)-trien-16α-ylmethyl acetate (21)

Compound **17b** (2 g, 5.6 mmol) was dissolved in acetone (50 ml), and Jones reagent (2 ml) was added dropwise with cooling in ice. The reaction mixture was poured onto ice and the precipitate separating out was filtered off and dried. The substance obtained was crystallized from acetone/hexane to give pure **21** (1.1 g, 57%). Mp: 117–119 °C; R_f = 0.60 (ss A); $[\alpha]_D^{25}$ = −21 (*c* 1 in $CHCl_3$). (Found: C, 74.35; H, 8.04. $C_{22}H_{28}O_4$ (356.48) requires: C, 74.13; H, 7.92%). ^{1}H NMR (δ, ppm, $CDCl_3$): 1.04 (s, 3H, 18-H_3), 2.04 (s, 3H, Ac-H_3), 2.84 (s, 2H, 6-H_2), 3.76 (s, 3H, 3-OCH_3), 4.29 (d, 2H, *J* = 3.0 Hz, 16a-H_2), 6.61 (s, 1H, 4-H), 6.70 (d, 1H, *J* = 6.5 Hz, 2-H), 7.18 (d, 1H, *J* = 8.0 Hz, 1-H). ^{13}C NMR (δ, ppm, $CDCl_3$): 20.8 (C-18), 24.5 (Ac-CH_3), 25.5, 28.4, 28.5, 30.3; 32.8, 41.4 (C-8), 41.9 (C-9), 45.2 (C-14), 47.6 (C-16), 50.2 (C-13), 55.2 (3-OCH_3), 63.3 (C-16a), 111.7 (C-2), 113.6 (C-4), 126.9 (C-1), 131.7 (C-10), 137.9 (C-5), 157.5 (C-3), 170.8 (Ac-C = O), 219.7 (C-17C = O).

2.7. 3-Methoxy-17-oxo-13α-estra-1,3,5(10)-trien-16β-ylmethyl acetate (22)

Compound **18b** (2 g, 5.6 mmol) was dissolved in acetone (100 ml) and a solution of Jones reagent (2 ml) was added dropwise with cooling in ice. The mixture was poured onto ice. The oily substance separating out was extracted with CH_2Cl_2, dried over Na_2SO_4 and evaporated *in vacuo*, giving product **22** (1.2 g, 60%). Mp: 144–145 °C; R_f = 0.60 (ss A); $[\alpha]_D^{25} = -18$ (*c* 1 in $CHCl_3$). (Found: C, 74.35; H, 8.04. $C_{22}H_{28}O_4$ (356.48) requires: C, 74.13; H, 7.92%). ^{1}H NMR (δ, ppm, $CDCl_3$): 0.90 (s, 3H, 18-H_3), 2.04 (s, 3H, Ac-H_3), 2.90 (m, 2H, 6-H_2), 3.78 (s, 3H, 3-OCH_3), 4.33 (s, 2H, 16a-H_2), 6.65 (s, 1H, 4-H), 6.72 (d, 1H, *J* = 7.5 Hz, 2-H), 7.20 (d, 1H, *J* = 8.5 Hz, 1-H). ^{13}C NMR (δ, ppm, $CDCl_3$): 13.1 (Ac-CH_3), 20.8 (C-18), 25.7, 25.9, 26.7, 29.6, 31.9, 37.8, 44.1, 48.2 (C-13), 48.8, 48.9, 55.2 (3-OCH_3), 63.1 (C-16a), 111.6 (C-2), 113.9 (C-4), 126.2 (C-1), 131.9 (C-10), 137.6 (C-5), 157.6 (C-3), 170.7 (Ac-C = O), 218.8 (C-17C = O).

2.8. 16α-Hydroxymethyl-3-methoxy-13α-estra-1,3,5(10)-trien-17α-ol (25a)

$LiAlH_4$ (1.2 g, 32 mmol) was suspended in anhydrous diethyl ether (100 ml), then *t*-BuOH (9 ml, 96 mmol) was added carefully during stirring and cooling with salt-ice. Compound **21** (2.3 g, 6.4 mmol) dissolved in diethyl ether (100 ml) was added dropwise to the suspension. The reaction mixture was stirred for 3 h and was decomposed by the careful addition of water (75 ml) during stirring and cooling. Next, it was acidified with dilute HCl to pH 5. The organic phase was separated and the aqueous phase was extracted with diethyl ether. The substance obtained on washing, drying and evaporation of the solvent was subjected to chromatographic separation on silica gel with CH_2Cl_2/ethyl acetate (99:1, v/v) to give pure compound **25a** (630 mg, 31%). Mp: 124–125 °C; R_f = 0.35 (ss A); $[\alpha]_D^{25} = +22$ (*c* 1 in $CHCl_3$). (Found: 76.03; H, 8.74. $C_{20}H_{28}O_3$ (316.44) requires: C, 75.91; H, 8.92%). ^{1}H NMR (δ, ppm, $CDCl_3$): 1.03 (s, 3H, 18-H_3), 2.81 (d, 2H, *J* = 5.0 Hz, 6-H_2), 3.78 (s, 3H, 3-OCH_3), 6.62 (s, 1H, 4-H), 6.72 (d, 1H, *J* = 7.0 Hz, 2-H), 7.22 (d, 1H, *J* = 8.5 Hz, 1-H). ^{13}C NMR (δ, ppm, $CDCl_3$): 23.7 (C-18), 26.9, 28.7, 30.4, 34.1, 41.7, 40.7, 40.7, 44.7 (C-13), 50.2 (C-16), 55.2 (3-OCH_3), 64.4 (C-16a), 76.2 (C-17), 111.7 (C-2), 113.5 (C-4), 126.9 (C-1), 132.5 (C-10), 138.2 (C-5), 157.4 (C-3). Further elution with CH_2Cl_2/ethyl acetate (95:5) gave **17a** (1.35 g, 67%).

2.9. 16α-Hydroxymethyl-3-methoxy-13α-estra-1,3,5(10)-trien-17α-ol acetonide (25c)

Compound **25a** (663 mg, 2 mmol) was dissolved in acetone (10 ml) in the presence of a catalytic amount of *p*-toluenesulfonic acid. The reaction mixture was treated at reflux temperature for 1 h. It was then neutralized with morpholine, diluted with CH_2Cl_2 (50 ml) and washed with water. The organic layer was dried over Na_2SO_4 and evaporated *in vacuo*. Recrystallization from methanol gave compound **25c** (680 mg, 95%). Mp: 138–140 °C; R_f = 0.85 (ss B); $[\alpha]_D^{25} = +18$ (*c* 1 in $CHCl_3$). (Found: C, 77.68; H, 8.92. $C_{23}H_{32}O_3$ (356.50) requires: C, 77.49; H, 9.05%). ^{1}H NMR (δ, ppm, $CDCl_3$): 1.08 (s, 3H, 18-H_3), 1.35 and 2.80 (two s, 6H, $(CH_3)_2C$), 2.80 (m, 2H, 6-H_2), 3.78 (s, 3H, 3-OCH_3), 6.61 (s, 1H, 4-H), 6.73 (d, 1H, *J* = 8.5 Hz, 2-H), 7.20 (d, 1H, *J* = 8.5 Hz, 1-H). ^{13}C NMR (δ, ppm, $CDCl_3$): 22.7 and 24.2 (two C, $(CH_3)_2C$), 27.0, 27.8 (C-18), 29.0, 30.1, 30.4, 33.2, 37.1, 40.1, 40.8, 45.1 (C-13), 50.7, 55.2 (3-OCH_3), 75.1 (C-17), 98.2 (C-20), 111.9 (C-2), 113.4 (C-4), 127.1 (C-1), 133.2 (C-10), 138.0 (C-5), 157.3 (C-3).

2.10. 16α-Hydroxymethyl-3-methoxy-13α-estra-1,3,5(10)-trien-17α-ol phenylboronate (25d)

Compound **25a** (95 mg, 0.3 mmol) was dissolved in ethanol (5 ml) and phenylboronic acid (45 mg, 0.3 mmol) was added. The precipitate formed in 15 min was filtered off and dried (**25d**: 116 mg, 86%). Mp: 128–130 °C; R_f = 0.70 (ss B); $[\alpha]_D^{25} = +8.5$ (*c* 1 in $CHCl_3$). (Found: C, 77.86; H, 7.98. $C_{26}H_{31}BO_3$ (402.35) requires: C, 77.62; H, 7.77%). ^{1}H NMR (δ, ppm, $CDCl_3$): 1.36 (s, 3H, 18-H_3), 2.77 (m, 2H, 6-H_2), 3.64 (d, 1H, *J* = 10.5 Hz, 16a-H_2), 3.78 (s, 3H, 3-OCH_3), 3.90 (t, 1H, *J* = 10.5 Hz, 16a-H_2), 4.33 (dd, 1H, *J* = 10.5 Hz, *J* = 5.0 Hz, 17-H), 6.59 (s, 1H, 4-H), 6.74 (dd, 1H, *J* = 8.5 Hz, *J* = 2.0 Hz, 2-H), 7.15 (d, 1H, *J* = 8.5 Hz, 1-H), 7.36 (t, 2H, *J* = 7.0 Hz, 3′- and 5′-H), 7.41 (t, 1H, *J* = 7.5 Hz, 1′-H), 7.82 (d, 2H, *J* = 7.5 Hz, 2′-H and 6′-H).

2.11. 17α-Hydroxy-3-methoxy-13α-estra-1,3,5(10)-trien-16α-ylmethyl p-toluenesulfonate (29)

Compound **25a** (316 mg, 1 mmol) was dissolved in anhydrous pyridine (10 ml) and then a solution of *p*-toluenesulfonyl chloride (285 mg, 1.5 mmol) in anhydrous pyridine (5 ml) was added dropwise during cooling with ice. The reaction mixture was allowed to stand for 24 h and then poured onto a mixture of ice (100 g) and sulfuric acid (5 ml). The precipitate separating out was filtered off and recrystallized from a mixture of acetone/hexane to give **29** (415 mg, 88%). Mp: 120–123 °C; R_f = 0.55 (ss A). (Found: C, 69.05; H, 7.36. $C_{27}H_{34}O_5S$ (470.63) requires: C, 68.90; H, 7.28%). ^{1}H NMR (δ, ppm, $CDCl_3$): 0.96 (s, 3H, 18-H_3), 2.45 (s, 3H, Ts-H_3), 2.78 (m, 2H, 6-H_2), 3.77 (s, 3H, 3-OCH_3), 4.06 (dd, 1H, *J* = 9.0 Hz, *J* = 7.0 Hz, 16a-H_2), 4.12 (d, 1H, *J* = 9.0 Hz, 17-H), 4.28 (dd, 1H, *J* = 9.0 Hz, *J* = 7.0 Hz, 16a-H_2), 6.60 (s, 1H, 4-H), 6.71 (dd, 1H, *J* = 9.0 Hz, *J* = 2.5 Hz, 2-H), 7.18 (d, 1H, *J* = 8.5 Hz, 1-H), 7.35 (d, 2H, *J* = 8.0 Hz, 3′-H and 5′-H), 7.80 (d, 2H, *J* = 8.0 Hz, 2′-H and 6′-H). ^{13}C NMR (δ, ppm, $CDCl_3$): 21.6 (C-18), 23.3 (Ts-CH_3), 26.8, 28.8, 30.2, 30.3, 33.1, 39.2, 40.5, 40.7, 44.8 (C-13), 49.7 (C-14), 55.2, 71.9 (C-16a), 75.4 (C-17), 111.9 (C-2), 113.4 (C-4), 127.0 (C-1), 129.8 (C-2′ and C-6′), 132.6 (C-3′ and C-5′), 132.6 (C-16), 133.1 (C-1′), 138.0 (C-5), 144.7 (C-4′), 157.4 (C-3).

2.12. 17α,16α-Epoxymethano-3-methoxy-13α-estra-1,3,5(10)-triene (33)

Compound **29** (380 mg, 1 mmol) was dissolved in methanol (15 ml) and heated at reflux with $NaOCH_3$ (162 mg, 3 mmol) for 2 h. The reaction mixture was diluted with water, the precipitate separating out was filtered off, dried and crystallized from a mixture of acetone/hexane to give **33** (265 mg, 88%). Mp: 115–116.5 °C; R_f = 0.75 (ss A); $[\alpha]_D^{25} = +19$ (*c* 1 in $CHCl_3$). (Found: C, 80.76; H, 8.92. $C_{20}H_{26}O_2$ (298.42) requires: C, 80.50; H, 8.78%). ^{1}H NMR (δ, ppm, $CDCl_3$): 1.25 (s, 3H, 18-H_3), 2.80 (m, 2H, 6-H_2), 3.19 (m, 1H, 16-H), 3.77 (s, 3H, 3-OCH_3), 4.15 (t, 1H, *J* = 6.0 Hz, 16a-H_2), 4.77 (t, 1H, *J* = 6.0 Hz, 16a-H_2), 4.84 (d, 1H, *J* = 6.0 Hz, 17-H), 6.60 (d, 1H, *J* = 2.0 Hz, 4-H); 6.72 (dd, 1H, *J* = 8.5 Hz, *J* = 2.5 Hz, 2-H); 7.19 (d, 1H, *J* = 8.5 Hz, 1-H). ^{13}C NMR (δ, ppm, $CDCl_3$): 23.3 (C-18), 27.2, 29.1, 30.5, 32.1, 35.8, 37.3, 39.2, 42.4, 45.2 (C-13), 53.4, 55.2, (3-OCH_3), 75.8 (C-16a), 94.2 (C-17), 111.8 (C-2), 113.4 (C-4), 127.2 (C-1), 133.0 (C-10), 137.9 (C-5), 157.3 (C-3).

2.13. 16β-Hydroxymethyl-3-methoxy-13α-estra-1,3,5(10)-trien-17β-ol (26a)

Compound **22** (356 mg, 1 mmol) was dissolved in methanol (15 ml) and $NaBH_4$ (378 mg, 10 mmol) was added in small portions at room temperature. The reaction mixture was allowed to stand for 24 h, then it was diluted with water and the precipitate was collected by filtration and recrystallized from acetone/hexane to obtain **26a** (260 mg, 82%). Mp: 104–106 °C; R_f = 0.30 (ss A); $[\alpha]_D^{25} = +24$ (*c* 1). (Found: C, 75.83; H, 8.77. $C_{20}H_{28}O_3$ (316.44) requires: C, 75.91; H, 8.92%). ^{1}H NMR (δ, ppm, $CDCl_3$): 0.95 (s, 3H, 18-H_3), 2.79 (m, 2H, 6-H_2), 3.72 (t, 1H, *J* = 7.5 Hz, 17-H), 3.77 (s, 3H, 3-OCH_3), 3.85 (d, 1H, *J* = 3.0 Hz, 16a-H_2), 3.88 (d, 1H, *J* = 4.5 Hz, 16a-H_2), 6.60 (s, 1H, 4-H), 6.71 (d, 1H, *J* = 7.0 Hz, 2-H), 7.19 (d, 1H, *J* = 8.5 Hz, 1-H). ^{13}C NMR (δ, ppm, $CDCl_3$): 28.9, 29.3, 30.0 (C-18), 30.4, 30.5, 32.1, 40.2, 43.3, 43.3, 45.3

(C-13), 51.2, 55.1 (3-OCH_3), 63.1 (C-16a), 85.4 (C-17), 111.8 (C-2), 113.3 (C-4), 127.4 (C-1), 133.2 (C-10), 138.3 (C-5), 157.2 (C-3).

2.14. 16β-Hydroxymethyl-3-methoxy-13α-estra-1,3,5(10)-trien-17β-ol acetonide (26c)

Compound **26a** (663 mg, 2 mmol) was dissolved in acetone (10 ml) in the presence of a catalytic amount of *p*-toluenesulfonic acid. The reaction mixture was treated at reflux temperature for 1 h. It was then neutralized with morpholine, the solution was diluted with CH_2Cl_2 (50 ml) and washed with water. The organic layer was dried over Na_2SO_4 and evaporated *in vacuo*. Recrystallization from methanol gave compound **26c** (665 mg, 93%). Mp: 137–139 °C; R_f = 0.80 (ss B); $[\alpha]_D^{25}$ = +15.5 (*c* 1 in $CHCl_3$). (Found: C, 77.58; H, 9.23. $C_{23}H_{32}O_3$ (356.50) requires: C, 77.49; H, 9.05%). ^{1}H NMR (δ, ppm, $CDCl_3$): 1.23 (s, 3H, 18-H_3), 1.36 and 2.17 (two s, 6H, $(CH_3)_2C$), 3.14 (m, 2H, 6-H_2), 3.77 (s, 3H, 3-OCH_3), 6.60 (d, 1H, *J* = 3.0 Hz, 4-H), 6.71 (dd, 1H, *J* = 9.0 Hz, *J* = 3.0 Hz, 2-H), 7.19 (dd, 1H, *J* = 17.0 Hz, *J* = 9.0 Hz, 1-H). ^{13}C NMR (δ, ppm, $CDCl_3$): 8.6, 19.8 (C-18), 28.5, 29.7, 29.8, 30.8, 32.5, 33.7, 36.4, 41.2, 44.5, 46.2, 51.5, 55.1, 55.2 (3-OCH_3), 62.1 (C-16a), 81.7 (C-17), 98.1 (C-20), 111.7 (C-2), 113.3 (C-4), 127.5 (C-1), 133.2 (C-10), 138.5 (C-5), 157.1 (C-3).

2.15. 16β-Hydroxymethyl-3-methoxy-13α-estra-1,3,5(10)-trien-17β-ol phenylboronate (26d)

Compound **26a** (79 mg, 0,25 mmol) was dissolved in ethanol (5 ml) and phenlyboronic acid (38 mg, 0.25 mmol) was added. The precipitate formed in 15 min was filtered off and dried (**26d**: 125 mg, 93%). Mp: 87–89 °C; R_f = 0.75 (ss B); $[\alpha]_D^{25}$ = +6 (*c* 1 in $CHCl_3$). (Found: C, 77.83; H, 7.96. $C_{26}H_{31}BO_3$ (402.35) requires: C, 77.62; H, 7.77%). ^{1}H NMR (δ, ppm, $CDCl_3$,): 1.16 (s, 3H, 18-H_3), 2.81 (m, 2H, 6-H_2), 3.79 (s, 3H, 3-OCH_3), 3. 87 (dd, 1H, *J* = 11.0 Hz, *J* = 7.0 Hz, 16a-H_2), 4.23 (d, 1H, *J* = 7.0 Hz, 17-H), 4.27 (dd, 1H, *J* = 6.0 Hz, *J* = 11.0 Hz, 16a-H_2), 6.62 (s, 1H, 4-H), 6.75 (dd, 1H, *J* = 1.5 Hz, *J* = 8.0 Hz, 2-H), 7. 21 (d, 1H, *J* = 8.5 Hz, 1-H), 7. 37 (t, 2H, *J* = 7.5 Hz, 3′-H and 5′-H), 7. 43 (d, 1H, *J* = 7.5 Hz, 4′-H), 7.86 (d, 2H, *J* = 7.5 Hz, 2′-H and 6′-H). ^{13}C NMR (δ, ppm, $CDCl_3$): 23.8 (C-18), 26.7, 29.1, 30.4, 30.5, 32.4, 35.9, 39.3, 41.4, 45.2 (C-13), 49.5, 55.2 (3-OCH_3), 63.9 (C-16a), 78.5 (C-17), 112.0 (C-2), 113.3 (C-4), 127.4 (C-1), 127.5 (C-2′ and C-6′), 130.6 (C-4′), 133.2 (C-10), 133.9 (C-3′ and C-5′), 137.8 (C-5), 157.3 (C-3).

2.16. 17β-Hydroxy-3-methoxy-13α-estra-1,3,5(10)-trien-16β-ylmethyl p-tolenesulfonate (30)

Compound **26a** (316 mg, 1 mmol) was dissolved in anhydrous pyridine (10 ml) and then a solution of *p*-toluenesulfonyl chloride (285 mg, 1.5 mmol) in anhydrous pyridine (5 ml) was added dropwise during cooling with ice. The reaction mixture was allowed to stand for 24 h and then poured onto a mixture of ice (100 g) and sulfuric acid (5 ml). The precipitate was filtered, dissolved in dichloromethane and chromatographed on silica gel with a mixture of dichloromethane/hexane (1:1, v/v) to obtain **30** (340 mg, 72%). Mp: 138–140 °C; R_f = 0.50 (ss A). (Found: 68.98; H, 7.41. $C_{27}H_{34}O_5S$ (470.63) requires: C, 68.90; H, 7.28%). ^{1}H NMR (δ, ppm, $CDCl_3$): 0.96 (s, 3H, 18-H_3), 2.45 (s, 3H, Ts-H_3), 2.78 (m, 2H, 6-H_2), 3.77 (s, 3H, 3-OCH_3), 4.07 (dd, 1H, *J* = 12.0 Hz, *J* = 8.0 Hz, 16a-H_2), 4.12 (d, 1H, *J* = 11.0 Hz, 17-H), 4.28 (dd, 1H, *J* = 12.0 Hz, *J* = 8.0 Hz, 16a-H_2), 6.60 (d, 1H, *J* = 3.5 Hz, 4-H), 6.71 (dd, 1H, *J* = 10.5 Hz, *J* = 3.5 Hz, 2-H), 7.18 (d, 1H, *J* = 10.5 Hz, 1-H), 7.35 (d, 2H, *J* = 10.5 Hz, 3′-H and 5′-H), 7.80 (d, 2H, *J* = 10.5 Hz, 2′-H and 6′-H). ^{13}C NMR (δ, ppm, $CDCl_3$): 21.6 (C-18), 23.3 (Ts-CH_3), 26.8, 28.8, 29.7, 30.3, 30.3, 33.1, 39.2, 40.5, 40.7, 44.8 (C-13), 49.8 (C-14), 55.2, 71.9 (C-16a), 75.5 (C-17), 111.9 (C-2), 113.4, (C-4), 127.0 (C-1), 127.9 (C-2′ and C-6′), 129.8 (C-3′ and C-5′), 132.6 (C-10), 133.2 (C-1), 138.0 (C-5), 144.7 (C-4′), 157.4 (C-3).

2.17. 17β,16β-Epoxymethano-3-methoxy-13α-estra-1,3,5(10)-triene (34)

Compound **30** (570 mg, 1.5 mmol) was dissolved in methanol (15 ml) and heated at reflux with $NaOCH_3$ (243 mg, 4.5 mmol) for 2 h. The reaction mixture was diluted with water, the precipitate separating out was filtered off, dried and crystallized from a mixture of acetone/hexane to give **34** (390 mg, 87%). Mp: 105–106 °C; R_f = 0.80 (ss A); $[\alpha]_D^{25}$ = +28 (*c* 1 in $CHCl_3$). (Found: C, 8.31; H, 8.96. $C_{20}H_{26}O_2$ (298.42) requires: C, 80.50; H, 8.78%). ^{1}H NMR (δ, ppm, $CDCl_3$): 1.25 (s, 3H, 18-H_3), 2.80 (m, 2H, 6-H_2), 4.15 (t, 1H, *J* = 5.5 Hz, 16a-H_2), 4.77 (t, 1H, *J* = 6.5 Hz, 16a-H_2), 4.84 (d, 1H, *J* = 6.5 Hz, 17-H), 6.60 (d, 1H, *J* = 3.0 Hz, 4-H), 6.72 (dd, 1H, *J* = 9.0 Hz, *J* = 3.0, Hz 2-H), 7.19 (d, 1H, *J* = 9.0 Hz, 1-H). ^{13}C NMR (δ, ppm, $CDCl_3$): 23.3 (C-18), 27.2, 29.2, 30.5, 32.1, 35.9, 37.3, 39.2, 42.4, 45.2 (C-13), 53.4, 55.2 (3-OCH_3), 75.8 (C-16a), 94.3 (C-17), 111.8 (C-2), 113.4 (C-4), 124.2 (C-1), 133.0 (C-10), 137.9 (C-5), 157.3 (C-3).

2.18. 16α-Acetoxymethyl-3-methoxy-13α-estra-1,3,5(10)-trien-17β-acetate (17c), 16β-acetoxymethyl-3-methoxy-13α-estra-1,3,5(10)-trien-17α-acetate (18c), 16α-acetoxymethyl-3-methoxy-13α-estra-1,3,5(10)-trien-17α-acetate (25b) and 16β-acetoxymethyl-3-methoxy-13α-estra-1,3,5(10)-trien-17β-acetate (26b)

2.18.1. General procedure

Compound **17a**, **18a**, **25a** or **26a** (150 mg, 0.47 mmol) was dissolved in a mixture of pyridine (3 ml) and acetic anhydride (3 ml) and the solution was allowed to stand at room temperature for 12 h Then it was diluted with water and the oil separating out was extracted with CH_2Cl_2 (3 × 15 ml). The organic phase was washed with $NaHCO_3$ solution, and then with water, dried and evaporated *in vacuo*. The residual oil was chromatographed on silica gel with a mixture of CH_2Cl_2/hexane (1:3, v/v). **17c**: Oil (186 mg, 98%); R_f = 0.65 (ss B); $[\alpha]_D^{25}$ = +37.4 (*c* 1 in $CHCl_3$). (Found: 72.14; H, 8.27. $C_{24}H_{32}O_5$ (400.51) requires: C, 71.97; H, 8.05%). ^{1}H NMR (δ, ppm, $CDCl_3$): 1.08 (s, 3H, 18-H_3), 2.00 (s, 3H, Ac-H_3), 2.05 (s, 3H, Ac-H_3), 2.84 (d, 2H, *J* = 3.0 Hz, 6-H_2), 3.79 (s, 3H, 3-OCH_3), 4.15 (d, 2H, *J* = 6.0 Hz, 16a-H_2), 4.81 (d, 1H *J* = 5.0 Hz, 17-H), 6.63 (s, 1H, 4-H), 6.73 (dd, 1H, *J* = 8.5 Hz, *J* = 2.5 Hz, 2-H), 7.20 (d, 1H, *J* = 8.5 Hz, 1-H). ^{13}C NMR (δ, ppm, $CDCl_3$): 20.9 (Ac-CH_3); 21.30 (Ac-CH_3), 28.4, 29.1, 29.6, 29.8 (C-18), 30.4, 33.1, 40.4 (C-8), 40.8 (C-9), 44.1 (C-13), 44.7 (C-14), 51.9 (C-16), 55.2 (3-OCH_3), 66.4 (C-16a), 84.6 (C-17), 111.9 (C-2), 113.4 (C-4), 127.3 (C-1), 132.7 (C-10), 138.2 (C-5), 157.4 (C-3), 170.6 (C = O), 171.0 (C = O). **18c**: Oil (179 mg, 95%); R_f = 0.65 (ss B); $[\alpha]_D^{25}$ = 0.0 (*c* 1 in $CHCl_3$). (Found: C, 71.63; H, 8.24. $C_{24}H_{32}O_5$ (400.51) requires: C, 71.97; H, 8.05%). ^{1}H NMR (δ, ppm, $CDCl_3$): 1.02 (s, 3H, 18-H_3), 2.00 (s, 3H, Ac-H_3), 2.07 (s, 3H, Ac-H_3), 2.82 (m, 2H, 6-H_2), 3.77 (s, 3H, 3-OCH_3), 4.05 (m, 2H, 16a-H_2), 5.30 (d, 1H, *J* = 9.0 Hz, 17-H), 6.61 (d, 1H, *J* = 3.5 Hz, 4-H), 6.71 (dd, 1H, *J* = 8.5 Hz, *J* = 2.5 Hz, 2-H), 7.22 (d, 1H, *J* = 8.5 Hz, 1-H). ^{13}C NMR (δ, ppm, $CDCl_3$): 20.9 (Ac-CH_3), 21.0 (Ac-CH_3), 23.8 (C-18), 26.2; 28.3, 30.5, 33.1, 39.7, 42.1, 42.9, 44.1 (C-13), 48.8, 55.2 (3-OCH_3), 66.9 (C-16a), 76.5 (C-17), 111.7 (C-2), 113.6 (C-4), 127.0 (C-1), 132.1 (C-10), 137.9 (C-5), 170.7 (C = O), 170.8 (C = O). **25b**: Oil (90 mg, 95%); R_f = 0.72 (ss B); $[\alpha]_D^{25}$ = −5.5 (*c* 1 in $CHCl_3$). (Found: C, 72.08; H, 8.28. $C_{24}H_{32}O_5$ (400.51) requires: C, 71.97; H, 8.05%). ^{1}H NMR (δ, ppm, $CDCl_3$): 1.05 (s, 3H, 18-H_3), 2.02 (s, 3H, Ac-H_3), 2.06 (s, 3H, Ac-H_3), 2.81 (t, 2H, *J* = 5.0 Hz, 6-H_2), 3.77 (s, 3H, 3-OCH_3), 4.12 (m, 2H, 16a-H_2), 5.34 (d, 1H, *J* = 9.5 Hz, 17-H), 6.61 (s, 1H, 4-H), 6.71 (dd, 1H, *J* = 8.5 Hz, *J* = 2.5 Hz, 2-H), 7.19 (d, 1H, *J* = 8.5 Hz, 1-H). ^{13}C NMR (δ, ppm, $CDCl_3$): 20.9 (18-CH_3), 20.9 (Ac-CH_3), 24.2 (C-18), 26.6, 28.7 (Ac-CH_3), 29.3, 30.3, 30.5, 33.4, 36.9 (C-8), 40.5 (C-9), 41.1 (C-14), 44.3 (C-13), 49.7 (C-16), 55.2 (3-OCH_3), 65.1 (C-16a), 111.8 (C-2), 113.5 (C-4), 126.9 (C-1), 132.4 (C-10), 137.9 (C-5), 157.4 (C-3), 170.8 (C = O), 170.9 (C = O). **26b**: Oil (109 mg, 96%); R_f = 0.70 (ss B); $[\alpha]_D^{25}$ = +26 (*c* 1 in $CHCl_3$). (Found: C, 72.15; H, 8.27. $C_{24}H_{32}O_5$ (400.51) requires: C, 71.97; H, 8.05%). ^{1}H NMR (δ, ppm, $CDCl_3$): 1.08 (s, 3H, 18-H_3), 1.98 (s, 3H, Ac-H_3), 2.02 (s, 3H, Ac-H_3), 2.81 (m, 2H, 6-

H_2), 3.77 (s, 3H, 3-OCH_3), 4.01 (dd, 1H, J = 11.0 Hz, J = 6.5 Hz, 16a-H_2); 4.10 (t, 1H, J = 11.0 Hz, 16a-H_2), 5.12 (d, 1H, J = 5.0 Hz, 17-H), 6.61 (d, 1H, J = 3.0 Hz, 4-H), 6.72 (dd, 1H, J = 8.5 Hz, J = 3.0 Hz, 2-H), 7.17 (d, 1H, J = 8.5 Hz, 1-H). ^{13}C NMR (δ, ppm, $CDCl_3$): 20.8 (Ac-CH_3), 21.2 (Ac-CH_3), 28.6, 29.7, 30.0 (C-18), 30.4, 31.3, 32.4, 39.8, 40.2, 43.5, 44.9 (C-13), 55.1 (3-OCH_3), 63.9 (C-16a), 83.4 (C-17), 111.9 (C-2), 113.0 (C-4), 127.5 (C-1), 132.8 (C-10), 138.0 (C-5), 157.3 (C-3), 170.4 (C = O), 171.0 (C = O).

2.19. 3-Benzyloxy-13α-estra-1,3,5(10)-trien-17-one (15)

A mixture of compound **3** (25 g, 70 mmol) in acetic acid (200 ml) and *o*-phenylenediamine (20 g, 183 mmol) was treated at reflux temperature for 3 h. After cooling, the mixture was carefully poured onto ice, the precipitate formed was filtered off, washed with water and dried. The solid was dissolved in CH_2Cl_2 (300 ml) and the solution was washed with water (3 × 250 ml), dried over Na_2SO_4 and evaporated *in vacuo*. The crude product was dissolved in methanol (250 ml) and Girard-P reagent (18.8 g, 100 mmol) and acetic acid (20 ml) were added to the solution. The reaction mixture was heated at reflux for 3 h and then allowed to stand overnight at room temperature. After neutralization with dilute Na_2CO_3, the precipitate was filtered off. The precipitate was dissolved in CH_2Cl_2 (250 ml) and the solution was washed with water (3 × 250 ml) to remove the water-soluble derivative of residual normal estrone-3-benzyl ether. After drying over Na_2SO_4, the solvent was evaporated *in vacuo* to give **15** (24.4 g, 97%). **15** is identical with the compound described in ref. [10].

2.20. (Z)-3-Benzyloxy-16-hydroxymethylidene-13α-estra-1,3,5(10)-trien-17-one (16)

Compound **15** (28 g, 77.7 mmol) was dissolved in anhydrous toluene (100 ml) and then NaOMe (10.6 g, 0.2 mmol) and freshly distilled ethyl formate (100 ml, 1.3 mmol) were added. The mixture was stirred for 6 h at 50 °C and allowed to stand overnight at room temperature. It was then diluted with water (1 L) and carefully poured onto a mixture of ice (100 g) and concentrated HCl (22 ml). The white precipitate separating out was filtered off, washed thoroughly with water and dried. Recrystallization from CH_2Cl_2/hexane gave **16** (27.5 g, 91%), as white crystals. Mp: 180–182 °C; R_f = 0.75 (ss A); $[\alpha]_D^{25}$ = −34 (*c* 1 in $CHCl_3$). (Found: C, 80.56; H, 7.12. $C_{26}H_{28}O_3$ (388.51) requires: C, 80.38; H, 7.26%. ^{1}H NMR (δ, ppm, $CDCl_3$): 1.15 (s, 3H, 18-H_3), 2.81 (m, 2H, 6-H_2), 5.02 (s, 2H, Bn-H_2), 6.68 (d, 1H, J = 2.4 Hz, 4-H), 6.77 (dd, 1H, J = 8.6 Hz, J = 2.4 Hz, 2-H), 7.09 (s, 1H, =CH), 7.18 (d, 1H, J = 8.6 Hz, 1-H), 7.30 (t, 1H, J = 7.3 Hz, 4′-H), 7.37 (t, 2H, J = 7.3 Hz, 3′- and 5′-H), 7.41 (d, 2H, J = 7.3 Hz, 2′-H and 6′-H). ^{13}C NMR (δ, ppm $CDCl_3$): 24.7, 25.9 (C-18), 27.7, 27.9, 30.4, 30.9, 41.1, 43.6, 44.6, 47.8, 51.2 (C-13), 62.1, 64.4, 69.9, 112.7 (C-2), 114.6 (C-4), 127.0 (C-1), 127.4 (C-2′ and -6′), 127.8 (C-4′), 128.5 (C-3′ and -5′), 132.1 (C-10), 137.2 (C-1′), 138.0 (C-5), 156.8 (C-3), 223.4 (C = O). **16** is identical with the compound described in ref. [10].

2.21. 3-Benzyloxy-16α-hydroxymethyl-13α-estra-1,3,5(10)-trien-17β-ol (19a) and 3-benzyloxy-16β-hydroxymethyl-13α-estra-1,3,5(10)-trien-17α-ol (20a)

Compound **16a** (9 g, 23.2 mmol) was suspended in MeOH (300 ml), and KBH_4 (6.2 g, 116 mmol) was added in small portions at room temperature. The mixture was allowed to stand for 5 h, then poured onto ice (750 g) and acidified with dilute HCl to pH 5. The precipitate separating out was filtered off, washed until free from acid and dried. The mixture of **19a** and **20a** (8.0 g, 98%) was obtained in a ratio of 6:1. **20a** is identical with the compound described in ref. [10].

2.22. 17β-Hydroxy-3-benzyloxy-13α-estra-1,3,5(10)-trien-16α-ylmethyl acetate (19b) and 17α-hydroxy-3-benzyloxy-13α-estra-1,3,5(10)-trien-16β-ylmethyl acetate (20b)

A mixture of **19a** and **20a** (10 g, 25.5 mmol) was dissolved in pyridine (40 ml) and a solution of Ac_2O (2.6 ml) in pyridine (55 ml) was added dropwise with cooling in salt-ice. The mixture was allowed to stand for 5 h at room temperature, and then poured onto a mixture of ice (400 g) and concentrated H_2SO_4 (40 ml). The precipitate separating out was filtered off and dissolved in CH_2Cl_2 (60 ml), and the solution was washed with water (3 × 60 ml), dried over Na_2SO_4 and evaporated *in vacuo*. The mixture of products was subjected to chromatographic separation (silica gel, CH_2Cl_2/hexane 25:75, v/v) to give **19c** and **20c** as oil (2.1 g, 17%). Continued elution with CH_2Cl_2 and CH_2Cl_2/ethyl acetate (99:1, v/v) resulted in **19b** as an oil (5.6 g, 51%), **20b** as a white powdery compound (1.0 g, 9%), and a residual mixture of **19a** and **20a** (2.0 g, 20%). After alkaline methanolysis of the mixture of diacetates (**19c** and **20c**) and diols (**19a** and **20a**), the products formed were recycled. **19b**: Oil; R_f = 0.45 (ss A); $[\alpha]_D^{25}$ = +75 (*c* 1 in $CHCl_3$). (Found: C, 77.46; H, 7.96. $C_{28}H_{34}O_4$ (434.58) requires: C, 77.39; H, 7.89%). ^{1}H NMR (δ, ppm, $CDCl_3$): 1.08 (s, 3H, 18-H_3), 2.08 (s, 3H, Ac-H_3), 2.79 (m, 2H, 6-H_2), 3.51 (d, 1H, J = 7.5 Hz, 17-H), 4.12 (dd, 1H, , J = 11.0 Hz, J = 6.5 Hz, 16a-H_2), 4.23 (dd, 1H, J = 11.0 Hz, J = 6.0 Hz, 16a-H_2), 5.03 (s, 2H, Bn-H_2), 6.68 (s, 1H, 4-H), 6.79 (dd, 1H, J = 8.5 Hz, J = 2.5 Hz, 2-H), 7.16 (d, 1H, J = 8.5 Hz, 1-H), 7.32 (t, 1H, J = 7.5 Hz, 4′-H), 7.37 (t, 2H, J = 7.5 Hz, 3′-H and 5′-H), 7.42 (d, 2H, J = 7.5 Hz, 2′-H and 6′-H). **20b**: Mp: 66–68 °C; R_f = 0.35 (ss A); $[\alpha]_D^{25}$ = +17 (*c* 1 in $CHCl_3$). (Found: C, 77.52; H, 8.02. $C_{28}H_{34}O_4$ (434.58) requires: 77.39; H, 7.89%). ^{1}H NMR (δ, ppm, $CDCl_3$): 0.99 (s, 3H, 18-H_3), 2.08 (s, 3H, Ac-H_3), 2.79 (m, 2H, 6-H_2), 3.65 (d, 1H, J = 7.5 Hz, 17-H), 4.05 (dd, 1H, J = 11.0 Hz, J = 5.0 Hz, 16a-H_2), 4.37 (m, 1H, 16a-H_2), 5.03 (s, 2H, Bn-H_2), 6.68 (d, 1H, J = 2.2 Hz, 4-H), 6.77 (dd, 1H, J = 8.5 Hz, J = 2.2 Hz, 2-H), 7.19 (d, 1H, J = 8.5 Hz, 1-H), 7.29 (t, 1H, J = 7.2 Hz, 4′-H), 7.35 (t, 2H, J = 7.2 Hz, 3′- and 5′-H), 7.40 (d, 2H, J = 7.2 Hz, 2′-H and 6′-H). ^{13}C NMR (δ, ppm, $CDCl_3$): 21.0 (Ac-CH_3), 28.9, 29.0 30.3 (C-18), 30.4, 31.8, 32.0, 39.9, 42.3, 43.8, 44.9 (C-13), 51.9, 64.5 (C-16a), 69.9 (Bn-CH_2), 82.2 (C-17), 112.7 (C-2), 114.3 (C-4), 127.4 (C-1), 127.6 (C-2′ and -6′), 127.8 (C-4′), 128.5 (C-3′ and -5′), 133.7 (C-10), 137.4 (C-1′), 138.1 (C-5), 156.4 (C-3), 171.8 (Ac-C = O).

2.23. 3-Benzyloxy-17-oxo-13α-estra-1,3,5(10)-trien-16α-ylmethyl acetate (23)

Compound **19b** (3 g, 8.4 mmol) was dissolved in acetone (100 ml) and Jones reagent was added dropwise during cooling with ice. The reaction mixture was poured onto ice (300 g) and extracted with CH_2Cl_2. The CH_2Cl_2 solution was washed with water, dried and evaporated. The substance obtained was crystallized from acetone/hexane to give **13** (1.1 g, 60%) as white crystals. Mp: 153–155 °C; R_f = 0.55 (ss A); $[\alpha]_D^{25}$ = −32.8 (*c* 1 in $CHCl_3$). (Found: C, 77.81; H, 7.65. $C_{28}H_{32}O_4$ (432.56) requires: C, 77.75; H, 7.46%). ^{1}H NMR (δ, ppm, $CDCl_3$): 1.05 (s, 3H, 18-H_3), 2.05 (s, 3H, Ac-H_3), 2.84 (m, 2H, 6-H_2), 4.30 (d, 2H, J = 4.0 Hz, 16a-H_2), 5.02 (s, 2H, Bn-H_2), 6.70 (d, 1H, J = 2.0 Hz, 4-H), 6.78 (dd, 1H, J = 2.0 Hz, J = 8.5 Hz, 2-H), 7.18 (d, 1H, J = 8.5 Hz, 1-H), 7.31 (t, 1H, J = 7.0 Hz, 4′-H), 7.38 (t, 2H, J = 7.5 Hz, 3′-H and 5′-H), 7.42 (d, 2H, J = 7.5 Hz, 2′-H and 6′-H). ^{13}C NMR (δ, ppm, $CDCl_3$): 20.8 (C-18), 24.5 (Ac-CH_3), 25.6, 28.5, 30.3, 32.8, 41.4, 41.8, 45.2, 47.6, 50.2 (C-13), 63.3 (C-16a), 69.9 (Bn-CH_2), 112.6 (C-2), 114.6 (C-4), 126.9 (C-1), 127.4 (C-2′ and C-6′), 127.8 (C-4′), 128.5 (C-3′ and C-5′), 132.0 (C-10), 137.2 (C-1′), 137.9 (C-5), 156.8 (C-3), 170.8 (Ac-C = O), 219.6 (C-17C = O).

2.24. 3-Benzyloxy-17-oxo-13α-estra-1,3,5(10)-trien-16β-ylmethyl acetate (24)

Compound **20b** (2 g, 5.6 mmol) was dissolved in acetone (80 ml) and Jones reagent was added dropwise during cooling in ice. The reaction mixture was poured onto ice (300 g) and extracted with CH_2Cl_2. The organic solution was washed with water, dried and evaporated. The residue is oily product **24** (1.45 g, 60%); $R_f = 0.50$ (ss A); $[\alpha]_D^{25} = -8.5$ (*c* 1 in $CHCl_3$). (Found: 77.63; H, 7.67. $C_{28}H_{32}O_4$ (432.56) requires: C, 77.75; H, 7.46%). ^{1}H NMR (δ, ppm, $CDCl_3$): 1.14 (s, 3H, 18-H_3), 1.96 (s, 3H, Ac-H_3), 2.83 (m, 2H, 6-H_2), 4.18 (dd, 1H, *J* = 11.0 Hz, *J* = 6.5 Hz, 16a-H_2), 4.30 (dd, 1H, *J* = 11.0 Hz, *J* = 4.5 Hz, 16a-H_2), 5.02 (s, 2H, Bn-H_2), 6.69 (s, 1H, 4-H), 6.78 (d, 1H, *J* = 8.5 Hz, 2-H), 7.18 (d, 1H, *J* = 9.0 Hz, 1-H), 7.32 (t, 1H, *J* = 7.0 Hz, 4′-H), 7.38 (t, 2H, *J* = 7.5 Hz, 3′-H and 5′-H), 7.42 (d, 2H, *J* = 7.5 Hz, 2′- H and 6′-H). ^{13}C NMR (δ, ppm, $CDCl_3$): 20.9 (C-18), 25.2, 26.1 (Ac-CH_3), 27.8, 27.9, 29.7, 30.3, 31.0, 41.0, 42.6, 42.9, 47.6, 50.4 (C-13), 64.3 (C-16a), 69.9 (Bn-CH_2), 112.6 (C-2), 114.5 (C-4), 127.0 (C-1), 127.4 (C-2′ and C-6′), 127.8 (C-4′), 128.5 (C-3′ and C-5′), 132.2 (C-10), 137.2 (C-1′), 137.8 (C-5), 156.7 (C-3), 170.8 (Ac-C = O), 218.5 (C-17C = O).

2.25. 3-Benzyloxy-16α-hydroxymethyl-13α-estra-1,3,5(10)-trien-17α-ol (27a)

$LiAlH_4$ (850 mg, 22.5 mmol) was carefully suspended in anhydrous diethyl ether (70 ml), then *t*-BuOH (6.3 ml, 67.5 mmol) was added dropwise during stirring and cooling with salt-ice. The mixture was allowed to warm up to room temperature, then the solution of compound **23** (2.3 g, 4.5 mmol) in a mixture of diethyl ether/THF (35 ml, 15 ml) was added slowly dropwise to the suspension. The reaction mixture was stirred for 3 h and then decomposed by the careful addition of water (50 ml) during stirring and cooling with salt-ice. Next, it was acidified with dilute HCl to pH 5 and then extracted with diethyl ether. The substance obtained on washing, drying and evaporation of the solvent was purified by column chromatography on silica gel. Elution with CH_2Cl_2/ethyl acetate (95:5, v/v) gave pure compound **27a** (530 mg, 30%). Mp: 124–126 °C; $R_f = 0.55$ (ss A); $[\alpha]_D^{25} = +25.8$ (*c* 1 in $CHCl_3$). (Found: C, 79.67; H, 8.34. $C_{26}H_{32}O_3$ (392.54) requires: C, 79.56; H, 8.22%). ^{1}H NMR (δ, ppm, DMSO): 0.88 (s, 3H, 18-H_3), 2.71 (d, 2H, *J* = 5.5 Hz, 6-H_2), 5.03 (s, 2H, Bn-H_2), 6.68 (s, 1H, 4-H), 6.75 (d, 1H, *J* = 8.5 Hz, 2-H), 7.18 (d, 1H, *J* = 8.5 Hz, 1-H), 7.31 (t, 1H, *J* = 5.5 Hz, 4′-H), 7.37 (t, 2H, *J* = 7.5 Hz, 3′-H and 5′-H), 7.41 (d, 2H, *J* = 7.5 Hz, 2′-H and 6′-H). ^{13}C NMR (δ, ppm, DMSO): 24.2 (C-18), 26.7, 28.5, 30.0, 30.5, 33.4, 40.3, 41.1, 41.1, 44.4 (C-13), 49.6, 63.4 (C-16a), 69.05 (Bn-CH_2), 73.8 (C-17), 112.5 (C-2), 114.3 (C-4), 126.9 (C-1), 127.5 (C-2′ and C-6′), 127.7 (C-4), 128.4 (C-3′ and C-5′), 132.7 (C-10), 137.4 (C-1′), 137.8 (C-5), 156.1 (C-3). Further elution with CH_2Cl_2/ethyl acetate (95:5, v/v) gave **19a** (1.0 g, 60%).

2.26. 3-Benzyloxy-16α-hydroxymethyl-13α-estra-1,3,5(10)-trien-17α-ol acetonide (27c)

Compound **27a** (393 mg, 1 mmol) was dissolved in acetone (3 ml) and a catalytic amount of *p*-toluenesulfonic acid was added. The reaction mixture was treated at reflux temperature for 1 h. It was then neutralized with morpholine, diluted with CH_2Cl_2 and washed with water. The organic layer was dried over Na_2SO_4 and evaporated *in vacuo*. Purification by column chromatography on silica gel with CH_2Cl_2/hexane (1:3, v/v) gives **27c** (389 mg, 90%). Mp: 134–136 °C; $R_f = 0.80$ (ss B); $[\alpha]_D^{25} = -2$ (*c* 1 in $CHCl_3$). (Found: C, 80.67; H, 8.41. $C_{29}H_{36}O_3$ (432.67) requires: C, 80.52; H, 8.39%). ^{1}H NMR (δ, ppm, $CDCl_3$): 0.93 (s, 3H, 18-H_3), 1.25 and 1.39 (two s, 6H $(CH_3)_2C$), 2.80 (m, 2H, 6-H_2), 3.74 (d, 1H, *J* = 3.0 Hz, 16a-H_2), 4.05 (dd, 1H, *J* = 11.5 Hz, *J* = 4.0 Hz, 16a-H_2), 5.04 (s, 2H, Bn-H_2), 6.71 (s, 1H, 4-H), 6.80 (dd, 1H, *J* = 8.5 Hz, *J* = 2.5 Hz, 2-H), 7.23 (d, 1H, *J* = 8.5 Hz, 1-H), 7.33 (t, 1H, *J* = 7.5 Hz, 4′-H), 7. 39 (t, 2H, *J* = 7.5 Hz, 3′-H and 5′-H), 7.45 (d, 2H, *J* = 7.5 Hz, 2′-H and 6′-H). ^{13}C NMR (δ, ppm, $CDCl_3$): 19.8 (C-18), 28.6 and 29.0 (two C, $(CH_3)_2C$), 29.8, 29.9, 30.8, 32.5, 33.7, 36.4, 41.2, 44.5, 45.0 (C-13), 51.6, 62.1 (C-16′), 69.9 (Bn-CH_2), 81.7 (C-17), 97.4 $(CH_3)_2C$), 112.43 (C-2), 114.3 (C-4), 127.4 (C-2′ and C-6′), 127.5 (C-1), 127.8 (C-4), 127.8 (C-3′ and C-5′), 133.5 (C-10), 137.4 (C-1′), 138.6 (C-5), 156.4 (C-3).

2.27. 3-Benzyloxy-16α-hydroxymethyl-13α-estra-1,3,5(10)-trien-17α-ol phenylboronate (27d)

Compound **27a** (130 mg, 0.3 mmol) was dissolved in ethanol (6 ml) and phenylboronic acid (45 mg, 0.3 mmol) was added. The precipitate formed in 15 min was filtered off and dried (**27d**: 132 mg, 92%). Mp: 111–113 °C; $R_f = 0.70$ (ss B); $[\alpha]_D^{25} = -14.0$ (*c* 1 in $CHCl_3$). (Found: C, 80.47; H, 7.23. $C_{32}H_{35}BO_3$ (478.45) requires: C, 80.33; H, 7.37%.). ^{1}H NMR (δ, ppm, $CDCl_3$): 1.16 (s, 3H, 18-H_3), 2.80 (m, 2H, 6-H_2), 3.87 (dd, 1H, *J* = 11.5 Hz, *J* = 7.0 Hz, 16a-H_2), 5.04 (s, 2H, Bn-CH_2); 6.70 (d, 1H, *J* = 2.0 Hz, 4-H); 6.82 (dd, 1H, *J* = 8.5 Hz, *J* = 2.5 Hz, 2-H), 7.21 (d, 1H, *J* = 8.5 Hz, 1-H), 7.32 (t, 1H, *J* = 7.5 Hz, 4′-H), 7.38 (dd, 4H, *J* = 16.0 Hz, *J* = 8.5 Hz, 3′- H and 5′-H, 3″-H and 5″-H), 7.44 (d, 3H, *J* = 7.5 Hz, 2′-H and 6′-H, 4″-H), 7.86 (d, 2H, *J* = 7.0 Hz, 2″-H and 6″-H). ^{13}C NMR (δ, ppm, $CDCl_3$): 23.8 (C-18), 26.7; 29.1, 30.4, 32.4, 35.9, 39.3, 41.4, 45.2 (C-13), 49.5, 63.7 (C-1″), 63.9 (C-16a), 70.0 (Bn-CH_2), 78.5 (C-17), 112.8 (C-2), 114.4 (C-4), 127.4 (C-2″ and C-6″), 127.5 (C-3″ and C-5″) 127.8 (C-1), 128.5 (C-2′ and C-6′), 133.5 (C-4″), 133.5 (C-10), 133.9 (C-3′ and C-5′), 137.3 (C-1′), 137.9 (C-5), 156.6 (C-3).

2.28. 3-Benzyl-16α-p-toluenesulfonyloxymethyl-13α-estra-1,3,5(10)-trien-17α-ol (31)

Compound **27a** (393 mg, 1 mmol) was dissolved in anhydrous pyridine (15 ml) and a solution of *p*-toluenesulfonyl chloride (285 mg, 1.5 mmol) in anhydrous pyridine (10 ml) was added dropwise while cooled in an ice-bath. The reaction mixture was allowed to stand for 24 h and then poured onto a mixture of ice (100 g) and sulfuric acid (10 ml). The precipitate was filtered off and crystallized from methanol to give **31** (490 mg, 89%). Mp: 115–116 °C; $R_f = 0.85$ (ss A). (Found: C, 72.67; H, 6.95. $C_{33}H_{38}O_5S$ (546.73) requires: C, 72.50; H, 7.01%). ^{1}H NMR (δ, ppm, $CDCl_3$): 0.97 (s, 3H, 18-H_3), 2.45 (s, 3H, Ts-H_3), 2.78 (m, 2H, 6-H_2), 4.07 (dd, 1H, *J* = 9.5 Hz, *J* = 7.0 Hz, 16a-H_2), 4.12 (d, 1H, *J* = 8.5 Hz, 17-H), 4.28 (dd. 1H, *J* = 9.5 Hz, *J* = 7.0 Hz, 16a-H_2), 5.03 (s, 2H, Bn-H_2), 6.69 (d, 1H, *J* = 2.0 Hz, 4-H), 6.79 (dd, 1H, *J* = 8.5 Hz, *J* = 2.0 Hz, 2-H), 7.18 (d, 1H, *J* = 9.0 Hz, 1-H), 7.35 (m, 5H, 2′-H, 3′-H, 4′-H, 5′-H and 6-H), 7.42 (d, 2H, *J* = 7.0 Hz, 3″-H and 5″-H), 7.81 (d, 2H, *J* = 8.0 Hz, 2″-H and 6″). ^{13}C NMR (δ, ppm, $CDCl_3$): 21.6 (C-18), 23.3 (Ts-CH_3) 26.8, 28.8, 30.2, 30.3, 33.1, 39.2, 40.5, 40.7, 44.8 (C-13), 49.7 (C-14), 69.9 (C-16a), 71.9 (Bn-CH_2), 75.5 (C-17), 112.7 (C-2), 114.5 (C-4), 127.0 (C-1), 127.4 (C-2′ and C-6′), 127.8 (C-4′), 127.9 (C-2″ and C-6″), 128.5 (C-3′ and C-5), 129.8 (C-3″ and C-5″), 132.9 (C-10), 133.1 (C-1″), 137.3 (C-1′), 138.0 (C-5), 144.7 (C-4″), 156.7 (C-3).

2.29. 16α,17α-Epoxymethano-3-benzyloxy-13α-estra-1,3,5(10)-triene (35)

Compound **31** (547 mg, 1 mmol) was dissolved in methanol (15 ml) and heated at reflux with $NaOCH_3$ (162 mg, 3 mmol) for 2 h. The reaction mixture was diluted with water, the precipitate was filtered off, dried, and crystallized from a mixture of acetone/hexane to give **35** (325 mg, 86%). Mp: 91–93 °C; $R_f = 0.75$ (ss B); $[\alpha]_D^{25} = +19.2$ (*c* 1 in $CHCl_3$). (Found: C, 83.62; H, 7.92. $C_{26}H_{30}O_2$ (374.53) requires: C, 83.38; H, 8.07%. ^{1}H NMR (δ, ppm, $CDCl_3$): 1.26 (s, 3H, 18-H_3), 2.80 (m, 2H, 6-H_2), 3.20 (m, 1H, 16-H), 4.15 (t, 1H, *J* = 5.5 Hz, 16a-H_2), 4.78 (t, 1H, *J* = 7.0 Hz, 16a-H_2), 4.85 (d, 1H, *J* = 7.0 Hz, 17-H), 5.04 (s, 2H, Bn-H_2), 6.70 (d, 1H, *J* = 2.0 Hz, 4-H), 6.80 (dd, 1H, *J* = 8.5 Hz,

J = 2.5 Hz, 2-H), 7.19 (d, 1H, J = 8.5 Hz, 1-H), 7.32 (t, 1H, J = 7.0 Hz, 4′-H), 7.39 (t, 2H, J = 7.5 Hz, 3′-H and 5′-H), 7.43 (d, 2H, J = 7.5 Hz, 2′-H and 6′-H). ^{13}C NMR (δ, ppm, $CDCl_3$): 23.3 (C-18), 27.2, 29.2, 30.4, 32.1, 35.9, 37.3, 39.2, 42.4, 45.2 (C-13), 53.4, 69.9 (Bn-CH_2), 75.8 (C-16a), 94.2 (C-17), 112.6 (C-2), 114.5 (C-4), 127.2 (C-1), 127.4 (C-2′ and C-6′), 127.8 (C-4′), 128.5 (C-3′ and C-5′), 133.3 (C-10), 137.3 (C-1′), 137.9 (C-5), 156.6 (C-3).

2.30. 3-Benzyloxy-16β-hydroxymethyl-13α-estra-1,3,5(10)-trien-17β-ol (28a)

Compound **24** (2.2 g, 5 mmol) was dissolved in methanol (50 ml) and $NaBH_4$ (570 mg, 15 mmol) was added in small portions at room temperature. The reaction mixture was allowed to stand for 12 h, then it was diluted with water and the precipitate was collected by filtration and recrystallized from acetone/hexane to obtain **28a** (890 mg, 45%). Mp: 119–121 °C; R_f = 0.50 (ss A); $[\alpha]_D^{25}$ = +31.9 (*c* 1 in $CHCl_3$). (Found: C, 79.33; H, 8.37. $C_{26}H_{32}O_3$ (392.54) requires: C, 79.56; H, 8.22%). ^{1}H NMR (δ, ppm, DMSO): 0.85 (s, 3H, 18-H_3), 2.71 (s, 2H, 6-H_2), 4.38 (m, 2H, 16a-H_2), 5.03 (s, 2H, Bn-H_2), 6.68 (s, 1H, 4-H), 6.75 (d, 1H, J = 8.0 Hz, 2-H), 7.19 (d, 1H, J = 8.5 Hz, 1-H), 7.31 (t, 1H, J = 6.5 Hz, 4′-H), 7.37 (t, 2H, J = 7.5 Hz, 3′-H and 5′-H), 7.41 (d, 2H, J = 7.0 Hz, 2′-H and 6′-H). ^{13}C NMR (δ, ppm, DMSO): 23.4 (C-18), 26.1; 27.8, 28.1, 30.0, 32.8, 41.9, 42.1, 43.4 (C-13), 45.0, 46.6, 63.6 (C-16a), 68.9 (Bn-CH_2), 72.9 (C-17), 112.3 (C-2), 114.2 (C-4), 126.7 (C-1), 127.4 (C-3′ and C-5′), 127.6 (C-4′), 128.3 (C-2′ and C-6′), 132.4 (C-10), 137.3 (C-1′), 137.8 (C-5), 156.0 (C-3).

2.31. 3-Benzyloxy-16β-hydroxymethyl-13α-estra-1,3,5(10)-trien-17β-ol acetonide (28c)

Compound **28a** (250 mg, 0.64 mmol) was dissolved in acetone (25 ml) and a catalytic amount of *p*-toluenesulfonic acid was added. The reaction mixture was treated at reflux temperature for 1 h, neutralized with morpholine, diluted with CH_2Cl_2 and then washed with water. The organic layer was dried over Na_2SO_4 and evaporated *in vacuo*. The crude product was recrystallized from methanol to give **28c** (240 mg, 86%). Mp: 118–120 °C; R_f = 0.70 (ss B); $[\alpha]_D^{25}$ = +2.0 (*c* 1 in $CHCl_3$). (Found: C, 80.36; H, 8.51. $C_{29}H_{36}O_3$ (432.67) requires: C, 80.52; H, 8.39%). ^{1}H NMR (δ, ppm, $CDCl_3$): 0.93 (s, 3H, 18-H_3), 1.25 and 1.39 (2 s, 6H, 2 $(CH_3)_2$C), 2.80 (m, 2H, 6-H_2), 3.74 (d, 1H, J = 4.0 Hz, 16a-H_2), 4.05 (dd, 1H, J = 11.5 Hz, J = 4.0 Hz, 16a-H_2), 6.72 (s, 1H, 4-H), 6.80 (dd, 1H, J = 8.5 Hz, J = 2.5 Hz, 2-H), 7.22 (d, 1H, J = 8.5 Hz, 1-H), 7.31 (m, 1H, 4′-H), 7.45 (t, 2H, J = 7.5 Hz, 3′- and 5′-H), 7.40 (d, 2H, J = 7.5 Hz, 2′- and 6′-H). ^{13}C NMR (δ, ppm, $CDCl_3$): 19.8 (C-18), 28.6 ($(CH_3)_2$C), 29.0, 29.7 ($(CH_3)_2$C), 29.9, 30.8, 32.5, 33.7, 36.4, 41.2, 44.5, 45.0 (C-13), 51.6, 62.1 (C-16a), 69.9 (Bn-CH_2), 81.7 (C-17), 97.4 ($(CH_3)_2$C), 112.4 (C-2), 114.3 (C-4), 127.4 (C-2′ and -6′), 127.5 (C-1), 127.6 (C-4′), 128.5 (C-3′ and -5′), 133.5 (C-10), 137.4 (C-1′), 138.5 (C-5), 156.4 (C-3).

2.32. 3-Benzyloxy-16β-hydroxymethyl-13α-estra-1,3,5(10)-trien-17β-ol phenylboronate (28d)

Compound **28a** (130 mg, 0.33 mmol) was dissolved in ethanol (2 ml) and phenlyboronic acid (45 mg, 0.3 mmol) was added. The precipitate formed in 20 min was filtered off and dried affording **28d** (147 mg, 93%). Mp: 112–114 °C; R_f = 0.68 (ss B); $[\alpha]_D^{25}$ = −12 (*c* 1 in $CHCl_3$). (Found C, 80.57; H, 7.62. $C_{32}H_{35}BO_3$ (478.45) requires: C, 80.33; H, 7.37%). ^{1}H NMR (δ, ppm, $CDCl_3$): 1.16 (s, 3H, 18-H_3), 2.80 (m, 2H, 6-H_2), 3.87 (dd, 1H, J = 11.5 Hz, J = 7.0 Hz, 16a-H_2), 4.23 (d, 1H, J = 7.5 Hz, 17-H), 4.26 (dd, 1H, J = 11.5 Hz, J = 6.0 Hz, 16a-H_2), 5.04 (s, 2H, Bn-H_2), 6.70 (d, 1H, J = 2.0 Hz, 4-H), 6.82 (dd, 1H, J = 8.5 Hz, J = 2.0 Hz, 2-H), 7.21 (d, 1H, J = 8.5 Hz, 1H), 7.33 (t, 1H, J = 7.0 Hz, 4′-H), 7.38 (dd, 4H, J = 16.0 Hz, J = 8.5 Hz, 3′-H and 5′-H, 3″-H and 5″-H), 7.44 (d, 3H, J = 7.0 Hz, 2′-H and 6′-H, 4″-H), 7.86 (d, 2H, J = 7.0 Hz, 2″-H and 6″-H). ^{13}C NMR (δ, ppm, $CDCl_3$): 23.8 (C-18), 26.7, 29.1, 30.4, 30.5, 32.4; 35.9, 39.3, 41.4, 45.2 (C-13), 49.5, 63.7 (C-1″), 63.9 (C-16a), 70.0 (Bn-CH_2), 78.5 (C-17), 112.8 (C-2), 114.4 (C-4), 127.4 (C-2″ and C-6″), 127.5 (C-3″ and C-5″), 127.8 (C-1), 128.5 (C-2′ and C-6′), 130.6 (C-4″), 133.5 (C-10), 133.9 (C-3′ and C-5′), 137.7 (C-1′), 137.9 (C-5), 156.6 (C-3).

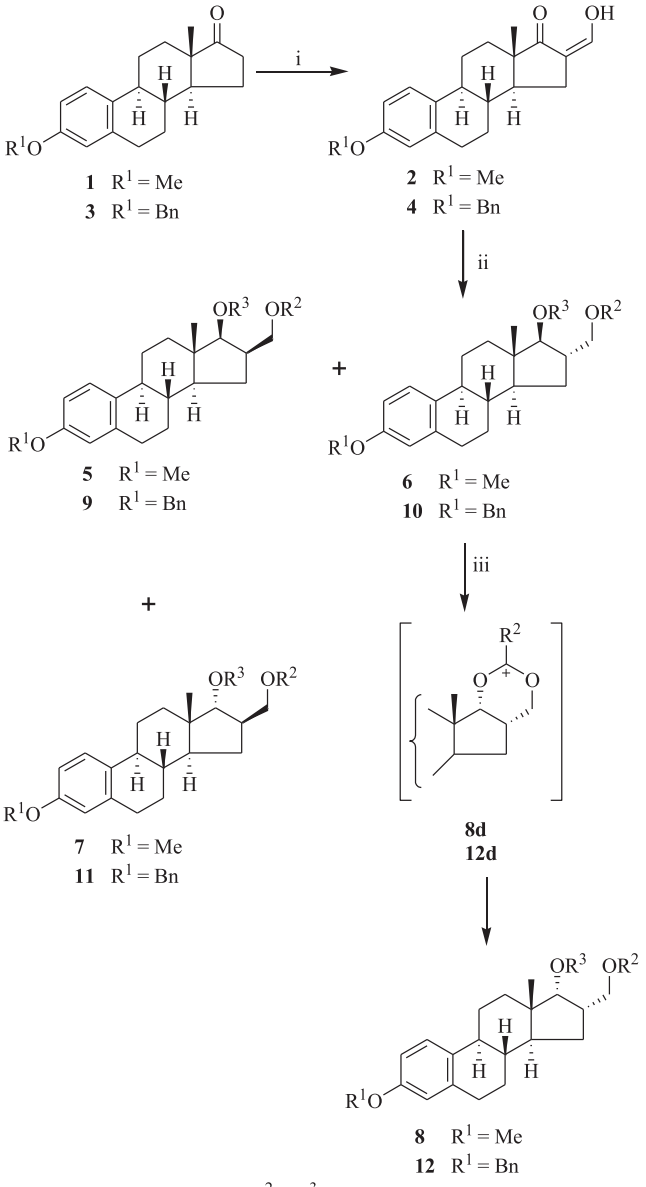

Scheme 1. Reagents and conditions: (i) NaOMe, HCOOEt, anhydrous toluene, 50 °C; (ii) KBH_4, MeOH; (iii) TsCl, pyridine; (iv) KOAc, AcOH.

2.33. 17β-Hydroxy-3-Benzyloxy-13α-estra-1,3,5,(10)-trien-16β-ylmethyl-p-toluenesulfonate (32)

Compound **28a** (393 mg, 1 mmol) was dissolved in anhydrous pyridine (15 ml) and a solution of *p*-toluenesulfonyl chloride (285 mg, 1.5 mmol) in anhydrous pyridine (10 ml) was added dropwise during cooling with ice. The reaction mixture was allowed to stand for 24 h and then poured onto a mixture of ice (100 g) and sulfuric acid (10 ml). The resulting precipitate was filtered off, dissolved in CH_2Cl_2 and

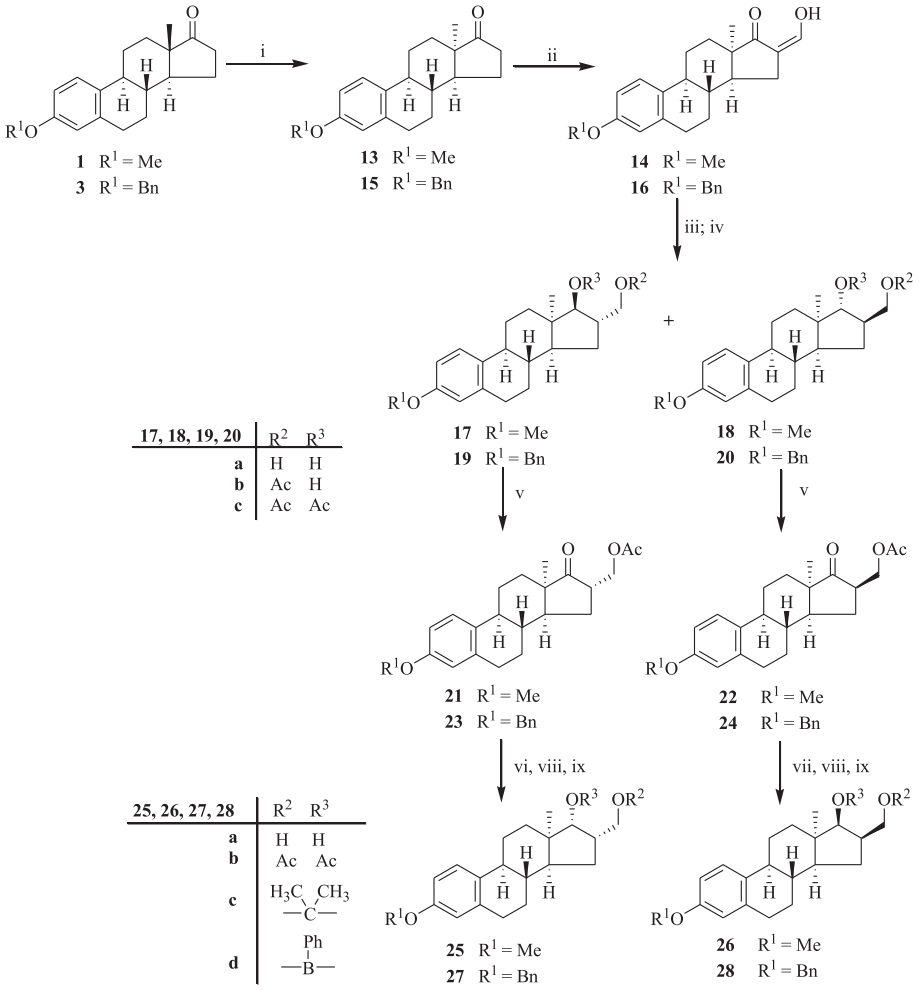

Scheme 2. Reagents and conditions: (i) 1,2-phenylenediamine, AcOH, 110 °C; (ii) NaOMe, HCOOEt, anhydrous toluene, 50 °C; (iii) KBH_4, MeOH; (iv) Ac_2O, pyridine; (v) CrO_3, acetone; (vi) $Li(OtBu)_3H$, diethyl ether; (vii) $NaBH_4$, MeOH; (viii) acetone, TsOH; (ix) EtOH, $PhB(OH)_2$.

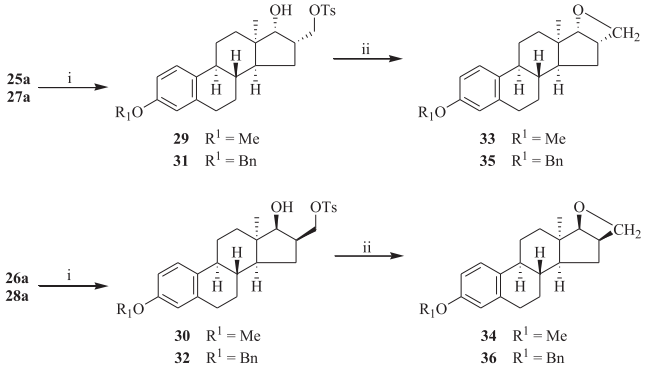

Scheme 3. Reagents and conditions: (i) TsCl, pyridine; (ii) NaOMe, MeOH.

chromatographed on silica gel. CH_2Cl_2/hexane (1:1, v/v) eluted pure **32**. Mp: 157–159 °C; R_f = 0.80 (ss A). (Found: C, 72.32; H, 6.87. $C_{33}H_{38}O_5S$ (546.73) requires: C, 72.50; H, 7.01%). ^{1}H NMR (δ, ppm, $CDCl_3$): 0.94 (s, 3H, 18-H_3), 2.45 (s, 3H, Ts-H_3), 2.73 (s, 2H, 6-H_2), 3.78 (d, 1H, *J* = 3.5 Hz, 17-H), 4.02 (dd, 1H, *J* = 8.5 Hz, *J* = 6.5 Hz, 16-H_2), 4.25 (t, 1H, *J* = 9.0 Hz, 16a-H_2), 5.02 (s, 2H, Bn-H_2), 6.67 (s, 1H, 4-H), 6.78 (d, 1H, *J* = 8.0 Hz, 2-H), 7.17 (d, 1H, *J* = 8.5 Hz, 1-H), 7.35 (m, 5H, 2′-H, 3′-H, 4′-H, 5′-H and 6′-H), 7.42 (d, 2H, *J* = 7.5 Hz, 3″-H and 5″-H), 7.80 (d, 2H, *J* = 7.5 Hz, 2″-H and 6″-H). ^{13}C NMR (δ, ppm, $CDCl_3$): 21. 6 (C-18), 28.8, 29.0, 30.0 (Ts-CH_3), 30.4, 31.5, 31.9, 39.9, 41.8, 43.7, 45.0 (C-13), 50.93 (C-14), 69.9 (C-16a), 70.9 (Bn-CH_2), 82.2 (C-17), 112.7 (C-2), 114.4 (C-4), 127.4 (C-2′ and C-6′), 127.6 (C-1), 127.8 (C-4′), 127.9 (C-2″ and C-6″), 128.5 (C-3′ and C-5′), 129.9 (C-3″ and C-5″), 133.1 (C-1″), 133.4 (C-10), 137.3 (C-1′), 138.1 (C-5), 144.7 (C-4″), 156.5 (C-3).

2.34. 16β,17β-Epoxymethano-3-benzyloxy-13α-estra-1,3,5(10)-triene (36)

Compound **32** (136 mg, 0.3 mmol) was dissolved in methanol (15 ml) and heated at reflux with $NaOCH_3$ (54 mg, 1 mmol) until full conversion (2.5 h). The solution was poured into water and mixed with NH_4Cl. The precipitate formed was filtered off, dried, and crystallized from a mixture of acetone/hexane to give **36** (95 mg, 84%). Mp: 118–120 °C; R_f = 0.70 (ss B); $[\alpha]_D^{25}$ = +17.0 (*c* 1 in $CHCl_3$). (Found: C, 83.56; H, 7.95. $C_{26}H_{30}O_2$ (374.53) requires: C, 83.38; H, 8.07%). ^{1}H NMR (δ, ppm, $CDCl_3$): 0.70 (s, 3H, 18-H_3), 2.90 (m, 2H, 6-H_2), 3.99 (dd, 1H, *J* = 4.0 Hz, *J* = 6.0 Hz, 16a-H_2), 4.77 (t, 1H, *J* = 7.0 Hz, 16a-H_2), 4.80 (d, 1H, *J* = 5.0 Hz, 17-H), 5.04 (s, 2H, Bn-H_2), 6.73 (d, 1H, *J* = 1.5 Hz, 4-H), 6.79 (dd, 1H, *J* = 8.5 Hz, *J* = 1.5 Hz, 2-H), 7.24 (s, 1H, 1-H), 7.32 (t, 1H, *J* = 7.5 Hz, 4′-H), 7.38 (t, 2H, *J* = 7.5 Hz, 3′-H and 5′-H), 7.44 (d, 2H, *J* = 7.5 Hz, 2′-H and 6′-H). ^{13}C NMR (δ, ppm, $CDCl_3$): 26.1 (C-18), 29.0, 29.5, 30.7, 32.7, 34.0, 38.0, 42.3, 42.5, 45 (C-13), 52.9, 69.9 (C-16a), 75.4 (Bn-CH_2), 75.8 , 98.1 (C-17), 112.4 (C-2), 114.5 (C-4), 127.2 (C-1), 127.4 (C-2′ and C-6′), 127.8 (C-4′), 128.5 (C-3′ and C-5′), 133.2 (C-10), 137.4 (C-1′), 138.4 (C-5), 156.6 (C-3).

Table 1
Antiproliferative activities of compounds **17a-20a** and **25a-28a**.

Compd.	Conc. (μM)	Growth Inhibition; % ± SEM [calculated IC_{50} value; μM]					
		231	MCF7	T47D	361	HeLa	A2780
26a	10	< 10	< 10	16.66 ± 1.42	< 10	47.46 ± 1.10	36.14 ± 0.87
	30	30.12 ± 0.98	26.81 ± 1.84	38.03 ± 0.68	17.83 ± 1.70	58.35 ± 1.52	55.23 ± 2.33
		–	–	–	–	[11.04]	[16.24]
17a	10	< 10	< 10	20.20 ± 1.74	22.87 ± 2.63	17.39 ± 2.03	23.62 ± 1.32
	30	32.08 ± 2.51	21.61 ± 2.30	36.68 ± 0.77	31.18 ± 2.94	58.61 ± 1.69	54.37 ± 1.97
		–	–	–	–	[24.68]	[23.16]
18a	10	10.11 ± 1.71	11.91 ± 2.11	31.69 ± 1.23	< 10	55.38 ± 2.11	38.69 ± 0.65
	30	40.43 ± 1.21	43.23 ± 1.64	57.02 ± 1.79	26.02 ± 1.29	66.04 ± 0.85	71.39 ± 0.56
		–	–	[22.51]	–	[8.35]	[13.34]
25a	10	27.10 ± 2.98	14.97 ± 2.16	28.01 ± 1.99	17.14 ± 1.26	56.54 ± 1.44	47.88 ± 1.89
	30	42.75 ± 2.13	31.29 ± 1.43	44.32 ± 2.06	39.26 ± 2.52	56.42 ± 1.52	63.68 ± 1.25
		–	–	–	–	[4.84]	[10.67]
28a	10	24.43 ± 2.89	37.28 ± 1.54	44.35 ± 1.16	15.21 ± 2.30	70.48 ± 1.33	54.59 ± 1.31
	30	88.29 ± 1.42	97.40 ± 0.34	93.46 ± 0.46	93.71 ± 0.25	98.05 ± 0.17	94.45 ± 0.81
		[11.54]	[11.95]	[10.31]	[13.23]	[4.91]	[7.94]
19a	10	18.24 ± 2.68	40.37 ± 1.69	46.30 ± 1.27	11.10 ± 1.85	50.87 ± 2.42	50.76 ± 0.79
	30	89.04 ± 1.53	96.65 ± 0.16	93.71 ± 0.29	96.53 ± 0.45	97.47 ± 0.08	94.89 ± 0.68
		[17.39]	[10.66]	[10.64]	[17.36]	[8.77]	[9.29]
20a	10	20.57 ± 0.91	26.44 ± 1.59	29.68 ± 0.72	15.69 ± 2.86	76.73 ± 0.72	51.90 ± 1.36
	30	94.18 ± 0.58	93.64 ± 0.65	46.81 ± 1.42	75.20 ± 1.10	89.60 ± 0.48	75.31 ± 0.69
		[16.04]	[14.62]	–	[13.54]	[3.36]	[7.74]
27a	10	22.31 ± 2.19	27.12 ± 1.96	44.31 ± 1.01	20.28 ± 2.84	55.27 ± 2.38	54.86 ± 1.86
	30	94.41 ± 0.73	95.43 ± 0.18	94.09 ± 0.87	88.12 ± 0.93	96.80 ± 0.53	93.68 ± 0.48
		[11.57]	[14.64]	[11.17]	[12.34]	[7.01]	[8.68]

		MRC-5
28a	10	< 10
	30	84.73 ± 0.98
		[26.01]
19a	10	< 10
	30	86.87 ± 0.59
		[15.65]

[#] IC_{50} values were calculated if the growth inhibition of the compound at 30 mM was > 75%.

*2.35. 16α-Acetoxymethyl-3-benzyloxy-13α-estra-1,3,5(10)-trien-17β-acetate (**19c**), 16β-acetoxymethyl-3-benzyloxy-13α-estra-1,3,5(10)-trien-17α-acetate (**20c**), 16α-acetoxymethyl-3-benzyloxy-13α-estra-1,3,5(10)-trien-17α-acetate (**27b**) and 16β-acetoxymethyl-3-benzyloxy-13α-estra-1,3,5(10)-trien-17β-acetate (**28b**)*

2.35.1. General procedure

Compound **19a**, **20a**, **27a** or **28a** (150 mg, 0.38 mmol) was dissolved in a mixture of pyridine (3 ml) and acetic anhydride (3 ml) and the solution was allowed to stand at room temperature for 12 h. It was then diluted with water and the oil separating out was extracted with CH_2Cl_2 (3 × 15 ml). The organic phase was washed with $NaHCO_3$ solution and then with water, dried and evaporated. The residual oil was chromatographed on silica gel with a mixture of CH_2Cl_2/hexane (1:3, v/v). Product **19c** (178 mg, 98%) was crystallized from methanol. Mp: 109–111 °C; R_f = 0.62 (ss B); $[\alpha]_D^{25}$ = +8.5 (*c* 1 in $CHCl_3$). (Found: 75.78; H, 7.85. $C_{30}H_{36}O_5$ (476.61) requires: C, 75.60; H, 7.61%). ^{1}H NMR (δ, ppm, $CDCl_3$): 1.08 (s, 3H, 18-H_3), 2.00 (s, 3H, Ac-H_3), 2.05 (s, 3H, Ac-H_3), 2.82 (m, 2H, 6-H_2), 4.15 (d, 2H, *J* = 6.0 Hz, 16a-H_2), 4.82 (d, 1H, *J* = 5.0 Hz, 17-H), 5.04 (s, 2H, Bn-H_2), 6.72 (d, 1H, *J* = 2.0 Hz, 4-H), 6.80 (dd, 1H, *J* = 8.5 Hz, *J* = 2.0 Hz, 2-H), 7.21 (d, 1H, *J* = 8.5 Hz, 1-H), 7.32 (t, 1H, *J* = 7.0 Hz, 4′-H), 7.38 (t, 2H, *J* = 7.0 Hz, 3′-H and 5′-H), 7.43 (d, 2H, *J* = 7.0 Hz, 2′-H and 6′-H). ^{13}C NMR (δ, ppm, $CDCl_3$): 20.9 (Ac-CH_3), 21.3 (Ac-CH_3), 28.4, 29.1, 29.6; 29.8 (C-18), 30.4, 33.1, 40.4, 40.8, 44.1 (C-13), 44.7, 51.9, 66.9 (C-16a), 69.9 (Bn-CH_2), 84.6 (C-17), 112.6 (C-2), 114.4 (C-4), 127.3 (C-1), 127.5 (C-2′ and C-6′), 127.8 (C-4′), 128.5 (C-3′ and C-5′), 132.9 (C-10), 137.3 (C-1′), 138.5 (C-5), 156.6 (C-3), 170.6 (C = O); 171.0 (C = O). **20c**: Mp: 71–72 °C; R_f = 0.60 (ss B); $[\alpha]_D^{25}$ = +11.5 (*c* 1 in $CHCl_3$). (Found: C, 75.38; H, 7,71. $C_{30}H_{36}O_5$ (476.61) requires: C, 75.60; H, 7.61%). ^{1}H NMR (δ, ppm, $CDCl_3$): 1.02 (s, 3H, 18-H_3); 2.00 (s, 3H, Ac-H_3), 2.07 (s, 3H, Ac-H_3), 2.82 (m, 2H, 6-H_2), 4.05 (m, 2H, 16a-H_2), 5.03 (s, 2H, Bn-H_2), 5.31 (d, 1H, *J* = 9.0 Hz, 17-H), 6.70 (s, 1H, 4-H); 6.79 (dd, 1H, *J* = 9.0 Hz, *J* = 2.0 Hz, 2-H), 7.22 (d, 1H, *J* = 9.0 Hz, 1-H); 7.31 (t, 1H, *J* = 7.0 Hz, 4′-H), 7.38 (t, 2H, *J* = 7.0 Hz, 3′-H and 5′-H), 7.43 (d, 2H, *J* = 7.0 Hz, 2′-H and 6′-H). ^{13}C NMR (δ, ppm, $CDCl_3$): 20.9 (Ac-CH_3), 21.0 (Ac-CH_3), 23.8 (18-CH_3), 26.2, 28.3, 30.5, 33.1, 39.7, 42.1, 42.8, 44.1 (C-13), 48.8, 66.9 (C-16a), 70.0 (Bn-CH_2), 76.5 (C-17), 112.6 (C-2), 114.6 (C-4), 126.9 (C-1), 127.4 (C-2′ and C-6′), 127.8 (C-4′), 128.5 (C-3′ and C-5′), 132.4 (C-10), 137.3 (C-1′), 138.0 (C-5), 156.7 (C-3), 170.7 (C = O), 171.0 (C = O). **27b**: Mp: 106–108 °C; R_f = 0.62 (ss B); $[\alpha]_D^{25}$ = + 15.6 (*c* 1 in $CHCl_3$). (Found: C, 75.42; H, 7.96. $C_{30}H_{36}O_5$ (476.61) requires: C, 75.60; H, 7.61%). ^{1}H NMR (δ, ppm, $CDCl_3$): 1.05 (s, 3H, 18-H_3); 2.03 (s, 3H, Ac-H_3), 2.07 (s, 3H, Ac-H_3), 2.80 (m, 2H 6-H_2), 4.02 (dd, 1H, *J* = 11.0 Hz, *J* = 7.0 Hz, 16a-H_2), 5.03 (s, 2H, Bn-H_2), 5.34 (d, 1H, *J* = 9.0 Hz, 17-H), 6.70 (d, 1H, *J* = 2.0 Hz, 4-H), 6.78 (dd, 1H, *J* = 8.5 Hz, *J* = 2.0 Hz, 2-H), 7.20 (d, 1H, *J* = 8.5 Hz, 1-H), 7.32 (t, 1H, *J* = 7.5 Hz, 4′-H), 7.38 (t, 2H, *J* = 7.5 Hz, 3′-H and 5′-H), 7.38 (t, 2H, *J* = 7.5 Hz, 3′-H and 5′-H), 7.43 (d, 2H, *J* = 7.5 Hz, 2′-H and 6′-H). ^{13}C NMR (δ, ppm, $CDCl_3$): 20.9 (Ac-CH_3), 20.9 (Ac-CH_3), 24.2 (C-18), 26.6, 28.7, 30.3, 30.5, 33.4; 36.9, 40.5, 41.2; 44.2 (C-13), 49.7, 65.1 (C-16a), 70.0 (Bn-CH_2), 76.0 (C-17), 112.6 (C-2), 114.5 (C-4), 126.9 (C-1), 127.4 (C-3′ and C-5′), 132.7 (C-10), 137.3 (C-1′), 138.0 (C-5), 156.7 (C-3), 170.8 (C = O), 170.9 (C = O). **28b**: Mp: 104–106 °C; R_f = 0.62 (ss B); $[\alpha]_D^{25}$ = +9.0 (*c* 1 in $CHCl_3$). (Found: 75.44; H, 7.82. $C_{30}H_{36}O_5$ (476.61) requires: C, 75.60; H, 7.61%). ^{1}H NMR (δ, ppm, $CDCl_3$): 1.26 (s, 3H, 18-H_3), 2.00 (s, 3H, Ac-H_3), 2.02 (s, 3H, Ac-H_3), 2.80 (m, 2H, 6-H_2), 4.01 (m, 16a-H_2), 4.11 (m, 1H, 16a-H_2), 5.03 (s, 2H, Bn-H_2), 5.12 (d, 1H, *J* = 5.0 Hz, 17-H), 6.70 (s, 1H, 4-H), 6.80 (dd, 1H, *J* = 8.5 Hz, *J* = 2.5 Hz, 2-H), 7.17 (d, 1H, *J* = 8.5 Hz, 1-H), 7.32 (t, 1H,

J = 7.5 Hz, 4′-H), 7.38 (t, 1H, J = 7.5 Hz, 3′-H and 5′-H), 7.32 (d, 2H, J = 7.5 Hz, 4′-H), 7.38 (t, 2H, J = 7.5 Hz, 3′-H and 5′-H), 7.43 (d, 2H, J = 7.5 Hz, 2′-H and 6′-H). ^{13}C NMR (δ, ppm, $CDCl_3$): 20.9 (Ac-CH_3), 21.2 (Ac-CH_3), 28.6, 29.7, 30.2 (C-18), 30.4, 31.3, 32.4, 39.9, 40.2, 43.5, 44.9 (C-13), 51.4, 64.0, (C-16a), 69.9 (Bn-CH_2); 83.4 (C-17), 112.7 (C-2), 114.4 (C-4), 127.4 (C-2′ and C-6′), 127.6 (C-1), 127.8 (C-4′), 128.5 (C-3′ and C-5′), 133.1 (C-10), 137.3 (C-1′), 138.1 (C-5), 156.6 (C-3), 170. 4 (C = O), 170.9 (C = O).

2.36. Cell cultures and antiproliferative assays

The growth-inhibitory effects of the compounds were tested *in vitro* by means of the MTT assay on HeLa, A2780, MCF-7, T47D, MDA-MB-231 and MDA-MB-361 cells, isolated from cervical, ovarian and breast cancer, and on noncancerous human fibroblasts (MRC-5 cell line). The growth-inhibitory effects of the compounds were tested *in vitro* by means of the MTT assay on a panel containing four breast cancer cell lines (MCF-7, T47D, MDA-MB-231 and MDA-MB-361), a cervical and an ovarian cancer cell line (HeLa and A2780, respectively).

The cell lines were obtained from the European Collection of Cell Cultures (Salisbury, UK). The cells were maintained in minimal essential medium supplemented with 10% fetal bovine serum (FBS), 1% non-essential aminoacids and an antibiotic-antimycotic mixture (AAM). All chemicals, if otherwise not specified, were purchased from Sigma-Aldrich Ltd. (Budapest, Hungary). All cell lines were grown in a humidified atmosphere of 5% CO_2 at 37 °C. For pharmacological investigations, 10 mM stock solutions of the tested compounds were prepared with dimethyl sulfoxide (DMSO). The highest applied DMSO concentration of the medium (0.3%) did not have any substantial effect on the determined cellular functions. All cell types were seeded into 96-well plates at a density of 5000 cells/well and allowed to stand overnight under cell culturing conditions, and the medium containing the tested compound was then added. After a 72 h incubation with two concentrations (10 and 30 μM) of the compounds, viability was determined by the addition of 20 μl 3-(4,5-dimethylthiazol-2-yl)-2,5-diphenyltetrazolium bromide (MTT) solution (5 mg/ml) for 4 h. The precipitated formazan crystals were solubilized in DMSO and the absorbance was determined at 545 nm with an ELISA reader [11]; wells with untreated cells were utilized as controls. Two independent experiments were performed with 5 parallel wells; cisplatin, an agent administered clinically in the treatment of certain gynecological malignancies, was used as positive control in the same concentration range as the test compounds. For the most effective compounds, the assays were repeated with a set of dilutions (0.03–30 μM), and sigmoidal dose–response curves were fitted to the measured data in order to determine the IC_{50} values by means of Graphpad Prism 4.0 (Graphpad Software; San Diego, CA, US).

3. Results and discussion

3.1. Synthetic studies

We have previously reported the preparation and determination of the configurations of the four possible isomers of the 3-methoxy-and 3-benzyloxy-16-hydroxymethyl-estra-1,3,5(10)-trien-17-ols (**5a-8a** and **9a-12a**) of 13β-estrone derivatives. Treatment of 3-methoxy- and 3-benzyloxyestra-1,3,6(10)-trienes (**1** and **3**) with NaOMe and ethyl formate gave 3-methoxy- and 3-benzyloxy-16-hydroxymethylidene-estra-1,3,5(10)-trien-17-ones (**2** and **4**). The 16-formyl compounds were reduced with KBH_4 in methanol yielding a mixture of three (**5a-7a** and **9a-11a**) of the four possible isomers of 3-methoxy- and 3-benzyloxy-16-hydroxymethylestra-1,3,5(10)-trienes in a ratio of 50:45:5 in 94% yield. Fourth isomers **8a** and **12a** were prepared from 16α-acetoxymethyl-17β-*p*-toluenesulfonate mixed esters (**6c** and **10c**) by neighboring group participation during solvolysis in aqueous AcOH. The structures of the isomers were confirmed unambiguously by their IR, ^{1}H and ^{13}C NMR spectra [6–8] (Scheme 1).

In contrast to the intensive research on 13β-estrone derivatives, reactions of 13α-estrones are much less studied [2,9,10,12]. Thus, due to our ongoing interest in 16-hydroxymethyl,17-hydroxy steroids, we extended the earlier investigations to 13α-estrone derivatives. In this publication we describe an extension of the C-16 hydroxymethylation to 3-methoxy- and 3-benzyloxy-13α-estra-1,3,5(10)-trien-17-ones (**13** and **15**). The 3-methoxy- and 3-benzyloxy-estra-1,3,5(10)-trien-17-ones (**1** and **3**) were epimerized by the method of Yaremenko and Khvat [5], resulting in 3-methoxy- and 3-benzyloxy-13α-estra-1,3,5(10)-trien-17-ones (**13** and **15**) in good yield [9,10]. Formylation of **13** and **15** with ethyl formate in the presence of NaOMe gave the 16-hydroxymethylidene-17-ketones (**14** and **16**) in high yield.

16-Hydroxymethylidene-17-ketones **14** and **16** were reduced with KBH_4 in methanol to give selectively **17**, **18** and **19**, **20**. Two new chiral centers are formed in this reaction, but only two of the possible four isomers could be obtained in a 6:1 ratio. These compounds could not be separated by flash chromatography on silica gel. Selective acetylation of the primary hydroxyl groups was therefore carried out and the resulting acetates (**17b**, **18b** and **19b**, **20b**) were separated on a silica gel column.

Compounds **17b**, **19b** and **18b**, **20b** were oxidized by the Jones method to 3-methoxy- and 3-benzyloxy-17-oxo-13α-estra-1,3,5(10)-trien-16α-ylmethyl acetates (**21**, **23**), and 3-methoxy- and 3-benzyloxy-17-oxo-13α-estra-1,3,5(10)-trien-16β-ylmethyl acetates (**22**, **24**). Reduction of **21** and **23** with lithium tri-*tert*-butoxyaluminum hydride afforded isomeric 16α-hydroxymethyl-3-methoxy- and 3-benzyloxy-16α-hydroxymethyl-13α-estra-1,3,5(10)-trien-17α-ols (**25a** and **27a**) and 16α-hydroxymethyl-3-methoxy- and 3-benzyloxy-16α-hydroxymethyl-13α-estra-1,3,5(10)-trien-17β-ols (**17a** and **19a**) in a ratio of 1:2. These isomers (**25a**, **17a** and **27a**, **19a**) are separable by flash chromatography. Repeated Jones oxidation of **17b** yields **21**, whereas the oxidation of **19b** gives **23**; both products can be reused in the reduction process.

Since reduction of the 17-ketone function in steroids normally yields a 17β group (for a few exceptions, see ref. [13]), the reduction of **22** and **24** with KBH_4 in methanol gave the isomers 16β-hydroxymethyl-3-methoxy- and l6β-hydroxymethyl-3-benzyloxy-13α-estra-1,3,5(10)-trien-17β-ols (**26a** and **28a**) (Scheme 2).

For confirmation of the configurations assumed for **25a**, **27a** and **26a**, **28a**, transformations were carried out with the individual isomers. Treatment of **25a**, **27a** and **26a**, **28a** with acetone in the presence of a catalytic amount of *p*-toluenesulfonic acid afforded the corresponding cyclic acetonide derivatives **25c**, **27c** and **26c**, **28c**. It is known from our earlier observations that only the *cis*-diols participate in acetonide building reaction [6]. Furthermore, they were reacted with phenylboronic acid to give the corresponding cyclic phenylboronic esters **25d**, **27d** and **26d**, **28d** in very good yields.

When treated with *p*-toluenesulfonyl chloride in pyridine at low temperature, the primary hydroxymethyl groups were tosylated yielding 17α-hydroxy-3-methoxy- and 17α-hydroxy-3-benzyloxy-13α-estra-1,3,5(10)-trien-16α-ylmethyl *p*-toluenesulfonates (**29** and **31**) and 17β-hydroxy-3-methoxy- and 17β-hydroxy-3-benzyloxy-13α-estra-1,3,5(10)-trien-16β-ylmethyl *p*-toluenesulfonates (**30** and **32**).

The alkaline reaction of these 1,3-tosylhydrines leads to the formation of oxetanes. The process can be regarded as a neighboring group participation characterized by the general symbol (O--4). Oxethane formation takes place readily when the participating groups are in a favourable steric configuration [14].

On alkaline methanolysis of **29** and **31**, α oxethanes **33** and **35** were formed, condensed to ring D. Alkaline methanolysis of **30** and **32**, in turn, gave β oxethanes **34** and **36** (Scheme 3).

In conclusion, we have synthesized two new *cis* 16-hydroxymethyl,17-hydroxy isomer pairs **25**, **27** and **26**, **28** in the 3-methoxy- and 3-benzyloxy-estra-13-*epi*-1,3,5(10)-triene-17-one series, respectively. These compounds were transformed quantitatively into their

cyclic acetonides and phenylboronic esters. Furthermore, alkaline methanolysis of their 16-*p*-toluensulfonyloxymethyl-17-hydroxy derivatives afforded the corresponding α and β oxetanes condensed to ring D ring in the sterane skeleton.

3.2. Determination of the antiproliferative properties of the 16-hydroxymethyl-3-methoxy- and 16-hydroxymethyl-3-benzyloxy-13α-estra-1,3,5(10)-trien-17-ol isomers

The antiproliferative activities of compounds **17a–20a** and **25a–28a** were determined *in vitro* by means of MTT assays against HeLa (cervical carcinoma), A2780 (ovarian carcinoma) and a set of breast cancer cell lines differing in receptor status [16]. These cell lines included MCF-7 (expressing estrogen and progesterone receptors), T47D (expressing estrogen, progesterone and androgen receptors), MDA-MB-361 (expressing estrogen and progesterone receptors and HER2), and a triple-negative cell line MDA-MB-231 (Table 1).

The antiproliferative activities of the compounds depended on the nature of the protecting group at the 3-hydroxy function and on the steric orientation of the substituents at C-16 and C-17. The 3-methyl ethers (**17a**, **18a**, **25a**, **26a**) did not influence the proliferation of the breast cancer cell lines markedly. Nevertheless, HeLa and A2780 seemed to be more sensitive to these compounds. 17α-Hydroxy derivatives (**18a** and **25a**) displayed outstanding cell growth-inhibitory properties against HeLa with IC_{50} values in the low micromolar range. The 16α,17β-diastereomer (**17a**) seemed to be the least potent in the methyl ether series, exerting remarkable antiproliferative action on HeLa and A2780 with IC_{50} values over 20 μM. This is in good agreement with the findings of Poirier et al. showing that in the 13-epimeric 3,17-estradiol series the 13α-methyl-3,17α-diol inhibits the proliferation of certain cancer cell lines mostly [15].

The 3-benzyl ethers (**19a**, **20a**, **27a**, **28a**), on the whole, proved to be more potent in comparison with their 3-methyl ether counterparts (**17a**, **18a**, **25a**, **26a**). These compounds (**19a**, **20a**, **27a**, **28a**) displayed moderate inhibitory properties with IC_{50} values in the range of 10–20 μM against the panel of breast cancer cell lines. The receptor status of the cells seems irrelevant, since no considerable cell line dependent differences between the IC_{50} values were observed. The 16β,17β-isomer (**28a**) may be concerned as the most active on the breast panel, because it displayed similar good potency against all four cell lines. All 3-benzyl ethers (**19a**, **20a**, **27a**, **28a**) inhibited the proliferation of HeLa and A2780 cell lines markedly. The 16β,17α-diastereomer (**20a**) was found to be the most potent and selective compound with an IC_{50} value of 3.36 μM against HeLa and 7.74 μM against A2780.

The two most potent 3-benzyl ethers (**19a** and **28a**) were selected for cancer selectivity investigations by means of the MTT assay, using the non-cancerous human fibroblast cell line MRC-5. Compounds **19a** and **28a** inhibited the proliferation of MRC-5 cell line dose-dependently. The 16β,17β-isomer (**28a**) proved to be tumor-selective by displaying IC_{50} values at least two times higher on healthy fibroblast cells than on cancer cell lines. The 16β,17β-isomer (**28a**) exerted a similar feature on fibroblasts in comparison with breast cancer cell lines but only a limited cancer selectivity could be identified when compared its action on HeLa or A2780 cells with that on MRC-5 cell line.

Acknowledgments

The work of Anita Kiss was supported by a PhD Fellowship of the Talentum Fund of Richter Gedeon Plc. (Budapest). Financial support from the Economic Development and Innovation Operative Programme of Hungary (GINOP-2.3.2-15-2016-00038) is gratefully acknowledged. This research was supported by the Hungarian Scientific Research Fund (OTKA K113150).

Appendix A. Supplementary data

Supplementary data associated with this article can be found, in the online version, at https://doi.org/10.1016/j.steroids.2018.02.008.

References

[1] E.E. Baulieu, Hormones, a complex communications network, in: E.E. Baulieu, P.A. Kelly (Eds.), Hormones, Herman Publishers, Paris and Chapman and Hall, New York, 1990, p. 147.
[2] B. Schönecker, C. Lange, M. Kötteritzsch, W. Günther, J. Weston, E. Anders, H. Görls, Conformation design for 13α-steroids, J. Org. Chem. 65 (2000) 5487–5497.
[3] D. Ayan, J. Roy, R. Maltais, D. Poirier, Impact of estradiol structural modifications (18-methyl and/or 17-hydroxy inversion of configuration) on the *in vitro* and *in vivo* estrogenic activity, J. Steroid Biochem. Mol. Biol. 127 (2011) 324–330.
[4] R. Minorics, N. Bózsity, J. Wölfling, E. Mernyák, G. Schneider, Á. Márki, G. Falkay, I. Ocsovszki, I. Zupkó, Antiproliferative effect of normal and 13-*epi*-D-homoestrone and their 3-methyl ethers on human reproductive cancer cell lines, J. Steroid Biochem. Mol. Biol. 132 (2012) 168–174.
[5] F.G. Yaramenko, A.V. Khvat, A new one-pot synthesis of 17-oxo-13α-steroids of the androstane series from their 13β-analogues, Mendeleev Commun. 122 (1994) 187–188.
[6] P. Taplcsányi, J. Wölfling, G. Falkay, Á. Márki, R. Minorics, G. Schneider, Synthesis and receptor binding examination of 16-hydroxymethyl-3,17-estradiol stereoisomers, Steroids 67 (2002) 671–678.
[7] G. Schneider, A. Vass, I. Vincze, P. Sohár, Neighbouring group participation in the 16- hydroxymethyl-3-methoxyestra-1,3,5(10)-trien-17β-ol series, Liebigs Ann. Chem. (1988) 267–273.
[8] G. Schneider, L. Hackler, P. Sohár, Preparation of 16α-hydroxymethyl-3-methoxyestra- 1,3,5(10)-trien-17α-ol and solvolysis investigations, Liebigs Ann. Chem. (1988) 679–683.
[9] E. Mernyák, J. Wölfling, G. Bunkóczi, L. Luo, T.R. Schneider, G. Schneider, Stereoselective synthesis of two *trans* 16-hydroxymethyl-3-methoxy-13α-estra-1,3,5(10)-trien-17-ol isomers, Collect. Czech. Chem. Commun. 68 (2003) 1121–1148.
[10] J. Wölfling, E. Mernyák, É. Frank, G. Falkay, Á. Márki, R. Minorics, G. Schneider, Synthesis and receptor-binding examinations of the normal and 13-*epi*-D-homoestrones and 3-methyl ethers, Steroids 68 (2003) 277–288.
[11] T. Mosmann, Rapid colorimetric assay for cellular growth survival: application to proliferation and cytotoxicity assay, J. Immunol. Methods 127 (1983) 324–330.
[12] S. Schwarz, B. Schönecker, K. Fritsche, A. Poser, C. Langer, W. Günther, S. Göttke, H. Görls, S. Bäsler, Synthesis and conformation of four 16,17-diols in the 3-methoxy-13α-estra-1,3,5(10)-triene series, Steroids 68 (2003) 113–123.
[13] W.R. Biggerstaff, T.F. Gallager, 3,16β-Dihydroxy-$\Delta^{1,3,5}$-estratrien-17-one and related compounds, J. Org. Chem. 22 (1957) 1220–1222.
[14] B. Capon, S.P. McManus, Neighbouring Group Participation vol. 1, (1976) 125.
[15] D. Ayan, J. Roy, R. Maltais, D. Poirier, Impact of estradiol structural modifications (18-methyl and/or 17-hydroxy inversion of configuration) on the *in vitro* and *in vivo* estrogenic activity, J. Steroid Biochem. Mol. Biol. (2011) 127324–127330.
[16] R.M. Neve, K. Chin, J. Fridlyand, J. Yeh, F.L. Baehner, T. Fevr, L. Clark, N. Bayani, J.P. Coppe, F. Tong, T. Speed, P.T. Spelman, A collection of breast cancer cell lines for the study of functionally distinct cancer subtypes, Cancer Cell 10 (2006) 515–527.

III.

Journal of Steroid Biochemistry & Molecular Biology 150 (2015) 123–134

Contents lists available at ScienceDirect

Journal of Steroid Biochemistry & Molecular Biology

journal homepage: www.elsevier.com/locate/jsbmb

Synthesis of *trans*-16-triazolyl-13α-methyl-17-estradiol diastereomers and the effects of structural modifications on their *in vitro* antiproliferative activities

Erzsébet Mernyák [a,*,1], Ida Kovács [b,1], Renáta Minorics [b], Péter Sere [a], Dóra Czégány [a], Izabella Sinka [b], János Wölfling [a], Gyula Schneider [a], Zsuzsanna Újfaludi [c], Imre Boros [c], Imre Ocsovszki [d], Mónika Varga [e], István Zupkó [b,**]

[a] Department of Organic Chemistry, University of Szeged, Dóm tér 8, H-6720 Szeged, Hungary
[b] Department of Pharmacodynamics and Biopharmacy, University of Szeged, Eötvös u. 6., H-6720 Szeged, Hungary
[c] Department of Biochemistry and Molecular Biology, University of Szeged, Közép fasor 52, H-6726 Szeged, Hungary
[d] Department of Biochemistry, University of Szeged, Dóm tér 9, H-6720 Szeged, Hungary
[e] Cereal Research Non-Profit Ltd., P.O. Box 391, H-6701 Szeged, Hungary

ARTICLE INFO

Article history:
Received 11 December 2014
Received in revised form 27 March 2015
Accepted 1 April 2015
Available online 3 April 2015

Keywords:
13α-estradiol
Azide–alkyne cycloaddition
Antiproliferative effect
Cell cycle blockade
Apoptosis

ABSTRACT

Novel 16-triazoles in the 13α-estrone series were synthesized *via* Cu(I)-catalyzed azide–alkyne cycloaddition of the two diastereomeric (on C-16 and on C-17) 16-azido-13α-estra-1,3,5(10)-trien-17-ol 3-benzyl ethers with substituted phenylacetylenes. The new heterocyclic derivatives were evaluated *in vitro* by means of MTT assays for antiproliferative activity against a panel of human adherent cancer cell lines (HeLa, MCF-7, A431, A2780, T47D, MDA-MB-231 and MDA-MB-361). The inversion of the configurations at C-16 and C-17 selectively affected the growth-inhibitory properties of the tested compounds. The 16β,17α isomers generally proved to be potent on all cell lines, with IC_{50} values comparable to those of the reference agent cisplatin. Change of the substitution pattern of the phenyl group of the acetylene led to great differences in antiproliferative properties. Exclusively the *p*-phenyl-substituted triazoles exerted high cytostatic effects. One of the most potent compounds activated caspase-3 and caspase-9 without influencing caspase-8, confirming the induction of apoptosis *via* the intrinsic pathway.

© 2015 Elsevier Ltd. All rights reserved.

1. Introduction

Structural modifications of estrone may lead to estrone-based anticancer agents [1–14]. There is a strict requirement in the development of this kind of drugs: the lack of estrogenic activity. Homologization of ring B or D or substitution at C-2 of the estrane skeleton usually leads to the complete loss of hormonal behavior [15,16,17–20]. An investigation of the effects of the inversion of the configuration at C-13 and/or C-17 of estradiol on the *in vitro* and *in vivo* estrogenic activity [20] revealed that the C-13 epimers of estradiol possess low affinity for the estrogen receptor, with no uterotropic activity when tested on mice. The probable explanation of the negligible receptor binding ability of the 13-*epi*-estradiols is the conformational change resulting from the *cis* junction of rings C and D [21,22]. 13α-Estrone is readily available from natural estrone by the epimerization method of Yaremenko and Khvat, using 1,2-phenylenediamine and acetic acid [23]. As the 13α-estradiols possess low affinity for the ER and are readily available, we chose these compounds as scaffolds for the design of 13α-estrone derivatives as potential antitumor agents. We set out to incorporate triazole rings into the 13α-estradiols in order to enhance their solubility and bioavailability and to diversify the drug structure [24]. Triazoles are attractive units because of their stability against metabolic degradation and their ability to form hydrogen-bonds. Additionally, these heterocycles are excellent mimetics of peptide bonds [25]. Cu(I)-catalyzed azide–alkyne cycloaddition (CuAAC) is a widely applicable and facile method for the introduction of a triazole moiety into natural products [26]. This regioselective reaction can be achieved with many compounds as Cu(I) catalysts and solvents and is unaffected by a variety

* Corresponding +3662544277
** Corresponding author.
E-mail addresses: bobe@chem.u-szeged.hu (E. Mernyák), zupko@pharm.u-szeged.hu (I. Zupkó).
[1] These authors contributed equally to this work.

http://dx.doi.org/10.1016/j.jsbmb.2015.04.001
0960-0760/© 2015 Elsevier Ltd. All rights reserved.

of functional groups. We recently reported the stereoselective synthesis of steroidal azidoalcohols and their CuAAC with terminal alkynes [27–31]. The triazoles formed by the 'click' reactions exerted moderate or pronounced cell-growth inhibition *in vitro* on human malignant cell lines.

In this paper, we describe CuAACs of the two diastereomeric (on C-16 and on C-17) *trans*-16-azido-13α-estra-1,3,5(10)-trien-17-ol 3-benzyl ethers with substituted phenylacetylenes. The *trans*-16-azido-17-alcohols were prepared by the ring-opening reactions of 16,17-epoxides with NaN_3. Novel 16-triazolyl-13α-methyl-17-estradiols and their precursors were tested *in vitro* on HeLa, MCF-7, A431 and A2780 cells, using MTT assays. The most potent derivatives were subjected to additional investigations on a panel of breast cancer cell lines. The effects of the configurations at C-16 and C-17 of the triazoles and the substitution patterns of the phenylacetylenes used as reagents were additionally examined. In order to clarify the mechanisms of antiproliferative action of the compounds, cell cycle analyses were performed by flow cytometry, and the caspase-3, caspase-8 and caspase-9 activities of one of the most potent derivatives were determined. The effects of the tested compounds on the mRNA expression pattern of p21 were investigated through real-time PCR analyses.

2. Methods and materials

2.1. Chemical synthesis

2.1.1. General methods

Melting points (mp) were determined with a Kofler hot-stage apparatus and are uncorrected. Elemental analyses were performed with a PerkinElmer CHN analyzer model 2400. Thin-layer chromatography: silica gel 60 F_{254}; layer thickness 0.2 mm (Merck); eluents: (A) EtOAc/hexane = 15/85, (B) EtOAc/hexane = 30/70; detection with iodine or UV (365 nm) after spraying with 5% phosphomolybdic acid in 50% aqueous phosphoric acid and heating at 100–120 °C for 10 min. Flash chromatography: silica gel 60, 40–63 μm (Merck). ^{1}H NMR spectra were recorded in $CDCl_3$ solution (if not otherwise stated) with a Bruker DRX-500 instrument at 500 MHz, with Me_4Si as internal standard. ^{13}C NMR spectra were recorded with the same instrument at 125 MHz under the same conditions. Full scan mass spectra of the compounds were acquired in the range 50–800 *m/z* with an Agilent 500MS Ion trap mass spectrometer equipped with an electrospray ionization source. Analyses were performed in positive ion mode. The spectra were collected by continous infusion of the steroid solution at a concentration of 10 ng μl^{-1} in MeCN/5 mM ammonium formate 50/50 (v/v %) at a flow rate of 15 μl min^{-1}. The analytical HPLC measurements were performed on an Agilent 1260 Infinity HPLC equipped with a Micro Vacuum Degasser, Binary Pump, Standard Autosampler, Thermostatted Column Compartment, and Variable Wavelength Detector. The chromatographic separation was achieved on Gemini NX C-18 analytical column (3 μm, 150 × 2 mm) from Phenomenex, equipped with a C-18 guard column, at 40 °C using gradient elution. Mobile phase A was water (Sigma–Aldrich Ltd., Budapest, Hungary), while mobile phase B was acetonitrile (Merck Ltd., Budapest, Hungary). A linear gradient was applied from 20% B to 100% B in 10 min (holding time: 5 min) then B content was lowered to 20% in 5 min and finally the column was re-equilibrated for 5 min. The flow rate was set to 0.2 ml/min.

2.1.2. Epoxidation of 3-benzyloxy-13α-estra-1,3,5(10), 16-tetraene (**1**)

A solution of 3-benzyloxy-13α-estra-1,3,5(10), 16-tetraene (**1**) (345 mg, 1.0 mmol) in CH_2Cl_2 (7 ml) was treated with a solution of magnesium monoperoxyphthalate hexahydrate (∼85%, 1.9 g, ∼4 mmol) in MeOH (7 ml) and the reaction mixture was stirred at room temperature for 24 h. Aqueous $NaHSO_3$ solution was then added. The mixture was diluted with CH_2Cl_2 (7 ml), the organic phase was separated and the aqueous phase was extracted with CH_2Cl_2. The combined organic phases were washed with water until neutral, dried over Na_2SO_4 and evaporated *in vacuo*. The crude product, analyzed by ^{1}H NMR spectroscopy, was a mixture of 16β,17β-epoxide (**2**) and 16α,17α-epoxide (**3**) in a ratio of 75:25. The residue was purified by flash chromatography with EtOAc/hexane = 10/90 as eluent. First-eluted compound **2** was obtained as a white solid after evaporation of the eluent (187 mg, 52%), mp 137–139 °C, R_f = 0.65 (ss A); ^{1}H NMR: δ_H 0.96 (s, 3H, 18-CH_3), 1.10–1.27 (overlapping multiplets, 3H), 1.50–1.64 (overlapping multiplets, 4H), 1.87–2.00 (overlapping multiplets, 3H), 2.12 (m, 1H), 2.21–2.26 (overlapping multiplets, 2H), 2.74–2.87 (m, 2H, 6-H_2), 3.10 (m, 1H) and 3.38 (m, 1H): 16-H and 17-H, 5.03 (s, 2H, OCH_2), 6.69 (d, 1H, *J* = 2.2 Hz, 4-H), 6.77 (dd, 1H, *J* = 8.6 Hz, *J* = 2.2 Hz, 2-H), 7.22 (d, 1H, *J* = 8.6 Hz, 1-H), 7.32 (t, 1H, *J* = 7.3 Hz, 4′-H), 7.38 (t, 2H, *J* = 7.3 Hz, 3′-H and 5′-H), 7.43 (d, 2H, *J* = 7.3 Hz, 2′-H and 6′-H). ^{13}C NMR: δ_C 26.7 (C-18), 27.8 (CH_2), 29.1 (CH_2), 30.6 (CH_2), 30.8 (CH_2), 35.4 (CH_2), 41.0 (C-13), 42.4 (CH), 44.5 (CH), 46.0 (CH), 54.1 and 66.0 (C-16 and C-17), 69.9 (OCH_2), 112.3 (C-2), 114.6 (C-4), 126.9 (C-1), 127.4 (2C: C-2′,6′), 127.8 (C-4′), 128.5 (2C: C-3′,5′), 132.9 (C-10), 137.4 (C-1′), 138.4 (C-5), 156.6 (C-3). MS *m/z* (%): 361 (100, $[M+H]^+$), 91 (50, Bn). Anal. Calcd. for $C_{25}H_{28}O_2$: C, 83.29; H, 7.83. Found: C, 83.35; H, 8.02. Purity from HPLC: 98.9%. Continued elution yielded a mixture of the epoxides **2** and **3** (102 mg, 28%) and finally compound **3** (53 mg, 15%), mp 97–99 °C, R_f = 0.57 (ss A); ^{1}H NMR: δ_H 1.27 (s, 3H, 18-CH_3), 1.22–1.34 (overlapping multiplets, 5H), 1.42–1.61 (overlapping multiplets, 4H), 1.91 (m, 1H), 2.44–2.65 (overlapping multiplets, 3H), 2.75 (m, 2H, 6-H_2), 3.07 (m, 1H) and 3.48 (m, 1H): 16-H and 17-H, 5.02 (s, 2H, OCH_2), 6.66 (d, 1H, *J* = 2.2 Hz, 4-H), 6.79 (dd, 1H, *J* = 8.6 Hz, *J* = 2.2 Hz, 2-H), 7.10 (d, 1H, *J* = 8.6 Hz, 1-H), 7.31 (t, 1H, *J* = 7.3 Hz, 4′-H), 7.38 (t, 2H, *J* = 7.3 Hz, 3′-H and 5′-H), 7.42 (d, 2H, *J* = 7.3 Hz, 2′-H and 6′-H). ^{13}C NMR: δ_C 23.6 (C-18), 26.2 (CH_2), 26.5 (CH_2), 29.3 (CH_2), 30.2 (CH_2), 34.6 (CH), 36.4 (CH_2), 41.2 (C-13), 43.0 (CH), 47.1 (CH), 58.4 and 67.1 (C-16 and C-17), 70.0 (OCH_2), 113.1 (C-2), 114.1 (C-4), 127.4 (2C: C-2′,6′), 127.8 (C-4′), 128.0 (C-1), 128.5 (2C: C-3′,5′), 134.4 (C-10), 137.3 (C-1′), 137.4 (C-5), 156.4 (C-3). MS *m/z* (%): 361 (100, $[M+H]^+$), 91 (23, Bn). Anal. Calcd. for $C_{25}H_{28}O_2$: C, 83.29; H, 7.83. Found: C, 83.42; H, 7.98. Purity from HPLC: 98.5%.

2.1.3. General procedure for the cleavage of epoxides **2** or **3** with hydrazoic acid

Epoxide **2** (360 mg, 1.0 mmol) or epoxide **3** (360 mg, 1.0 mmol) or a mixture of **2** and **3** (360 mg, 1.0 mmol) was dissolved in abs. DMSO (10 ml), and AcOH (1 ml) and NaN_3 (455 mg, 7.0 mmol) were added. The mixture was refluxed for 3 h. After cooling to room temperature, the mixture was poured into ice–water, treated with NaCl and extracted with CH_2Cl_2. The combined organic phases were washed with water until neutral, dried over Na_2SO_4 and evaporated *in vacuo*. The residue was purified by flash chromatography with EtOAc/hexane = 30/70 as eluent.

2.1.3.1. 16α-Azido-3-benzyloxy-13α-estra-1,3,5(10)-trien-17β-ol (4). As described in Section 2.1.3, epoxide **2** (360 mg, 1.0 mmol) was reacted with NaN_3 (455 mg, 7.0 mmol). Compound **4** was obtained as a white solid (351 mg, 87%), mp 86–88 °C, R_f = 0.43 (ss A); ^{1}H NMR: δ_H δ 1.16 (s, 3H, 18-CH_3), 1.21–1.35 (overlapping multiplets, 3H), 1.44–1.54 (overlapping multiplets, 2H), 1.63 (m, 1H), 1.73 (m, 1H), 1.82–1.88 (overlapping multiplets, 2H), 2.00–2.05 (overlapping multiplets, 2H), 2.33–2.46 (overlapping multiplets, 2H), 2.78 (m, 2H, 6-H_2), 3.65 (t, 1H, *J* = 5.1 Hz, 17-H), 3.82 (m, 1H, 16-H), 5.03 (s, 2H, OCH_2), 6.69 (d, 1H, *J* = 2.2 Hz, 4-H), 6.80 (dd, 1H, *J* = 8.6 Hz, *J* = 2.2 Hz, 2-H), 7.14 (d, 1H, *J* = 8.6 Hz, 1-H), 7.32 (t, 1H, *J* = 7.3 Hz, 4′-H), 7.38 (t, 2H, *J* = 7.3 Hz, 3′-H and 5′-H), 7.43 (d, 2H, *J* = 7.3 Hz, 2′-H and 6′-H). ^{13}C NMR: δ_C 27.2 (CH_2), 27.9 (CH_2), 28.7 (C-

18), 28.8 (CH_2), 30.2 (CH_2), 31.5 (CH_2), 37.7 (CH), 41.1 (CH), 42.1 (C-13), 49.0 (CH), 66.9 (C-16), 70.0 (OCH_2), 86.2 (C-17), 112.9 (C-2), 114.2 (C-4), 127.4 (2C: C-2′,6′), 127.6 (C-1), 127.8 (C-4′), 128.5 (2C: C-3′,5′), 133.8 (C-10), 137.3 (C-1′), 137.7 (C-5), 156.5 (C-3). MS *m/z* (%): 404 (57, $[M+H]^+$), 145 (100), 91 (89, Bn). Anal. Calcd. for $C_{25}H_{29}N_3O_2$: C, 74.41; H, 7.24. Found: C, 74.32; H, 7.37. Purity from HPLC: 97.9%.

2.1.3.2. 16β-Azido-3-benzyloxy-13α-estra-1,3,5(10)-trien-17α-ol (5). As described in Section 2.1.3, epoxide **3** (360 mg, 1.0 mmol) was reacted with NaN_3 (455 mg, 7.0 mmol). Compound **5** was obtained as a white solid (343 mg, 85%), mp 97–99 °C, R_f = 0.37 (ss A); ^{1}H NMR: δ_H 0.98 (s, 3H, 18-CH_3), 1.13–1.17 (m, 1H), 1.22–1.46 (overlapping multiplets, 5H), 1.52 (m, 1H), 1.79 (m, 1H), 1.94 (m, 2H), 2.25 (m, 2H), 2.50 (m, 1H), 2.82 (m, 2H, 6-H_2), 3.86 (m, 1H) and 4.03 (m, 1H): 16-H and 17-H, 5.04 (s, 2H, OCH_2), 6.71 (d, 1H, *J* = 2.2 Hz, 4-H), 6.80 (dd, 1H, *J* = 8.6 Hz, *J* = 2.2 Hz, 2-H), 7.21 (d, 1H, *J* = 8.6 Hz, 1-H), 7.32 (t, 1H, *J* = 7.3 Hz, 4′-H), 7.38 (t, 2H, *J* = 7.3 Hz, 3′-H and 5′-H), 7.43 (d, 2H, *J* = 7.3 Hz, 2′-H and 6′-H). ^{13}C NMR: δ_C 23.0 (C-18), 26.5 (CH_2), 28.3 (CH_2), 30.3 (CH_2), 31.3 (CH_2), 33.2 (CH_2), 42.0 (CH), 43.0 (C-13), 43.1 (CH), 48.3 (CH), 66.9 (C-16), 69.9 (OCH_2), 79.2 (C-17), 112.6 (C-2), 114.6 (C-4), 126.9 (C-1), 127.4 (2C: C-2′,6′), 127.8 (C-4′), 128.5 (2C: C-3′,5′), 132.1 (C-10), 137.2 (C-1′), 138.2 (C-5), 156.7 (C-3). MS *m/z* (%): 404 (100, $[M+H]^+$), 91 (54, Bn). Anal. Calcd. for $C_{25}H_{29}N_3O_2$: C, 74.41; H, 7.24. Found: C, 74.45; H, 7.18. Purity from HPLC: 98.6%.

*2.1.4. General procedure for the preparation of triazoles **7** and **8***

To a stirred solution of 16α-azido-3-benzyloxy-13α-estra-1,3,5(10)-trien-17β-ol **4** (100 mg, 0.25 mmol) or 16β-azido-3-benzyloxy-13α-estra-1,3,5(10)-trien-17α-ol **5** (100 mg, 0.25 mmol) in toluene (5 ml), Ph_3P (13 mg, 0.05 mmol), CuI (4.7 mg, 0.025 mmol), DIPEA (0.13 ml, 0.75 mmol) and the appropriate terminal alkyne (**6**, 1.1 equiv.) were added. The reaction mixture was refluxed for 2 h, allowed to cool and evaporated *in vacuo*. The residue was purified by flash chromatography with EtOAc/hexane = 20/80 as eluent.

2.1.4.1. 3-Benzyloxy-16α-[4-phenyl-1H-1,2,3-triazol-1-yl]-13α-estra-1,3,5(10)-trien-17β-ol (7a). As described in Section 2.1.4, azidoalcohol **4** (100 mg, 0.25 mmol) was reacted with phenylacetylene (**6a**, 0.030 ml). Compound **7a** was obtained as a white solid (123 mg, 97%), mp 95–97 °C, R_f = 0.41 (ss B); ^{1}H NMR: δ_H 1.31 (s, 3H, 18-CH_3), 1.29–1.36 (overlapping multiplets, 3H), 1.40–1.47 (overlapping multiplets, 2H), 1.62–1.71 (overlapping multiplets, 2H), 1.82 (m, 1H), 2.05 (m, 1H), 2.29 (m, 1H), 2.43 (m, 1H), 2.49–2.56 (overlapping multiplets, 2H), 2.81 (m, 2H, 6-H_2), 4.19 (m, 1H, 17-H), 4.77 (m, 1H, 16-H), 5.04 (s, 2H, OCH_2), 6.70 (d, 1H, *J* = 2.2 Hz, 4-H), 6.82 (dd, 1H, *J* = 8.6 Hz, *J* = 2.2 Hz, 2-H), 7.17 (d, 1H, *J* = 8.6 Hz, 1-H), 7.32 (overlapping multiplets, 2H, 4′-H and 4″-H), 7.39 (overlapping multiplets, 4H, 3′-H, 3″-H, 5′-H, 5″-H), 7.43 (d, 2H, *J* = 7.3 Hz, 2′-H and 6′-H), 7.76 (d, 2H, *J* = 7.5 Hz, 2″-H and 6″-H), 7.79 (s, 1H, C=CH). ^{13}C NMR: δ_C 27.0 (CH_2), 27.5 (CH_2), 28.7 (C-18), 28.9 (CH_2), 30.2 (CH_2), 31.9 (CH_2), 37.4 (CH), 41.0 (CH), 42.1 (C-13), 48.6 (CH), 66.2 (C-16), 70.0 (OCH_2), 85.3 (C-17), 113.0 (C-2), 114.2 (C-4), 119.4 (C=CH), 125.6 (2C) and 128.8 (2C): C-2″,3″,5″,6″; 127.4 (2C: C-2′,6′), 127.7 (C-1), 127.8 (C-4′), 128.1 (C-4″), 128.5 (2C: C-3′,5′), 130.5 (C-1″), 133.8 (C-10), 137.3 (C-1′), 137.6 (C-5), 147.3 (C=CH), 156.6 (C-3). MS *m/z* (%): 506 (100, $[M+H]^+$), 146 (23). Anal. Calcd. for $C_{33}H_{35}N_3O_2$: C, 78.38; H, 6.98. Found: C, 78.54; H, 7.05. Purity from HPLC: 97.3%.

2.1.4.2. 3-Benzyloxy-16α-[4-(3-tolyl)-1H-1,2,3-triazol-1-yl]-13α-estra-1,3,5(10)-trien-17β-ol (7b). As described in Section 2.1.4, azidoalcohol **4** (100 mg, 0.25 mmol) was reacted with 3-ethynyltoluene (**6b**, 0.036 ml). Compound **7b** was obtained as a white solid (125 mg, 96%), mp 149–150 °C, R_f = 0.43 (ss B); ^{1}H NMR: δ_H 1.26 (s, 3H, 18-CH_3), 1.29–1.36 (overlapping multiplets, 2H), 1.41–1.47 (overlapping multiplets, 2H), 1.62–1.72 (overlapping multiplets, 3H), 1.83 (m, 1H), 2.05 (m, 1H), 2.30 (m, 1H), 2.41–2.51 (overlapping multiplets, 3H), 2.39 (s, 3H, tolyl-CH_3), 2.81 (m, 2H, 6-H_2), 4.18 (d, 1H, *J* = 7.9 Hz, 17-H), 4.77 (m, 1H, 16-H), 5.04 (s, 2H, OCH_2), 6.70 (d, 1H, *J* = 2.2 Hz, 4-H), 6.82 (dd, 1H, *J* = 8.6 Hz, *J* = 2.2 Hz, 2-H), 7.14 (d, 1H, *J* = 7.3 Hz, 4″-H), 7.17 (d, 1H, *J* = 8.6 Hz, 1-H), 7.29 (t, 1H, *J* = 7.3 Hz, 5″-H), 7.32 (t, 1H, *J* = 7.3 Hz, 4′-H), 7.38 (t, 2H, *J* = 7.3 Hz, 3′-H and 5′-H), 7.43 (d, 2H, *J* = 7.3 Hz, 2′-H and 6′-H), 7.56 (d, 1H, *J* = 7.3 Hz, 6″-H), 7.62 (s, 1H, 2″-H), 7.79 (s, 1H, C=CH). ^{13}C NMR: δ_C 21.4 (tolyl-CH_3), 27.0 (CH_2), 27.5 (CH_2), 28.7 (C-18), 28.9 (CH_2), 30.2 (CH_2), 31.9 (CH_2), 37.4 (CH), 41.0 (CH), 42.1 (C-13), 48.6 (CH), 66.1 (C-16), 70.0 (OCH_2), 85.3 (C-17), 113.0 (C-2), 114.2 (C-4), 119.3 (C=CH), 122.7 (C-6″), 126.3 (C-2″), 127.4 (2C: C-2′,6′), 127.7 (C-1), 127.8 (C-4′), 128.5 (2C: C-3′,5′), 128.7 and 128.9 (C-4″ and C-5″), 130.5 (C-1″), 133.8 (C-10), 137.3 (C-1′), 138.5 (C-3″), 137.6 (C-5), 147.5 (C=CH), 156.6 (C-3). MS *m/z* (%): 520 (100, $[M+H]^+$), 160 (29). Anal. Calcd. for $C_{34}H_{37}N_3O_2$: C, 78.58; H, 7.18. Found: C, 78.67; H, 7.05. Purity from HPLC: 96.9%.

2.1.4.3. 3-Benzyloxy-16α-[4-(4-tolyl)-1H-1,2,3-triazol-1-yl]-13α-estra-1,3,5(10)-trien-17β-ol (7c). As described in Section 2.1.4, azidoalcohol **4** (100 mg, 0.25 mmol) was reacted with 4-ethynyltoluene (**6c**, 0.035 ml). Compound **7c** was obtained as a white solid (121 mg, 93%), mp 96–98 °C, R_f = 0.43 (ss B); ^{1}H NMR: δ_H 1.27 (s, 3H, 18-CH_3), 1.38–1.47 (overlapping multiplets, 3H), 1.61–1.70 (overlapping multiplets, 4H), 1.83 (m, 1H), 2.05 (m, 1H), 2.27 (m, 1H), 2.42 (m, 1H), 2.47–2.54 (overlapping multiplets, 2H), 2.37 (s, 3H, tolyl-CH_3), 2.80 (m, 2H, 6-H_2), 4.17 (d, 1H, *J* = 7.9 Hz, 17-H), 4.76 (m, 1H, 16-H), 5.04 (s, 2H, OCH_2), 6.70 (d, 1H, *J* = 2.2 Hz, 4-H), 6.82 (dd, 1H, *J* = 8.6 Hz, *J* = 2.2 Hz, 2-H), 7.17–7.21 (overlapping multiplets, 3H, 1-H, 3″-H and 5″-H), 7.32 (t, 1H, *J* = 7.3 Hz, 4′-H), 7.38 (t, 2H, *J* = 7.3 Hz, 3′-H and 5′-H), 7.44 (d, 2H, *J* = 7.3 Hz, 2′-H and 6′-H), 7.65 (d, 2H, *J* = 7.5 Hz, 2″-H and 6″-H), 7.75 (s, 1H, C=CH). ^{13}C NMR: δ_C 21.3 (tolyl-CH_3), 27.0 (CH_2), 27.5 (CH_2), 28.7 (C-18), 28.9 (CH_2), 30.2 (CH_2), 31.9 (CH_2), 37.4 (CH), 41.0 (CH), 42.1 (C-13), 48.6 (CH), 66.2 (C-16), 70.0 (OCH_2), 85.3 (C-17), 113.0 (C-2), 114.2 (C-4), 119.0 (C=CH), 125.5 (2C) and 129.5 (2C): C-2″,3″,5″,6″; 127.4 (2C: C-2′,6′), 127.6 (C-1″), 127.7 and 127.8 (C-1 and C-4′), 128.5 (2C: C-3′,5′), 133.9 (C-10), 137.3 and 137.6 and 137.9 (C-1′ and C-5 and C-4′), 147.4 (C=CH), 156.6 (C-3). MS *m/z* (%): 520 (54, $[M+H]^+$), 160 (100). Anal. Calcd. for $C_{34}H_{37}N_3O_2$: C, 78.58; H, 7.18. Found: C, 78.42; H, 7.35. Purity from HPLC: 98.9%.

2.1.4.4. 3-Benzyloxy-16α-[4-{4-(trifluoromethyl) phenyl}-1H-1,2,3-triazol-1-yl]-13α-estra-1,3,5(10)-trien-17β-ol (7d). As described in Section 2.1.4, azidoalcohol **4** (100 mg, 0.25 mmol) was reacted with 1-ethynyl-4-(trifluoromethyl) benzene (**6d**, 0.039 ml). Compound **7d** was obtained as a white solid (136 mg, 95%), mp 133–135 °C, R_f = 0.52 (ss B); ^{1}H NMR: δ_H 1.32 (s, 3H, 18-CH_3), 1.33 (m, 1H), 1.44 (m, 1H), 1.64–1.74 (overlapping multiplets, 4H), 1.81 (m, 1H), 2.05 (m, 1H), 2.29 (m, 1H), 2.43 (m, 1H), 2.51–2.61 (overlapping multiplets, 2H), 2.81 (m, 2H, 6-H_2), 3.26 (d, 1H, *J* = 4.7 Hz, OH), 4.21 (m, 1H, 17-H), 4.78 (m, 1H, 16-H), 5.04 (s, 2H, OCH_2), 6.70 (d, 1H, *J* = 2.2 Hz, 4-H), 6.82 (dd, 1H, *J* = 8.6 Hz, *J* = 2.2 Hz, 2-H), 7.18 (d, 1H, *J* = 8.6 Hz, 1-H), 7.32 (t, 1H, *J* = 7.3 Hz, 4′-H), 7.39 (t, 2H, *J* = 7.3 Hz, 3′-H and 5′-H), 7.43 (d, 2H, *J* = 7.3 Hz, 2′-H and 6′-H), 7.62 (d, 2H, *J* = 8.2 Hz, 2″-H and 6″-H), 7.82 (d, 2H, *J* = 8.2 Hz, 3″-H and 5″-H), 7.87 (s, 1H, C=CH). ^{13}C NMR: δ_C 26.7 (CH_2), 27.1 (CH_2), 28.5 (C-18), 28.8 (CH_2), 30.1 (CH_2), 31.6 (CH_2), 37.1 (CH), 40.9 (CH), 41.8 (C-13), 48.2 (CH), 66.6 (C-16), 69.9 (OCH_2), 85.1 (C-17), 112.9 (C-2), 114.1 (C-4), 120.6 (C=CH), 123.9 (d, *J* = 272.5 Hz, CF_3), 125.3 (2C: C-2″ and C-6″), 125.6 (d, 2C, *J* = 3.4 Hz, C-3″ and C-5″), 127.4 (2C: C-2′,6′), 127.7 (C-1), 127.8 (C-4′), 128.4 (2C: C-3′,5′), 129.7 (d, *J* = 32.6 Hz, C-4″), 133.5 (C-1″), 133.8 (C-10), 137.2 (C-1′), 137.5 (C-5), 145.3 (C=CH), 156.5 (C-3). MS *m/z* (%): 574 (58, $[M+H]^+$), 145 (64),

115 (100). Anal. Calcd. for $C_{34}H_{34}F_3N_3O_2$: C, 71.19; H, 5.97. Found: C, 71.37; H, 6.11. Purity from HPLC: 97.9%.

2.1.4.5. 3-Benzyloxy-16α-[4-(4-ethylphenyl)-1H-1,2,3-triazol-1-yl]-13α-estra-1,3,5(10)-trien-17β-ol (7e). As described in Section 2.1.4, azidoalcohol **4** (100 mg, 0.25 mmol) was reacted with 1-ethynyl-4-ethynylbenzene (**6e**, 0.039 ml). Compound **7e** was obtained as a white solid (127 mg, 95%), mp 100–101 °C, R_f = 0.46 (ss B); ^{1}H NMR: δ_H 1.30 (s, 3H, 18-CH_3), 1.26 (t, 3H, J = 7.6 Hz, CH_2–CH_3), 1.32 (m, 1H), 1.38–1.47 (overlapping multiplets, 2H), 1.61–1.71 (overlapping multiplets, 4H), 1.83 (m, 1H), 2.05 (m, 1H), 2.27 (m, 1H), 2.43 (m, 1H), 2.49–2.55 (overlapping multiplets, 2H), 2.66 (q, 2H, J = 7.6 Hz, CH_2–CH_3), 2.81 (m, 2H, 6-H_2), 3.26 (s, 1H, OH), 4.19 (m, 1H, 17-H), 4.75 (m, 1H, 16-H), 5.04 (s, 2H, OCH_2), 6.70 (d, 1H, J = 2.2 Hz, 4-H), 6.82 (dd, 1H, J = 8.6 Hz, J = 2.2 Hz, 2-H), 7.17 (d, 1H, J = 8.6 Hz, 1-H), 7.22 (d, 2H, J = 7.9 Hz, 3″-H and 5″-H), 7.32 (t, 1H, J = 7.3 Hz, 4′-H), 7.39 (t, 2H, J = 7.3 Hz, 3′-H and 5′-H), 7.44 (d, 2H, J = 7.3 Hz, 2′-H and 6′-H), 7.66 (d, 2H, J = 7.9 Hz, 2″-H and 6″-H), 7.75 (s, 1H, C=CH). ^{13}C NMR: δ_C 15.5 (CH_2–CH_3), 26.9 (CH_2), 27.4 (CH_2), 28.6 (CH_2), 28.7 (C-18), 28.9 (CH_2), 30.2 (CH_2), 31.9 (CH_2), 37.4 (CH), 41.0 (CH), 42.1 (C-13), 48.5 (CH), 66.1 (C-16), 70.0 (OCH_2), 85.3 (C-17), 113.0 (C-2), 114.2 (C-4), 119.1 (C=CH), 125.6 (2C) and 128.3 (2C): C-2″,3″,5″,6″; 127.4 (2C: C-2′,6′), 127.7 (C-1), 127.8 (C-4′), 127.9 (C-1″), 128.5 (2C: C-3′,5′), 133.9 (C-10), 137.3 (C-1′), 137.6 (C-5), 144.3 and 147.4 (C-4″ and C=CH), 156.5 (C-3). MS m/z (%): 534 (100, $[M+H]^+$), 174 (55). Anal. Calcd. for $C_{35}H_{39}N_3O_2$: C, 78.77; H, 7.37. Found: C, 78.95; H, 7.52. Purity from HPLC: 96.9%.

2.1.4.6. 3-Benzyloxy-16β-[4-{4-(tert-butyl) phenyl}-1H-1,2,3-triazol-1-yl]-13α-estra-1,3,5(10)-trien-17α-ol (7f). As described in Section 2.1.4, azidoalcohol **4** (100 mg, 0.25 mmol) was reacted with 4-(*tert*-butyl) phenylacetylene (**6f**, 0.050 ml). Compound **7f** was obtained as a white solid (129 mg, 92%), mp 90–92 °C, R_f = 0.54 (ss B); ^{1}H NMR: δ_H 1.30 (s, 3H, 18-CH_3), 1.35 (s, 9H, $C(CH_3)_3$), 1.32 (m, 1H), 1.44 (m, 1H), 1.61–1.71 (overlapping multiplets, 4H), 1.82 (m, 1H), 2.05 (m, 1H), 2.21 (m, 1H), 2.27 (m, 1H), 2.43 (m, 1H), 2.50–2.57 (overlapping multiplets, 2H), 2.81 (m, 2H, 6-H_2), 4.18 (d, 1H, J = 7.9 Hz, 17-H), 4.75 (m, 1H, 16-H), 5.04 (s, 2H, OCH_2), 6.70 (d, 1H, J = 2.2 Hz, 4-H), 6.82 (dd, 1H, J = 8.6 Hz, J = 2.2 Hz, 2-H), 7.18 (d, 1H, J = 8.6 Hz, 1-H), 7.34 (t, 1H, J = 7.3 Hz, 4′-H), 7.37–7.44 (overlapping multiplets, 6H, 2′-H, 6′-H, 3′-H, 5′-H, 3″-H and 5″-H), 7.60 (d, 2H, J = 7.5 Hz, 2″-H and 6″-H), 7.76 (s, 1H, C=CH). ^{13}C NMR: δ_C 27.0 (CH_2), 27.4 (CH_2), 28.7 (C-18), 28.9 (CH_2), 30.2 (CH_2), 31.3 (3C: C $(CH_3)_3$), 31.8 (CH_2), 37.4 (CH), 41.0 (CH), 42.1 (C-13), 48.5 (CH), 51.1 ($C(CH_3)_3$), 66.1 (C-16), 70.0 (OCH_2), 85.3 (C-17), 113.0 (C-2), 114.2 (C-4), 119.2 (C=CH), 125.3 (2C) and 125.7 (2C): C-2″,3″,5″,6″; 127.4 (2C: C-2′,6′), 127.6 (C-1″), 127.7 and 127.8 (C-1 and C-4′), 128.5 (2C: C-3′,5′), 133.9 (C-10), 137.2 (C-1′), 137.6 (C-5), 147.2 (C=CH), 151.1 (C-4″), 156.6 (C-3). MS m/z (%): 562 (100, $[M+H]^+$), 202 (44). Anal. Calcd. for $C_{37}H_{43}N_3O_2$: C, 79.11; H, 7.72. Found: C, 79.28; H, 7.95. Purity from HPLC: 98.9%.

2.1.4.7. 3-Benzyloxy-16β-[4-(4-bromophenyl)-1H-1,2,3-triazol-1-yl]-13α-estra-1,3,5(10)-trien-17α-ol (7g). As described in Section 2.1.4, azidoalcohol **4** (100 mg, 0.25 mmol) was reacted with 4-bromophenylacetylene (**6g**, 50 mg). Compound **7g** was obtained as a white solid (129 mg, 88%), mp 72–74 °C, R_f = 0.39 (ss B); ^{1}H NMR: δ_H 1.31 (s, 3H, 18-CH_3), 1.33 (m, 1H), 1.43 (m, 1H), 1.62–1.72 (overlapping multiplets, 3H), 1.81 (m, 1H), 2.05 (m, 1H), 2.29 (m, 1H), 2.43 (m, 1H), 2.52 (m, 2H), 2.81 (m, 2H, 6-H_2), 4.18 (d, 1H, J = 7.9 Hz, 17-H), 4.77 (m, 1H, 16-H), 5.04 (s, 2H, OCH_2), 6.70 (d, 1H, J = 2.2 Hz, 4-H), 6.81 (dd, 1H, J = 8.6 Hz, J = 2.2 Hz, 2-H), 7.17 (d, 1H, J = 8.6 Hz, 1-H), 7.32 (t, 1H, J = 7.3 Hz, 4′-H), 7.38 (t, 2H, J = 7.3 Hz, 3′-H and 5′-H), 7.43 (d, 2H, J = 7.3 Hz, 2′-H and 6′-H), 7.52 (d, 2H, J = 7.5 Hz, 2″-H and 6″-H), 7.63 (d, 2H, J = 7.5 Hz, 3″-H and 5″-H), 7.81 (s, 1H, C=CH). ^{13}C NMR: δ_C 27.0 (CH_2), 27.5 (CH_2), 28.7 (C-18), 28.9 (CH_2), 30.2 (CH_2), 31.8 (CH_2), 37.4 (CH), 41.0 (CH), 42.1 (C-13), 48.6 (CH), 66.3 (C-16), 70.0 (OCH_2), 85.4 (C-17), 113.1 (C-2), 114.3 (C-4), 119.6 (C=CH), 122.0 (C-4″), 127.1 (2C, C-2″ and C-6″), 127.4 (2C, C-2′ and C-6′), 127.7 (C-1), 127.9 (C-4′), 128.5 (2C, C-3′ and C-5′), 129.4 (C-1″), 132.0 (2C, C-3″ and C-5″), 133.8 (C-10), 137.3 (C-1′), 137.5 (C-5), 148.2 (C=CH), 156.6 (C-3). MS m/z (%): 584 (100, $[M+H]^+$). Anal. Calcd. for $C_{33}H_{34}BrN_3O_2$: C, 67.81; H, 5.86. Found: C, 69.28; H, 6.15. Purity from HPLC: 97.4%.

2.1.4.8. 3-Benzyloxy-16β-[4-(4-fluorophenyl)-1H-1,2,3-triazol-1-yl]-13α-estra-1,3,5(10)-trien-17α-ol (7h). As described in Section 2.1.4, azidoalcohol **4** (100 mg, 0.25 mmol) was reacted with 4-fluorophenylacetylene (**6h**, 33 mg). Compound **7h** was obtained as a white solid (113 mg, 86%), mp 84–86 °C, R_f = 0.41 (ss B); ^{1}H NMR: δ_H 1.31 (s, 3H, 18-CH_3), 1.44 (m, 1H), 1.62–1.74 (overlapping multiplets, 4H), 1.81 (m, 1H), 2.05 (m, 1H), 2.27 (m, 1H), 2.43 (m, 1H), 2.50–2.54 (overlapping multiplets, 2H), 2.81 (m, 2H, 6-H_2), 4.19 (d, 1H, J = 8.0 Hz, 17-H), 4.76 (m, 1H, 16-H), 5.04 (s, 2H, OCH_2), 6.70 (d, 1H, J = 2.2 Hz, 4-H), 6.82 (dd, 1H, J = 8.6 Hz, J = 2.2 Hz, 2-H), 7.08 (t, 2H, J = 7.8 Hz, 3″-H and 5″-H), 7.18 (d, 1H, J = 8.6 Hz, 1-H), 7.32 (t, 1H, J = 7.3 Hz, 4′-H), 7.38 (t, 2H, J = 7.3 Hz, 3′-H and 5′-H), 7.42 (d, 2H, J = 7.3 Hz, 2′-H and 6′-H), 7.72 (m, 2H, 2″-H and 6″-H), 7.77 (s, 1H, C=CH). ^{13}C NMR: δ_C 26.9 (CH_2), 27.5 (CH_2), 28.7 (C-18), 28.9 (CH_2), 30.1 (CH_2), 31.6 (CH_2), 37.4 (CH), 41.0 (CH), 42.1 (C-13), 48.5 (CH), 66.3 (C-16), 69.9 (OCH_2), 85.3 (C-17), 113.0 (C-2), 114.2 (C-4), 115.8 (d, 2C, J = 21.7 Hz, C-3″ and C-5″), 119.3 (C=CH), 126.6 (C-1″), 127.3 (d, 2C, J = 8.0 Hz, C-2″ and C-6″), 127.4 (2C: C-2′,6′), 127.7 (C-1), 127.8 (C-4′), 128.5 (2C: C-3′,5′), 133.7 (C-10), 137.3 (C-1′), 137.5 (C-5), 146.4 (C=CH), 156.5 (C-3), 162.6 (d, J = 247.6 Hz, C-4″). MS m/z (%): 524 (100, $[M+H]^+$). Anal. Calcd. for $C_{33}H_{34}FN_3O_2$: C, 75.69; H, 6.54. Found: C, 76.53; H, 7.06. Purity from HPLC: 98.9%.

2.1.4.9. 3-Benzyloxy-16β-[4-phenyl-1H-1,2,3-triazol-1-yl]-13α-estra-1,3,5(10)-trien-17α-ol (8a). As described in Section 2.1.4, azidoalcohol **5** (100 mg, 0.25 mmol) was reacted with phenylacetylene (**6a**, 0.030 ml). Compound **8a** was obtained as a white solid (116 mg, 92%), mp 132–134 °C, R_f = 0.33 (ss B); ^{1}H NMR: δ_H 1.11 (s, 3H, 18-CH_3), 1.27–1.50 (overlapping multiplets, 5H), 1.56 (m, 1H), 1.97–2.02 (overlapping multiplets, 2H), 2.11 (m, 1H), 2.24–2.30 (overlapping multiplets, 2H), 2.72–2.81 (overlapping multiplets, 2H), 2.89 (m, 2H, 6-H_2), 4.57 (d, 1H, J = 8.0 Hz, 17-H), 4.80 (m, 1H, 16-H), 5.02 (s, 2H, OCH_2), 6.70 (d, 1H, J = 2.2 Hz, 4-H), 6.77 (dd, 1H, J = 8.6 Hz, J = 2.2 Hz, 2-H), 7.19 (d, 1H, J = 8.6 Hz, 1-H), 7.28–7.33 (overlapping multiplets, 2H, 4′-H and 4″-H), 7.36–7.39 (overlapping multiplets, 4H, 3′-H, 3″-H, 5′-H, 5″-H), 7.43 (d, 2H, J = 7.3 Hz, 2′-H and 6′-H), 7.73 (d, 2H, J = 8.4 Hz, 2″-H and 6″-H), 7.74 (s, 1H, C=CH). ^{13}C NMR: δ_C 23.0 (C-18), 26.5 (CH_2), 28.4 (CH_2), 30.4 (CH_2), 31.7 (CH_2), 33.1 (CH_2), 42.0 (CH), 42.9 (CH), 43.2 (C-13), 48.4 (CH), 66.5 (C-16), 69.9 (OCH_2), 78.8 (C-17), 112.7 (C-2), 114.6 (C-4), 119.5 (C=CH), 125.6 (2C) and 128.8 (2C): C-2″,3″,5″,6″, 127.0 (C-1), 127.4 (2C: C-2′,6′), 127.8 (C-4′), 128.0 (C-4″), 128.5 (2C: C-3′,5′), 130.5 (C-1″), 132.1 (C-10), 137.3 (C-1′), 138.2 (C-5), 147.4 (C=CH), 156.7 (C-3). MS m/z (%): 506 (100, $[M+H]^+$), 146 (29). Anal. Calcd. for $C_{33}H_{35}N_3O_2$: C, 78.38; H, 6.98. Found: C, 78.54; H, 7.06. Purity from HPLC: 97.1%.

2.1.4.10. 3-Benzyloxy-16β-[4-(3-tolyl)-1H-1,2,3-triazol-1-yl]-13α-estra-1,3,5(10)-trien-17α-ol (8b). As described in Section 2.1.4, azidoalcohol **5** (100 mg, 0.25 mmol) was reacted with 3-ethynyltoluene (**6b**, 0.036 ml). Compound **8b** was obtained as a white solid (122 mg, 94%), mp 114–116 °C, R_f = 0.37 (ss B); ^{1}H NMR: δ_H 1.11 (s, 3H, 18-CH_3), 1.25–1.58 (overlapping multiplets, 7H), 1.56 (m, 1H), 1.96–2.03 (overlapping multiplets, 2H), 2.09 (m, 1H), 2.24–2.31 (overlapping multiplets, 2H), 2.71–2.91 (overlapping

multiplets, 3H), 2.36 (s, 3H, tolyl-CH_3), 2.81 (m, 2H, 6-H_2), 4.55 (m, 1H, 17-H), 4.80 (m, 1H, 16-H), 5.02 (s, 2H, OCH_2), 6.70 (d, 1H, J = 2.2 Hz, 4-H), 6.76 (dd, 1H, J = 8.6 Hz, J = 2.2 Hz, 2-H), 7.11 (d, 1H, J = 7.3 Hz, 4″-H), 7.19 (d, 1H, J = 8.6 Hz, 1-H), 7.27 (t, 1H, J = 7.7 Hz, 5″-H), 7.31 (t, 1H, J = 7.3 Hz, 4′-H), 7.38 (t, 2H, J = 7.3 Hz, 3′-H and 5′-H), 7.43 (d, 2H, J = 7.3 Hz, 2′-H and 6′-H), 7.52 (d, 1H, J = 7.7 Hz, 6″-H), 7.56 (s, 1H, 2″-H), 7.72 (s, 1H, C=CH). ^{13}C NMR: δ_C 21.4 (tolyl-CH_3), 23.0 (C-18), 26.5 (CH_2), 28.4 (CH_2), 30.4 (CH_2), 31.8 (CH_2), 33.2 (CH_2), 42.0 (CH), 42.9 (CH), 43.2 (C-13), 48.4 (CH), 66.4 (C-16), 69.9 (OCH_2), 78.7 (C-17), 112.7 (C-2), 114.6 (C-4), 119.4 (C=CH), 122.7 (C-6″), 126.3 (C-2″), 127.0 (C-1), 127.4 (2C: C-2′,6′), 127.8 (C-4′), 128.5 (2C: C-3′,5′), 128.7 and 128.8 (C-4″ and C-5″), 130.3 (C-1″), 132.1 (C-10), 137.3 (C-1′), 138.4 (C-3″), 138.2 (C-5), 147.6 (C=CH), 156.7 (C-3). MS m/z (%): 520 (100, $[M+H]^+$), 160 (38). Anal. Calcd. for $C_{34}H_{37}N_3O_2$: C, 78.58; H, 7.18. Found: C, 78.63; H, 7.31. Purity from HPLC: 96.9%.

2.1.4.11. 3-Benzyloxy-16β-[4-(4-tolyl)-1H-1,2,3-triazol-1-yl]-13α-estra-1,3,5(10)-trien-17α-ol (8c). As described in Section 2.1.4, azidoalcohol **5** (100 mg, 0.25 mmol) was reacted with 4-ethynyltoluene (**6c**, 0.035 ml). Compound **8c** was obtained as a white solid (118 mg, 91%), mp 151–153 °C, R_f = 0.37 (ss B); ^{1}H NMR: δ_H 1.11 (s, 3H, 18-CH_3), 1.29–1.58 (overlapping multiplets, 7H), 1.96–2.03 (overlapping multiplets, 2H), 2.09 (m, 1H), 2.24–2.32 (overlapping multiplets, 2H), 2.35 (s, 3H, tolyl-CH_3), 2.71–2.92 (overlapping multiplets, 3H), 4.55 (d, 1H, J = 8.0 Hz, 17-H), 4.80 (m, 1H, 16-H), 5.02 (s, 2H, OCH_2), 6.71 (d, 1H, J = 2.2 Hz, 4-H), 6.77 (dd, 1H, J = 8.6 Hz, J = 2.2 Hz, 2-H), 7.17–7.20 (overlapping multiplets, 3H, 1-H, 3″-H and 5″-H), 7.32 (t, 1H, J = 7.3 Hz, 4′-H), 7.38 (t, 2H, J = 7.3 Hz, 3′-H and 5′-H), 7.43 (d, 2H, J = 7.3 Hz, 2′-H and 6′-H), 7.61 (d, 2H, J = 7.5 Hz, 2″-H and 6″-H), 7.69 (s, 1H, C=CH). ^{13}C NMR: δ_C 21.2 (tolyl-CH_3), 23.0 (C-18), 26.5 (CH_2), 28.4 (CH_2), 30.4 (CH_2), 31.8 (CH_2), 33.1 (CH_2), 42.0 (CH), 42.9 (CH), 43.2 (C-13), 48.4 (CH), 66.4 (C-16), 70.0 (OCH_2), 78.7 (C-17), 112.7 (C-2), 114.6 (C-4), 119.1 (C=CH), 125.5 (2C) and 129.4 (2C): C-2″,3″,5″,6″; 127.0 (C-1), 127.4 (2C: C-2′,6′), 127.6 (C-1″), 127.8 (C-4′), 128.5 (2C: C-3′,5′), 132.2 (C-10), 137.3 and 137.9 and 138.2 (C-1′ and C-4″ and C-5), 147.5 (C=CH), 156.7 (C-3). MS m/z (%): 520 (100, $[M+H]^+$), 160 (41). Anal. Calcd. for $C_{34}H_{37}N_3O_2$: C, 78.58; H, 7.18. Found: C, 78.42; H, 7.35. Purity from HPLC: 98.4%.

2.1.4.12. 3-Benzyloxy-16β-[4-{4-(trifluoromethyl) phenyl}-1H-1,2,3-triazol-1-yl]-13α-estra-1,3,5(10)-trien-17α-ol (8d). As described in Section 2.1.4, azidoalcohol **5** (100 mg, 0.25 mmol) was reacted with 1-ethynyl-4-(trifluoromethyl) benzene (**6d**, 0.039 ml). Compound **8d** was obtained as a white solid (132 mg, 92%), mp 104–105 °C, R_f = 0.38 (ss B); ^{1}H NMR: δ_H 1.11 (s, 3H, 18-CH_3), 1.26–1.59 (overlapping multiplets, 7H), 1.99–2.01 (overlapping multiplets, 2H), 2.14 (m, 1H), 2.26–2.33 (overlapping multiplets, 2H), 2.73–2.90 (overlapping multiplets, 3H), 4.57 (d, 1H, J = 8.1 Hz, 17-H), 4.82 (m, 1H, 16-H), 5.02 (s, 2H, OCH_2), 6.71 (d, 1H, J = 2.2 Hz, 4-H), 6.78 (dd, 1H, J = 8.6 Hz, J = 2.2 Hz, 2-H), 7.19 (d, 1H, J = 8.6 Hz, 1-H), 7.32 (t, 1H, J = 7.3 Hz, 4′-H), 7.38 (t, 2H, J = 7.3 Hz, 3′-H and 5′-H), 7.43 (d, 2H, J = 7.3 Hz, 2′-H and 6′-H), 7.61 (d, 2H, J = 7.5 Hz, 2″-H and 6″-H), 7.83 (d, 2H, J = 7.5 Hz, 3″-H and 5″-H), 7.84 (s, 1H, C=CH). ^{13}C NMR: δ_C 23.0 (C-18), 26.4 (CH_2), 28.4 (CH_2), 30.4 (CH_2), 31.7 (CH_2), 33.1 (CH_2), 41.9 (CH), 42.9 (CH), 43.2 (C-13), 48.4 (CH), 66.6 (C-16), 69.9 (OCH_2), 78.9 (C-17), 112.7 (C-2), 114.6 (C-4), 120.4 (C=CH), 123.9 (d, J = 272.5 Hz, CF_3), 125.6 (2C: C-2″ and C-6″), 125.8 (d, 2C, J = 3.4 Hz, C-3″ and C-5″), 127.0 (C-1), 127.4 (2C: C-2′,6′), 127.8 (C-4′), 128.5 (2C: C-3′,5′), 129.8 (d, J = 32.7 Hz, C-4″), 132.0 (C-10), 133.9 (C-1″), 137.3 (C-1′), 138.1 (C-5), 146.1 (C=CH), 156.3 (C-3). MS m/z (%): 596 (100, [M + Na]), 574 (88, $[M+H]^+$), 214 (97). Anal. Calcd. for $C_{34}H_{34}F_3N_3O_2$: C, 71.19; H, 5.97. Found: C, 71.28; H, 6.15. Purity from HPLC: 98.2%.

2.1.4.13. 3-Benzyloxy-16β-[4-(4-ethylphenyl)-1H-1,2,3-triazol-1-yl]-13α-estra-1,3,5(10)-trien-17α-ol (8e). As described in Section 2.1.4, azidoalcohol **5** (100 mg, 0.25 mmol) was reacted with 1-ethynyl-4-ethynylbenzene (**6e**, 0.039 ml). Compound **8e** was obtained as a white solid (125 mg, 94%), mp 162–164 °C, R_f = 0.36 (ss B); ^{1}H NMR: δ_H 1.11 (s, 3H, 18-CH_3), 1.25 (t, 3H, J = 7.6 Hz, CH_2–CH_3), 1.26–1.59 (overlapping multiplets, 7H), 1.97–2.03 (overlapping multiplets, 2H), 2.11 (m, 1H), 2.25–2.32 (overlapping multiplets, 2H), 2.66 (q, 2H, J = 7.6 Hz, CH_2–CH_3), 2.72–2.93 (overlapping multiplets, 3H), 4.56 (m, 1H, 17-H), 4.80 (m, 1H, 16-H), 5.02 (s, 2H, OCH_2), 6.70 (d, 1H, J = 2.2 Hz, 4-H), 6.77 (dd, 1H, J = 8.6 Hz, J = 2.2 Hz, 2-H), 7.19 (d, 1H, J = 8.6 Hz, 1-H), 7.21 (d, 2H, J = 7.9 Hz, 3″-H and 5″-H), 7.31 (t, 1H, J = 7.3 Hz, 4′-H), 7.38 (t, 2H, J = 7.3 Hz, 3′-H and 5′-H), 7.43 (d, 2H, J = 7.3 Hz, 2′-H and 6′-H), 7.65 (d, 2H, J = 7.5 Hz, 2″-H and 6″-H), 7.71 (s, 1H, C=CH). ^{13}C NMR: δ_C 15.5 (CH_2–CH_3), 23.0 (C-18), 26.5 (CH_2), 28.4 (CH_2), 28.6 (CH_2), 30.4 (CH_2), 31.7 (CH_2), 33.2 (CH_2), 42.0 (CH), 42.9 (CH), 43.2 (C-13), 48.4 (CH), 66.4 (C-16), 69.9 (OCH_2), 78.8 (C-17), 112.7 (C-2), 114.6 (C-4), 119.1 (C=CH), 125.6 (2C) and 128.3 (2C): C-2″,3″,5″,6″; 126.9 (C-1), 127.4 (2C: C-2′,6′), 127.8 (C-4′), 127.9 (C-1″), 128.5 (2C: C-3′,5′), 132.1 (C-10), 137.2 (C-1′), 138.2 (C-5), 144.3 and 147.6 (C=CH and C-4″), 156.7 (C-3). MS m/z (%): 534 (100, $[M+H]^+$), 174 (49). Anal. Calcd. for $C_{35}H_{39}N_3O_2$: C, 78.77; H, 7.37. Found: C, 78.95; H, 7.42. Purity from HPLC: 97.8%.

2.1.4.14. 3-Benzyloxy-16β-[4-{4-(tert-butyl) phenyl}-1H-1,2,3-triazol-1-yl]-13α-estra-1,3,5(10)-trien-17α-ol (8f). As described in Section 2.1.4, azidoalcohol **5** (100 mg, 0.25 mmol) was reacted with 4-(*tert*-butyl) phenylacetylene (**6f**, 0.050 ml). Compound **8f** was obtained as a white solid (126 mg, 90%), mp 187–190 °C, R_f = 0.44 (ss B); ^{1}H NMR: δ_H 1.11 (s, 3H, 18-CH_3), 1.27–1.55 (overlapping multiplets, 7H), 1.33 (s, 9H, $C(CH_3)_3$), 1.96–2.03 (overlapping multiplets, 2H), 2.08 (m, 1H), 2.24–2.29 (overlapping multiplets, 2H), 2.72–2.89 (overlapping multiplets, 3H), 4.55 (d, 1H, J = 8.0 Hz, 17-H), 4.79 (m, 1H, 16-H), 5.01 (s, 2H, OCH_2), 6.70 (d, 1H, J = 2.2 Hz, 4-H), 6.76 (dd, 1H, J = 8.6 Hz, J = 2.2 Hz, 2-H), 7.19 (d, 1H, J = 8.6 Hz, 1-H), 7.32 (t, 1H, J = 7.3 Hz, 4′-H), 7.37 (overlapping multiplets, 4H, 3′-H, 5′-H, 3″-H and 5″-H), 7.42 (d, 2H, J = 7.3 Hz, 2′-H and 6′-H), 7.60 (d, 2H, J = 7.5 Hz, 2″-H and 6″-H), 7.68 (s, 1H, C=CH). ^{13}C NMR: δ_C 23.0 (C-18), 26.5 (CH_2), 28.3 (CH_2), 30.4 (CH_2), 31.3 (3C: $C(CH_3)_3$), 31.8 (CH_2), 33.2 (CH_2), 41.9 (CH), 42.9 (CH), 43.1 (C-13), 48.4 (CH), 51.2 ($C(CH_3)_3$), 66.5 (C-16), 69.9 (OCH_2), 78.7 (C-17), 112.6 (C-2), 114.6 (C-4), 119.2 (C=CH), 125.3 (2C) and 125.6 (2C): C-2″,3″,5″,6″; 127.0 (C-1), 127.4 (2C: C-2′,6′), 127.5 (C-1″), 127.8 (C-4′), 128.5 (2C: C-3′,5′), 132.2 (C-10), 137.3 (C-1′), 137.8 (C-5), 147.3 (C=CH), 151.0 (C-4″), 156.7 (C-3). MS m/z (%): 584 (82, [M + Na]), 562 (100, $[M+H]^+$), 202 (53). Anal. Calcd. for $C_{37}H_{43}N_3O_2$: C, 79.11; H, 7.72. Found: C, 79.43; H, 7.96. Purity from HPLC: 98.9%.

2.1.4.15. 3-Benzyloxy-16β-[4-(4-bromophenyl)-1H-1,2,3-triazol-1-yl]-13α-estra-1,3,5(10)-trien-17α-ol (8g). As described in Section 2.1.4, azidoalcohol **5** (100 mg, 0.25 mmol) was reacted with 4-bromophenylacetylene (**6g**, 50 mg). Compound **8g** was obtained as a white solid (127 mg, 87%), mp 87–89 °C, R_f = 0.31 (ss B); ^{1}H NMR: δ_H 1.11 (s, 3H, 18-CH_3), 1.26–1.59 (overlapping multiplets, 5H), 1.96–2.02 (overlapping multiplets, 2H), 2.11 (m, 1H), 2.25–2.32 (overlapping multiplets, 2H), 2.75–2.92 (overlapping multiplets, 3H), 4.55 (m, 1H, 17-H), 4.80 (m, 1H, 16-H), 5.02 (s, 2H, OCH_2), 6.70 (d, 1H, J = 2.2 Hz, 4-H), 6.77 (dd, 1H, J = 8.6 Hz, J = 2.2 Hz, 2-H), 7.19 (d, 1H, J = 8.6 Hz, 1-H), 7.31 (t, 1H, J = 7.3 Hz, 4′-H), 7.38 (t, 2H, J = 7.3 Hz, 3′-H and 5′-H), 7.42 (d, 2H, J = 7.3 Hz, 2′-H and 6′-H), 7.50 (d, 1H, J = 7.7 Hz, 2″-H and 6″-H), 7.61 (d, 2H, 3″-H and 5″-H), 7.78 (s, 1H, C=CH). ^{13}C NMR: δ_C 23.0 (C-18), 26.5 (CH_2), 28.4 (CH_2), 30.4 (CH_2), 31.7 (CH_2), 33.1 (CH_2), 41.9 (CH), 42.9 (CH), 43.2 (C-13), 48.4 (CH), 66.6 (C-16), 69.9 (OCH_2), 78.8 (C-

17), 112.7 (C-2), 114.6 (C-4), 119.6 (C=CH), 122.1 (C-4″), 127.0 (C-1), 127.1 (2C: C-2″ and C-6″), 127.4 (2C: C-2′ and C-6′), 127.8 (C-4′), 128.5 (2C: C-3′ and C-5′), 129.4 (C-1″), 132.0 (2C, C-3″ and C-5″), 132.1 (C-10), 137.3 (C-1′), 138.2 (C-5), 146.3 (C=CH), 156.8 (C-3). MS *m*/*z* (%): 584 (100, $[M+H]^+$). Anal. Calcd. for $C_{33}H_{34}BrN_3O_2$: C, 67.81; H, 5.86. Found: C, 68.13; H, 6.06. Purity from HPLC: 99.0%.

2.1.4.16. 3-Benzyloxy-16β-[4-(4-fluorophenyl)-1H-1,2,3-triazol-1-yl]-13α-estra-1,3,5(10)-trien-17α-ol (8h). As described in Section 2.1.4, azidoalcohol **5** (100 mg, 0.25 mmol) was reacted with 4-fluorophenylacetylene (**6h**, 33 mg). Compound **8h** was obtained as a white solid (110 mg, 84%), mp 76–78 °C, R_f = 0.29 (ss B); ^{1}H NMR: δ_H 1.11 (s, 3H, 18-CH_3), 1.26–1.58 (overlapping multiplets, 5H), 1.97–2.02 (overlapping multiplets, 2H), 2.12 (m, 1H), 2.25–2.33 (overlapping multiplets, 2H), 2.73–2.93 (overlapping multiplets, 3H), 4.56 (d, 1H, *J* = 7.8 Hz, 17-H), 4.82 (m, 1H, 16-H), 5.02 (s, 2H, OCH_2), 6.71 (d, 1H, *J* = 2.2 Hz, 4-H), 6.78 (dd, 1H, *J* = 8.6 Hz, *J* = 2.2 Hz, 2-H), 7.08 (t, 2H, *J* = 7.8 Hz, 3″-H and 5″-H), 7.19 (d, 1H, *J* = 8.6 Hz, 1-H), 7.31 (t, 1H, *J* = 7.3 Hz, 4′-H), 7.38 (t, 2H, *J* = 7.3 Hz, 3′-H and 5′-H), 7.42 (d, 2H, *J* = 7.3 Hz, 2′-H and 6′-H), 7.78 (m, 3H, C=CH, 2″-H and 6″-H). ^{13}C NMR: δ_C 23.0 (C-18), 26.5 (CH_2), 28.4 (CH_2), 30.4 (CH_2), 31.7 (CH_2), 33.1 (CH_2), 42.0 (CH), 42.9 (CH), 43.2 (C-13), 48.4 (CH), 66.6 (C-16), 69.9 (OCH_2), 78.8 (C-17), 112.7 (C-2), 114.6 (C-4), 115.8 (d, 2C, *J* = 21.7 Hz, C-3″ and C-5″), 119.3 (C=CH), 126.5 (C-1″), 127.3 (d, 2C, *J* = 8.0 Hz, C-2″ and C-6″), 127.4 (2C: C-2′,6′), 127.7 (C-1), 127.8 (C-4′), 128.5 (2C: C-3′,5′), 132.1 (C-10), 137.3 (C-1′), 138.2 (C-5), 146.5 (C=CH), 156.8 (C-3), 161.7 (d, *J* = 247.6 Hz, C-4″). MS *m*/*z* (%): 524 (100, $[M+H]^+$). Anal. Calcd. for $C_{33}H_{34}FN_3O_2$: C, 75.69; H, 6.54. Found: C, 77.13; H, 6.96. Purity from HPLC: 98.9%.

2.1.4.17. 16β-[4-(4-Fluorophenyl)-1H-1,2,3-triazol-1-yl]-3-hydroxy-13α-estra-1,3,5(10)-trien-17α-ol (9). A suspension of **8e** (100 mg, 0.19 mmol) and Pd/C (0.30 g, 10%) in EtOAc (10 ml) was subjected to 20 bar of H_2 pressure at room temperature for 3 h. The catalyst was then removed by filtration through a short pad of silica gel. After evaporation of the solvent *in vacuo*, the residue was purified by flash chromatography with CH_2Cl_2 as eluent. Compound **9** was obtained as a white solid (70 mg, 82%), mp 115–117 °C, R_f = 0.12 (ss B); ^{1}H NMR: δ_H 0.99 (s, 3H, 18-CH_3), 1.21–1.37 (overlapping multiplets, 7H), 1.50 (m, 1H), 1.80 (m, 1H), 1.87–1.94 (overlapping multiplets, 2H), 2.20 (m, 2H), 2.61 (q, 2H, *J* = 6.6 Hz, CH_2–CH_3), 2.73 (m, 2H, 6-H_2), 4.39 (m, 1H, 17-H), 4.84 (m, 1H, 16-H), 5.20 (d, 1H, *J* = 5.7 Hz, 17-OH), 6.64 (d, 1H, *J* = 2.2 Hz, 4-H), 6.54 (dd, 1H, *J* = 8.6 Hz, *J* = 2.2 Hz, 2-H), 7.12 (d, 1H, *J* = 8.6 Hz, 1-H), 7.26 (d, 2H, *J* = 7.3 Hz, 3″-H and 5″-H), 7.75 (d, 2H, *J* = 7.5 Hz, 2″-H and 6″-H), 8.85 (s, 1H, C=CH), 9.01 (s, 1H, 3-OH). ^{13}C NMR: δ_C 15.4 (CH_2–CH_3), 22.9 (C-18), 27.8 (CH_2), 28.0 (CH_2), 28.9 (CH_2), 29.2 (CH_2), 31.2 (CH_2), 32.0 (CH_2), 41.6 (CH), 42.4 (CH), 42.6 (C-13), 47.4 (CH), 65.6 (C-16), 76.9 (C-17), 112.9 (C-2), 114.7 (C-4), 119.2 (C=CH), 125.0 (2C) and 128.1 (2C): C-2″,3″,5″,6″; 126.6 (C-1), 128.4 (C-1″), 143.2 (C-10), 146.1 (C-5), 148.1 and 148.4 (C=CH and C-4″), 154.8 (C-3). MS *m*/*z* (%): 444 (100, $[M+H]^+$). Anal. Calcd. for $C_{28}H_{33}N_3O_2$: C, 75.81; H, 7.50. Found: C, 76.05; H, 7.40. Purity from HPLC: 97.9%.

2.2. Pharmacology

2.2.1. Cell cultures and antiproliferative assays

The human cancer cell lines HeLa, A2780 and A431 (isolated from cervical, ovarian and skin carcinoma, respectively), four breast cancer cell lines (MCF7, T47D, MDA-MB-231 and MDA-MB-361) and noncancerous MRC5 fibroblasts (isolated from a fetal human lung) were maintained in minimal essential medium supplemented with 10% fetal bovine serum, 1% non-essential aminoacids and an antibiotic–antimycotic mixture. These cell lines were purchased from the European Collection of Cell Cultures (Salisbury, UK) and maintained in a humidified atmosphere of 5% CO_2 at 37 °C. All the chemicals, if otherwise not specified, were purchased from Sigma–Aldrich Ltd. (Budapest, Hungary). For pharmacological investigations, 10 mM stock solutions of the tested compounds were prepared with DMSO. The highest applied DMSO concentration of the medium (0.3%) did not have a substantial effect on the measured cellular functions. The antiproliferative effects were determined *in vitro* by means of the MTT assay. Cells were seeded onto 96-well plates at a density of 5000 cells/well and allowed to stand overnight, after which the medium containing the tested compound was added. After a 72-h incubation, viability was determined by the addition of 20 μl of 3-(4,5-dimethylthiazol-2-yl)-2,5-diphenyltetrazolium bromide solution (5 mg ml^{-1}). The precipitated formazan crystals were solubilized in DMSO and the absorbance was determined at 545 nm with an ELISA reader [32]. Two independent experiments were performed with 5 parallel wells. Cisplatin, an agent administered clinically in the treatment of certain gynecological malignancies, was used as a positive control. For the most effective compounds, the assays were repeated with a set of dilutions, and sigmoidal dose–response curves were fitted to the measured data in order to determine the IC_{50} values by means of GraphPad Prism 4.0 (GraphPad Software; San Diego, CA, USA).

2.2.2. Cell cycle analysis by flow cytometry

Flow cytometric analysis was performed in order to characterize the cellular DNA content of treated HeLa cells. After treatment for 24 or 48 h, cells (200,000 per condition) were trypsinized (Gibco BRL, Paisley, U.K.), washed with phosphate-buffered saline (PBS) and fixed in 1.0 ml of cold 70% EtOH. After two washing steps in cold PBS, DNA was stained with propidium iodide (10 μg ml^{-1}) in the presence of RNA-ase (50 μg ml^{-1}). The samples were then analyzed with CyFlow (Partec GmbH, Münster, Germany). In each analysis, 20,000 events were recorded, and the percentages of the cells in the different cell-cycle phases (subG1, G1, S and G2/M) were calculated by using ModFit LT (Verity Software House, Topsham, ME, USA) [33].

2.2.3. Hoechst 33258 – propidium iodide double staining

Near-confluent HeLa cells were seeded onto a 96-well plate (5000 cells/well). After incubation for 24 h with the test compound, Hoechst 33,258 and propidium iodide were added to the culture medium to give final concentrations of 5 and 2 μg ml^{-1}, respectively. The cells were incubated with the staining mixture for 1 h at 37 °C and were then photographed by means of a Nikon Eclipse microscope equipped with an epifluorescence attachment containing the appropriate optical blocks and a QCapture CCD camera. The staining allowed the identification of live, early-apoptotic, late-apoptotic and necrotic cells. Hoechst 33258 permeates all the cells and makes the nuclei appear blue. Apoptosis was revealed by nuclear changes such as chromatin condensation and nuclear fragmentation. The necrotic and the late-apoptotic cells were identified as cells with propidium iodide uptake, which indicates the loss of membrane integrity, the cell nuclei being stained red [34].

2.2.4. Determination of in situ caspase-3 activity

The activity of caspase-3 from treated cells was determined in triplicate by means of a commercially available colorimetric kit in accordance with the instructions of the supplier (Sigma–Aldrich, Budapest, Hungary). Briefly, near-confluent HeLa cells were seeded in tissue culture flasks (10^6 cells/flask) and grown overnight under standard cell culturing conditions. The cells were next incubated with two concentrations (3 and 10 μM) of the test compound for 48 h and then scraped, counted and resuspended in lysis buffer (10 μl for 10^6 cells). The caspase-3 activity was measured by the

Table 1
Nucleotide sequences of the utilized primers.

Target gene	Forward primer (5′-3′)	Reverse primer (5′-3′)
p21	GGATTAGGGCTTCCTCTTGG	GACTCTCAGGGTCGAAAACG
Rps11	GCTGCTGCCCCTTTCTTTTT	TTGAAGCCCAGACCGATGTT

addition of substrate (Ac-DEVD-*p*NA) and the amount of product (*p*NA, *p*-nitroaniline) was measured at 405 nm after incubation for 2 h. Results on treated cells are given as fold increase by direct comparison with the untreated control results.

2.2.5. Determination of in situ *caspase-8 activity*

Caspase-8 activity was determined by using a colorimetric assay kit (Sigma–Aldrich Ltd., Budapest, Hungary), Ac-IETD-*p*NA serving as substrate. During the assay, the peptide substrate was cleaved by caspase-8, resulting in the release of *p*NA, which was measured on a microplate reader at an absorbance wavelength of 405 nm. All further conditions were identical with those of the caspase-3 assay.

2.2.6. Determination of in situ *caspase-9 activity*

The activity of caspase-9 from treated cells was determined in triplicate by means of a commercially available colorimetric kit in accordance with the instructions of the supplier (Invitrogen; Carlsbad, CA, USA). Caspase-9 was determined similarly as for caspase-3, but the substrate utilized was LEHD-*p*NA; the amount of *p*NA was measured as described above.

2.2.7. Quantitative real-time PCR (QPCR)

Total RNA samples were prepared with TRizol from HeLa cells treated for 24 or 48 h with **8e** (200,000/well). First-strand cDNA was synthetized by using TaqMan Reverse Transcription Reagents (Applied Biosystems, Life Technologies). QPCR reactions were performed on the PikoReal 96 Real-Time PCR System (Thermo Scientific), using SYBR Green chemistry. Primers (see Table 1) were designed by Primer3 software [35]. Rps11 ribosomal protein was used as internal control. The Ct value for each studied mRNA was normalized to the internal control and the changes in expression levels of the examined genes were calculated by the DDCt method [36]. The presented results were obtained from three independent experiments.

2.2.8. Statistical analysis

Statistical analysis of the obtained data was carried out by analysis of variance (ANOVA), followed by the Dunnett post-test. All analyses were performed with GraphPad Prism 4.0 (GraphPad Software, San Diego, CA, USA).

3. Results and discussion

3.1. Chemical synthesis

The 16-olefin (**1**) was readily synthetized from 13α-estrone 3-benzyl ether as described in the literature for 3-methyl ether derivatives [37]. The epoxidation of **1** with magnesium monoperoxyphthalate resulted in a 3:1 mixture of the 16β,17β- (**2**) and the 16α,17α-epoxide (**3**, Scheme 1). This diastereomeric ratio was higher than that described earlier in the 3-methyl ether series (ratio β-epoxide:α-epoxide = 56:44) [37]. The opening of the epoxides with NaN_3 gave the new *trans* 16-azido-17-alcohols (**4** and **5**) regioselectively.

The 16-azido-17-hydroxy derivatives (**4** or **5**) were subjected to azide–alkyne 'click' reactions with substituted phenylacetylenes according to the earlier-published synthetic procedure (**6**, Scheme 2, [28]). Full conversion of the starting materials was achieved by using a catalytic amount of CuI as catalyst and PPh_3 as stabilizing ligand. Reactions were carried out in refluxing toluene with an excess of DIPEA as base. Each of the reactions proceeded in a regioselective manner, yielding the desired triazoles (**7** or **8**) in excellent yields (Entries 1–12, Table 2). Removal of the benzyl protecting group from **8e** furnished **9**.

The structures of the new compounds (**1**–**8**) were confirmed by ^1H and ^{13}C NMR measurements. In the ^{13}C NMR spectra of *trans*-azidoalcohols **4** and **5**, the signals of C-16 and C-17 appear at higher chemical shifts (around 70 and 80 ppm) than in the spectra of epoxides **2** and **3** (around 55–58 and 66 ppm). These upfield shifts clearly indicate the ring opening of the epoxide and the formation of alcoholic hydroxy and azido functions on C-17 and C-16. The multiplets of 16-H and 17-H appear at around 4.2 and 4.7 ppm in the ^1H NMR spectra of triazoles **7**, but at around 4.5 and 4.8 ppm in the spectra of **8**. In the ^{13}C spectra of **7d** and **8d**, signals of CF_3, C-4″ and C-3″ —C-5″ appear together as doublets with coupling constants of around 270 Hz, 30 Hz and 3 Hz, indicating the presence of the CF_3 function on C-4".

3.2. Characterization of antiproliferative properties of the newly synthetized compounds

In the light of the significant cytostatic properties of our recently synthetized triazoles [27–31] and the low affinity of the readily available 13α-estradiols for the ER [21], we combined the triazole and 13α-estradiol moieties and investigated the cell-growth-inhibitory potencies of the resulting heterocyclic compounds. The aims of our present study included characterization of the synthetized triazoles (**7**, **8**) and their precursors (**1**–**5**) on a panel of human adherent cancer cell lines (HeLa, MCF-7, A431 and

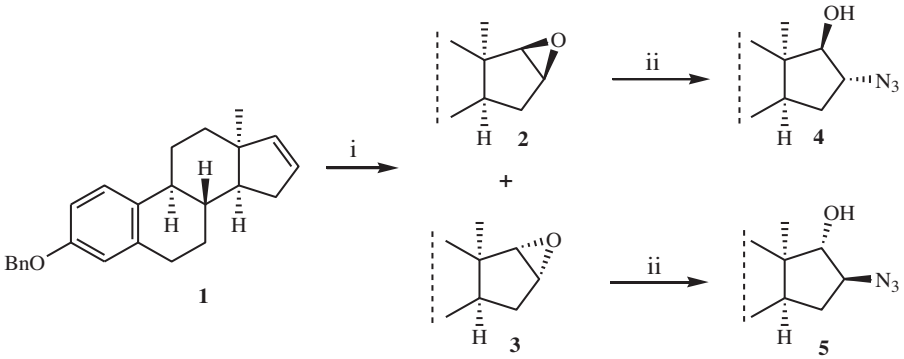

Scheme 1. Synthesis of *trans*-16,17-azidoalcohols in the 13α-estrone series. Reagents and conditions: (i) magnesium monoperoxyphthalate hexahydrate (4 equiv.), CH_2Cl_2/MeOH, rt, 24 h; (ii) NaN_3 (7 equiv.), DMSO/MeCOOH = 10/1, reflux, 3 h.

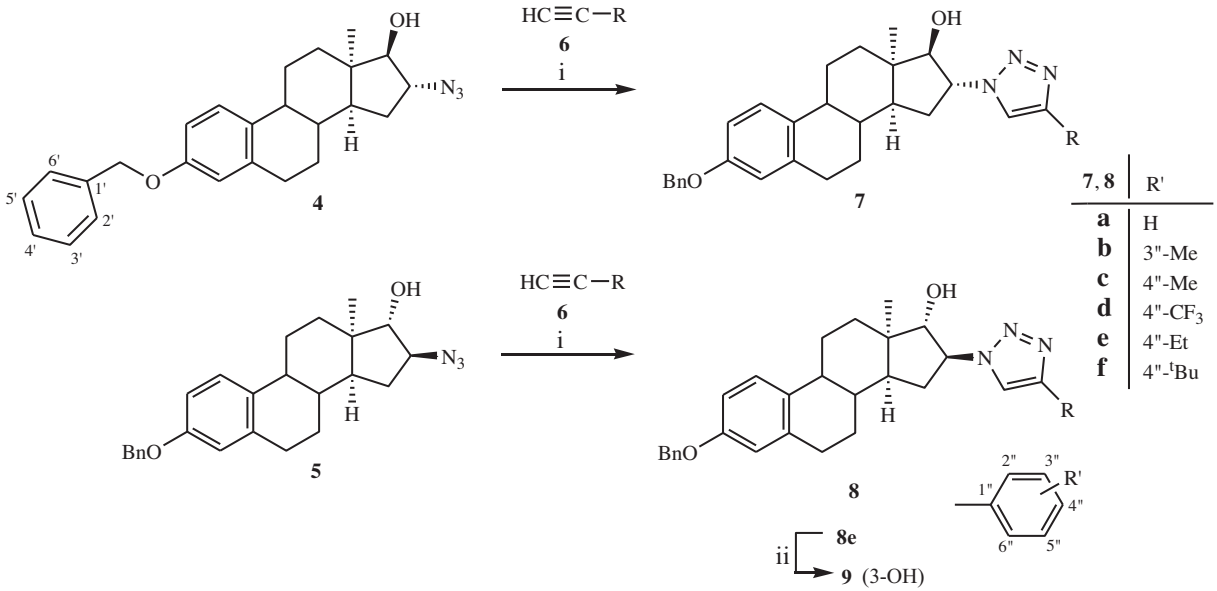

Scheme 2. Synthesis of 16-triazoles in the 13α-estradiol series. Reagents and conditions: (i) CuI (0.1 equiv.), Ph_3P (0.2 equiv.), DIPEA (3 equiv.), reflux, 2 h; (ii) H_2 (20 bar), Pd/C, EtOAc, 3 h.

A2780). Compounds **1**–**5** exerted only moderate cell-growth inhibition, since none of the derivatives at 10 μM achieved 50% cell-growth inhibition, but compounds **7** and **8** exhibited higher antiproliferative activities. We set out to determine the impact of inversion of the configurations at C-16 and C-17 on the *in vitro* biological activity. In order to investigate the structure–activity relationships, the effect of the substitution pattern (considering the nature and the electronic properties of the 4″-substituent) of the phenyl ring of the terminal alkyne was additionally tested. Compounds containing 16β,17α functions (**8**) proved more efficient than their 16α,17β counterparts, except for the halogenated derivatives **7g** and **7h**, which exerted substantial growth inhibition selectively on Hela cells (Table 3). The potency of compounds **8** depended greatly on the substitution pattern of the phenyl ring derived from the phenylacetylene. The unsubstituted (**8a**) or *m*-ethyl (**8b**) derivatives were less active than the *p*-tolyltriazole (**8c**). In order to establish whether the alkyl moiety is necessary for the cytostatic effect, the *p*-trifluoromethyl compound (**8d**) was also tested; it displayed a similar antiproliferative effect to that of the methyl derivative (**8c**). The *p*-alkylphenyl derivatives bearing an ethyl or *tert*-butyl group (**8e** and **8f**) proved to be the most potent against all the tested cell lines, with IC_{50} values in the range 2.4–3.4 μM, displaying a broad spectrum of activities. Halogen-containing derivatives **8g** and **8h** were less potent than their alkyl-substituted counterparts. Compound **9**, containing 3-OH was totally inactive, indicating that the benzyl ether protecting group is necessary for the antiproliferative activity.

The potent derivatives (**8c**–**g**) were subjected to additional investigations in order to determine their antiproliferative properties against a panel of breast cancer cell lines differing in receptorial status [38]: T47D (expressing estrogen, progesterone and androgen receptors), MDA-MB-361 (expressing estrogen receptor and HER2) and triple-negative MDA-MB-231. Compounds **8c**–**g** proved to be antiproliferative against all three cell lines, with IC_{50} values in the range 5–11 μM (Table 4), **8d** and **8g** exerting the lowest growth inhibition. The activities of the triazoles exceeded that of cisplatin on T47D and on MDA-MB-231.

The cancer selectivity of the selected potent compound (**8e**) was tested by means of the MTT assay, using noncancerous MRC5 human fibroblast cells. Treatment with 30 μM **8e** resulted in a 22.2 ± 2.9% inhibition of the proliferation of MRC5 cells, while the reference agent cisplatin at the same concentration caused a more substantial inhibition (70.7 ± 1.3%). Since **8e** exhibited limited growth inhibition against MRC5 cells at 30 μM, while its calculated IC_{50} values on cancer cell lines were 2.4–6.5 μM, it can be considered cancer-selective.

In order to shed light on the growth-inhibitory action of compound **8e**, cell cycle analyses were performed after exposure for 24 h or 48 h. A 24-h treatment of HeLa cells with 10 μM **8e** resulted in significant increase in the ratio of cells in the S and G2/M states at the expense of the G1 phase (Fig. 1). After a 48-h exposure, marked increases in the subdiploid (subG1) and G2/M populations were observed, again with decreased presence of G1 cells. These results indicate blockade of the cell cycle at the G2–M transition and apoptosis induction.

The presence of apoptosis or necrosis was determined according to the nuclear morphology and membrane integrity. HeLa cells were incubated with increasing concentrations of **8e** (3 and 10 μM) for 24 or 48 h. Separate photos were recorded, in which Hoechst 33258 and propidium iodide fluorescence served as morphological markers. At 10 μM, **8e** significantly increased the ratio of early apoptotic and secondary necrotic cells at the expense

Table 2
Synthesis of 16-triazoles (**7**,**8**) in the 13α-estradiol series.

Entry	Azide	Alkyne	Product	Yield (%)
1	**4**	**6a**	**7a**	89
2	**4**	**6b**	**7b**	91
3	**4**	**6c**	**7c**	90
4	**4**	**6d**	**7d**	88
5	**4**	**6e**	**7e**	92
6	**4**	**6f**	**7f**	93
7	**4**	**6g**	**7g**	88
8	**4**	**6h**	**7h**	86
9	**5**	**6a**	**8a**	94
10	**5**	**6b**	**8b**	91
11	**5**	**6c**	**8c**	91
12	**5**	**6d**	**8d**	89
13	**5**	**6e**	**8e**	93
14	**5**	**6f**	**8f**	90
15	**5**	**6g**	**8g**	87
16	**5**	**6h**	**8h**	84

Table 3
Antiproliferative properties of the synthetized compounds.

Comp.	Concn. (μM)	Inhibition (%) ± SEM [calculated IC_{50} value][a]			
		HeLa	MCF7	A2780	A431
1	10	–[b]	–	–	–
	30	–	27.3 ± 1.6	24.6 ± 0.4	–
2	10	–	–	–	–
	30	28.9 ± 0.8	48.3 ± 1.2	36.3 ± 1.0	46.7 ± 1.1
3	10	–	–	–	–
	30	39.9 ± 1.4	48.8 ± 1.3	44.8 ± 0.6	68.8 ± 1.2
4	10	21.5 ± 0.7	36.2 ± 1.4	33.3 ± 0.8	–
	30	98.3 ± 0.1	90.3 ± 0.4	96.4 ± 0.2	97.7 ± 0.1
5	10	20.4 ± 0.5	34.6 ± 1.4	39.0 ± 1.0	–
	30	96.0 ± 0.4	77.3 ± 1.3	96.0 ± 0.4	82.3 ± 1.1
7a	10	64.7 ± 1.7	–	46.5 ± 1.1	44.9 ± 0.9
	30	80.3 ± 0.4	–	50.7 ± 2.0	36.1 ± 1.3
7b	10	23.9 ± 0.9	28.3 ± 1.0	38.9 ± 0.2	–
	30	27.4 ± 1.0	30.0 ± 0.5	38.6 ± 0.4	–
7c	10	57.3 ± 2.4	35.2 ± 2.0	46.9 ± 0.8	–
	30	55.5 ± 1.0	37.6 ± 2.0	56.5 ± 0.9	36.6 ± 0.4
7d	10	58.3 ± 1.0	42.9 ± 1.2	53.5 ± 1.5	25.5 ± 2.6
	30	56.7 ± 1.2	43.6 ± 0.4	55.4 ± 1.1	19.0 ± 4.4
7e	10	28.1 ± 1.4	30.4 ± 0.6	41.4 ± 0.5	–
	30	24.1 ± 1.2	28.7 ± 2.3	40.5 ± 0.3	–
7f	10	46.2 ± 2.4	36.4 ± 1.4	43.6 ± 0.7	38.7 ± 0.4
	30	52.0 ± 2.4	39.6 ± 2.1	51.0 ± 1.4	37.0 ± 1.1
7g	10	61.2 ± 2.7	22.9 ± 1.5	38.8 ± 0.98	18.5 ± 2.8
	30	65.1 ± 2.0 [2.0 μM]	27.9 ± 1.0	39.8 ± 1.2	33.7 ± 2.1
7h	10	55.5 ± 1.0	22.3 ± 2.0	40.2 ± 2.2	13.1 ± 0.5
	30	62.8 ± 2.2	23.4 ± 0.8	36.8 ± 1.4	26.2 ± 2.8
8a	10	45.7 ± 2.7	–	33.3 ± 1.6	–
	30	84.9 ± 0.5	74.7 ± 0.7	81.7 ± 0.8	53.4 ± 0.4
8b	10	58.4 ± 0.1	41.5 ± 1.9	56.4 ± 0.6	–
	30	79.3 ± 0.4	66.8 ± 1.5	82.9 ± 1.0	–
8c	10	72.0 ± 2.0	82.0 ± 0.9	80.9 ± 2.3	49.3 ± 1.3
	30	88.3 ± 1.3 [7.6 μM]	93.6 ± 0.3 [6.0 μM]	88.8 ± 1.5 [6.0 μM]	64.8 ± 2.4 [10.2 μM]
8d	10	75.8 ± 1.0	67.7 ± 2.6	69.5 ± 2.6	44.9 ± 0.5
	30	89.2 ± 0.9 [8.8 μM]	94.3 ± 0.2 [9.3 μM]	90.7 ± 1.8 [7.5 μM]	46.8 ± 1.1
8e	10	93.5 ± 0.2	83.3 ± 2.1	92.7 ± 0.2	87.5 ± 0.7
	30	97.3 ± 0.1 [2.6 μM]	89.5 ± 1.1 [2.4 μM]	96.9 ± 0.1 [2.6 μM]	92.3 ± 0.6 [2.9 μM]
8f	10	76.0 ± 0.8	73.5 ± 0.9	88.4 ± 0.9	68.6 ± 0.6
	30	89.6 ± 0.5 [3.4 μM]	84.8 ± 0.5 [2.9 μM]	95.0 ± 0.3 [2.9 μM]	76.6 ± 0.3 [3.2 μM]
8g	10	60.5 ± 1.1	35.1 ± 2.6	47.8 ± 1.0	31.2 ± 1.2
	30	86.3 ± 0.9 [8.5 μM]	73.5 ± 1.2	58.5 ± 2.1	42.6 ± 1.4
8h	10	31.6 ± 2.4	18.4 ± 2.4	16.7 ± 2.4	4.3 ± 1.4
	30	49.6 ± 0.4	34.2 ± 2.3	38.1 ± 1.7	12.8 ± 2.8
9	10	24.3 ± 1.6	8.8 ± 1.0	9.9 ± 0.9	4.6 ± 1.1
	30	24.5 ± 1.9	57.9 ± 0.9	39.0 ± 1.0	30.0 ± 1.3

Table 3 (*Continued*)

Comp.	Concn. (μM)	Inhibition (%) ± SEM [calculated IC_{50} value][a]			I-n
		HeLa	MCF7	A2780	A431
Cisplatin	10	42.6 ± 2.3	53.0 ± 2.3	83.6 ± 1.2	88.6 ± 0.5
	30	99.9 ± 0.3	86.9 ± 1.3	95.0 ± 0.3	90.2 ± 1.8
		[12.4 μM]	[9.6 μM]	[1.3 μM]	[2.8 μM]

[a] Mean value from two independent determinations with five parallel wells; standard deviation <15%.
[b] Inhibition values <20% are not presented.

Table 4
Antiproliferative properties of **8c–g**.

Comp.	Concn. (μM)	Inhibition (%) ± SEM [calculated IC_{50} value][a]		
		T47D	MDA-MB-231	MDA-MB-361
8c	10	85.9 ± 1.1	84.5 ± 1.01	83.6 ± 0.6
	30	92.0 ± 0.4	94.5 ± 0.5	89.2 ± 0.5
		[5.9 μM]	[6.5 μM]	[5.3 μM]
8d	10	58.4 ± 0.9	41.8 ± 2.5	57.2 ± 1.8
	30	90.9 ± 0.5	82.2 ± 0.7	74.1 ± 1.2
		[9.7 μM]	[10.3 μM]	[9.7 μM]
8e	10	85.6 ± 0.6	85.3 ± 1.8	74.1 ± 0.9
	30	92.0 ± 0.4	92.4 ± 0.9	83.6 ± 1.6
		[5.9 μM]	[6.5 μM]	[5.4 μM]
8f	10	65.4 ± 0.8	57.0 ± 1.3	61.4 ± 0.3
	30	87.7 ± 0.6	84.5 ± 0.7	74.3 ± 1.2
		[6.2 μM]	[8.3 μM]	[6.6 μM]
8g	10	56.5 ± 1.0	48.5 ± 1.5	56.0 ± 2.0
	30	81.1 ± 1.4	76.9 ± 1.9	73.7 ± 1.3
		[9.0 μM]	[10.3 μM]	[8.8 μM]
Cisplatin	10	51.0 ± 2.0	20.08 ± 0.8	67.5 ± 1.0
	30	57.9 ± 1.4	71.7 ± 1.2	87.7 ± 1.1
		[9.8 μM]	[19.1 μM]	[3.7 μM]

[a] Mean value from two independent determinations with five parallel wells; standard deviation.

of intact cells, even after incubation for 24 h (Fig. 2). This tendency was substantially more pronounced after exposure for 48 h. While substances that predominantly initiate apoptotic cell death are preferred during the development of anticancer agents, treatment with **8e** resulted in necrosis too.

The latter observation was supported by the results obtained from the determination of the apoptosis executive enzyme caspase-3. After the incubation of HeLa cells for 48 h with 10 μM **8e**, the caspase-3 concentration was significantly increased (Fig. 3). Since the intrinsic or mitochondrial pathway of programmed cell death is initiated by caspase-9, the activity of this apoptotic enzyme was additionally determined under the same conditions. Compound **8e** at 10 μM increased the activity of caspase-9, which indicates that a mitochondrial dysfunction may contribute to the activation of the apoptotic machinery. In order to clarify the role of the extrinsic pathway of apoptosis in the action of **8e**, the activity of caspase-8 was determined in the same way. Since no caspase-8 activation was detected, the involvement of extrinsic apoptotic initiation can be excluded.

To the best of our knowledge, there is only one literature example of an efficient antiproliferative 13α-estrone derivative on the malignant cell lines that we tested [39]. The 16-oxime propionate in the 3-benzyl ether series caused a cell cycle blokade of HeLa cells at the G1–S transition with induction in the subdiploid ratio after exposure for 48 h, indicating apoptotic cell death [39]. Its noteworthy that 16-triazolyl derivative **8e** led to blockade at a later phase (G2–M) of the cell cycle, in contrast with the effect of the oxime ester on the first checkpoint (G1–S).

order to investigate the reason for the G2–M arrest, HeLa cells were treated with low and high concentrations of **8e**. 24 and 48 h later, the mRNA levels of p21, one of the key regulators of a G2–M arrest [40], were determined by QPCR. The induction of p21 was observed

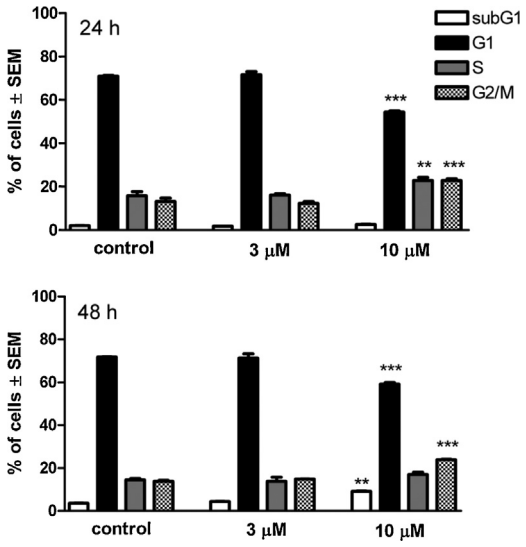

Fig. 1. Compound **8e** causes disturbance in the cell cycle distribution of HeLa cells after incubation for 24 or 48 h. ** and *** indicate $p < 0.01$ and $p < 0.001$, respectively, as compared with the control cells.

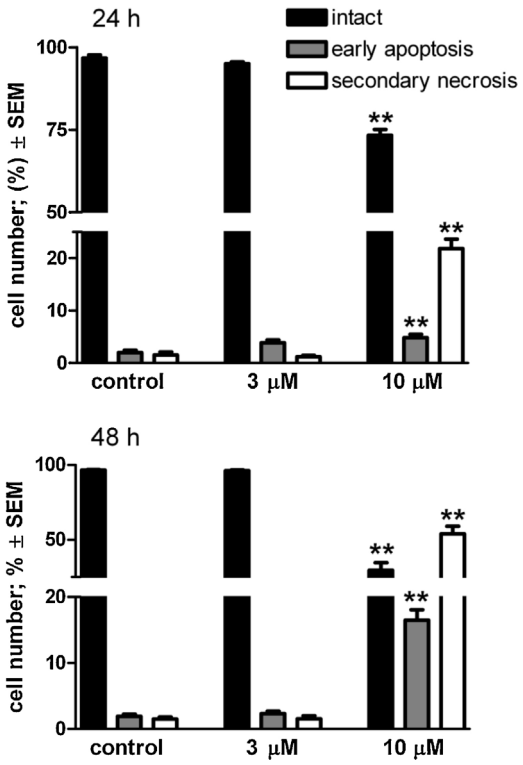

Fig. 2. Compound **8e** elicits apoptosis and necrosis in HeLa cells after incubation for 24 or 48 h. ** indicates $p < 0.01$ as compared with the control conditions.

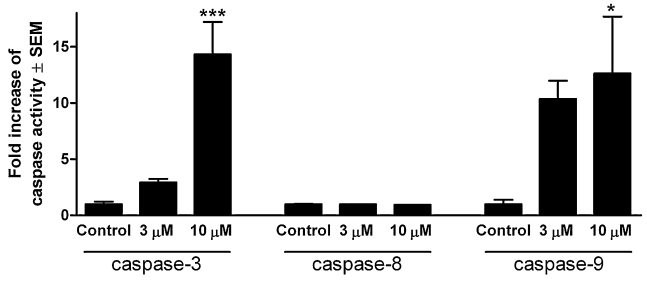

Fig. 3. Compound **8e** induces caspase-3 and caspase-9 but not caspase-8 activities after incubation for 48 h. The activities of the untreated cells were taken as one unit. * and *** indicate $p < 0.05$ and $p < 0.001$, respectively, as compared with the control cells.

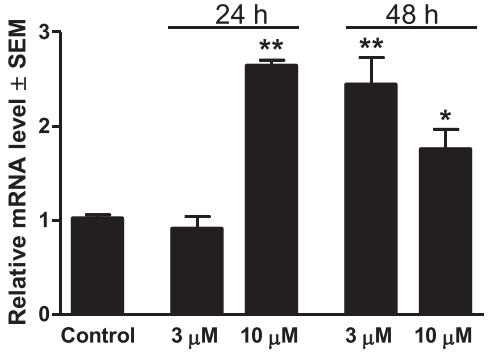

Fig. 4. Compound **8e** increases p21 mRNA expression in HeLa cells treated for 24 or 48 h. * and ** indicate $p < 0.05$ and $p < 0.01$, respectively, as compared with the control conditions.

both 24 and 48 h after exposure to 10 μM **8e** (Fig. 4). At 3 μM **8e**, the mRNA levels of p21 were significantly increased only 48 h after the treatment, indicating that **8e** has the capacity to induce p21 in a time- and concentration-dependent manner.

4. Conclusions

In summary, novel 16-triazolyl-17-estradiol 3-benzyl ethers were synthetized in the 13α-estrone series. Some compounds proved to exert *in vitro* cytostatic activity against the examined human adherent cancer cell lines, with IC_{50} values comparable to those of the reference agent cisplatin. The antiproliferative activities of the tested compounds were greatly affected by the configurations at C-16 and C-17 and by the substitution pattern of the triazolyl-phenyl ring. It can be stated that 16β,17α isomers bearing *p*-alkyl substituents on the triazolyl-phenyl ring displayed outstanding activities. It was confirmed that one of the most potent compounds (**8e**) induces apoptosis *via* the intrinsic pathway. Our results indicate that 17α-hydroxy-13α-estradiol 3-benzyl ether is a promising scaffold for the design of hormonally inactive cytostatic derivatives, especially with a 16β-heterocyclic substituent.

Acknowledgments

The authors are grateful for financial support from the Hungarian Scientific Research Fund (OTKA K101659 and K109293) and Richter Gedeon Plc. This research was supported by the European Union and the State of Hungary, co-financed by the European Social Fund in the framework of TÁMOP 4.2.4. A/2-11-1-2012-0001 'National Excellence Program'.

References

[1] A. Billich, P. Nussbaumer, P. Lehr, Stimulation of MCF-7 breast cancer cell proliferation by estrone sulfate and dehydroepiandrosterone sulfate: inhibition by novel non-steroidal steroid sulfatase inhibitors, J. Steroid Biochem. Mol. Biol. 73 (2000) 225–235.
[2] H. Ishida, T. Nakata, M. Suzuki, Y. Shiotsu, H. Tanaka, N. Sato, Y. Terasaki, M. Takebayashi, H. Anazawa, C. Murata, P.K. Li, T. Kuwabara, S. Akinaga, A novel steroidal selective steroid sulfatase inhibitor KW-2581 inhibits sulfated-estrogen dependent growth of breast cancer cells in vitro and in animal models, Breast Cancer Res. Treat. 106 (2007) 215–217.
[3] F. Jourdan, M.P. Leese, W. Dohle, E. Ferrandis, S.P. Newman, S. Chander, A. Purohit, B.V.L. Potter, Structure-activity relationships of C-17-substituted estratriene-3-*O*-sulfamates as anticancer agents, J. Med. Chem. 51 (2008) 1295–1308.
[4] M. Numazawa, M. Ando, Y. Watari, T. Tominaga, Y. Hayata, A. Yoshimura, Structure-activity relationships of 2-,4-, or 6-substituted estrogens as aromatase inhibitors, J. Steroid Biochem. Mol. Biol. 96 (2005) 51–58.
[5] C. Cadot, Y. Laplante, F. Kamal, V. Luu, D. Poirier, C6-(*N*,*N*-butyl-methyl-heptanamide) derivatives of estrone and estradiol as inhibitors of type 1 17β-hydroxysteroid dehydrogenase: chemical synthesis and biological evaluation, Bioorg. Med. Chem. 15 (2007) 714–726.
[6] H. Lawrence, H. Vicker, N. Allan, G.M. Smith, A. Mahon, M. Tutill, H.J. Purohit, A. Reed, M.J. Reed, B.V.L. Potter, Novel and potent 17β-hydroxysteroid dehydrogenase type 1 inhibitors, J. Med. Chem. 48 (2005) 2759–2762.
[7] D. Poirier, R.P. Boivin, M.R. Tremblay, M. Berube, W. Qiu, S.X. Lin, Estradiol-adenosine hybrid compounds designed to inhibit type 1, 17β-hydroxysteroid dehydrogenase, J. Med. Chem. 48 (2005) 8134–8147.
[8] B. Husen, K. Huhtinen, T. Saloniemi, J. Messinger, H.H. Thole, M. Poutanen, Human hydroxysteroids dehydrogenase 1 expression enhances estrogen sensitivity of MCF-7 breast cancer cell xenografts, Endocrinology 147 (2006) 5333–5339.
[9] D. Deluka, G. Moller, A. Rosinus, W. Elger, A. Hillisch, J. Adamski, Inhibitory effects of fluorine-substituted estrogens on the activity of 17β-hydroxysteroid dehydrogenases, Mol. Cell. Endocrinol. 248 (2006) 218–224.
[10] G.M. Allan, C. Bubert, N. Vicker, A. Smith, H.J. Tutill, A. Purohit, M.J. Reed, B.V.L. Potter, Novel, potent inhibitors of 17β-hydroxysteroid dehydrogenase type1, Mol. Cell. Endocrinol. 248 (2006) 204–207.
[11] D. Poirier, H.J. Chang, A. Azzi, R.P. Boivin, S.X. Lin, Estrone and estradiol C-16 derivatives as inhibitors of type 1 17β-hydroxysteroid dehydrogenase, Mol. Cell. Endocrinol. 248 (2006) 236–238.
[12] G. Moller, D. Deluca, C. Gege, A. Rosinus, D. Kowalik, O. Peters, P. Droescher, W. Elger, J. Adamski, A. Hillisch, Structure-based design, synthesis and in vitro

characterization of potent 17β-hydroxysteroid dehydrogenase type1 inhibitors based on 2-substitutions of estrone and D-homo-estrone, Bioorg. Med. Chem. Lett. 19 (2009) 6740–6744.
[13] S. Ray, I. Dwivedy, Development of estrogen antagonists as pharmaceutical agents, Adv. Drug Res. 29 (1997) 171–270.
[14] A. Claussner, L. Nedelec, F. Nique, D. Philibert, G. Teutsch, P. Van De Velde, 11β-Amidoalkyl estradiols, a new series of pure antiestrogens, J. Steroid Biochem. Mol. Biol. 41 (1992) 609–614.
[15] M. Cushman, H.M. He, J.A. Katzenellenbogen, R.K. Varma, E. Hamel, C.M. Lin, S. Ram, Y.P. Sachdeva, Synthesis of analogs of 2-methoxyestradiol with enhanced inhibitory effects on tubulin polymerization and cancer cell growth, J. Med. Chem. 40 (1997) 2323–2334.
[16] Z. Wang, D. Yang, A.K. Mohanakrishnan, P.E. Fanwick, P. Nampoothiri, E. Hamel, M. Cushman, Synthesis of B-ring homologated estradiol analogues that modulate tubulin polymerization and microtubule stability, J. Med. Chem. 43 (2000) 2419–2429.
[17] G. Möller, D. Deluca, C. Gege, A. Rosinus, D. Kowali, O. Peters, P. Droescher, W. Elger, J. Adamski, A. Hillisch, Structure-based design, synthesis and in vitro characterization of potent 17β-hydroxysteroid dehydrogenase type 1 inhibitors based on 2-substitutions of estrone and D-homo-estrone, Bioorg. Med. Chem. Lett. 19 (2009) 6740–6744.
[18] A. Hillisch, O. Peters, C. Gege, G. Siemeister, E. Unger, B. Menzenbach, Antitumoral D-homoestra-1,3,5(10)-trien-3-yl 2-substituted sulfamates, US RE42,132 E (2011).
[19] R. Minorics, N. Bózsity, J. Wölfling, E. Mernyák, G. Schneider, Á. Márki, G. Falkay, I. Ocsovszki, I. Zupkó, Antiproliferative effect of normal and 13-*epi*-D-homoestrone and their 3-methyl ethers on human reproductive cancer cell lines, J. Steroid Biochem. Mol. Biol. 132 (2012) 168–174.
[20] J. Wölfling, E. Mernyák, É. Frank, G. Falkay, Á. Márki, R. Minorics, G. Schneider, Synthesis and receptor-binding examinations of the normal and 13-epi-D-homoestrones and their 3-methyl ethers, Steroids 68 (2003) 277–288.
[21] D. Ayan, J. Roy, R. Maltais, D. Poirier, Impact of estradiol structural modifications (18-methyl and/or 17-hydroxy inversion of configuration) on the *in vitro* and *in vivo* estrogenic activity, J. Steroid Biochem. 127 (2011) 324–330.
[22] B. Schönecker, C. Lange, M. Kötteritzsch, W. Günther, J. Weston, E. Anders, H. Görls, Conformational design for 13α-steroids, J. Org. Chem. 65 (2000) 5487–5497.
[23] F.G. Yaremenko, A.V. Khvat, A new one-pot synthesis of 17-oxo-13α-steroids of the androstane series from their 13β-analogues, Mendeleev Commun. 187 (1994) 187–188 Chem. Abstr. 122 (1995) 214318w.
[24] L. Liang, D. Astruc, The copper(I)-catalyzed alkyne-azide cycloaddition (CuAAC) "click" reaction and its applications. An overview, Coord. Chem. Rev. 255 (2011) 2933–2945.
[25] C.W. Tornøe, S.J. Sanderson, J.C. Mottram, G.H. Coombs, M. Meldal, Combinatorial library of peptidotriazoles: identification of [1,2,3]-triazole inhibitors against a recombinant *Leishmania mexicana* cysteine protease, J. Comb. Chem. 6 (2004) 312–324.
[26] A.M. Deobald, L.R.S. Camargo, D. Alves, J. Zukerman-Schpector, A.G. Corrêa, M. W. Paixão, Click chemistry: an efficient synthesis of heterocycles substituted with steroids, saponins, and digitalis analogues, Synthesis 24 (2011) 4003–4010.
[27] Z. Kadar, E. Frank, G. Schneider, J. Molnar, I. Zupko, J. Koti, B. Schönecker, J. Wölfling, Efficient synthesis of novel A-ring-substituted 1,2,3-triazolylcholestane derivatives via catalytic azide–alkyne cycloaddition, Arkivoc 3 (2012) 279–296.
[28] Z. Kadar, J. Molnar, G. Schneider, I. Zupko, E. Frank, A facile 'click' approach to novel 15β-triazolyl-5α-androstane derivatives, and an evaluation of their antiproliferative activities in vitro, Bioorg. Med. Chem. 20 (2012) 1396–1402.
[29] Z. Kadar, A. Baji, I. Zupko, T. Bartok, J. Wölfling, E. Frank, Efficient approach to novel 1α-triazolyl-5α-androstane derivatives as potent antiproliferative agents, Org. Biomol. Chem. 9 (2011) 8051–8057.
[30] E. Frank, J. Molnar, I. Zupko, Z. Kadar, J. Wölfling, Synthesis of novel steroidal 17α-triazolyl derivatives via Cu(I)-catalyzed azide–alkyne cycloaddition, and an evaluation of their cytotoxic activity in vitro, Steroids 76 (2011) 1141–1148.
[31] Z. Kadar, D. Kovacs, E. Frank, G. Schneider, J. Huber, I. Zupko, T. Bartok, J. Wölfling, Synthesis and *in vitro* antiproliferative activity of novel androst-5-ene triazolyl and tetrazolyl derivatives, Molecules 16 (2011) 4786–4806.
[32] T. Mosmann, Rapid colorimetric assay for cellular growth and survival: application to proliferation and citotoxicity assays, J. Immunol. Methods 65 (1983) 55–63.
[33] I. Vermes, C. Haanen, C. Reutelingsperger, Flow cytometry of apoptotic cell death, J. Immunol. Methods 243 (2000) 167–190.
[34] D. Ribble, N.B. Goldstein, D.A. Norris, Y.G. Shellman, A simple technique for quantifying apoptosis in 96-well plates, BMC Biotechnol. 5 (2005) 12.
[35] S. Rozen, H. Skaletsky, Primer3 on the WWW for general users and for biologist programmers, Methods Mol. Biol. 132 (2000) 365–386.
[36] M.R. Johnson, K. Wang, J.B. Smith, M.J. Heslin, R.B. Diasio, Quantitation of dihydropyrimidine dehydrogenase expression by real-time reverse transcription polymerase chain reaction, Anal. Biochem. 278 (2000) 175–184.
[37] E. Mernyák, B. Schönecker, C. Lange, M. Kötteritzsch, H. Görls, J. Wölfling, G. Schneider, Addition reactions at the 16(17) double bond of 3-methoxy-13α-estra-1 3,5(10), 16-tetraene, Steroids 68 (2003) 289–295.
[38] R.M. Neve, K. Chin, J. Fridlyand, J. Yeh, F.L. Baehner, T. Fevr, L. Clark, et al., A collection of breast cancer cell lines for the study of functionally distinct cancer subtypes, Cancer Cell 10 (2006) 515–527.
[39] A. Berényi, R. Minorics, Z. Iványi, I. Ocsovszki, E. Ducza, M. Thole, J. Messinger, J. Wölfling, G. Mótyán, E. Mernyák, E. Frank, G. Schneider, I. Zupkó, Synthesis and investigation of the anticancer effects of estrone-16-oxime ethers *in vitro*, Steroids 78 (2013) 69–78.
[40] W.R. Taylor, G.R. Stark, Regulation of the G2/M transition by p53, Oncogene 20 (2001) 1803–1815.